GLOBAL WARMING EFFECTS ON ECTOTHERM SPECIES

ARTICLES FOR FACULTY MEMBERS

Title/Author	A common temperature dependence of nutritional demands in ectotherms / Laspoumaderes, C., Meunier, C. L., Magnin, A., Berlinghof, J., Elser, J. J., Balseiro, E., Torres, G., Modenutti, B., Tremblay, N., & Boersma, M.
Source	*Ecology Letters* Volume 25 Issue 10 (2022) Pages 2189–2202 https://doi.org/10.1111/ele.14093 (Database: Wiley Online Library)

Title/Author	Adding climate change to the mix: Responses of aquatic ectotherms to the combined effects of eutrophication and warming / Rodgers, E. M.
Source	*Biology Letters* Volume 17 Issue 10 (2021) Pages 1-6 https://doi.org/10.1098/rsbl.2021.0442 (Database: Royal Society Publishing)

Title/Author	Climate change and ageing in ectotherms / Burraco, P., Orizaola, G., Monaghan, P., & Metcalfe, N. B.
Source	*Global Change Biology* Volume 26 Issue 10 (2020) Pages 5371–5381 https://doi.org/10.1111/gcb.15305 (Database: Wiley Online Library)

GLOBAL WARMING EFFECTS ON ECTOTHERM SPECIES

ARTICLES FOR FACULTY MEMBERS

Title/Author	Evidence of stronger range shift response to ongoing climate change by ectotherms and high-latitude species / Ramalho, Q., Vale, M. M., Manes, S., Diniz, P., Malecha, A., & Prevedello, J. A
Source	*Biological Conservation* Volume 279 (2023) 109911 Pages 1-9 https://doi.org/10.1016/j.biocon.2023.109911 (Database: ScienceDirect)

Title/Author	Extreme escalation of heat failure rates in ectotherms with global warming / Jørgensen, L. B., Ørsted, M., Malte, H., Wang, T., & Overgaard, J.
Source	*Nature* Volume 611 Issue 7934 (2022)Pages 93–98 https://doi.org/10.1038/s41586-022-05334-4 (Database: Nature Portfolio)

Title/Author	Fish shrinking, energy balance and climate change / Queiros, Q., McKenzie, D. J., Dutto, G., Killen, S., Saraux, C., & Schull, Q.
Source	*Science of the Total Environment* Volume 906 (2024) 167310 Pages 1-12 https://doi.org/10.1016/j.scitotenv.2023.167310 (Database: Science Direct)

GLOBAL WARMING EFFECTS ON ECTOTHERM SPECIES

ARTICLES FOR FACULTY MEMBERS

Title/Author	Global warming is projected to lead to increased freshwater growth potential and changes in pace of life in Atlantic salmon Salmo salar / Rinaldo, A., de Eyto, E., Reed, T., Gjelland, K. Ø., & McGinnity, P.
Source	*Journal of Fish Biology* Volume 104 Issue 3 (2024) Pages 647–661 https://doi.org/10.1111/jfb.15603 (Database: Wiley Online Library)

Title/Author	Predicting the fundamental thermal niche of ectotherms / Simon, M. W., & Amarasekare, P.
Source	*Ecology* Volume 105, Issue 5 (2024) e4289 Pages 1-18 https://doi.org/10.1002/ecy.4289 (Database: Wiley Online Library)

Title/Author	Temperature change effects on marine fish range shifts: A meta-analysis of ecological and methodological predictors / Dahms, C., & Killen, S. S.
Source	*Global Change Biology* Volume 29 Issue 16 (2023)Pages 4459–4479 https://doi.org/10.1111/gcb.16770 (Database: Wiley Online Library)

ARTICLES FOR FACULTY MEMBERS

GLOBAL WARMING EFFECTS ON ECTOTHERM SPECIES

Title/Author	**A common temperature dependence of nutritional demands in ectotherms / Laspoumaderes, C., Meunier, C. L., Magnin, A., Berlinghof, J., Elser, J. J., Balseiro, E., Torres, G., Modenutti, B., Tremblay, N., & Boersma, M.**
Source	***Ecology Letters*** **Volume 25 Issue 10 (2022) Pages 2189–2202** **https://doi.org/10.1111/ele.14093** **(Database: Wiley Online Library)**

Received: 14 March 2022 | Revised: 25 July 2022 | Accepted: 26 July 2022

DOI: 10.1111/ele.14093

LETTER

ECOLOGY LETTERS cnrs WILEY

A common temperature dependence of nutritional demands in ectotherms

Cecilia Laspoumaderes[1,2,3] | **Cedric L. Meunier**[2] | **Amaru Magnin**[1,2] | **Johanna Berlinghof**[2,4] | **James J. Elser**[3,5] | **Esteban Balseiro**[1] | **Gabriela Torres**[2] | **Beatriz Modenutti**[1] | **Nelly Tremblay**[2,6,7] | **Maarten Boersma**[2,8]

[1]INIBIOMA, CONICET-Universidad Nacional del Comahue, Bariloche, Argentina

[2]Biologische Anstalt Helgoland, Alfred-Wegener-Institut, Helmholtz-Zentrum für Polar- und Meeresforschung (AWI), Germany

[3]School of Life Sciences, Arizona State University, Tempe, Arizona, USA

[4]Department of Marine Ecology, University of Bremen, Bremen, Germany

[5]Flathead Lake Biological Station, University of Montana, Polson, Montana, USA

[6]Pêches et Océans Canada, Mont-Joli, Quebec, Canada

[7]Département de Biologie, de Chimie et de Géographie, Université du Québec à Rimouski, Rimouski, Canada

[8]FB2, University of Bremen, Bremen, Germany

Correspondence
Cecilia Laspoumaderes, Quintral 1250, San Carlos de Bariloche (8400), Río Negro, Argentina.
Email: claspoumaderes@comahue-conicet.gob.ar

Funding information
Alexander von Humboldt-Stiftung; Dynatrait programme of the German Science Foundation; Fulbright Association; NSF Rules of Life grant, Grant/Award Number: DEB-1930816; Deutsche Forschungsgemeinschaft; Bundesministerium für Bildung und Forschung, Grant/Award Number: 01LN1702A; Fondo Para la Investigación Científica y Tecnológica, Grant/Award Number: PICT 2017-1940 and PICT 2019-00950; Alexander von Humboldt Foundation

Editor: Cameron Ghalambor

Abstract

In light of ongoing climate change, it is increasingly important to know how nutritional requirements of ectotherms are affected by changing temperatures. Here, we analyse the wide thermal response of phosphorus (P) requirements via elemental gross growth efficiencies of Carbon (C) and P, and the Threshold Elemental Ratios in different aquatic invertebrate ectotherms: the freshwater model species *Daphnia magna*, the marine copepod *Acartia tonsa*, the marine heterotrophic dinoflagellate *Oxyrrhis marina*, and larvae of two populations of the marine crab *Carcinus maenas*. We show that they all share a non-linear cubic thermal response of nutrient requirements. Phosphorus requirements decrease from low to intermediate temperatures, increase at higher temperatures and decrease again when temperature is excessive. This common thermal response of nutrient requirements is of great importance if we aim to understand or even predict how ectotherm communities will react to global warming and nutrient-driven eutrophication.

KEYWORDS
carbon, ecological stoichiometry, gross growth efficiency, growth, metabolism, nutrients, phosphorus, respiration, thermal gradient, threshold elemental ratio

INTRODUCTION

Temperature is among the most influential determinants of fitness in ectotherms, as it directly drives their metabolism (Clissold & Simpson, 2015; Cross et al., 2015). Within biologically relevant ranges below the optimum temperature, ectotherm metabolic rates scale exponentially with temperature. Hence, even a small increase in environmental temperature may lead to large changes in performance (Brown et al., 2004; Gillooly et al., 2001). Furthermore, to ensure the achievement of the Darwinian functions of survival and reproduction, all consumers must obtain a diet containing the appropriate balance of biochemical nutrients (Simpson & Raubenheimer, 2012) including essential fatty acids, amino acids and vitamins. On a more basic level, specific chemical elements, such as nitrogen (N) and phosphorus (P), are also essential components of the food (Sterner & Elser, 2002). Given the overriding importance of temperature for metabolic rates of ectotherms, understanding the interactions of temperature and nutritional demands is critical (Cross et al., 2015). The most straightforward way to assess temperature–food quality interactions is to investigate temperature effects on the Threshold Elemental Ratio (TER) (Frost et al., 2006; Sterner, 1997; Urabe & Watanabe, 1992). The $TER_{C:X}$ is the carbon:nutrient (C:X) ratio in the food that matches the current physiological requirements for metabolism and growth of the consumer, with neither C nor X being limiting or in excess. The TER is a quantitative tool that integrates multiple responses of organism biochemistry and physiology. A low $TER_{C:X}$ indicates higher needs for the nutrient X relative to C, while a higher $TER_{C:X}$ indicates the opposite. Cross et al. (2015) noted that there were few studies on how temperature affects the TER and made a strong case to measure the $TER_{C:X}$ at different temperatures.

The integration of two theoretical frameworks may lead to a general theory to understand how energy and nutrient availability act in combination: the metabolic theory of ecology (MTE) from Brown et al. (2004), which focuses on the importance of individuals energetics; and ecological stoichiometry theory (EST) that focuses on the importance of element availability (Sterner & Elser, 2002). In the frame of MTE, a positive relation of an organism's C requirements with temperature is expected as a consequence of the over-proportional increase in respiration rates with temperature, resulting in an increasing $TER_{C:X}$ with temperature as seen by Boersma et al. (2016) and Malzahn et al. (2010). However, assuming that respiration and feeding rates scale equally with temperature (same Q_{10}) and that invertebrates facing nutrient limitation at increasing temperatures might use their excess C to meet the increased demands for energy without the need for extra dietary C, Anderson et al. (2017) modelled a constant $TER_{C:N}$ with temperature. On the other hand, growth has a lower C:nutrient than metabolism so a decreasing $TER_{C:P}$ with temperature is expected if growth scales faster (larger Q_{10}) than respiration.

Studies on stoichiometric impacts of temperature are, unfortunately, rather equivocal, with reports of increasing, decreasing or constant TER with increasing temperature (Anderson et al., 2017; Boersma et al., 2016; Malzahn et al., 2016; Persson et al., 2011; Ruiz et al., 2020; Wojewodzic et al., 2011). The most parsimonious explanation for these findings is that the response of the nutritional demands to temperature is not monotonic and that most studies conducted so far have not covered a sufficiently broad temperature range. Indeed, based on the parametrisation of $TER_{C:P}$ model from Frost et al. (2006) with literature data on the temperature dependencies of all parameters in the model and with experimental data on growth-based $TER_{C:P,}$ Ruiz et al. (2020) predicted a U-shaped response of the $TER_{C:P}$ with temperature. Hence, the question remains whether there is a common response of ectotherm nutrient requirements to changing temperatures that would help in making predictions about secondary production responses to global change. Alternatively, the diversity of findings to date may reflect true idiosyncrasies in temperature responses among taxa, consequently preventing general overarching predictions.

In this study, we aim to shed light on the interactions between macronutrient requirements of ectotherms and temperature. We experimentally determined the response of the $TER_{C:P}$ to temperature for different aquatic invertebrates. We used two different clones of the freshwater cladoceran *Daphnia magna* with different thermal histories to determine the growth-based $TER_{C:P}$. Further, we characterised the thermal response of fundamental parameters of the bioenergetics $TER_{C:P}$ model (respiration, ingestion, growth, gross growth efficiencies of C and P, and body C:P) (Doi et al., 2010; Frost et al., 2006; Halvorson et al., 2015) across ecologically relevant temperature ranges, using one clone of *D. magna* (same as growth-based TER), the marine copepod *Acartia tonsa*, the marine heterotrophic dinoflagellate *Oxyrrhis marina*, and larvae of two populations of the marine crab *Carcinus maenas*.

Thermal performance curves of respiration and ingestion vary with increasing temperature, usually displaying an ascending phase, a peak, which indicates the thermal optimum, and a descending phase of metabolic inhibition (Shah et al., 2021). Growth rate increases with increasing temperature and is in part responsible for the increase in ingestion, due to the extra demands for substrates (Hayes et al., 2015). Body C:P is expected to increase with temperature (Balseiro et al., 2021; Woods et al., 2003), while for GGEs decreasing, increasing and constant thermal responses were reported (Doi et al., 2010; Hagerty et al., 2014; Smith et al., 2021; Ye et al., 2019; Zheng et al., 2019). Based on these hypothesised mechanisms, we predict that ectotherm nutrient

requirements change with temperature in a nonlinear fashion, as a response to nonlinear thermal reaction norms of metabolism and growth.

MATERIALS AND METHODS

First, we determined the thermal response of the $TER_{C:P}$ from growth rates as a function of temperature and food C:P (growth-based $TER_{C:P}$) for two clones of *Daphnia magna*. The $TER_{C:P}$ is obtained from the diet C:P, which maximises growth, at different temperatures. Secondly, to explore the mechanisms underlying the thermal response of the $TER_{C:P}$, we determined the thermal response of body C and P contents and ingestion (IR), respiration (RR) and growth (GR) rates, the gross growth efficiency of C and P (GGE_C and GGE_P) and the $TER_{C:P}$ bioenergetic model proposed by (Doi et al., 2010; Frost et al., 2006) following Halvorson et al. (2015). This was done for *Acartia tonsa*, *Oxyrrhis marina* and larvae of two different populations of *Carcinus maenas*, and one clone of *D. magna* (same used in the growth-based $TER_{C:P}$). With this second set of experiments, we obtained information on how nutrient requirements of the studied organisms change with temperature, as well as the thermal response of all underlying variables that determine the TER (model details in Appendix S1).

Growth-based $TER_{C:P}$ as a function of temperature

We determined the diet C:P, which maximises growth ($TER_{C:P}$) at different temperatures for two clones of *D. magna*. These two clones differ in their thermal histories. Clone US was maintained in the laboratory at 24–25°C, and Clone AR at 20°C, both for at least 3 years prior to experiments (see below for details). The thermal optimum for *D. magna* ranges between 16 and 22°C (Bruijning et al., 2018).

Culturing conditions

The first experiment was carried out at Arizona State University, USA, with a clone of *D. magna* (Clone US) that was maintained in the laboratory in COMBO media (Kilham et al., 1998) on a diet of the green alga *Scenedesmus acutus* (C:P ~ 120) at room temperature (24–25°C). The experiment was carried out at 18, 23 and 28°C in a food quality gradient consisting of food with five C:P ratios ranging from 51 to 816. The second experiment was carried out at Universidad Nacional del Comahue, Argentina, with a clone of *D. magna* (Clone AR) that had been maintained in the laboratory in COMBO media (Kilham et al., 1998) on a diet of the green algae *Chlamydomonas reinhardtii* (C:P ~ 150) at 20°C. We used 15, 20 and 24°C as temperatures and a C:P gradient ranging from 40 to 746.

Experimental design

Both experiments lasted 3 days to avoid the confounding effect of shifts in allocation between growth and ovary development of *Daphnia* reaching maturity (Acharya et al., 2004). To exclude the influence of indirect effects of P limitation on the biochemistry of the algae, the gradients in food quality (C:P) were created with a short-term P-spiking technique following Rothhaupt (1995) and Plath and Boersma (2001) (Details in Appendix S2).

For both experiments, we placed one 24-h-old *D. magna* in a 30 ml beaker with 11 replicates in a factorial design of 3 temperatures and 5 food qualities (n = 165). Food and media were replaced daily at a concentration of 1.5 $mg\,C\,L^{-1}$. To determine growth rate, the area of each animal was measured by taking lateral images and then processing the image via Image-Pro Plus (Media Cybernetics) software. These measurements were converted to dry weight based on our own area–weight regressions obtained from our *D. magna* cultures at different food qualities. We determined the growth rate of each individual as the difference in the natural logarithm of the dry weight at the end and the beginning of the experiment divided by the time in days. In some cases, one or two replicates were missing at the end of the experiment due to mortality during the daily handling of the animals.

Data analyses

The shape of the $TER_{C:P}$ thermal reaction norm was obtained following Ruiz et al. (2020). For each temperature level separately, the following modified Gaussian function was fitted to the relationship between individual growth rate versus the food C:P from which $TER_{C:P}$ estimates were derived:

$$GR = a + b * e^{-E * \frac{C:P - c^2}{d^2}} \quad (1)$$

where $C:P$ is the food C:P ratio, a is the minimum growth rate, b is the height of the curve, c is the estimated $TER_{C:P}$ (i.e., curve's maximum), d is the curve breadth and E is a scaling parameter. All the parameters were estimated by nonlinear least squares regression (Baty et al., 2015). The confidence intervals around the $TER_{C:P}$ were estimated by nonparametric bootstrapping (Efron & Tibshirani, 1986). At each temperature, the dataset was resampled 1000 times and the nonlinear regression procedure and $TER_{C:P}$ estimations were reiterated. This was used to calculate the mean $TER_{C:P}$ and the 95% confidence intervals ($CI_{95\%}$) for each temperature. A

significant difference between $TER_{C:P}$ estimates at each temperature was inferred in the absence of overlap between their $CI_{95\%}$.

Thermal response of the bioenergetic $TER_{C:P}$ and underlying variables

Culturing conditions

Experiments were carried out at the Universidad Nacional del Comahue, Argentina (*D. magna* AR) and the Biologische Anstalt Helgoland (BAH), AWI, Helgoland, Germany, for the rest of the species. *D. magna* (AR) is the same clone as the growth-based $TER_{C:P.}$ *O. marina* was obtained from the Göttingen culture collection (Strain B21.89), and the stock culture used to inoculate the experimental containers was grown in batch cultures at 18°C in the dark. Eggs of *A. tonsa* were obtained from a permanent laboratory culture at 18°C and incubated in filtered seawater for hatching, and only those hatched between 24–36 h of incubation were used. Berried females of *C. maenas* were collected manually at the intertidal area of the bay of Cadiz (Spain) and Helgoland (Germany) during the reproductive periods. Suitable temperature for embryonic development and larval release occurs in February–March (15.3–16°C) for the Cadiz population, and in May–July (9–15°C) for the Helgoland population. Animals were transported to the BAH in individual containers with seawater and constant temperature (15.7 and 12.5°C for Cadiz and Helgoland, respectively). To ensure a successful embryonic development, and to reflect the temperature of the natural habitat at the time of hatching in summer, females were maintained in individual aquaria where temperature was gradually increased (0.2°C per day) until 18°C, when hatching occurred. We used four hatches from different females from the Cadiz population and three from Helgoland to account for maternal effects on the results (Torres et al., 2020), and each of them was considered a replicate.

Experimental design

24-h-old *D. magna* (AR) were placed in beakers with COMBO and food (*C. reinhardtii*) ad libitum. Individuals of *O. marina*, or recently hatched *A. tonsa* (nauplii) and *C. maenas* (Zoea I) were placed in beakers with filtered seawater (0.2 μm) and food ad libitum. *A. tonsa* and *O. marina* were fed *Rhodomonas salina*, and *C. maenas* was fed with *Artemia salina*. *D. magna* (15 and 24°C), *A. tonsa* and *C. maenas* (12–24°C) were distributed in temperature-controlled rooms, and *O. marina* beakers were placed in a gradient temperature table (15.2–22.8°C) following Malzahn et al. (2016). Media and food were replaced daily. The length of the experiment varied according to each species (Details in Appendix S3, Table S1).

Carbon and phosphorus analyses

At the beginning and the end of the experiments, we determined C and P contents for individuals of *D. magna*, *A. tonsa* and *C. maenas*. Carbon and P contents per beaker of *O. marina*, *C. reinhardtii* and *R. salina* were measured by filtering a known amount through acid-washed precombusted (450°C, 2 h) Whatman GF/F filters. Analyses for *D. magna*, *A. tonsa* and *A. salina* were carried out by placing a known number of individuals on GF/F filters and for *C. maenas* by placing individuals directly into pre-weighed tin capsules for C analysis or in 1.5 ml Eppendorf tubes for P analysis, following by re-weighing before analysis. C was analysed with a Vario MICRO cube CHNS analyser (Elementar Analysensysteme), and P as orthophosphate after acidic oxidative hydrolysis (Grasshoff et al., 2009). Using these data, we calculated initial and final body C:P ratios and growth rate in terms of C and P for each species (*GR*, see calculations).

Ingestion (IR) and respiration (RR)

At the end of the growth periods, we determined ingestion rates in terms of C and P and respiration rates for all the organisms in the dark. Ingestion rates of *D. magna* were obtained with the fluorescent microspheres method following DeMott (1986); Wiedner and Vareschi (1995); Laspoumaderes et al. (2017). Ingestion rates of the other species were determined through the difference in final food concentration versus a control for *O. marina* and *A. tonsa*, or versus initial concentration for *C. maenas* (details in Appendix S3b and S3, Table S2).

Respiration rates were assessed as oxygen consumption over time in glass vials with the organisms, media without food, in the dark, stoppered to ensure that no air bubbles were present, in temperature-controlled rooms set to the experimental temperature. Vials without organisms (n = 5–6) were used as controls to account for microbial oxygen consumption. Oxygen consumption was determined by linear regression of O_2 concentration against time, standardised to μgC (details in Appendix S3c and S3, Table S3).

Calculations

We determined the $TER_{C:P}$ as a function of temperature for *D. magna* (AR), *A. tonsa*, *O. marina* and *C. maenas* using the model of Frost et al. (2006) modified by Doi et al. (2010) and further analysed by Halvorson et al. (2015) (Equation 2):

$$TER_{C:P} = \frac{GGE_P}{GGE_C} \times \frac{Q_C}{Q_P} \quad (2)$$

where Q_C and Q_P are the final body C and P contents (for alternatives see Appendix S1), GGE_P and GGE_C are the gross growth efficiencies of P and C calculated following Doi et al. (2010) as the ratio of the growth rate of P or C to the ingestion rate of P or C (for GGE_P and GGE_C, respectively):

$$GGE = \frac{GR}{IR} \quad (3)$$

where *GR* is the amount of C or P fixed as new biomass in a certain period, it is calculated as the difference in C or P content (per individual for *D. magna*, *A. tonsa* and *C. maenas*, and per beaker for *O. marina*) at the end and the beginning of the experiment over time in days, and *IR* is the ingestion rate in terms of C or P in the same period.

We calculated the Q_{10} of *RR*, *IR* and *GR* in the thermal gradient with the formula:

$$Q_{10} = (\frac{R_2}{R_1})^{10/T_2 - T_1}$$

where R_1 and R_2 are the specific rates at temperatures 1 and 2, respectively (T_1 and T_2). When the $TER_{C:P}$ was nonlinear, we calculated the Q_{10} separately for the increasing and decreasing thermal range. We compared the Q_{10} of respiration with the Q_{10} of ingestion and growth for each thermal range.

Data analyses

One-way analysis of variance (ANOVA) was performed to compare the organisms' C:P ratios, respiration, growth and ingestion rates, GGE and $TER_{C:P}$ values with temperature as a factor, followed by Holm-Šídák post hoc tests. When assumptions were not met, Kruskal-Wallis ANOVA on ranks was used. The temperature where the $TER_{C:P}$ is the highest ($MaxTER_{C:P}$ temperature) and its $CI_{95\%}$ for *A. tonsa*, *O. marina* and *C. maenas* were obtained through nonlinear regression fit of the thermal response of the $TER_{C:P}$ to a Gaussian function, with the R package nlstools (Baty et al., 2015). The Q_{10} were compared with *t*-tests. Analyses were performed using the software R v.4.1.2 (R-Core-Team, 2021).

RESULTS

Growth-based $TER_{C:P}$ as a function of temperature

Growth rates of both clones of *D. magna* showed a hump-shaped response to the food C:P gradient and fitted to the Gaussian equation (Equation 1) at all temperatures (Figure 1a,b), except for *D. magna* (US) at 15°C (lowest temperature), which showed a nearly flat response of growth rates to changing food quality (Figure 1a) (See Appendix S4a model fitting). The $TER_{C:P}$, at each temperature (maximum of the gaussian function, except for *D. magna* (US) at 15°C), showed a hump-shaped relation with temperature. The maximum $TER_{C:P}$ was found at intermediate temperatures for both clones (Figure 1c,d), with decreasing $TER_{C:P}$ at low and high temperatures (Figure 1c,d).

Thermal response of the bioenergetic $TER_{C:P}$ and underlying variables

Ingestion, respiration and growth rates in the thermal gradient

Ingestion and respiration rates showed the same response to temperature within species but were not consistent between them (Figure 2). The change in ingestion rates in *D. magna* (AR) with temperature was not significant; however, respiration increased (Figure 2a,b). Ingestion and respiration rates showed a hump-shaped response to temperature for *A. tonsa* and *O. marina*, with maximum values in the range of 18–21°C for *A. tonsa*, and at 18°C for *O. marina* (Figure 2d,e,j,k). In contrast, both populations of *C. maenas* presented a consistent increase in ingestion and respiration (Figure 2g,h,m,n). Growth rates had an increasing trend in the thermal gradient for all species (Figure 2c,f,i,l,o). However, growth rates of both populations of *C. maenas* seemed to reach a maximum growth at around 21°C (Figure 2i,o).

Body C:P in the thermal gradient

Body C:P of *D. magna* was higher at 24°C than at 15°C (Figure 3a). C:P of *A. tonsa*, *O. marina* and *C. maenas* (Cadiz (C)) had a U-shaped response to temperature, with minimum values at intermediate temperatures (around 18°C) (Figure 3b–d). C:P ratios of *C. maenas* (Helgoland [H]) showed the same U-shaped response to temperature but also had a second minimum in the highest temperatures resulting in an "inverse N-response" of body C:P to temperature (Figure 3e).

Gross growth efficiency of C and P (GGE_C and GGE_P) in the thermal gradient

The thermal response of gross growth efficiency of carbon presented some differences between species (Figure 3f–j). GGE_C in *A. tonsa* increased at the highest temperature (Figure 3g), had a U-shaped response to temperature in *O. marina* (Figure 3h), and had no variation with temperature for both *C. maenas* populations

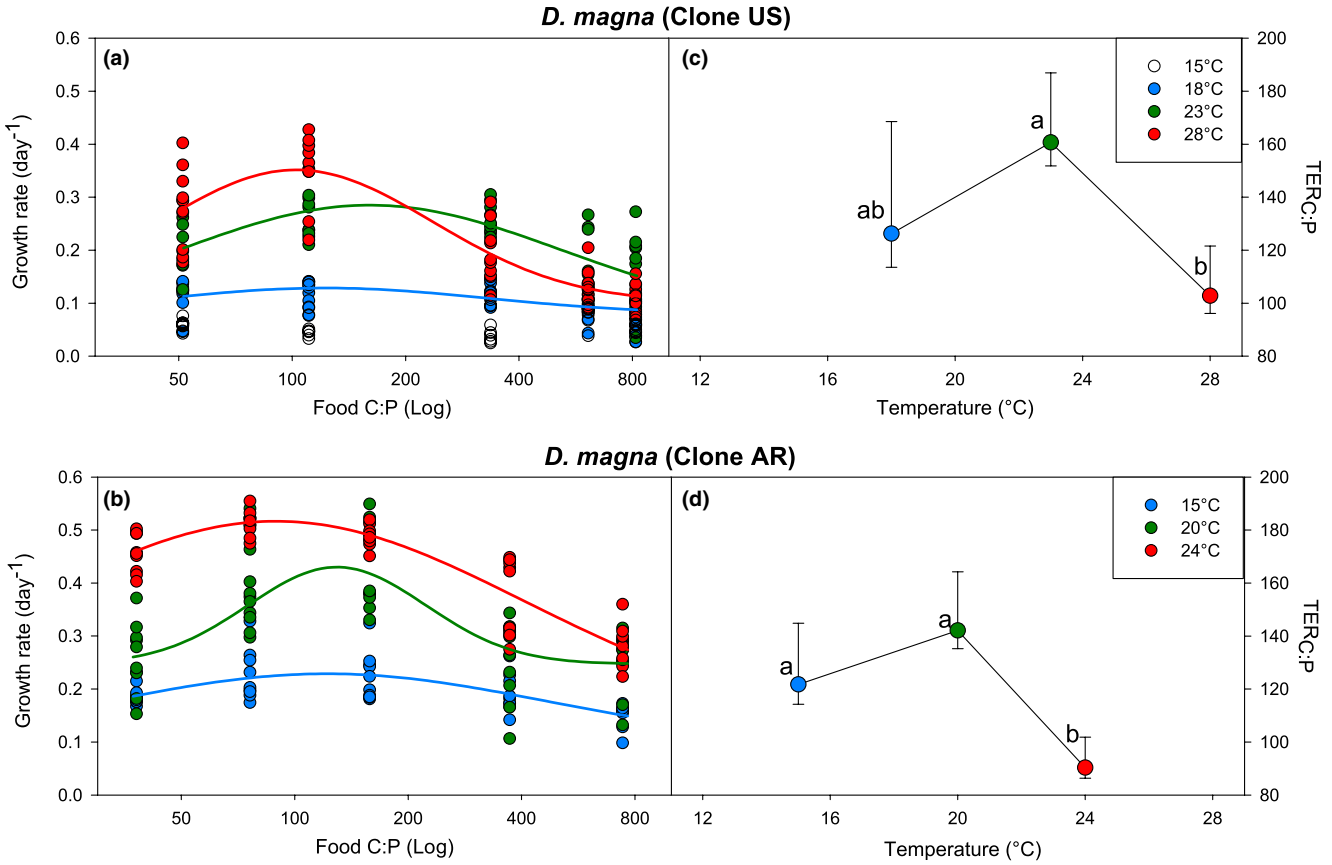

FIGURE 1 (a) and (b) Growth rate as a function of food C:P ratio in the thermal gradient for clone US (a) and clone AR (b) of *Daphnia magna*. Dots are individual data, and the lines are the best fit to the Gaussian Function (Equation 1) estimated by nonlinear least squares regression, the maximum of the gaussian function is the C:P threshold elemental ratio ($TER_{C:P}$). (c) and (d) $TER_{C:P}$ as a function of temperature and the 95% confidence intervals ($CI_{95\%}$) estimated by nonparametric bootstrapping ($n = 1000$) for clone US and clone AR, respectively. Lower-case letters inside the graphs indicate homogeneous groups according to overlapping $CI_{95\%}$. Lines and dot colours represent different temperatures (see reference in figure)

and *D. magna* (Figure 3f, i, j). On the other hand, GGE_P showed larger responses to temperature with patterns that differed among the study taxa (Figure 3f–j).

Bioenergetic $TER_{C:P}$

For *D. magna*, the $TER_{C:P}$ was higher at 15°C than at 24°C. This was consistent with the growth-based and bioenergetic $TER_{C:P}$ calculated with final and initial body C:P (Figure 1d and 4a, and Appendix S5). However, using initial body C:P, the $TER_{C:P}$ was closer to growth-based $TER_{C:P}$ than using final body C:P. As only two temperatures were tested for *D. magna* with the bioenergetic model, we do not know the shape of the response in the complete thermal gradient. For the other species, the bioenergetic $TER_{C:P}$ was determined for a broad temperature range and we obtained a hump-shaped response of the $TER_{C:P}$ to temperature for *A. tonsa*, *O. marina* and *C. maenas* (C) (Figure 4b–d), with a maximum $TER_{C:P}$ ($MaxTER_{C:P}$) at intermediate temperatures. This $MaxTER_{C:P}$ is indicative of the organism's lowest P-requirements. The unimodal shape of the $TER_{C:P}$ indicates that at both lower and higher temperatures animals need food with higher P content relative to C to grow maximally. In the case of *C. maenas* (H), we obtained an N-shaped response of the $TER_{C:P}$ as a function of temperature (Figure 4e). The lower temperatures of the gradient (12–18°C) resulted in a hump-shaped response for this population similar to the other taxa, while the warmer temperatures (18–24°C) formed a U-shaped thermal response of the $TER_{C:P}$ (Figure 4e).

Q_{10} for respiration, ingestion and growth

The Q_{10} values for respiration, ingestion and growth showed different patterns in the different areas of the $TER_{C:P}$ (increasing and decreasing arms) for all species (Table 1). The Q_{10} of respiration was higher than the Q_{10} of ingestion and growth in the increasing arm of the $TER_{C:P}$ for *O. marina* and the opposite pattern was observed for the decreasing arm (Table 1). For the other species, we observed that Q_{10} of respiration was higher than Q_{10} of ingestion or growth in the increasing arm, and that the Q_{10} of

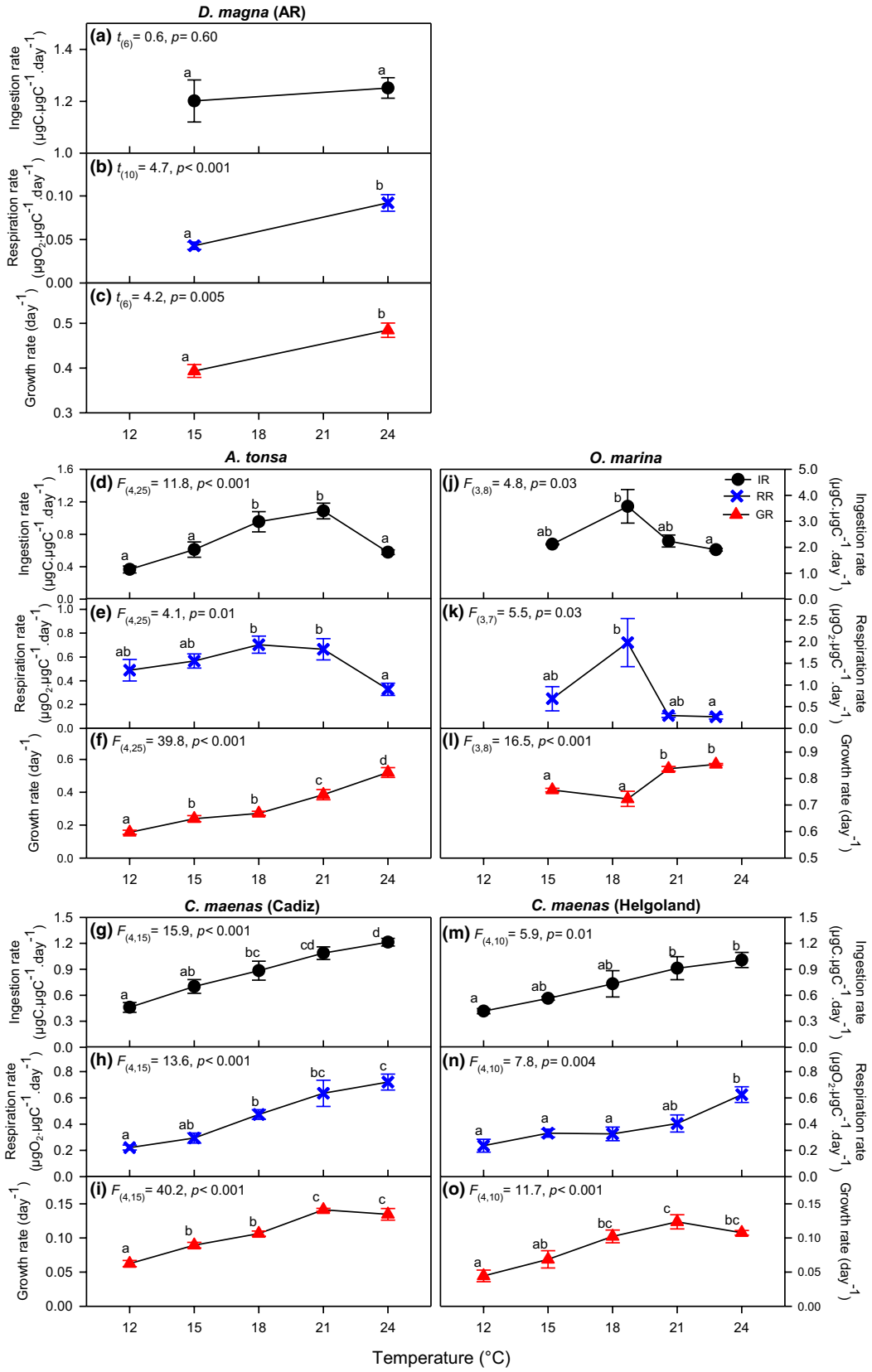

FIGURE 2 Thermal response of ingestion rate (a, d, g, j, m), respiration rate (b, e, h, k, n) and growth rate (c, f, i, l, o), for *Daphnia magna* (AR) (a–c), *Acartia tonsa* (d–f), *Carcinus maenas* (Cadiz) (g–i), *Oxyrrhis marina* (j–l) and *C. maenas* (Helgoland) (m–o). Symbols are mean values and bars SE. In some cases, the error bars are not visible, because they are smaller than the symbols. Lower-case letters inside the graphs indicate homogeneous groups according to the post hoc Holm-Šídák multiple comparison test results

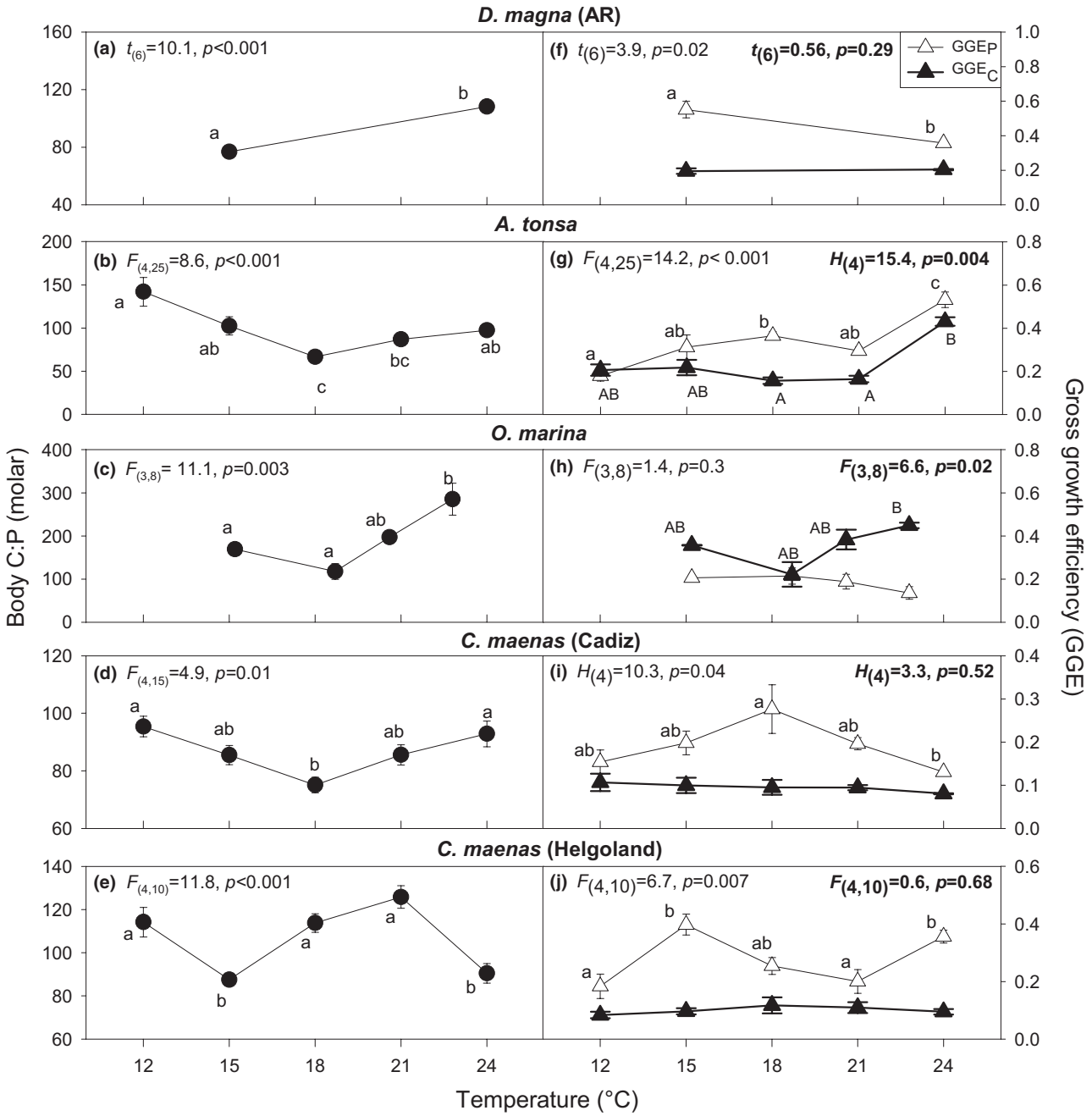

FIGURE 3 Thermal response of the body C:P ratios (a–e) and gross growth efficiency (GGE) of C and P (f–j) for all studied taxa. Dots are for body C:P, filled triangles are for GGE_C and empty triangles for GGE_P, symbols and bars are mean values and SE. In some cases, the error bars are not visible, because they are smaller than the symbols. Lower-case letters inside the graphs indicate homogeneous groups according to the *t*-test (a and f), post hoc Holm-Šídák multiple comparison test results, or Kruskal-Wallis ANOVA on ranks (i) for body C:P, and GGE_P and upper-case letters are for GGE_C

respiration was lower than the Q_{10} of ingestion or growth in the decreasing arm of the $TER_{C:P}$ (Table 1).

DISCUSSION

Considering all the studied taxa, we observed a common thermal response in their interactive temperature-nutrient requirements with a hump-shaped $TER_{C:P}$. These results were obtained applying two different methods, the growth-based and the bioenergetic $TER_{C:P}$. Somatic growth can be constrained by the reduction in metabolism due to low temperatures (Brown et al., 2004), and also as a consequence of P-limitation or excess when food contains too high or low C:P ratios (Plath & Boersma, 2001). When we analysed growth of *Daphnia* in the food C:P and temperature gradient, we found support for the knife-edge

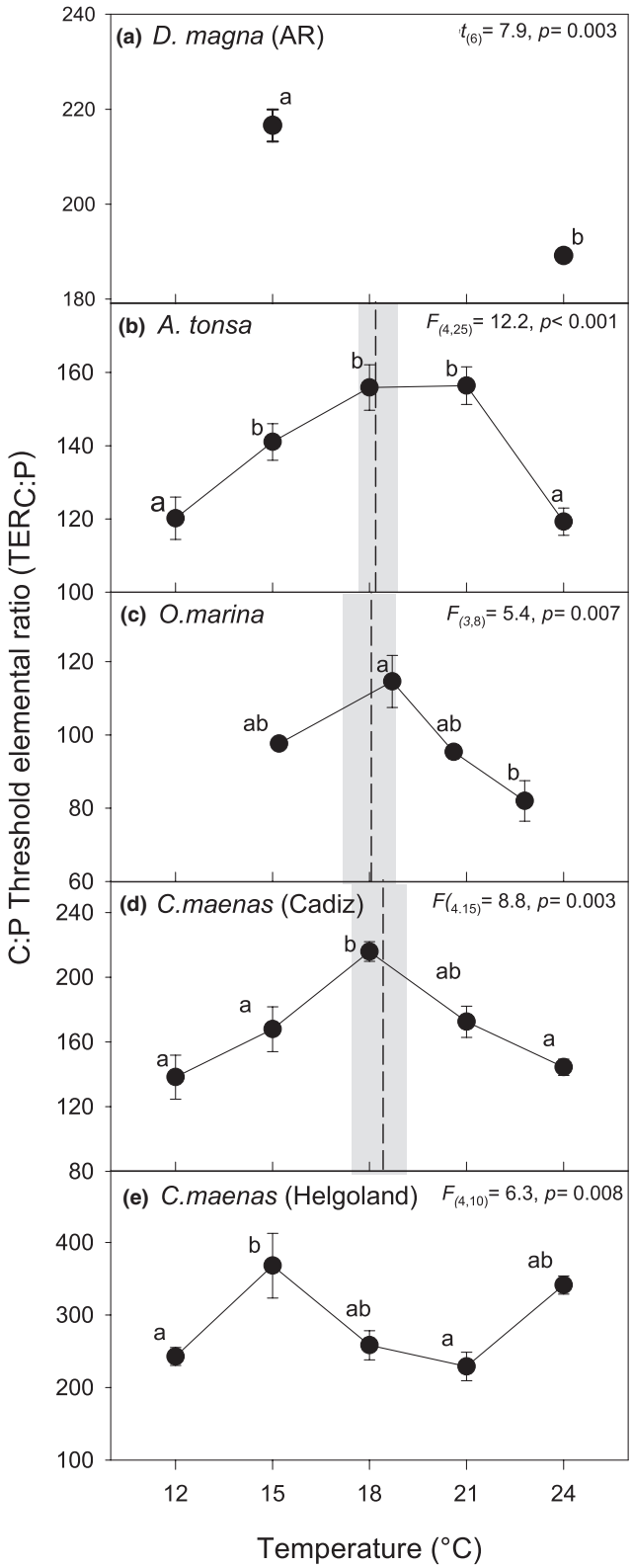

FIGURE 4 C:P Threshold Elemental Ratio ($TER_{C:P}$) as a function of temperature for (a) *Daphnia magna* (AR), (b) *Acartia tonsa*, (c) *Oxyrrhis marina*, (d) *Carcinus maenas* Cadiz and (e) *C. maenas* Helgoland. Symbols are mean values and bars SE. In some cases, the error bars are not visible, because they are smaller than the symbols. In (b–d), dashed vertical lines represent the mean $MaxTER_{C:P}$ temperature and the shaded areas the $CI_{95\%}$ obtained through non-linear regression fit of the thermal response of the $TER_{C:P}$ to a Gaussian function, with the R package nlstools (Baty et al., 2015). Dots and bars are mean values and SE. Lower-case letters inside the graphs indicate homogeneous groups according to –-tests (a), or the post hoc Holm- Šídák multiple comparison test results

hypothesis and the metabolic theory, as growth was depressed at extreme food C:P, and at low temperature (Figure 1a,b). The flattening of the growth curves with decreasing temperature implies that the effect of food quality on growth decrease with temperature (Persson et al., 2011), suggesting that the constrain imposed by low temperature is stronger than that by food quality. The lack of a $TER_{C:P}$ identification in the cold *D. magna* treatment implies poor energy availability for somatic and gonadic growth, which agrees with identified thermal optimal range for growth (from 16 to 22°C (Bruijning et al., 2018)). The bioenergetic $TER_{C:P}$ for *D. magna* tested at two different temperatures, showed the same thermal pattern as the growth-based TER at the same two temperatures, but different absolute values (Figure 1b and 4a, Appendix S5). Because we obtained the same pattern in the $TER_{C:P}$ of *D. magna* (AR) with the growth-based and bioenergetic model, we determined the bioenergetic $TER_{C:P}$ in a thermal gradient for the other species, as it provides information on the thermal reaction norms of the underlying variables driving the $TER_{C:P}$ (Details in Appendix S1).

The observed hump-shaped $TER_{C:P}$, indicates that P requirements are high at low temperatures, decrease when temperatures increase to intermediate values, and increase again when temperatures are higher. The low $TER_{C:P}$ at low temperatures provides support for the "Compensatory Hypothesis" (Persson et al., 2011) which states that P requirements should be high at low temperatures to compensate for the thermal constrain on enzymatic activity. Metabolic theory predicts that the shape of the $TER_{C:X}$ can be explained by the relation between the Q_{10} of respiration and ingestion (Anderson et al., 2017; Ruiz et al., 2020). When respiration has a lower Q_{10} than ingestion, the $TER_{C:X}$ is expected to decrease. In agreement with the metabolic theory, Ruiz et al. (2020) found the minimum $TER_{C:P}$ in their "U-shaped TER" at the temperature where respiration starts increasing faster than ingestion. On the other hand, metabolism has higher C:nutrient requirements than growth, so an increasing $TER_{C:P}$ with temperature is expected if respiration scales faster than growth. We suggest that the relation between Q_{10} of respiration, ingestion and growth can contribute to explain the hump-shaped $TER_{C:P}$. An increasing $TER_{C:P}$ is expected when Q_{10} of respiration is larger than Q_{10} of ingestion and/or growth; and a decreasing $TER_{C:P}$ should be expected when Q_{10} of respiration is smaller than the Q_{10} of ingestion and/or growth. In our study, this combination was observed as predicted in the increasing arm of the $TER_{C:P}$ of *O. marina*,

TABLE 1 Q_{10} of respiration rates (RR), ingestion rates (IR) and growth rates (GR), for all taxa in the analyses, for the increasing and decreasing arms of the $TER_{C:P}$

	Variable	Increasing $TER_{C:P}$	Decreasing $TER_{C:P}$	Increasing $TER_{C:P}$
	RR	3.12 (1.10)	0.34 (0.10)	
A. tonsa	IR	6.10 (2.00)^{ns}	0.51 (0.10)^{ns}	
	GR	2.78 (0.26)^{ns}	3.08 (0.42)***	
	RR	20.73 (2.00)	0.008 (0.006)	
O. marina	IR	4.48 (2.4)**	0.22 (0.09)*	
	GR	0.87 (0.10)***	1.51 (0.15)***	
	RR	3.63 (0.42)	2.16 (0.46)	
C. maenas (C)	IR	3.50 (0.96)^{ns}	1.99 (0.63)^{ns}	
	GR	2.47 (0.24)*	1.50 (0.16)^{ns}	
	RR	3.13 (0.98)	1.22 (0.13)	6.37 (2.25)
C. maenas (H)	IR	2.46 (0.63)^{ns}	2.26 (0.48)^{ns}	1.56 (0.67)^{ns}
	GR	4.35 (0.46)^{ns}	2.87 (0.52)*	0.67 (0.15)*

Note: Superscripts indicate the results of the *t*-test of RR versus IR, and RR versus GR. ns indicates no significant differences, *$p<0.05$, **$p<0.01$, ***$p<0.001$.

C. maenas (C) and on the second increase of *C. maenas* (H), while for *A. tonsa* and the first increase in *C. maenas* (H) the Q_{10} of respiration did not differ for ingestion and growth. In addition, as predicted, in the decreasing arm of the $TER_{C:P}$ of *A. tonsa*, *O. marina* and *C. maenas* (H), Q_{10} of respiration was lower than Q_{10} for ingestion and/or growth (Table 1, Appendix S4b, Table S3). The Q_{10} in *D. magna* was not included in this study as we are likely to have an optimum between the two temperatures that would lead to misleading results.

Ingestion, respiration, growth and GGEs are affected not only by temperature but also by food quality. This can lead to confounding effects of food quality on the thermal response of all underlying variables of the $TER_{C:P}$. Ingestion rates increase when facing imbalanced food to increase the acquisition of the limiting element (Hessen et al., 2013), respiration rates increase when food is C-rich as a pathway to dispose of excess C (Darchambeau et al., 2003), and GGEs of C and P tend to decrease when the element is non-limiting (Frost et al., 2004). In our study, food C:P was the same at all temperatures for each species but consumer nutrient requirements ($TER_{C:P}$) differed with temperature. Hence, the imbalance accounted for the difference in elemental composition of the food and that required by the consumer ($TER_{C:P}$) differed with temperature. This may affect the response of the variables driving the $TER_{C:P}$ to temperature.

Understanding the thermal dependencies of nutrient GGEs may open the path towards integrating metabolic theory and ecological stoichiometry. In an attempt to do so, Doi et al. (2010) compiled data from the literature, but were not able to find a universal relationship between GGE_P and temperature. They concluded that it is difficult to make robust inferences due to limited number of assessments of GGE_P. We find, GGE_P to be an important driver of the $TER_{C:P}$ in the thermal gradient for three (both *C. maenas* and *D. magna*) out of five organisms in the analyses and we found that, in general, GGE_P seems to be high at the $MaxTER_{C:P}$ temperature. We do not know whether there is a universal pattern for the thermal dependence of GGE. However, the nonlinear thermal responses of GGE_C and GGE_P result in a complex nonlinear thermal response of nutrient requirements. The humped-shaped and N-shaped thermal responses of the $TER_{C:P}$ were a result of the relation between the GGE of P and C, while the body C:P ratio generated changes in the absolute values of the $TER_{C:P}$ but not in the thermal shape or the response (Appendix S5).

We observed that body C:P stoichiometry changes significantly with temperature, as indicated in previous work (Balseiro et al., 2021; Kendrick & Benstead, 2013; Woods et al., 2003) but in contrast to Ruiz et al. (2020). Body C:P had a nonlinear U-shaped thermal response, with a minimum C:P located at the $MaxTER_{C:P}$ temperature. In addition, for *C. maenas* (H) we found a second body C:P minimum at the highest temperature of the range we studied. The response of body C:P to temperature showed the opposite pattern compared to the thermal response of the $TER_{C:P}$ (Figures 3 and 4). This pattern is expected to be stronger when C:P is more variable, as the calculation of the $TER_{C:P}$ involves the ratio of the growth of P and C. However, differential use efficiencies of C and P will lead to deviations from this inverse relation between $TER_{C:P}$ and body C:P, until GGE_P equals GGE_C then $TER_{C:P}$ equals body C:P.

Our hump-shaped $TER_{C:P}$–temperature relationship may appear to conflict with the study of Ruiz et al. (2020), which reported a U-shaped $TER_{C:P}$ response to temperature. In Ruiz et al. (2020), however, temperatures were mainly above the optimal ones of the studied organisms. Here, we aimed to study more ecologically relevant temperatures, so our experiments did not include high temperatures, except for *C. maenas* (H). Interestingly, when we extended the model of Ruiz

et al. (2020) to lower temperatures (below 18°C), we obtained an N-shaped TER response to temperature (See Appendix S4c). Indeed, the *C. maenas* (H) population (Figure 4d) seem to provide experimental support for the extension of the model by Ruiz et al. (2020) to lower temperatures. Based on the observed results, our working hypothesis is that the observed N-shaped $TER_{C:P}$ is likely a general pattern. We suggest that more studies exploring broad thermal ranges are needed to determine if encompassing the entire operating temperature range of a species, the hump-shaped $TER_{C:P}$ responses, that we observed here, can be combined with the U-shape found by Ruiz et al. (2020), resulting in a cubic thermal response of the $TER_{C:P}$ (See Figure 5 for our hypothesised N-shaped $TER_{C:P}$).

The $maxTER_{C:P}$ temperature might be related to the temperature of acclimation or the normal habitat temperature of the organisms in the study. The $MaxTER_{C:P}$ temperature was higher for *D. magna* (US) than for *D. magna* (AR), whose historical temperatures were 24–25 and 20°C, respectively. The same happened for both populations of *C. maenas*. The $MaxTER_{C:P}$ temperature was around 18°C for the population from Cadiz and around 15°C for the colder Helgoland population, while for *O. marina* and *A. tonsa*, the $MaxTER_{C:P}$ temperature was around 18°C, the temperatures in the laboratory cultures. So, we propose that the $MaxTER_{C:P}$ observed for all species at intermediate temperatures might reflect lower P requirements at temperatures that are close to the species' thermal environment in nature (Figure 5). This response would optimise P metabolism, given that this element is often limiting in aquatic environments.

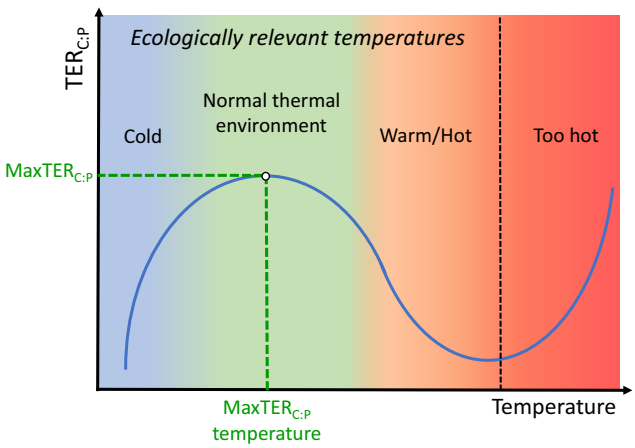

FIGURE 5 Hypothesised response of the $TER_{C:P}$ to a broad temperature range. Light blue, green and orange areas, until the vertical dashed line, represent temperatures within the ecological environment of the species (is the experimental temperature range for *A. tonsa*, O. marina and *C. maenas* (C)). The red area represents temperatures beyond the thermal optimum (Pörtner, 2012; Pörtner & Farrell, 2008) that might be experienced by the species only in rare conditions (we suggest that this was the case of *C. maenas* (H) in the highest temperature in our experiments). In this hypothesised concept, the increasing demands of C relative to P when temperatures increase from cold (light blue) to intermediate (middle green) are the result of increasing respiration rates and P use efficiency, until the $MaxTER_{C:P}$ is reached. When temperatures increase above the normal thermal environment of the organism (from green to orange area), the increasing demands of P relative to C are the result of the decrease in P use efficiency, the higher Q_{10} of growth and ingestion in relation to respiration, and might prevent an excessive increase in metabolism that can result from the combination of low P diets (Ruiz et al., 2018; Ruiz et al., 2020) and increased temperatures. The increase in C demands relative to P when temperature is excessive may reflect the physiological stress that amplifies C-demands for respiratory and catabolic processes (Schmitz, 2013) with higher Q_{10} of respiration than ingestion and growth

Human activities have altered, and will continue to alter, biogeochemical cycles and the nutritional value of the resources for consumers (Peñuelas et al., 2013; Sardans et al., 2012). Nutrient supplies directly influence the stoichiometry of autotrophs, either by changing the autotroph C:X, or by changing autotroph community composition. These shifts affect primary consumers, either by changing the C:X of weakly homeostatic herbivores, or by changing herbivore community composition. Such shifts have already been observed by a number of studies (Laspoumaderes et al., 2013; Sardans et al., 2012; Teurlincx et al., 2017). Furthermore, nutrient recycling is related to organism nutrient requirements. Animals with high P-requirements recycle low amounts of P (C:P of excretion is high), and vice versa. Here we identified that the sensitivity of consumers to nutrient imbalance varies with temperature, and that for organisms living at temperatures above their $MaxTER_{C:P}$, warming would increase their sensitivity to nutrient limitation (or C excess). These thermal changes in organism nutrient requirements should lead to changes in nutrient recycling in food webs exacerbating the impact of warming, creating simultaneous shifts in resource quality driven by alterations of biogeochemical cycles, that may create or strengthen nutritional mismatches between resources and consumers in food webs.

Although the temperature range we used in our experiments is much wider than expected by global warming (IPCC, 2014), in some extreme climatic conditions (i.e., heat waves), some freshwater ecosystems may suffer from these high temperatures. Hence, even the response to high or very low temperatures may be important to understand how extreme climatic events may affect consumer requirements. Indeed, we show that, depending on where the thermal environment sits relative to the $MaxTER_{C:P}$ temperature and the direction of change in nutrient availability, even relatively small predicted temperature increases can have strong effects on consumer performance. However, the effects of these temperature changes might be counteracted if changes in nutrient availability move in the same direction as the thermal response of nutrient requirements, i.e., further eutrophication of waters would increase P-availability. At the same time, warming would increase organism P-requirements. Based on our results, we predict that the ongoing nutrient reductions in many water bodies globally may ironically

exacerbate the impacts of warming temperatures. We propose that an accurate mechanistic understanding of the complex relationship between temperature and stoichiometric requirements of consumers is essential if we are to predict how ectotherms will respond to ongoing changes in nutrient supplies and environmental temperature.

AUTHORSHIP

C.L. conceived the idea. C.L., J.J.E., E.B., B.M., M.B. and C.L.M. conceived the study design. C.L., A.M., J.B., N.T. and G.T. performed the experiments. G.T. provided field samples. C.L., A.M. and J.B. performed all analyses. C.L., M.B. and C.L.M. wrote the manuscript with input from all other authors. All authors read and agreed on the last version of the manuscript.

ACKNOWLEDGEMENTS

C.L. acknowledges support from the Alexander von Humboldt Foundation and the Fulbright Foundation. C.L., A.M., E.B. and B.M. are CONICET Researchers. We acknowledge support from Fondo Para la Investigación Científica y Tecnológica (Argentina FONCyT PICT 2019-0950, PICT 2017-1940). C.L.M. was supported by the Bundesministerium für Bildung und Forschung (BMBF grant no. 01LN1702A). M.B. was supported by the Dynatrait programme of the German Science Foundation. J.J.E. was supported by an NSF Rules of Life grant (DEB-1930816). We thank Dr Thomas Ruiz for providing the R scripts for parameter bootstrapping. We are thankful to Siri Rohwer and Zoran Šargač for their help with the larval cultures of C. maenas while funded by the Deutsche Forschungsgemeinschaft (Research Training Group 2010: RESPONSE). We acknowledge Dr Enrique González-Ortegón (Instituto de Ciencias Marinas de Andalucía, Spain) for providing the C. maenas berried females from Cadiz. Open Access funding enabled and organized by Projekt DEAL.

COMPLIANCE WITH ETHICAL STANDARDS

The research presented in this paper complies with the national (German) laws, and the guidelines from the directives 2010/63/EU of the European Parliament and of the Council of 22nd September 2010 on the protection of animals used for scientific purposes.

FUNDING INFORMATION

Alexander von Humboldt-Stiftung; Dynatrait programme of the German Science Foundation; Fulbright Association; NSF Rules of Life grant, Grant/Award Number: DEB-1930816; Deutsche Forschungsgemeinschaft; Bundesministerium für Bildung und Forschung, Grant/Award Number: 01LN1702A; Fondo Para la Investigación Científica y Tecnológica, Grant/Award Number: PICT 2017-1940PICT 2019-00950; Alexander von Humboldt Foundation

PEER REVIEW

The peer review history for this article is available at https://publons.com/publon/10.1111/ele.14093.

DATA AVAILABILITY STATEMENT

Data supporting the results of this study is openly available in the public repository Zenodo at https://doi.org/10.5281/zenodo.6944193.

ORCID

Cecilia Laspoumaderes https://orcid.org/0000-0001-7790-2975
Cedric L. Meunier https://orcid.org/0000-0002-4070-4286
Amaru Magnin https://orcid.org/0000-0002-6957-4710
Johanna Berlinghof https://orcid.org/0000-0002-1622-1938
James J. Elser https://orcid.org/0000-0002-1460-2155
Esteban Balseiro https://orcid.org/0000-0002-5052-0587
Gabriela Torres https://orcid.org/0000-0002-4064-0585
Beatriz Modenutti https://orcid.org/0000-0002-8683-5679
Nelly Tremblay https://orcid.org/0000-0002-8221-4680
Maarten Boersma https://orcid.org/0000-0003-1010-026X

REFERENCES

Acharya, K., Kyle, M. & Elser, J.J. (2004) Biological stoichiometry of *Daphnia* growth: an ecophysiological test of the growth rate hypothesis. *Limnology and Oceanography*, 49, 656–665.

Anderson, T.R., Hessen, D.O., Boersma, M., Urabe, J. & Mayor, D.J. (2017) Will invertebrates require increasingly carbon-rich food in a warming world? *The American Naturalist*, 190, 725–742.

Balseiro, E., Laspoumaderes, C., Smufer, F., Wolinski, L. & Modenutti, B. (2021) Short term fluctuating temperature alleviates *Daphnia* stoichiometric constraints. *Scientific Reports*, 11, 1–10.

Baty, F., Ritz, C., Charles, S., Brutsche, M., Flandrois, J.-P. & Delignette-Muller, M.-L. (2015) A toolbox for nonlinear regression in R: the package nlstools. *Journal of Statistical Software*, 66, 1–21.

Boersma, M., Mathew, K.A., Niehoff, B., Schoo, K.L., Franco-Santos, R.M. & Meunier, C.L. (2016) Temperature driven changes in the diet preference of omnivorous copepods: no more meat when it's hot? *Ecology Letters*, 19, 45–53.

Brown, J.H., Gillooly, J.F., Allen, A.P., Savage, V.M. & West, G.B. (2004) Toward a metabolic theory of ecology. *Ecology*, 85, 1771–1789.

Bruijning, M., ten Berge, A.C. & Jongejans, E. (2018) Population-level responses to temperature, density and clonal differences in *Daphnia magna* as revealed by integral projection modelling. *Functional Ecology*, 32, 2407–2422.

Clissold, F.J. & Simpson, S.J. (2015) Temperature, food quality and life history traits of herbivorous insects. *Current Opinion in Insect Science*, 11, 63–70.

Cross, W.F., Hood, J.M., Benstead, J.P., Huryn, A.D. & Nelson, D. (2015) Interactions between temperature and nutrients across levels of ecological organization. *Global Change Biology*, 21, 1025–1040.

Darchambeau, F., Faeovig, P.J. & Hessen, D.O. (2003) How *Daphnia* copes with excess carbon in its food. *Oecologia*, 136, 336–346.

DeMott, W.R. (1986) The role of taste in food selection by freshwater zooplankton. *Oecologia*, 69, 334–340.

Doi, H., Cherif, M., Iwabuchi, T., Katano, I., Stegen, J.C. & Striebel, M. (2010) Integrating elements and energy through the metabolic dependencies of gross growth efficiency and the threshold elemental ratio. *Oikos*, 119, 752–765.

Efron, B. & Tibshirani, R. (1986) Bootstrap methods for standard errors, confidence intervals, and other measures of statistical accuracy. *Statistical Science*, 1, 54–77.

Frost, P.C., Benstead, J.P., Cross, W.F., Hillebrand, H., Larson, J.H., Xenopoulos, M.A. et al. (2006) Threshold elemental ratios of carbon and phosphorus in aquatic consumers. *Ecology Letters*, 9, 774–779.

Frost, P.C., Xenopoulos, M.A. & Larson, J.H. (2004) The stoichiometry of dissolved organic carbon, nitrogen, and phosphorus release by a planktonic grazer. *Daphnia. Limnol. Oceanogr.*, 49, 1802–1808.

Gillooly, J.F., Brown, J.H., West, G.B., Savage, V.M. & Charnov, E.L. (2001) Effects of size and temperature on metabolic rate. *Science*, 293, 2248–2251.

Grasshoff, K., Kremling, K. & Ehrhardt, M. (2009) *Methods of seawater analysis*. Weinheim, Germany: John Wiley & Sons.

Hagerty, S.B., van Groenigen, K.J., Allison, S.D., Hungate, B.A., Schwartz, E., Koch, G.W. et al. (2014) Accelerated microbial turnover but constant growth efficiency with warming in soil. *Nature Climate Change*, 4, 903–906.

Halvorson, H.M., Scott, J.T., Sanders, A.J. & Evans-White, M.A. (2015) A stream insect detritivore violates common assumptions of threshold elemental ratio bioenergetics models. *Freshwater Science*, 34, 508–518.

Hayes, M.B., Jiao, L., Tsao, T.H., King, I., Jennings, M. & Hou, C. (2015) High temperature slows down growth in tobacco hornworms (*Manduca sexta* larvae) under food restriction. *Insect Sci.*, 22, 424–430.

Hessen, D.O., Elser, J.J., Sterner, R.W. & Urabe, J. (2013) Ecological stoichiometry: an elementary approach using basic principles. *Limnology and Oceanography*, 58, 2219–2236.

IPCC (2014). Climate Change 2014: Synthesis Report. Contribution of Working Groups I, II and III to the Fifth Assessment Report of the Intergovernmental Panel on Climate Change. Geneva, Switzerland, 151 pp. (eds Pachauri, RK & Meyer, L) Geneva, Switzerland, p. 138.

Kendrick, M.R. & Benstead, J.P.J.F.B. (2013) Temperature and nutrient availability interact to mediate growth and body stoichiometry in a detritivorous stream insect. *Freshwater Biology*, 58, 1820–1830.

Kilham, S.S., Kreeger, D.A., Lynn, S.G., Goulden, C.E. & Herrera, L. (1998) COMBO - A defined freshwater culture medium for algae and zooplankton. *Hydrobiologia*, 377, 147–159.

Laspoumaderes, C., Modenutti, B., Souza, M.S., Navarro, M.B., Cuassolo, F. & Balseiro, E. (2013) Glacier melting and stoichiometric implications for lake community structure: zooplankton species distributions across a natural light gradient. *Global Change Biology*, 19, 316–326.

Laspoumaderes, C., Souza, M.S., Modenutti, B. & Balseiro, E. (2017) Glacier melting and response of *Daphnia* oxidative stress. *Journal of Plankton Research*, 39, 675–686.

Malzahn, A., Hantzsche, F., Schoo, K., Boersma, M. & Aberle, N. (2010) Differential effects of nutrient-limited primary production on primary, secondary or tertiary consumers. *Oecologia*, 162, 35–48.

Malzahn, A.M., Doerfler, D. & Boersma, M. (2016) Junk food gets healthier when it's warm. *Limnology and Oceanography*, 61, 1677–1685.

Peñuelas, J., Poulter, B., Sardans, J., Ciais, P., Van Der Velde, M., Bopp, L. et al. (2013) Human-induced nitrogen–phosphorus imbalances alter natural and managed ecosystems across the globe. *Nature Communications*, 4, 1–10.

Persson, J., Wojewodzic, M.W., Hessen, D.O. & Andersen, T. (2011) Increased risk of phosphorus limitation at higher temperatures for *Daphnia magna*. *Oecologia*, 165, 123–129.

Plath, K. & Boersma, M. (2001) Mineral limitation of zooplankton: stoichiometric constraints and optimal foraging. *Ecology*, 82, 1260–1269.

Pörtner, H.-O. (2012) Integrating climate-related stressor effects on marine organisms: unifying principles linking molecule to ecosystem-level changes. *Marine Ecology Progress Series*, 470, 273–290.

Pörtner, H.O. & Farrell, A.P. (2008) Physiology and climate change. *Science*, 322, 690–692.

R-Core-Team (2021). *R: A language and environment for statistical computing*. Vienna, Austria: R Foundation for Statistical Computing.

Rothhaupt, K.O. (1995) Algal nutrient limitation affects rotifer growth rate but not ingestion rate. *Limnology and Oceanography*, 40, 1201–1208.

Ruiz, T., Bec, A., Danger, M., Koussoroplis, A.M., Aguer, J.P., Morel, J.P. et al. (2018) A microcalorimetric approach for investigating stoichiometric constraints on the standard metabolic rate of a small invertebrate. *Ecology Letters*, 21, 1714–1722.

Ruiz, T., Koussoroplis, A.M., Danger, M., Aguer, J.P., Morel-Desrosiers, N. & Bec, A. (2020) U-shaped response Unifies views on temperature dependency of stoichiometric requirements. *Ecology Letters*, 23, 860–869.

Sardans, J., Rivas-Ubach, A. & Peñuelas, J. (2012) The C: N: P stoichiometry of organisms and ecosystems in a changing world: a review and perspectives. *Perspectives in Plant Ecology, Evolution and Systematics*, 14, 33–47.

Schmitz, O.J. (2013) Global climate change and the evolutionary ecology of ecosystem functioning. *Annals of the New York Academy of Sciences*, 1297, 61–72.

Shah, A.A., Woods, H.A., Havird, J.C., Encalada, A.C., Flecker, A.S., Funk, W.C. et al. (2021) Temperature dependence of metabolic rate in tropical and temperate aquatic insects: support for the Climate Variability Hypothesis in mayflies but not stoneflies. *Global Change Biology*, 27, 297–311.

Simpson, S.J. & Raubenheimer, D. (2012) *The nature of nutrition: a unifying framework from animal adaptation to human obesity*. Princeton, NJ: Princeton University press.

Smith, T.P., Clegg, T., Bell, T. & Pawar, S. (2021) Systematic variation in the temperature dependence of bacterial carbon use efficiency. *Ecology Letters*, 24, 2123–2133.

Sterner, R.W. (1997) Modelling interactions of food quality and quantity in homeostatic consumers. *Freshwater Biology*, 38, 473–481.

Sterner, R.W. & Elser, J.J. (2002) *Ecological stoichiometry*. The biology of elements from molecules to the biosphere: Princeton University Press, Princeton, NJ USA.

Teurlincx, S., Velthuis, M., Seroka, D., Govaert, L., van Donk, E., Van de Waal, D.B. et al. (2017) Species sorting and stoichiometric plasticity control community C: P ratio of first-order aquatic consumers. *Ecology Letters*, 20, 751–760.

Torres, G., Thomas, D.N., Whiteley, N.M., Wilcockson, D. & Giménez, L. (2020) Maternal and cohort effects modulate offspring responses to multiple stressors. *Proceedings of the Royal Society B*, 287, 20200492.

Urabe, J. & Watanabe, Y. (1992) Possibility of N or P limitation for planktonic cladocerans: an experimental test. *Limnology and Oceanography*, 37, 244–251.

Wiedner, C. & Vareschi, E. (1995) Evaluation of a fluorescent microparticle technique for measuring filtering rates of *Daphnia*. *Hydrobiologia*, 302, 89–96.

Wojewodzic, M.W., Kyle, M., Elser, J.J., Hessen, D.O. & Andersen, T. (2011) Joint effect of phosphorus limitation and temperature on alkaline phosphatase activity and somatic growth in *Daphnia magna*. *Oecologia*, 165, 837–846.

Woods, H., Makino, W., Cotner, J.B., Hobbie, S.E., Harrison, J., Acharya, K. et al. (2003) Temperature and the chemical composition of poikilothermic organisms. *Functional Ecology*, 17, 237–245.

Ye, J.S., Bradford, M.A., Dacal, M., Maestre, F.T. & Garcia-Palacios, P. (2019) Increasing microbial carbon use efficiency with warming predicts soil heterotrophic respiration globally. *Global Change Biology*, 25, 3354–3364.

Zheng, Q., Hu, Y., Zhang, S., Noll, L., Bockle, T., Richter, A. et al. (2019) Growth explains microbial carbon use efficiency across soils differing in land use and geology. *Soil Biology and Biochemistry*, 128, 45–55.

SUPPORTING INFORMATION

Additional supporting information can be found online in the Supporting Information section at the end of this article.

How to cite this article: Laspoumaderes, C., Meunier, C.L., Magnin, A., Berlinghof, J., Elser, J.J. & Balseiro, E. et al. (2022) A common temperature dependence of nutritional demands in ectotherms. *Ecology Letters*, 25, 2189–2202. Available from: https://doi.org/10.1111/ele.14093

ARTICLES FOR FACULTY MEMBERS

GLOBAL WARMING EFFECTS ON ECTOTHERM SPECIES

Title/Author	**Adding climate change to the mix: Responses of aquatic ectotherms to the combined effects of eutrophication and warming / Rodgers, E. M.**
Source	***Biology Letters*** **Volume 17 Issue 10 (2021) Pages 1-6** **https://doi.org/10.1098/rsbl.2021.0442** **(Database: Royal Society Publishing)**

BIOLOGY LETTERS

royalsocietypublishing.org/journal/rsbl

Opinion piece

Cite this article: Rodgers EM. 2021 Adding climate change to the mix: responses of aquatic ectotherms to the combined effects of eutrophication and warming. *Biol. Lett.* **17**: 20210442.
https://doi.org/10.1098/rsbl.2021.0442

Received: 19 August 2021
Accepted: 4 October 2021

Subject Areas:
ecology

Keywords:
nutrients, climate warming, global change, eutrophication, algal blooms, fish

Author for correspondence:
Essie M. Rodgers
e-mail: essie.rodgers@canterbury.ac.nz

THE ROYAL SOCIETY PUBLISHING

Global change biology

Adding climate change to the mix: responses of aquatic ectotherms to the combined effects of eutrophication and warming

Essie M. Rodgers

School of Biological Sciences, University of Canterbury, Private Bag 4800, Christchurch 8140, New Zealand

EMR, 0000-0003-3514-3653

The threat of excessive nutrient enrichment, or eutrophication, is intensifying across the globe as climate change progresses, presenting a major management challenge. Alterations in precipitation patterns and increases in temperature are increasing nutrient loadings in aquatic habitats and creating conditions that promote the proliferation of cyanobacterial blooms. The exacerbating effects of climate warming on eutrophication are well established, but we lack an in-depth understanding of how aquatic ectotherms respond to eutrophication and warming in tandem. Here, I provide a brief overview and critique of studies exploring the cumulative impacts of eutrophication and warming on aquatic ectotherms, and provide forward direction using mechanistically focused, multi-threat experiments to disentangle complex interactions. Evidence to date suggests that rapid warming will exacerbate the negative effects of eutrophication on aquatic ectotherms, but gradual warming will induce physiological remodelling that provides protection against nutrients and hypoxia. Moving forward, research will benefit from a greater focus on unveiling *cause and effect* mechanisms behind interactions and designing treatments that better mimic threat dynamics in nature. This approach will enable robust predictions of species responses to ongoing eutrophication and climate warming and enable the integration of climate warming into eutrophication management policies.

1. Introduction

Anthropogenic eutrophication (hereafter, eutrophication) is the world's most widespread form of habitat degradation affecting aquatic ecosystems [1,2]. Excessive nutrient inputs trigger eutrophication events where rapid, uncontrolled growth of aquatic plants is spurred and harmful algal blooms spread [3,4]. Phosphorus (P) and nitrogen (N) are the key nutrients of concern because their availability drives aquatic plant primary production. In freshwater habitats, plant growth is limited by P availability, whereas N is generally the limiting nutrient in marine habitats [5,6]. Aquatic habitats transform during eutrophication; floating plants and cyanobacteria become over-abundant and dominant over other plant life, creating low light conditions for underwater life and nightly hypoxic (low oxygen) episodes [7]. Water quality also declines, with increased turbidity levels and high concentrations of dissolved nutrients, many of which can disrupt homeostasis in aquatic ectotherms by passively diffusing across the gills and epithelium [3,8,9]. Following eventual bloom die-off, bacterial decomposition consumes large amounts of oxygen and produces carbon dioxide causing hypoxia and acidification, respectively [10]. The

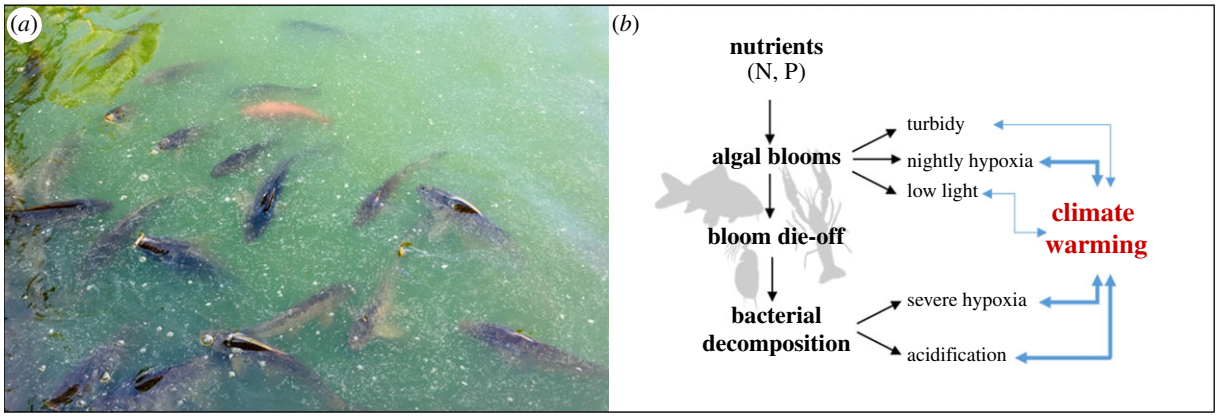

Figure 1. (*a*) Fish inhabiting a eutrophic lake in Seville, Spain (photo credit: Daniel Gomez Isaza). (*b*) Diagram showing the sequence (black arrows) of threats that aquatic ectotherms face during eutrophication, with the added threat of climate warming. Some threats are experienced sequentially, while others are experienced simultaneously. Excessive nutrient enrichment (nitrogen [N] in marine habitats, phosphorus [P] in freshwater habitats) leads to accelerated algal and cyanobacteria bloom growth, causing increased turbidity, nightly hypoxia and low light levels. When blooms die, bacterial decomposition of the plant matter consumes oxygen and produces carbon dioxide, causing hypoxia and acidification, respectively. Blue arrows represent the interactions between climate warming and eutrophication threats and arrow thickness reflects the extent of literature on these interactions (thicker arrows reflect more literature than thinner arrows). Multi-way threat interactions are not shown, but much less literature exists for these compared to two-way interactions.

degraded habitat conditions driven by eutrophication have been linked to mass mortalities of aquatic life the world over [4,11–13], and this loss of life is becoming more common as habitats warm [14].

The environmental consequences and economic burden of eutrophication are predicted to surge under forecasted climate change [15,16]. In 2009, the annual economic cost of eutrophication (e.g. lost tourism revenue and commercial fisheries) was estimated to be £114 million in England and Wales [17], and USD$2.2 billion in the United States (US) [18], but these estimates have not factored in the catalysing effects of climate change [15]. Heatwaves are increasing in intensity, frequency and duration around the world [14]. For example, the 2018 European heatwave lasted several weeks and had devastating impacts on aquatic life [19]; over 5 t of dead fish were found in the Rhine, Elbe and other rivers in Germany when water temperature increased 4°C above summertime normal. The heatwave was linked to the formation of one of the largest algal blooms in the Baltic Sea and a 'dead zone', with insufficient oxygen to support life, spanning 70 km^2. Here, I provide an overview of how aquatic ectotherms are affected by eutrophication and climate warming in tandem and highlight knowledge gaps to direct further research.

2. Climate change catalyses eutrophication

Climate change catalyses eutrophication by creating conditions that increase nutrient loadings in aquatic habitats and support rapid algal growth [15,16,20]. Elevated temperatures can indirectly increase the release of nutrients from lake sediment and catchment soils, promoting more rapid algal growth [21]. Additionally, cyanobacteria typically grow more efficiently at high temperatures compared to other phytoplankton species, suggesting it will have a competitive advantage under future warming [22,23]. Heat-accelerated growth of cyanobacteria suggests that blooms will form faster, earlier in the year and reach larger sizes with climate warming. More expansive algal blooms may cause more severe hypoxic episodes, which occur nightly when plants cannot photosynthesize and during the eventual die-off and microbial decomposition of blooms [12].

Altered precipitation patterns can also exacerbate eutrophication [24]. Increases in storm frequency and severity are projected to result in greater groundwater and surface nutrient discharge into freshwater and coastal habitats. In the United States, for example, total N loadings in riverine habitats are predicted to increase by approximately 19% by 2100 due to changes in precipitation patterns, and similar increases are expected to occur in India, China and Southeast Asia [24]. More frequent drought periods can also increase nutrient loadings by reducing habitat water levels and increasing the dissolved concentrations of nutrients [21]. Recent evidence suggests that eutrophication, in itself, may be contributing to climate change by lowering the carbon sequestration rates of seagrass beds [25], and releasing nitrous oxide and methane into the atmosphere [26,27]. Evidence supporting the strengthening of eutrophication under climate warming and the positive feedback loops between these threats is strong, but how aquatic organisms will respond to both threats in concert remains less clear.

3. Eutrophication: a cocktail of interacting threats

Although eutrophication is often referred to as a single threat (or 'stressor'), the process of eutrophication exposes organisms to complex combinations of challenges, including elevated nutrient concentrations, harmful algal blooms, increased turbidity, low light levels, hypoxic conditions, pH reductions and altered plant and animal communities (figure 1). Many of these threats are experienced sequentially (e.g. nutrient exposure and subsequent hypoxia), but most multi-threat studies have exposed organisms to threats simultaneously. To understand how organisms cope with eutrophication, threat interactions must be characterized in an ecologically relevant manner, alongside assessments of how climate warming may compound or alleviate these interactions. Investigations into the interactions among eutrophication threats and climate warming are still in their infancy, but

simultaneous exposure to these threats may have dire consequences for aquatic ectotherms.

Nutrient loadings are a persistent background threat in eutrophic habitats, because animals must contend with regular influxes (e.g. nitrate, nitrite, ammonia and phosphorus) from wastewater discharges, aquaculture operations and run-off from urban, agricultural and mining sources [3]. Nitrate is the most stable and abundant form of nitrogen in aquatic habitats [3], and most eutrophication studies have, therefore, focused on nitrate effects. Chronic nitrate exposure can exert a range of lethal and sub-lethal effects on aquatically respiring species. A recent meta-analysis, based on data from 68 studies on freshwater fish, amphipods and amphibians, showed that long-term exposure to nitrate pollution reduced activity levels by 79%, growth by 29% and survival by 68% [28]. Moreover, the effects of nitrate pollution were shown to be worsened by the presence of additional threats, such as hypoxia and low pH, which are common threats in eutrophic habitats [10,28].

Recent evidence is mounting to show that chronic nitrate exposure can make fish more susceptible to hypoxia. For example, silver perch (*Bidyanus bidyanus*) exposed to nitrate pollution (50 or 100 NO_3^- mg l^{-1}) for three weeks suffered reduced hypoxia tolerance [29]. Similar findings have also been reported in a freshwater salmonid (*Thymallus thymallus*), where hypoxia tolerance decreased by 15% in fish exposed to nitrate (50 or 200 NO_3^- mg l^{-1}) for eight weeks, compared to controls (0 NO_3^- mg l^{-1}) [30]. Heightened hypoxia susceptibility in nitrate-exposed fish is linked to the toxic action of nitrate (and nitrite). Once nitrite enters the body of fish via the gills, it directly lowers blood oxygen-carrying capacity by oxidizing haemoglobin to a non-oxygen binding form, called methaemoglobin [9]. This reduction in blood oxygen-carrying capacity can scale up to reduce aerobic scope (maximum resting metabolic rate) [31–33], which is a measure of the oxygen available to support aerobic activities like locomotion and digestion. Compared to freshwater fishes, marine and estuarine fishes are more tolerant of nitrate/nitrite because chloride in sea/brackish water competitively inhibits nitrate/nitrite uptake across the gills [9].

4. Heatwave and warming impacts

Mass mortalities of aquatic ectotherms, or fish kills, during summer heatwaves are becoming a new norm, and are often associated with eutrophic conditions [14,34–36]. Understanding how eutrophication interacts with elevated temperatures is, therefore, key to preventing further loss of aquatic life. Elevated temperatures have profound, direct impacts on the physiology and fitness of aquatic ectotherms due to the tight relationship between environmental temperature and body temperature. Rapid increases in environmental temperature can raise the 'cost of living' in ectotherms by increasing resting metabolic rates in an exponential manner [37]. If resting metabolic rates increase without a matched increase in maximum metabolic rates, ectotherms suffer from reduced aerobic scope, and a reduced capacity to perform aerobically supported activities [38]. Gradual increases in mean habitat temperatures allow time for thermal acclimatization responses in ectotherms, where underlying physiology is remodelled so that performance is maintained at elevated temperatures [39]. By contrast, heatwaves involve rapid spikes in environmental temperature, often leaving ectotherms insufficient time for acclimatization. Interactions between eutrophication processes and gradual increases in habitat temperatures may, therefore, be distinct to interactions with heatwaves.

Nutrient exposure can reduce aerobic scope in fish [33,40], but this effect reveals an ecological surprise when fish are acclimated to elevated temperatures. For example, five to eight weeks of acclimation to elevated temperatures offset the negative effects of nitrate on aerobic scope in silver perch [40], and caused synergistic increases in aerobic scope in both European grayling and common carp (*Cyprinus carpio*) [41,42]. These protective benefits were attributed to thermal acclimation responses, involving changes to oxygen supply and delivery systems. Thermal acclimation also confers increased tolerance to hypoxia in many fish and aquatic invertebrates [43]. Both Arctic charr (*Salvelinus alpinus*) and landlocked salmon (*Salmo salar m. sebago*) showed improved hypoxia tolerance (22–200% improvement) when fish were acclimated to high temperatures and nightly hypoxia together, and this improvement was related to remodelling of cardiac tissue [44]. By contrast, acute increases in temperature typically decrease hypoxia tolerance in aquatic ectotherms, because there is insufficient time for thermal acclimation to take place [43]. Taken together, these findings suggest that gradual habitat warming, where thermal acclimatization can occur, will enhance species resilience to nutrients and hypoxia, but rapid temperature spikes will exacerbate these threats.

For gilled-organisms like fish, tadpoles and crustaceans, heatwaves pose the added threat of increasing the uptake and accumulation of unwanted substances via increased respiration rates [45]. Dissolved nutrients, suspended sediments and contaminants can enter their gills at an increased rate as temperatures rise, but disentangling these interactions can be challenging because chemical availability and organismal detoxification mechanisms are also temperature-dependent [45]. Moreover, fish exposed to nutrients (nitrite or nitrate) generally suffer reduced heat tolerance compared to unexposed fish [30,46]. Specifically, the upper thermal limit of common carp was reduced by 1.2°C following 7 days of nitrite exposure (1 mM) [46], and dropped by 1°C in European grayling following eight weeks of exposure to nitrate (50 or 100 NO_3^- mg l^{-1}) [30]. Nitrate and phosphate exposure can also compromise the resilience of corals to warming [47], and lower coral bleaching thresholds [48]. Limiting nutrient loads in habitats may, therefore, have the added benefit of increasing species resilience to heatwaves.

At the population level, dire effects have been observed in fish when warming and nutrients are combined under experimental conditions. For example, the interactive effects of climate warming (+4°C) and nutrient loadings (250–2500 µg l^{-1} N; 50 µg l^{-1} P) were examined in three-spined stickleback (*Gasterosteus aculeatus*) populations, using a full-factorial design with 24 freshwater mesocosms across 16 months [49]. Stickleback populations became extinct in treatments where warming and nutrient loadings were coupled and fish losses were attributed to frequent, severe hypoxic episodes. At an ecosystem level, eutrophication in lakes can lower ecological specialization and promote genetic and phenotypic homogenization [50], but it remains unknown if these effects hold with climate warming. Models based on field data suggest that nutrient pollution and high temperatures in

combination will drive population declines in macroinvertebrates and fish at regional scales [51]. Scaling up interactions between eutrophication and warming from species- to population-level effects should be a priority for future investigations.

5. New directions and conclusion

Conserving and managing aquatic ectotherms is becoming increasingly challenging as climate change interacts with threatening processes. Investigations have primarily focused on understanding how climate warming interacts with the process of eutrophication (e.g. algal bloom formation and sediment loads), rather than understanding how aquatic ectotherms are affected by the combination of these threats. Current understanding suggests that chronic exposure to particular nutrients can increase fish susceptibility to acute temperature spikes and hypoxia [29,30,46], but research is needed on a greater diversity of species to test the wider applicability of this interaction. Nonetheless, these data suggest that nutrient pollution is not only causing a range of sub-lethal effects on aquatic ectotherms [28], but is also increasing their vulnerability to climate change.

Available evidence also suggests that gradual warming and heatwaves have divergent interactions with nutrient pollution. Thermal acclimation responses, associated with gradual warming, induce physiological changes in aquatic ectotherms (e.g. gill, ventricle and haematological remodelling) that offer protection against nutrients and hypoxia [40–42]. By contrast, acute increases in temperature increase the susceptibility of many aquatic ectotherms to hypoxia [43]. Therefore, gradual climate warming may aid aquatic ectotherms in coping with eutrophication, but heatwaves pose a threat.

Well-designed, mechanistically focused studies offer a fruitful approach to elucidating *cause and effect* behind interacting threats in a changing world. Only full-factorial experimental designs, which examine both the isolated and combined effects of threats, can effectively disentangle interactions. Mimicking threats in ways that enhance ecological realism is vital. Most studies have only assessed two-way threat interactions, and very little is known about how three or more threats interact, despite eutrophication involving a mixture of threats. Moreover, multi-threat studies generally expose organisms to threats simultaneously, but this approach does not always reflect natural processes, with some threats experienced sequentially in nature (figure 1*b*). Manipulating the order that organisms are exposed to threats can reveal insightful cross-tolerance or cross-susceptibility interactions, which may inform management practices [52]. Management practices often operate to remove threats; for example, restricting nutrient loads in habitats. Therefore, we also need to understand how species respond to the removal of a threat and track the recovery of populations.

Better mimicking climate change scenarios in experiments will also enhance ecological relevance. Ectotherms are projected to be more vulnerable to increases in temperature variability than increases in mean temperatures [53]. Despite this, we lack an understanding of how increased thermal variability interacts with eutrophication because studies have only used stable, constant temperatures. Mesocosm experiments [54] and ecological/mechanistic niche modelling [55] will be paramount to testing if mechanisms identified in tightly controlled experiments scale up to impact population and community level dynamics under increasingly natural conditions. Current research suggests there is a looming threat of combined climate warming and eutrophication for aquatic ectotherms, but the impacts of gradual warming and heatwaves will likely be distinct. Further mechanistic research on taxonomically diverse species is required to deepen our understanding of these interactions and to develop management solutions.

Data accessibility. This article does not contain any additional data.

Competing interests. I declare, I have no competing interests.

Funding. E.M.R. was supported by a Brian Mason Trust grant (no. E7300) and a Fisheries Society of the British Isles grant (no. E7318).

References

1. Malone TC, Newton A. 2020 The globalization of cultural eutrophication in the coastal ocean: causes and consequences. *Front. Marine Sci.* **7**, 670. (doi:10.3389/fmars.2020.00670)
2. Khan FA, Naushin F, Rehman F, Masoodi A, Irfan M, Hashmi F, Ansari AA. 2014 Eutrophication: global scenario and local threat to dynamics of aquatic ecosystems. In *Eutrophication: causes, consequences and control* (eds AA Ansari, SS Gill), pp. 17–27. Dordrecht, Netherlands: Springer.
3. Camargo JA, Alonso Á. 2006 Ecological and toxicological effects of inorganic nitrogen pollution in aquatic ecosystems: a global assessment. *Environ. Int.* **32**, 831–849. (doi:10.1016/j.envint.2006.05.002)
4. Smith VH. 2003 Eutrophication of freshwater and coastal marine ecosystems: a global problem. *Environ. Sci. Pollut. Res.* **10**, 126–139. (doi:10.1065/espr2002.12.142)
5. Smith VH, Joye SB, Howarth RW. 2006 Eutrophication of freshwater and marine ecosystems. *Limnol. Oceanogr.* **51**, 351–355. (doi:10.4319/lo.2006.51.1_part_2.0351)
6. Blomqvist S, Gunnars A, Elmgren R. 2004 Why the limiting nutrient differs between temperate coastal seas and freshwater lakes: a matter of salt. *Limnol. Oceanogr.* **49**, 2236–2241. (doi:10.4319/lo.2004.49.6.2236)
7. Bonsdorff E. 2021 Eutrophication: early warning signals, ecosystem-level and societal responses, and ways forward: this article belongs to Ambio's 50th anniversary collection. Theme: eutrophication. *Ambio* **50**, 753–758. (doi:10.1007/s13280-020-01432-7)
8. Camargo JA, Alonso A, Salamanca A. 2005 Nitrate toxicity to aquatic animals: a review with new data for freshwater invertebrates. *Chemosphere* **58**, 1255–1267. (doi:10.1016/j.chemosphere.2004.10.044)
9. Kroupova H, Machova J, Svobodova Z. 2005 Nitrite influence on fish: a review. *Vet. Med.* **50**, 461–471. (doi:10.17221/5650-VETMED)
10. Cai WJ *et al.* 2011 Acidification of subsurface coastal waters enhanced by eutrophication. *Nat. Geosci.* **4**, 766–770. (doi:10.1038/ngeo1297)
11. Smith VH, Schindler DW. 2009 Eutrophication science: where do we go from here? *Trends Ecol. Evol.* **24**, 201–207. (doi:10.1016/j.tree.2008.11.009)
12. Diaz RJ, Rosenberg R. 2008 Spreading dead zones and consequences for marine ecosystems. *Science* **321**, 926–929. (doi:10.1126/science.1156401)
13. Kahru M, Elmgren R, Kaiser J, Wasmund N, Savchuk O. 2020 Cyanobacterial blooms in the Baltic sea: correlations with environmental factors. *Harm. Algae* **92**, 101739. (doi:10.1016/j.hal.2019.101739)

14. Stillman JH. 2019 Heat waves, the new normal: summertime temperature extremes will impact animals, ecosystems, and human communities. *Physiology* **34**, 86–100. (doi:10.1152/physiol.00040.2018)
15. Moss B *et al*. 2011 Allied attack: climate change and eutrophication. *Inland Waters* **2**, 101–105. (doi:10.5268/IW-1.2.359)
16. Paerl HW, Huisman J. 2008 Climate: blooms like it hot. *Science* **320**, 57–58. (doi:10.1126/science.1155398)
17. Pretty JN, Mason CF, Nedwell DB, Hine RE, Leaf S, Dils R. 2003 Environmental costs of freshwater eutrophication in England and Wales. *Environ. Sci. Technol.* **37**, 201–208. (doi:10.1021/es020793k)
18. Dodds WK, Bouska WW, Eitzmann JL, Pilger TJ, Pitts KL, Riley AJ, Schloesser JT, Thornbrugh DJ. 2009 Eutrophication of U. S. freshwaters: analysis of potential economic damages. *Environ. Sci. Technol.* **43**, 12–19. (doi:10.1021/es801217q)
19. Woolway RI, Jennings E, Carrea L. 2020 Impact of the 2018 European heatwave on lake surface water temperature. *Inland Waters* **10**, 322–332. (doi:10.1080/20442041.2020.1712180)
20. Glibert PM. 2020 Harmful algae at the complex nexus of eutrophication and climate change. *Harm. Algae* **91**, 101583. (doi:10.1016/j.hal.2019.03.001)
21. Nazari-Sharabian M, Ahmad S, Karakouzian M. 2018 Climate change and eutrophication: a short review. *Eng. Technol. Appl. Sci. Res.* **8**, 3668–3672. (doi:10.48084/etasr.2392)
22. Jöhnk KD, Huisman J, Sharples J, Sommeijer B, Visser PM, Stroom JM. 2008 Summer heatwaves promote blooms of harmful cyanobacteria. *Glob. Change Biol.* **14**, 495–512. (doi:10.1111/j.1365-2486.2007.01510.x)
23. Elliott JA, Jones ID, Thackeray SJ. 2006 Testing the sensitivity of phytoplankton communities to changes in water temperature and nutrient load, in a temperate lake. *Hydrobiologia* **559**, 401–411. (doi:10.1007/s10750-005-1233-y)
24. Sinha E, Michalak AM, Balaji V. 2017 Eutrophication will increase during the 21st century as a result of precipitation changes. *Science* **357**, 405–408. (doi:10.1126/science.aan2409)
25. Jiang Z, Liu S, Zhang J, Wu Y, Zhao C, Lian Z, Huang X. 2018 Eutrophication indirectly reduced carbon sequestration in a tropical seagrass bed. *Plant Soil* **426**, 135–152. (doi:10.1007/s11104-018-3604-y)
26. Beaulieu JJ, DelSontro T, Downing JA. 2019 Eutrophication will increase methane emissions from lakes and impoundments during the 21st century. *Nat. Commun.* **10**, 1375. (doi:10.1038/s41467-019-09100-5)
27. Jameson BD, Berg P, Grundle DS, Stevens CJ, Juniper SK. 2020 Continental margin sediments underlying the NE Pacific oxygen minimum zone are a source of nitrous oxide to the water column. *Limnol. Oceanogr. Lett.* **6**, 68–76. (doi:10.1002/lol2.10174)
28. Gomez Isaza DF, Cramp RL, Franklin CE. 2020 Living in polluted waters: a meta-analysis of the effects of nitrate and interactions with other environmental stressors on freshwater taxa. *Environ. Pollut.* **261**, 114091. (doi:10.1016/j.envpol.2020.114091)
29. Gomez Isaza DF, Cramp RL, Franklin CE. 2021 Exposure to nitrate increases susceptibility to hypoxia in fish. *Physiol. Biochem. Zool.* **94**, 124–142. (doi:10.1086/713252)
30. Rodgers EM, Opinion AGR, Gomez Isaza DF, Rašković B, Poleksić V, De Boeck G. 2021 Double whammy: nitrate pollution heightens susceptibility to both hypoxia and heat in a freshwater salmonid. *Sci. Total Environ.* **765**, 142777. (doi:10.1016/j.scitotenv.2020.142777)
31. Gomez Isaza DF, Cramp RL, Franklin CE. 2018 Negative impacts of elevated nitrate on physiological performance are not exacerbated by low pH. *Aquat. Toxicol.* **200**, 217–225. (doi:10.1016/j.aquatox.2018.05.004)
32. Gomez Isaza DF, Cramp RL, Franklin CE. 2020 Simultaneous exposure to nitrate and low pH reduces the blood oxygen-carrying capacity and functional performance of a freshwater fish. *Conserv. Physiol.* **8**, coz092. (doi:10.1093/conphys/coz092)
33. Lefevre S, Jensen FB, Huong D, Wang T, Phuong NT, Bayley M. 2011 Effects of nitrite exposure on functional haemoglobin levels, bimodal respiration, and swimming performance in the facultative air-breathing fish *Pangasianodon hypophthalmus*. *Aquat. Toxicol.* **104**, 86–93. (doi:10.1016/j.aquatox.2011.03.019)
34. San Diego-McGlone ML, Azanza RV, Villanoy CL, Jacinto GS. 2008 Eutrophic waters, algal bloom and fish kill in fish farming areas in Bolinao, Pangasinan, Philippines. *Mar. Pollut. Bull.* **57**, 295–301. (doi:10.1016/j.marpolbul.2008.03.028)
35. Obrist-Farner J, Brenner M, Curtis JH, Kenney WF, Salvinelli C. 2019 Recent onset of eutrophication in Lake Izabal, the largest water body in Guatemala. *J. Paleolimnol.* **62**, 359–372. (doi:10.1007/s10933-019-00091-3)
36. Godinho FN, Segurado P, Franco A, Pinheiro P, Pádua J, Rivaes R, Ramos P. 2019 Factors related to fish kill events in Mediterranean reservoirs. *Water Res.* **158**, 280–290. (doi:10.1016/j.watres.2019.04.027)
37. Fry FJ. 1971 The effect of environmental factors on the physiology of fish. In *Fish physiology* (eds W Hoar, D Randall), pp. 1–87. New York, NY: Academic Press Inc.
38. Johansen JL, Jones GP. 2011 Increasing ocean temperature reduces the metabolic performance and swimming ability of coral reef damselfishes. *Glob. Change Biol.* **17**, 2971–2979. (doi:10.1111/j.1365-2486.2011.02436.x)
39. Seebacher F, White CR, Franklin CE. 2015 Physiological plasticity increases resilience of ectothermic animals to climate change. *Nat. Clim. Change* **5**, 61–66. (doi:10.1038/nclimate2457)
40. Gomez Isaza DF, Cramp RL, Franklin CE. 2021 Thermal plasticity of the cardiorespiratory system provides cross-tolerance protection to fish exposed to elevated nitrate. *Comp. Biochem. Physiol. Part C Toxicol. Pharmacol.* **240**, 108920. (doi:10.1016/j.cbpc.2020.108920)
41. Opinion AGR, De Boeck G, Rodgers EM. 2020 Synergism between elevated temperature and nitrate: impact on aerobic capacity of European grayling, *Thymallus thymallus* in warm, eutrophic waters. *Aquat. Toxicol.* **226**, 105563. (doi:10.1016/j.aquatox.2020.105563)
42. Opinion AGR, Çakir R, De Boeck G. 2021 Better together: cross-tolerance induced by warm acclimation and nitrate exposure improved the aerobic capacity and stress tolerance of common carp *Cyprinus carpio*. *Ecotoxicol Environ. Saf.* **225**, 112777. (doi:10.1016/j.ecoenv.2021.112777)
43. Collins M, Truebano M, Verberk WCEP, Spicer JI. 2021 Do aquatic ectotherms perform better under hypoxia after warm acclimation? *J. Exp. Biol.* **224**, jeb.232512. (doi:10.1242/jeb.232512)
44. Anttila K, Lewis M, Prokkola JM, Kanerva M, Seppanen E, Kolari I, Nikinmaa M. 2015 Warm acclimation and oxygen depletion induce species-specific responses in salmonids. *J. Exp. Biol.* **218**, 1471–1477. (doi:10.1242/jeb.119115)
45. Sokolova IM, Lannig G. 2008 Interactive effects of metal pollution and temperature on metabolism in aquatic ectotherms: implications of global climate change. *Clim. Res.* **37**, 181–201. (doi:10.3354/cr00764)
46. Rodgers EM, De Boeck G. 2019 Nitrite-induced reductions in heat tolerance are independent of aerobic scope in a freshwater teleost. *J. Exp. Biol.* **22**, jeb.212035. (doi:10.1242/jeb.212035)
47. Hall ER, Muller EM, Goulet T, Bellworthy J, Ritchie KB, Fine M. 2018 Eutrophication may compromise the resilience of the Red Sea coral *Stylophora pistillata* to global change. *Mar. Pollut. Bull.* **131**, 701–711. (doi:10.1016/j.marpolbul.2018.04.067)
48. Wooldridge SA. 2009 Water quality and coral bleaching thresholds: formalising the linkage for the inshore reefs of the Great Barrier Reef, Australia. *Mar. Pollut. Bull.* **58**, 745–751. (doi:10.1016/j.marpolbul.2008.12.013)
49. Moran R, Harvey I, Moss B, Feuchtmayr H, Hatton K, Heyes T, Atkinson D. 2010 Influence of simulated climate change and eutrophication on three-spined stickleback populations: a large scale mesocosm experiment. *Freshw. Biol.* **55**, 315–325. (doi:10.1111/j.1365-2427.2009.02276.x)
50. Alexander TJ, Vonlanthen P, Seehausen O. 2017 Does eutrophication-driven evolution change aquatic ecosystems? *Phil. Trans. R. Soc. B* **372**, 20160041. (doi:10.1098/rstb.2016.0041)
51. Mantyka-Pringle CS, Martin TG, Moffatt DB, Linke S, Rhodes JR. 2014 Understanding and predicting the combined effects of climate change and land-use change on freshwater macroinvertebrates and fish. *J. Appl. Ecol.* **51**, 572–581. (doi:10.1111/1365-2664.12236)
52. Rodgers EM, Gomez Isaza DF. 2021 Harnessing the potential of cross-protection stressor interactions for conservation: a review. *Conserv. Physiol.* **9**, coab037. (doi:10.1093/conphys/coab037)

53. Paaijmans KP, Heinig RL, Seliga RA, Blanford JI, Blanford S, Murdock CC, Thomas MB. 2013 Temperature variation makes ectotherms more sensitive to climate change. *Glob. Change Biol.* **19**, 2373–2380. (doi:10.1111/gcb.12240)

54. Piggott JJ, Lange K, Townsend CR, Matthaei CD. 2012 Multiple stressors in agricultural streams: a mesocosm study of interactions among raised water temperature, sediment addition and nutrient enrichment. *PLoS ONE* **7**, e49873. (doi:10.1371/journal.pone.0049873)

55. Bossier S, Nielsen JR, Almroth-Rosell E, Höglund A, Bastardie F, Neuenfeldt S, Wåhlström I, Christensen A. 2021 Integrated ecosystem impacts of climate change and eutrophication on main Baltic fishery resources. *Ecol. Modell.* **453**, 109609. (doi:10.1016/j.ecolmodel.2021.109609)

ARTICLES FOR FACULTY MEMBERS

GLOBAL WARMING EFFECTS ON ECTOTHERM SPECIES

Title/Author	**Climate change and ageing in ectotherms / Burraco, P., Orizaola, G., Monaghan, P., & Metcalfe, N. B.**
Source	***Global Change Biology*** **Volume 26 Issue 10 (2020) Pages 5371–5381** **https://doi.org/10.1111/gcb.15305** **(Database: Wiley Online Library)**

Received: 7 April 2020 | Revised: 31 July 2020 | Accepted: 31 July 2020

DOI: 10.1111/gcb.15305

OPINION

Global Change Biology WILEY

Climate change and ageing in ectotherms

Pablo Burraco[1,2] | Germán Orizaola[3,4] | Pat Monaghan[1] | Neil B. Metcalfe[1]

[1]Institute of Biodiversity, Animal Health, and Comparative Medicine, College of Medical, Veterinary, and Life Sciences, University of Glasgow, Glasgow, UK

[2]Animal Ecology, Department of Ecology and Genetics, Evolutionary Biology Centre, Uppsala University, Uppsala, Sweden

[3]IMIB-Biodiversity Research Institute (Univ. Oviedo-CSIC-Principado Asturias), Mieres-Asturias, Spain

[4]Zoology Unit, Department of Organisms and Systems Biology, University of Oviedo, Oviedo-Asturias, Spain

Correspondence
Pablo Burraco, Institute of Biodiversity, Animal Health, and Comparative Medicine, College of Medical, Veterinary, and Life Sciences, University of Glasgow, Graham Kerr Building, Glasgow G12 8QQ, UK.
Email: pablo.burraco@glasgow.ac.uk

Funding information
European Research Council Advanced Grant, Grant/Award Number: 834653; Ministerio de Ciencia e Innovación, Grant/Award Number: RYC-2016-20656; Natural Environment Research Council, Grant/Award Number: NE/R001510/1; H2020 Marie Skłodowska-Curie Actions, Grant/Award Number: 797879-METAGE; Carl Tryggers Stiftelse för Vetenskaplig Forskning, Grant/Award Number: CT 16:344

Abstract

Human activity is changing climatic conditions at an unprecedented rate. The impact of these changes may be especially acute on ectotherms since they have limited capacities to use metabolic heat to maintain their body temperature. An increase in temperature is likely to increase the growth rate of ectothermic animals, and may also induce thermal stress via increased exposure to heat waves. Fast growth and thermal stress are metabolically demanding, and both factors can increase oxidative damage to essential biomolecules, accelerating the rate of ageing. Here, we explore the potential impact of global warming on ectotherm ageing through its effects on reactive oxygen species production, oxidative damage, and telomere shortening, at the individual and intergenerational levels. Most evidence derives primarily from vertebrates, although the concepts are broadly applicable to invertebrates. We also discuss candidate mechanisms that could buffer ectotherms from the potentially negative consequences of climate change on ageing. Finally, we suggest some potential applications of the study of ageing mechanisms for the implementation of conservation actions. We find a clear need for more ecological, biogeographical, and evolutionary studies on the impact of global climate change on patterns of ageing rates in wild populations of ectotherms facing warming conditions. Understanding the impact of warming on animal life histories, and on ageing in particular, needs to be incorporated into the design of measures to preserve biodiversity to improve their effectiveness.

KEYWORDS

global warming, oxidative stress, senescence, telomere, thermal stress

1 | INTRODUCTION

Climatic conditions are currently changing at unprecedented rate (Diffenbaugh & Field, 2013). Climate projections forecast a global temperature increase up to 4°C by the end of the current century, and an increasing likelihood of extreme climatic events such as heat waves and droughts (IPCC, 2014). Climatic changes have already impacted on many organisms and ecosystems (Parmesan, 2006), even though individuals often have the ability to detect such changes and modify their behaviour, physiology or life history to reduce the impact on fitness (Hoffmann & Sgrò, 2011). Understanding the influence of climate change on wild organisms is crucial if we are to devise appropriate conservation research plans and policies.

The impact of climate change is expected to be particularly severe on ectothermic animals (Kingsolver, Diamond, & Buckley, 2013). The limited abilities of ectotherms to use metabolic heat to maintain their body temperature makes them especially vulnerable to temperature fluctuations (Bickford, Sheridan, & Howard, 2011; Seebacher, White, & Franklin, 2015). Despite most ectotherms exhibit behavioural plasticity that allows them to adjust their body temperature to

environmental conditions, rising temperatures can put ectotherms outside their physiological optima and closer, or even above, their thermal tolerance limits (Kingsolver et al., 2013; Sunday et al., 2014). A mismatch between the rate of change in environmental conditions and the capacity of ectotherms to cope with these changes may severely affect their physiology and lead to decreases in fitness.

While the effects of global warming on several components of ectothermic physiology are well understood (Abram, Boivin, Moiroux, & Brodeur, 2017; Gunderson, Dillon, & Stillman, 2017; Gunderson & Stillman, 2015), one particular aspect that has hitherto received little attention is its effect on the dynamics of ageing. Ageing can broadly be defined as the time-dependent functional decline that affects most living organisms (López-Otín, Blasco, Partridge, Serrano, & Kroemer, 2013). Here, we highlight three routes by which climate change might alter the rate of ageing in ectotherms: (a) warmer average temperatures causing an acceleration of growth rates; (b) more frequent heat waves inducing thermal stress; and (c) changes in the pace-of-life of parents affecting the ageing rate of their offspring. As we show below, all three scenarios can induce the loss of organismal homeostasis and accelerate senescence in ectotherms. Here, in using the term 'ectotherm', we are primarily referring to vertebrates, since this is where most relevant existing data on ageing mechanisms occur, but the processes are likely to be also relevant to invertebrates. At present, it is unclear whether organisms have the capacity to compensate for these potential changes in lifespan, or the demographic consequences for populations. Further research is clearly needed to fully evaluate the effects of climate change on rates of ageing of wild organisms, and to incorporate these issues into biodiversity conservation actions.

2 | GLOBAL WARMING, FAST GROWTH, AND AGEING IN ECTOTHERMS

At the individual level, warmer environments induce thermal plasticity in most ectotherms, resulting in fast growth but often smaller size later in life, a process that can be also mediated through size-dependent feedbacks (Ohlberger, 2013). This is a common pattern in arthropods (Angilletta & Dunham, 2003), fish (Baudron, Needle, Rijnsdorp, & Tara Marshall, 2014), amphibians (Ruthsatz, Peck, Dausmann, Sabatino, & Glos, 2018), and reptiles (Price et al., 2017). Thermally induced alterations in growth can be particularly costly for ectotherms at early ontogenetic stages, since at this point resources are prioritized towards the development of new structures and away from somatic maintenance (Dmitriew, 2011; Metcalfe & Monaghan, 2001). Many ectotherms develop complex life cycles and are especially sensitive to warming impacts on growth if these occur in early life stages, that is, before metamorphosis (Huey et al., 2012).

Environmentally induced acceleration of growth is known to impact on lifespan. The costs of rapid growth were first demonstrated in fish showing a negative relationship between growth rate and longevity (Comfort, 1963). A negative relationship between faster growth in early life and later survival has been found in other fish species, and also in insects (e.g. Lee & Roh, 2010), amphibians (e.g. Altwegg & Reyer, 2003), and reptiles (e.g. Olsson & Shine, 2002). While most of these studies have been correlational, a trade-off between growth rate and lifespan has been demonstrated experimentally in sticklebacks (Lee, Monaghan, & Metcalfe, 2013). In this study, temperature-induced faster growth was associated with reduced longevity, while experimental slowing of growth was associated with increased longevity, confirming the role of thermally induced growth in shaping the pattern and pace of ageing in ectotherms.

Across-species comparisons indicate that larger endotherms live longer than smaller ones (r^2 = .46 and .39 in birds and mammals, respectively; Speakman, 2005). In contrast, body size explains only a small portion of the variance in longevity in vertebrate ectotherms, as observed in amphibians (r^2 = .07–.14; Stark & Meiri, 2018) or reptiles (r^2 = .04–.23; Stark, Tamar, Itescu, Feldman, & Meiri, 2018). The weaker correlation between body size and maximum lifespan in vertebrate ectotherms than in endotherms probably indicates that the traits have evolved at least partially independently in species with indeterminate growth. Ectotherms can potentially show some degree of thermal independence via a reduced heat exchange rate with the environment. The ability to be thermally independent mainly benefits larger-bodied ectotherms under cold environments rather than warming conditions. However, reductions in body size due to induced fast growth caused by warming may facilitate heat loss in large species. Among-species differences in the rate of growth from birth to maturation, and the variation in this rate caused by rising temperatures, may be even more relevant than differences in body size to understand the impact of warming on ageing in ectotherms. Another unexplored topic is how among-species differences in life expectancy at birth can affect responses to warming. The likelihood of being exposed to warming and thermal stress during a single lifetime is, obviously, higher in long-lived species, but these species have often evolved protective mechanisms to slow the ageing process (Tian, Seluanov, & Gorbunova, 2017). Further comparative research will help to disentangle the relative importance of growth, body size, and lifespan on ectotherms ageing under a global warming scenario.

2.1 | Fast growth and oxidative damage

The reduction in lifespan of ectotherms experiencing faster growth could be due to greater mitochondrial activity (Figure 1a). Rapid growth requires the formation in the mitochondria of increased amounts of ATP, and this can lead to the generation of reactive oxygen species (ROS) as a by-product. While ROS have many beneficial physiological functions such as maintenance of homeostasis and cell signalling, they can also cause oxidative damage to essential biomolecules like membrane lipids, proteins, and DNA when their concentration exceeds the antioxidant capacity of cells to detoxify them (Halliwell & Gutteridge, 2015). This damage can lead to accelerated ageing of the cells and ultimately the whole organism (Halliwell & Gutteridge, 2015). A meta-analysis across all animal groups has

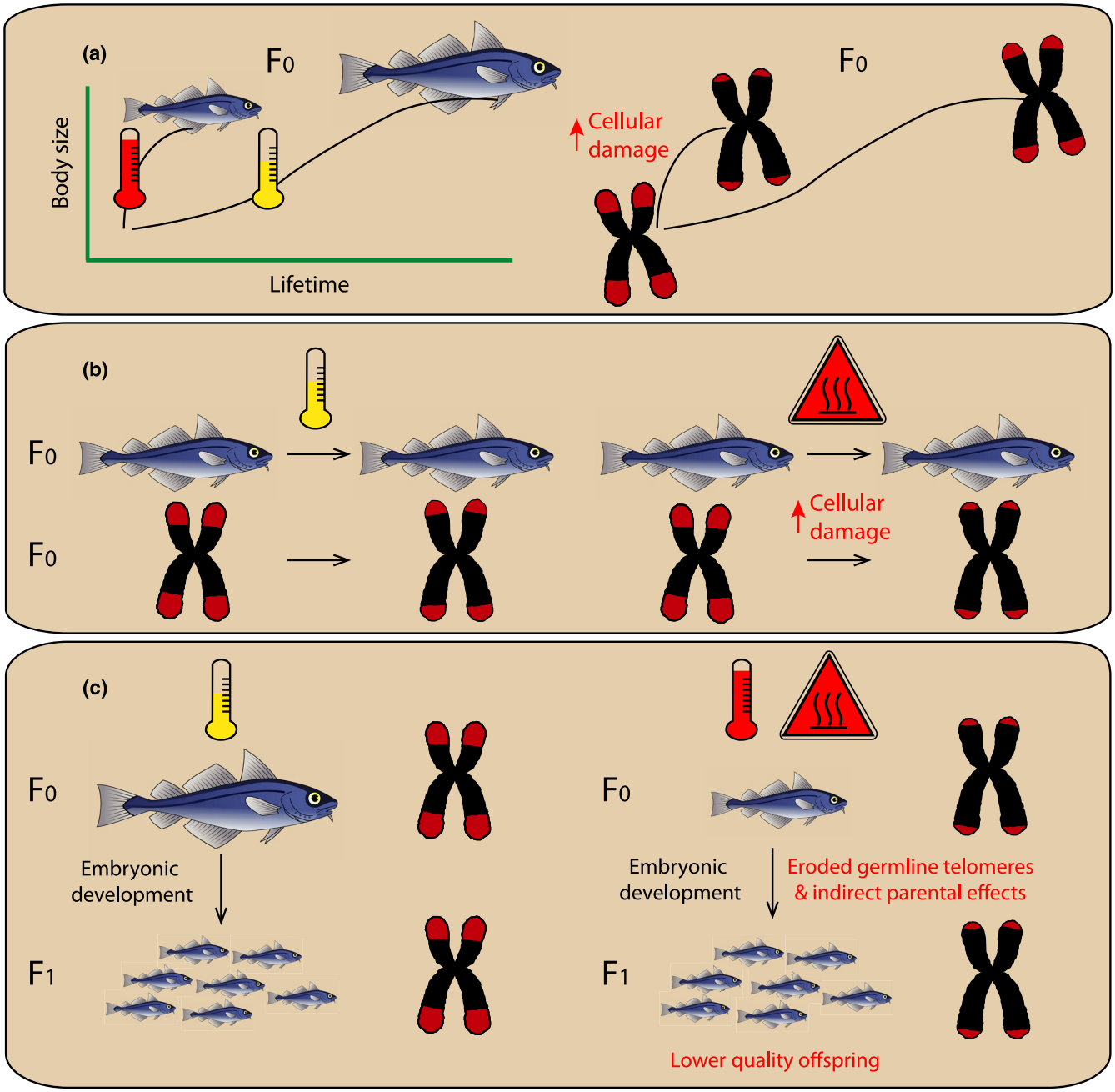

FIGURE 1 Mechanisms whereby environmental warming could increase the rates of ageing in ectotherms. (a) Left side: differences in individual growth trajectories and body size at maturation in response to normal (yellow thermometer) or warm (red thermometer) thermal conditions; right side: fast growth may include cellular damage and a consequent increase in the rate of shortening of the telomeres (the red caps on the ends of the chromosomes). (b) Left side: ectotherms have evolved to cope with normal temperature regimes without incurring in thermal stress; right side: heat waves induce thermal stress, leading to cellular damage and consequent faster erosion of telomeres. Such responses would not necessarily include significant changes in growth since they often take place during a brief period of time. (c) Possible intergenerational effects of climate warming on telomere length. Left side: normal thermal regimes result in normal telomere lengths in offspring; right side: higher mean temperatures and heat waves in parental generation have deleterious effects on offspring. Such effects, evident at very early offspring life stages, could be caused by faster erosion of germline telomeres, by poor parental condition and/or impaired parental care during post-natal stages during post-natal stages

shown that faster growth is associated with greater oxidative damage (Smith, Nager, & Costantini, 2016). In ectotherms, fast growth can alter the redox status in insects (e.g. De Block & Stoks, 2008), fish (e.g. Guerra, Zenteno-Savín, Maeda-Martínez, Philipp, & Abele, 2012), amphibians (e.g. Burraco, Valdés, & Orizaola, 2020), and reptiles (e.g. Furtado-Filho, Polcheira, Machado, Mourão, & Hermes-Lima, 2007). These effects can persist over long time periods, even across life stages. For instance, juvenile fish growing faster in response to elevated winter temperatures experienced severe oxidative and DNA damage later in life at the time of breeding (Kim,

Noguera, & Velando, 2019). Amphibians can also experience redox imbalances at metamorphosis as a negative consequence of growing at high rates earlier in life, when compensating for delayed hatching (Burraco et al., 2020).

2.2 | Warmer temperature and telomeres

Oxidative stress can also induce faster ageing through its impact on telomeres. Telomeres are specialized sections of non-coding DNA that mark and protect the ends of chromosomes. Telomere regions are essential for maintaining genome stability by preventing end-to-end fusion of chromosomes, and also protect the coding sequences from loss at the ends of the lagging DNA strands that occurs during DNA replication (Richter & von Zglinicki, 2007). The length of the telomeres becomes shorter at each cell division. Cells enter a state of replicative senescence once their telomeres reach a critically short length; this is followed by either cell death or a change in cell secretory profile to a more pro-inflammatory state (Aubert & Lansdorp, 2008). Such changes can provide a link between the rate of telomere shortening and tissue (and hence organismal) senescence. The causal relationship between oxidative stress and the rate of telomere shortening has been evidenced via the administration of antioxidants, which slow the rate of telomere erosion (Badás et al., 2015; Pineda-Pampliega et al., 2020), and confirmed through field and laboratory studies (reviewed in Barnes, Fouquerel, & Opresko, 2018; Monaghan & Ozanne, 2018; Reichert & Stier, 2017). A recent meta-analysis (Chatelain, Drobniak, & Szulkin, 2020) supports the idea that oxidative stress mediates telomere shortening, although this relationship is mainly linked to differences in the levels of the antioxidant machinery.

Differences in telomere length or loss rate can predict life expectancy, but the telomere–fitness relationship is highly variable in ectotherms and still need further research (Olsson, Wapstra, & Friesen, 2018a, 2018b). Telomere loss can also indicate the degree of stress exposure of an individual across the life course, although as yet most of the evidence of this comes from endotherms (Bateson & Poirier, 2019; Tricola et al., 2018; Wilbourn et al., 2018). The variation in telomere length among populations of brown trout correlates negatively with the river temperatures they experienced in the previous summer, and thus telomere length has been suggested as a marker of past thermal stress in fish (Debes, Visse, Panda, Ilmonen, & Vasemägi, 2016). In ectotherms, fast growth can lead to accelerated telomere shortening, as found in juvenile fish (McLennan et al., 2016; Pauliny, Devlin, Johnsson, & Blomqvist, 2015) or amphibian larvae (Burraco, Díaz-Paniagua, & Gomez-Mestre, 2017). Since differences in length-at-age and rate of loss of telomeres can be considered as ageing biomarkers, a detailed understanding of telomere dynamics over a species' lifetime, and across taxa, will improve our predictions of the impact of warming on ectotherm ageing. To this end, knowing the age of individuals is helpful in studies in the wild. In temperate vertebrate ectotherms, growth shows seasonal variation and age can be determined through skeletochronology, for example, by counting lines of arrested growth in reptiles and amphibians, growth rings in fish scales or bands in fish otoliths (Zhao, Klaassen, Lisovski, & Klaassen, 2019).

However, when faster growth is induced by higher temperatures, the relationship with telomere attrition is not always straightforward since adult ectotherms can undergo partial telomere restoration as a result of expressing the enzyme telomerase. Telomerase restores telomere length and is more often active in somatic tissue after birth in ectotherms than in endotherms (Olsson, Wapstra, & Friesen, 2018a). Telomerase expression is predicted to be higher in warmer environments, so potentially compensating for damage to telomeres in those organisms experiencing temperature-induced fast growth (Olsson et al., 2018a). This hypothesis is supported by recent research showing that lizards held in hot basking conditions for 3 months experienced increases in telomere length, unlike those held in cooler conditions (Fitzpatrick et al., 2019). Further empirical studies will clarify the possible interaction between temperature, growth, and telomerase expression.

The study of telomere dynamics in populations inhabiting divergent temperature conditions might allow us to evaluate the effects of human-induced thermal stress on ageing rates. This would be particularly relevant for populations of ectotherms living in regions of rapid thermal change, especially if they have long generation times that slow the potential rate of adaptation to changing environments (Morley, Peck, Sunday, Heiser, & Bates, 2019). Species with shorter generation time and larger populations are predicted to evolve quickly while maintaining genetic variation (Hoffmann & Sgrò, 2011). Artificial selection experiments comparing the genetic responses to warming conditions will help to evaluate the relative importance of generation time, population size, and plasticity, in evolutionary adaptation processes. Unfortunately, there is a lack of studies combining biogeographical and gerontological approaches which would allow us to appropriately predict the impact that global warming will have on the comparative rates of ageing of ectotherms along climatic gradients.

3 | HEAT WAVES AND AGEING IN ECTOTHERMS

Forecasts for the next 50 years predict a dramatic increase in the likelihood of heat waves (IPCC, 2014), characterized by sudden rises in air or water temperature that could reach the upper thermal limits for many ectotherms (Gunderson & Stillman, 2015). Heat waves are one of the most powerful environmental forces affecting the welfare and physiology of ectotherms (Kingsolver et al., 2013), and may cause the acceleration of senescence by inducing thermal stress. Similar to the alterations caused by other stressful conditions, thermal stress can disrupt individual's homeostasis and compromise organismal health. In vertebrates, the response to stressful conditions is mainly regulated by neuroendocrine pathways. These pathways mediate biological processes such as growth or reproduction (Crespi, Williams, Jessop, & Delehanty, 2013) but also accelerate the rate of ageing, as determined, for example, by a higher rate of telomere

attrition (Angelier, Costantini, Blevin, & Chastel, 2018; Haussmann & Heidinger, 2015). Stress often leads to a higher secretion of hormones that enhances cellular catabolism and exacerbates the generation of ROS, with putative impacts on antioxidant defences and the rate of telomere shortening (Haussmann & Heidinger, 2015; Haussmann & Marchetto, 2010; Monaghan, 2014). The antioxidant machinery of ectotherms seems to be particularly sensitive to extreme thermal events, as indicated by strong redox responses to high temperatures observed in arthropods (e.g. Yang, Huang, & Wang, 2010) and fish (e.g. Banh, Wiens, Sotiri, & Treberg, 2016). On the other hand, the redox machinery of some reptiles seems relatively insensitive to thermal stress (e.g. Stahlschmidt, French, Ahn, Webb, & Butler, 2017), which may be a consequence of the downregulation of particular genes in response to warming (Bentley, Haas, Tedeschi, & Berry, 2017).

Exposure to heat waves can result in accelerated erosion of telomeres in ectothermic animals likely as a consequence of enhanced cellular metabolism under thermal fluctuations (Figure 1b). For instance, sturgeons facing thermal stress experience higher rate of telomere shortening (Simide, Angelier, Gaillard, & Stier, 2016) and show increased juvenile mortality (Kappenman, Fraser, Toner, Dean, & Webb, 2009). Desert lizards, which do not show signs of telomere shortening or reductions in survival when exposed to gradual warming, experience telomere shortening and lower overwinter survival after a week of simulated heat wave conditions (Zhang et al., 2018). This is perhaps surprising, given the lack of oxidative stress induced by high temperatures in other reptiles, and highlights the need for more comprehensive studies investigating the impact of temperature on physiological indicators of ageing in ectotherms.

4 | INTERGENERATIONAL EFFECTS OF CLIMATE CHANGE ON AGEING RATES IN ECTOTHERMS

Stress experienced by parents can influence the physiology of their offspring. To establish whether the environmental conditions experienced by parents can influence the rates of ageing of their offspring, we need to understand the mechanisms whereby rates of ageing could be transmitted between generations. In the absence of detailed information on life expectancy (not normally available over multiple generations), the usual approach is to use a biomarker of the rate of ageing, such as telomere length. Telomere length at a given developmental stage is a function of their initial length (i.e. at zygote), minus the accumulated shortening, plus the amount of restoration experienced until that point (Dugdale & Richardson, 2018).

Heritability estimates for telomere length in animals range from 0.18 to >1 (reviewed in Dugdale & Richardson, 2018; Haussmann & Heidinger, 2015; Reichert et al., 2015), tending to be higher when measured earlier in life (Dugdale & Richardson, 2018). However, in ectotherms (in contrast to most endotherms), telomeres show signs of elongation after birth in several species (reptiles: Ujvari et al., 2017; fish: McLennan et al., 2018; amphibians: Burraco et al., 2020). This makes it far from straightforward to decide the point in ontogeny at which telomere length should be compared between parents and offspring.

If climate warming causes a reduction in the physiological condition of ectotherms at the time of breeding, this could lead to shorter telomeres in their offspring through two different routes. First, stressors could affect germline telomere lengths, causing offspring to inherit shorter telomeres from parents that were exposed to more stressful environments. Second, indirect parental effects can cause faster ageing in offspring, either during the embryonic stages (e.g. through maternally derived stress hormones or suboptimal temperatures during development), or in the early post-natal stages (e.g. through changes in parental behaviour or care; Haussmann & Heidinger, 2015). Both routes may be particularly important for ectotherms in a warming world because higher temperatures can induce maturation earlier in life and at a smaller size (Angilletta, Steury, & Sears, 2004). Smaller size at breeding is often associated with the production of lower-quality offspring and poor parental care, which can negatively affect offspring performance at embryonic and post-birth stages (Angilletta et al., 2004), and cause accelerated ageing (Haussmann & Heidinger, 2015; Figure 1c). Detrimental thermal conditions experienced by parents can lead to poor offspring condition as a consequence of a reduction in the energy invested by the parents in each offspring. However, although rare, compensatory responses by parents or changes in breeding strategies could mitigate this effect, for example by reducing clutch size to allocate a larger amount of energy to each offspring (Charnov & Ernest, 2006).

There are several other factors that ideally should be considered when studying the intergenerational effects of warming on ageing dynamics in ectotherms. Many ectotherms show sexual dimorphism, with females typically larger than males, and temperature-dependent sex determination during embryogenesis can also occur. The negative consequences on ageing caused by warming may be exacerbated in species producing females at higher incubation temperatures. Embryos developing as females, and hatching at smaller sizes due to warming, could then show compensatory growth responses, which may result in a lifespan penalty (Metcalfe and Monaghan, 2003). Sex differences in lifespan and ageing can also be driven by the reproductive strategy of species. For example, in polygynous species, survival declines with age faster in males than in females (Clutton-Brock & Isvaran, 2007); warming could exacerbate such sex differences in lifespan by uncoupling the time at which each sex reaches sexual maturation, a process that may be particularly important in semelparous species.

5 | CANDIDATE MECHANISMS TO BUFFER THE EFFECTS OF WARMING ON AGEING IN ECTOTHERMS

Different mechanisms could allow ectotherms to counteract the negative effects of climate change on their ageing rate (Figure 2). Temperature-induced plasticity is a ubiquitous feature of ectothermic

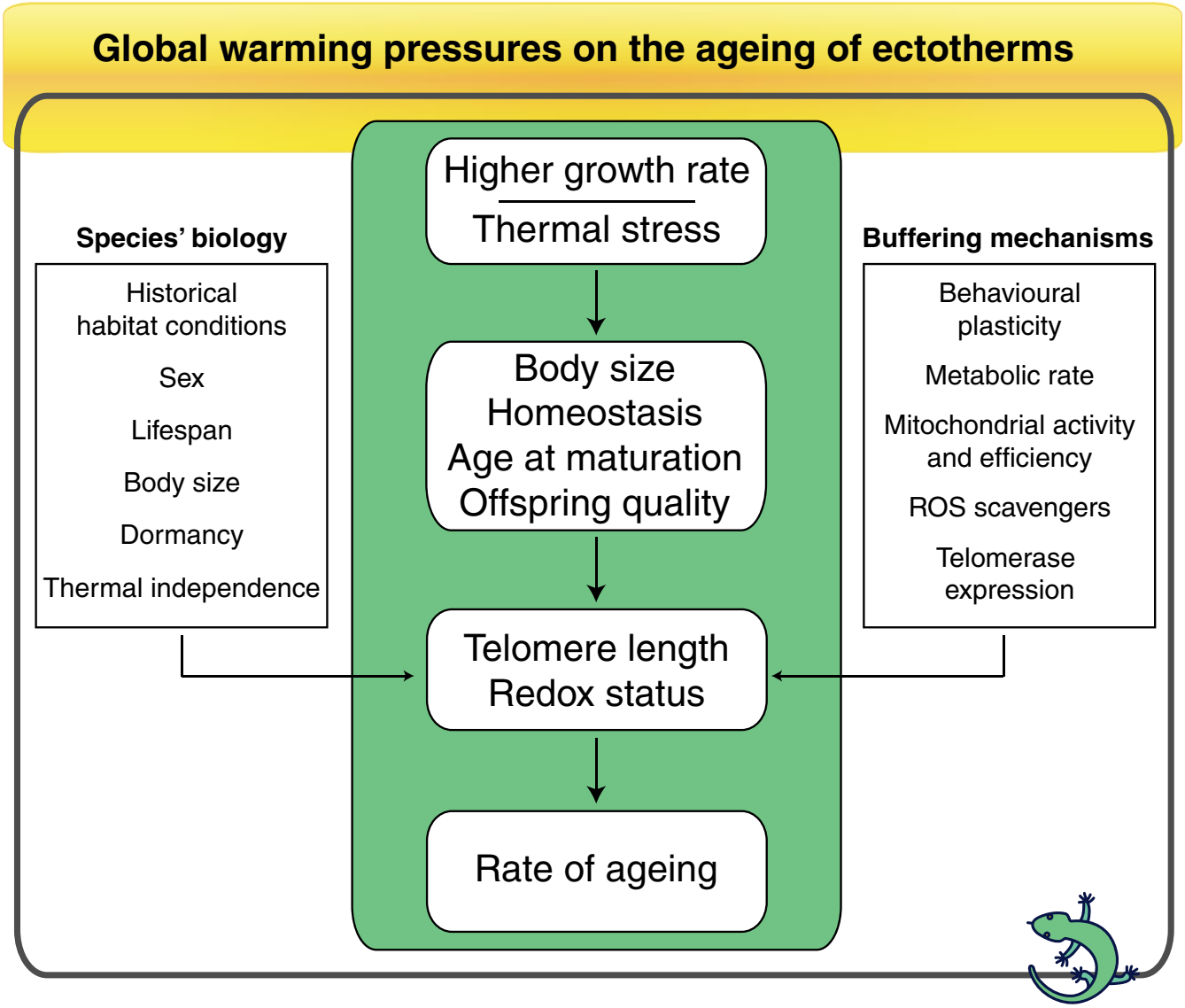

FIGURE 2 Putative impacts of warming conditions on ageing in ectotherms. Higher temperatures are predicted to cause faster growth or thermal stress in ectotherms, which can involve changes in body size, physiological homeostasis, age at maturation, and/or offspring quality. Both faster growth and thermal stress can cause a detrimental impact on ageing-related mechanisms, as for example inducing telomere attrition or oxidative stress. From an eco-evolutionary point of view, a species' biology and buffering mechanisms will likely define the extent to which warming will impact on ageing both at the individual or intergenerational levels

animals (Gunderson et al., 2017). Adaptive behavioural plasticity can be essential for thermoregulation in mobile ectotherms and may play an important role both under gradual warming and during thermal stress events. At low and medium latitudes, where exposure to the sun can otherwise cause body temperatures to increase above an organism's thermal limits, many ectotherms have developed behavioural strategies to avoid overheating (Abram et al., 2017). This is mainly explained by the fact that metabolic responses do not follow a linear pattern, and at those latitudes small increases in temperature may induce significant changes in metabolism. However, species at higher latitudes, including polar environments, may be as vulnerable to global warming as those in the tropics because they may have very narrow thermal tolerances (Johansson, Orizaola, & Nilsson-Örtman, 2020; Somero, 2010).

The ability to plastically modify the onset of some life strategies can reduce the negative impact of warming on ectotherm ageing. Dormancy, diapause and resting egg stages, processes very common in ectotherms living in highly seasonal environments, involve a significant decrease in development and physical activity. In an endotherm, the edible dormouse, a reduction in telomere attrition has been observed during hibernation (Turbill, Ruf, Smith, & Bieber, 2013), although intermittent arousal also carries costs in terms of increased telomere loss (Hoelzl, Cornils, Smith, Moodley, & Ruf, 2016). Under a global warming scenario, dormant ectotherms will probably experience a reduction in the duration and number of dormancy events. Therefore, individuals may need to adjust their use of dormancy in response to environmental temperatures, to reduce the negative effects on ageing. The possible role of this process

in regulating ageing dynamics has not been tested yet in ectotherms, but a recent study shows that higher winter and summer temperatures impact positively and negatively, respectively, on telomere lengths in a hibernating lizard (Axelsson, Wapstra, Miller, Rollings, & Olsson, 2020).

Adaptive physiological plasticity can also help ectotherms acclimate to warmer conditions (Gunderson et al., 2017; Norin & Metcalfe, 2019; Seebacher et al., 2015). However, both behavioural and physiological plasticity may prove insufficient to fully compensate for the effects of warming (Gunderson et al., 2017; Gunderson & Stillman, 2015). This is exemplified by the fact that physiological (e.g. locomotor, metabolic, heart, enzymatic activity) rates in ectotherms have increased up to 20% over the last 20 years as result of climate change, and chronic exposure to higher temperatures has resulted in reductions in their thermal sensitivity (Norin & Metcalfe, 2019; Seebacher et al., 2015). Metabolic rates of terrestrial, freshwater, and marine ectothermic species are predicted to keep increasing in the coming decades (Seebacher et al., 2015). Plasticity is, on average, higher in aquatic than terrestrial ectotherms (Gunderson & Stillman, 2015; Huey et al., 2012; Morley et al., 2019), and it may buffer the negative impact of warming on ectotherm physiology. However, plasticity alone cannot fully protect aquatic ectotherms from overheating (Gunderson et al., 2017). Among ectotherms, crustacea and fish are expected to have smaller decreases in thermal safety margins when environmental temperatures rise than insects, reptiles, and amphibians (Gunderson & Stillman, 2015). Measured impacts of past and current global warming on ectothermic metabolism would suggest that there will be a global acceleration in the rate of senescence of ectotherms as warming continues.

There are also potential molecular mechanisms that could buffer warming impact on ageing. These mechanisms might either prevent damage in cells by reducing the generation of ROS, or repair the damage already caused. Both metabolic rate, usually measured in terms of whole-body oxygen consumption, and mitochondrial efficiency, defined as the amount of ATP generated per molecule of oxygen consumed, show great within- and among-individual variation, and can change in response to environmental conditions (Salin, Auer, Rey, Selman, & Metcalfe, 2015; Salin et al., 2019). Metabolic plasticity at the organelle and tissue/organ level may allow organisms to adjust ROS production to increase their resilience to climate change (Norin & Metcalfe, 2019; Seebacher et al., 2015). Greater mitochondrial uncoupling, which reduces the rate of ROS production at the expense of ATP production efficiency, has been proposed as a mechanism to reduce the rate of senescence (the 'uncoupling to survive' hypothesis, Mookerjee, Divakaruni, Jastroch, & Brand, 2010). This mitigation measure comes at a cost of reduced ATP availability and also increased body heat, since the uncoupling process involves a thermogenic reaction; there is thus an interesting trade-off between ROS production and body temperature in organisms facing warming. Animals may respond by increasing their production of ROS scavenger molecules so as to prevent excessive oxidative damage caused by responses to warming. As an example, one of the first cellular lines of defence against pro-oxidants is the reduced form of glutathione, the production of which can increase in response to stress events (Angelier et al., 2018). An increased availability of ROS scavengers can allow greater metabolic activity, as demonstrated in endotherms through enhanced growth (Velando, Noguera, da Silva, & Kim, 2019). However, there is little knowledge about the costs of increased ROS scavenger production—note that ROS are known to play an essential role in signalling pathways (Costantini, 2019).

The enhancement of repair mechanisms might also slow down ageing in ectotherms. The enzyme telomerase restores telomere length and may play a key role in the extensive regenerative capacity in organisms with indeterminate growth (Gomes, Shay, & Wright, 2010). If selection favours higher levels of telomerase expression in response to warming, it may mitigate the potential damage to telomeres caused by growth acceleration or by thermal stress (Olsson et al., 2018a). However, the prolonged action of telomerase can induce 'immortal cells' and tumorigenesis (Blasco, 2007), which may expose adult ectotherms to a higher risk of cancer (Olsson et al., 2018a; Young, 2018), although our knowledge of the prevalence of cancer in wild animals is very limited.

Field and laboratory studies, ideally including cross-fostering and transgenerational approaches, will help us to understand whether the action of buffering mechanisms is driven either by plasticity or local adaptation across populations. A higher degree of complexity can be added by considering the possibility that the dynamics of ageing-related mechanisms may be tissue-specific. Although telomere lengths seem to correlate among tissues (e.g. in reptiles: Rollings et al., 2019, 2020), differences in cell division and turnover rate, together with the possible tissue-specific expression of buffering mechanisms, may imply divergent responses in ageing-related mechanisms at the tissue level. Evidence from mammals suggests that telomere attrition rates are similar across tissues in adults, but not necessarily so in early life (Daniali et al., 2013; Sabharwal et al., 2018), so the life stage at which the temperature effects occur could be important. Conducting longitudinal studies on the variation of ageing mechanisms at the tissue level is challenging, since terminal sampling is often required, but cross-sectional studies should help to disentangle this topic. It is clear that much more research is needed to fully understand the role that behavioural, physiological, and molecular mechanisms can play in buffering the effects of climate change on the ageing of ectotherms.

6 | HOW MIGHT THESE CONCEPTS HELP IN THE CONSERVATION OF ECTOTHERMS—AND WHAT DO WE STILL NEED TO FIND OUT?

There are issues that need to be taken into account in the context of ectotherm conservation in the face of environmental warming. It is crucial to know how different environmental conditions affect the ageing rate of ectotherms at the individual level and across developmental stages or lifetimes, as well as to understand how among-species differences in life histories can influence the

impact of environmental change on ageing dynamics. Studies of the ageing machinery in ectotherms inhabiting contrasting environments may provide insights into the current health status of populations that may aid in defining conservation actions. As an example, forest clearing reduces canopy cover and leads to an increase in the duration of sunlight exposure, modifying the thermal regime in nest sites of lizards (e.g. Shine, Barrott, & Elphick, 2002). Comparing the ageing dynamics of populations with different access to forest shade would help to better evaluate the impact that forest management can have in mitigating the adverse effect of rising temperatures on these lizard populations. A similar approach can be applied to aquatic ectotherms. Climate change is increasing the likelihood of droughts and the sudden change of water temperature in small ponds. The evaluation of ageing dynamics across populations may help to identify those populations under risk due to thermal stress and to implement conservation actions such as the installation of microclimate refuges, the restoration of breeding sites, or the manipulation of hydroperiod at breeding ponds (Shoo et al., 2011).

Several research questions are still unresolved regarding the impact of warming on the ageing of ectotherms. We need to know the relative importance of high average temperature versus heat waves in affecting rates of ageing, and which ectothermic taxa are most vulnerable to changes in ageing. This is particularly important for invertebrates, where there is currently virtually no information on ageing mechanisms in wild populations. An understanding of these differences will allow managers to develop effective conservation measures that will protect not only declining populations but also others that are apparently healthy. Furthermore, it will allow more accurate modelling of the impact of future warming scenarios on ageing rates in ectotherms that can feed into population models used to set conservation priorities.

7 | CONCLUSIONS

Temperature increases associated with climate change may alter ageing-related processes in ectotherms, as a consequence of changes in their growth trajectories or an increased risk of thermal stress, and both processes may include intergenerational effects (Figure 2). However, there is a need for more ecological, biogeographical, and evolutionary studies on the impact of global climate change on patterns of senescence in wild populations of ectotherms (even more in invertebrates) facing warming conditions. This research should also investigate the possible role of candidate behavioural, cellular, and physiological mechanisms for buffering the predicted negative consequences of warming on the rate of ageing. We also need to understand the putative population consequences of changes in ageing rate, and to link these to location-specific predictions of climate change, to determine which populations and/or species are most vulnerable. Ideally, this information needs to be combined with species-specific knowledge on plasticity or evolutionary adaptability in response to thermal changes (Morley et al., 2019). Understanding the basic effects of climate warming on the ageing rates of ectothermic species will help in developing global and local scientific-based policies aiming at reducing the negative consequences of climatic change on biodiversity.

ACKNOWLEDGEMENTS

We thank three anonymous referees for helpful comments on the manuscript. P.B. was supported by a Marie-Skłodowska-Curie individual fellowship (797879-METAGE project) and by Carl Tryggers Foundation project CT 16:344. G.O. was supported by a Spanish Ministry of Science, Innovation and Universities 'Ramón y Cajal' contract (RYC-2016-20656). P.M. and N.M. were funded by Natural Environment Research Council grant NE/R001510/1, and N.M. by European Research Council Advanced Grant 834653.

CONFLICT OF INTEREST

We declare no conflict of interest.

ORCID

Pablo Burraco https://orcid.org/0000-0002-9007-2643
Germán Orizaola https://orcid.org/0000-0002-6748-966X
Pat Monaghan https://orcid.org/0000-0003-2430-0326
Neil B. Metcalfe https://orcid.org/0000-0002-1970-9349

REFERENCES

Abram, P. K., Boivin, G., Moiroux, J., & Brodeur, J. (2017). Behavioural effects of temperature on ectothermic animals: Unifying thermal physiology and behavioural plasticity. *Biological Reviews*, *92*, 1859–1876. https://doi.org/10.1111/brv.12312

Altwegg, R., & Reyer, H. U. (2003). Patterns of natural selection on size at metamorphosis in water frogs. *Evolution*, *57*, 872–882.

Angelier, F., Costantini, D., Blevin, P., & Chastel, O. (2018). Do glucocorticoids mediate the link between environmental conditions and telomere dynamics in wild vertebrates? A review. *General and Comparative Endocrinology*, *256*, 99–111. https://doi.org/10.1016/j.ygcen.2017.07.007

Angilletta, J. R., & Dunham, A. E. (2003). The temperature-size rule in ectotherms: Simple evolutionary explanations may not be general. *American Naturalist*, *162*, 332–342. https://doi.org/10.1086/377187

Angilletta Jr., M. J., Steury, T. D., & Sears, M. W. (2004). Temperature, growth rate, and body size in ectotherms: Fitting pieces of a life-history puzzle. *Integrative and Comparative Biology*, *44*, 498–509.

Aubert, G., & Lansdorp, P. M. (2008). Telomeres and aging. *Physiological Reviews*, *88*, 557–579. https://doi.org/10.1152/physrev.00026.2007

Axelsson, J., Wapstra, E., Miller, E., Rollings, N., & Olsson, M. (2020). Contrasting seasonal patterns of telomere dynamics in response to environmental conditions in the ectothermic sand lizard, *Lacerta agilis*. *Scientific Reports*, *10*, 1–9. https://doi.org/10.1038/s41598-019-57084-5

Badás, E. P., Martínez, J., de Aguilar, R., Cachafeiro, J., Miranda, F., Figuerola, J., & Merino, S. (2015). Ageing and reproduction: Antioxidant supplementation alleviates telomere loss in wild birds. *Journal of Evolutionary Biology*, *28*, 896–905. https://doi.org/10.1111/jeb.12615

Banh, S., Wiens, L., Sotiri, E., & Treberg, J. R. (2016). Mitochondrial reactive oxygen species production by fish muscle mitochondria: Potential role in acute heat-induced oxidative stress. *Comparative Biochemistry and Physiology Part B: Biochemistry and Molecular Biology*, *191*, 99–107. https://doi.org/10.1016/j.cbpb.2015.10.001

Barnes, R. P., Fouquerel, E., & Opresko, P. L. (2018). The impact of oxidative DNA damage and stress on telomere homeostasis. *Mechanisms of Ageing and Development*, *177*, 37–45.

Bateson, M., & Poirier, C. (2019). Can biomarkers of biological age be used to assess cumulative lifetime experience. *Animal Welfare*, *28*, 41–56. https://doi.org/10.7120/09627286.28.1.041

Baudron, A. R., Needle, C. L., Rijnsdorp, A. D., & Tara Marshall, C. (2014). Warming temperatures and smaller body sizes: Synchronous changes in growth of North Sea fishes. *Global Change Biology*, *20*, 1023–1031. https://doi.org/10.1111/gcb.12514

Bentley, B. P., Haas, B. J., Tedeschi, J. N., & Berry, O. (2017). Loggerhead sea turtle embryos (*Caretta caretta*) regulate expression of stress response and developmental genes when exposed to a biologically realistic heat stress. *Molecular Ecology*, *26*, 2978–2992.

Bickford, D. P., Sheridan, J. A., & Howard, S. D. (2011). Climate change responses: Forgetting frogs, ferns and flies? *Trends in Ecology & Evolution*, *26*, 553–554. https://doi.org/10.1016/j.tree.2011.06.016

Blasco, M. A. (2007). Telomere length, stem cells and aging. *Nature Chemical Biology*, *3*, 640. https://doi.org/10.1038/nchembio.2007.38

Burraco, P., Díaz-Paniagua, C., & Gomez-Mestre, I. (2017). Different effects of accelerated development and enhanced growth on oxidative stress and telomere shortening in amphibian larvae. *Scientific Reports*, *7*, 7494. https://doi.org/10.1038/s41598-017-07201-z

Burraco, P., Valdés, A. E., & Orizaola, G. (2020). Metabolic costs of altered growth trajectories across life transitions in amphibians. *Journal of Animal Ecology*, *89*, 855–866. https://doi.org/10.1111/1365-2656.13138

Charnov, E. L., & Ernest, S. M. (2006). The offspring-size/clutch-size trade-off in mammals. *American Naturalist*, *167*, 578–582. https://doi.org/10.1086/501141

Chatelain, M., Drobniak, S. M., & Szulkin, M. (2020). The association between stressors and telomeres in non-human vertebrates: A meta-analysis. *Ecology Letters*, *23*, 381–398. https://doi.org/10.1111/ele.13426

Clutton-Brock, T. H., & Isvaran, K. (2007). Sex differences in ageing in natural populations of vertebrates. *Proceedings of the Royal Society B: Biological Sciences*, *274*, 3097–3104. https://doi.org/10.1098/rspb.2007.1138

Comfort, A. (1963). Effect of delayed and resumed growth on the longevity of a fish (*Lebistes reticulatus*, Peters) in captivity. *Gerontology*, *8*, 150–155. https://doi.org/10.1159/000211216

Costantini, D. (2019). Understanding diversity in oxidative status and oxidative stress: The opportunities and challenges ahead. *Journal of Experimental Biology*, *222*, jeb194688. https://doi.org/10.1242/jeb.194688

Crespi, E. J., Williams, T. D., Jessop, T. S., & Delehanty, B. (2013). Life history and the ecology of stress: How do glucocorticoid hormones influence life-history variation in animals? *Functional Ecology*, *27*, 93–106. https://doi.org/10.1111/1365-2435.12009

Daniali, L., Benetos, A., Susser, E., Kark, J. D., Labat, C., Kimura, M., … Aviv, A. (2013). Telomeres shorten at equivalent rates in somatic tissues of adults. *Nature Communications*, *4*, 1–7. https://doi.org/10.1038/ncomms2602

De Block, M., & Stoks, R. (2008). Compensatory growth and oxidative stress in a damselfly. *Proceedings of the Royal Society B: Biological Sciences*, *275*, 781–785. https://doi.org/10.1098/rspb.2007.1515

Debes, P. V., Visse, M., Panda, B., Ilmonen, P., & Vasemägi, A. (2016). Is telomere length a molecular marker of past thermal stress in wild fish? *Molecular Ecology*, *25*, 5412–5424. https://doi.org/10.1111/mec.13856

Diffenbaugh, N. S., & Field, C. B. (2013). Changes in ecologically critical terrestrial climate conditions. *Science*, *341*, 486–492. https://doi.org/10.1126/science.1237123

Dmitriew, C. M. (2011). The evolution of growth trajectories: What limits growth rate? *Biological Reviews*, *86*, 97–116. https://doi.org/10.1111/j.1469-185X.2010.00136.x

Dugdale, H. L., & Richardson, D. S. (2018). Heritability of telomere variation: It is all about the environment! *Philosophical Transactions of the Royal Society B*, *373*, 20160450. https://doi.org/10.1098/rstb.2016.0450

Fitzpatrick, L. J., Olsson, M., Parsley, L. M., Pauliny, A., Pinfold, T. L., Pirtle, T., … Wapstra, E. (2019). Temperature and telomeres: Thermal treatment influences telomere dynamics through a complex interplay of cellular processes in a cold-climate skink. *Oecologia*, *191*, 767–776. https://doi.org/10.1007/s00442-019-04530-w

Furtado-Filho, O. V., Polcheira, C., Machado, D. P., Mourão, G., & Hermes-Lima, M. (2007). Selected oxidative stress markers in a South American crocodilian species. *Comparative Biochemistry and Physiology Part C: Toxicology & Pharmacology*, *146*, 241–254. https://doi.org/10.1016/j.cbpc.2006.11.017

Gomes, N. M., Shay, J. W., & Wright, W. E. (2010). Telomere biology in Metazoa. *FEBS Letters*, *584*, 3741–3751. https://doi.org/10.1016/j.febslet.2010.07.031

Guerra, C., Zenteno-Savín, T., Maeda-Martínez, A. N., Philipp, E. E. R., & Abele, D. (2012). Changes in oxidative stress parameters in relation to age, growth and reproduction in the short-lived catarina scallop *Argopecten ventricosus* reared in its natural environment. *Comparative Biochemistry and Physiology Part A: Molecular & Integrative Physiology*, *162*, 421–430. https://doi.org/10.1016/j.cbpa.2012.04.018

Gunderson, A. R., Dillon, M. E., & Stillman, J. H. (2017). Estimating the benefits of plasticity in ectotherm heat tolerance under natural thermal variability. *Functional Ecology*, *31*, 1529–1539. https://doi.org/10.1111/1365-2435.12874

Gunderson, A. R., & Stillman, J. H. (2015). Plasticity in thermal tolerance has limited potential to buffer ectotherms from global warming. *Proceedings of the Royal Society B: Biological Sciences*, *282*, 20150401. https://doi.org/10.1098/rspb.2015.0401

Halliwell, B., & Gutteridge, J. M. (2015). *Free radicals in biology and medicine*. New York, NY: Oxford University Press.

Haussmann, M. F., & Heidinger, B. J. (2015). Telomere dynamics may link stress exposure and ageing across generations. *Biology Letters*, *11*, 20150396. https://doi.org/10.1098/rsbl.2015.0396

Haussmann, M. F., & Marchetto, N. M. (2010). Telomeres: Linking stress and survival, ecology and evolution. *Current Zoology*, *56*, 714–727. https://doi.org/10.1093/czoolo/56.6.714

Hoelzl, F., Cornils, J. S., Smith, S., Moodley, Y., & Ruf, T. (2016). Telomere dynamics in free-living edible dormice (*Glis glis*): The impact of hibernation and food supply. *Journal of Experimental Biology*, *219*, 2469–2474.

Hoffmann, A. A., & Sgrò, C. M. (2011). Climate change and evolutionary adaptation. *Nature*, *470*, 479. https://doi.org/10.1038/nature09670

Huey, R. B., Kearney, M. R., Krockenberger, A., Holtum, J. A., Jess, M., & Williams, S. E. (2012). Predicting organismal vulnerability to climate warming: Roles of behaviour, physiology and adaptation. *Philosophical Transactions of the Royal Society B*, *367*, 1665–1679. https://doi.org/10.1098/rstb.2012.0005

IPCC. (2014). *Climate change 2014: Synthesis report. Contribution of working groups I, II and III to the fifth assessment report of the Intergovernmental Panel on Climate Change*. Core Writing Team, R. K. Pachauri, & L. A. Meyer (Eds.). Geneva, Switzerland: IPCC, 151 pp.

Johansson, F., Orizaola, G., & Nilsson-Örtman, V. (2020). Temperate insects with narrow seasonal activity periods can be as vulnerable to climate change as tropical insect species. *Scientific Reports*, *10*, 8822.

Kappenman, K. M., Fraser, W. C., Toner, M., Dean, J., & Webb, M. A. (2009). Effect of temperature on growth, condition, and survival of juvenile shovelnose sturgeon. *Transactions of the American Fisheries Society*, *138*, 927–937. https://doi.org/10.1577/T07-265.1

Kim, S. Y., Noguera, J. C., & Velando, A. (2019). Carry-over effects of early thermal conditions on somatic and germline oxidative damages are mediated by compensatory growth in sticklebacks. *Journal of Animal Ecology*, *88*, 473–483.

Kingsolver, J. G., Diamond, S. E., & Buckley, L. B. (2013). Heat stress and the fitness consequences of climate change for terrestrial ectotherms. *Functional Ecology*, *27*, 1415–1423. https://doi.org/10.1111/1365-2435.12145

Lee, K. P., & Roh, C. (2010). Temperature-by-nutrient interactions affecting growth rate in an insect ectotherm. *Entomologia Experimentalis et Applicata*, *136*, 151–163. https://doi.org/10.1111/j.1570-7458.2010.01018.x

Lee, W. S., Monaghan, P., & Metcalfe, N. B. (2013). Experimental demonstration of the growth rate–lifespan trade-off. *Proceedings of the Royal Society B: Biological Sciences*, *280*, 20122370. https://doi.org/10.1098/rspb.2012.2370

López-Otín, C., Blasco, M. A., Partridge, L., Serrano, M., & Kroemer, G. (2013). The hallmarks of aging. *Cell*, *153*, 1194–1217. https://doi.org/10.1016/j.cell.2013.05.039

McLennan, D., Armstrong, J. D., Stewart, D. C., McKelvey, S., Boner, W., Monaghan, P., & Metcalfe, N. B. (2016). Interactions between parental traits, environmental harshness and growth rate in determining telomere length in wild juvenile salmon. *Molecular Ecology*, *25*, 5425–5438. https://doi.org/10.1111/mec.13857

McLennan, D., Armstrong, J. D., Stewart, D. C., Mckelvey, S., Boner, W., Monaghan, P., & Metcalfe, N. B. (2018). Telomere elongation during early development is independent of environmental temperatures in Atlantic salmon. *Journal of Experimental Biology*, *221*, jeb-178616. https://doi.org/10.1242/jeb.178616

Metcalfe, N. B., & Monaghan, P. (2001). Compensation for a bad start: Grow now, pay later? *Trends in Ecology & Evolution*, *16*, 254–260. https://doi.org/10.1016/S0169-5347(01)02124-3

Metcalfe, N. B., & Monaghan, P. (2003). Growth versus lifespan: Perspectives from evolutionary ecology. *Experimental Gerontology*, *38*, 935–940. https://doi.org/10.1016/S0531-5565(03)00159-1

Monaghan, P. (2014). Organismal stress, telomeres and life histories. *Journal of Experimental Biology*, *217*, 57–66. https://doi.org/10.1242/jeb.090043

Monaghan, P., & Ozanne, S. E. (2018). Somatic growth and telomere dynamics in vertebrates: Relationships, mechanisms and consequences. *Philosophical Transactions of the Royal Society B*, *373*, 20160446. https://doi.org/10.1098/rstb.2016.0446

Mookerjee, S. A., Divakaruni, A. S., Jastroch, M., & Brand, M. D. (2010). Mitochondrial uncoupling and lifespan. *Mechanisms of Ageing and Development*, *131*, 463–472. https://doi.org/10.1016/j.mad.2010.03.010

Morley, S. A., Peck, L. S., Sunday, J. M., Heiser, S., & Bates, A. E. (2019). Physiological acclimation and persistence of ectothermic species under extreme heat events. *Global Ecology and Biogeography*, *28*, 1018–1037. https://doi.org/10.1111/geb.12911

Norin, T., & Metcalfe, N. B. (2019). Ecological and evolutionary consequences of metabolic rate plasticity in response to environmental change. *Philosophical Transactions of the Royal Society B: Biological Sciences*, *374*, 20180180. https://doi.org/10.1098/rstb.2018.0180

Ohlberger, J. (2013). Climate warming and ectotherm body size–From individual physiology to community ecology. *Functional Ecology*, *27*, 991–1001. https://doi.org/10.1111/1365-2435.12098

Olsson, M., & Shine, R. (2002). Growth to death in lizards. *Evolution*, *56*, 1867–1870.

Olsson, M., Wapstra, E., & Friesen, C. (2018a). Ectothermic telomeres: It's time they came in from the cold. *Philosophical Transactions of the Royal Society B: Biological Sciences*, *373*, 20160449. https://doi.org/10.1098/rstb.2016.0449

Olsson, M., Wapstra, E., & Friesen, C. R. (2018b). Evolutionary ecology of telomeres: A review. *Annals of the New York Academy of Sciences*, *1422*, 5–28.

Parmesan, C. (2006). Ecological and evolutionary responses to recent climate change. *Annual Review of Ecology, Evolution, and Systematics*, *37*, 637–669. https://doi.org/10.1146/annurev.ecolsys.37.091305.110100

Pauliny, A., Devlin, R. H., Johnsson, J. I., & Blomqvist, D. (2015). Rapid growth accelerates telomere attrition in a transgenic fish. *BMC Evolutionary Biology*, *15*, 159. https://doi.org/10.1186/s12862-015-0436-8

Pineda-Pampliega, J., Herrera-Dueñas, A., Mulder, E., Aguirre, J. I., Höfle, U., & Verhulst, S. (2020). Antioxidant supplementation slows telomere shortening in free-living white stork chicks. *Proceedings of the Royal Society B: Biological Sciences*, *287*, 20191917. https://doi.org/10.1098/rspb.2019.1917

Price, E. R., Sirsat, T. S., Sirsat, S. K. G., Kang, G., Keereetaweep, J., Aziz, M., … Dzialowski, E. M. (2017). Thermal acclimation in American alligators: Effects of temperature regime on growth rate, mitochondrial function, and membrane composition. *Journal of Thermal Biology*, *68*, 45–54. https://doi.org/10.1016/j.jtherbio.2016.06.016

Reichert, S., Rojas, E. R., Zahn, S., Robin, J. P., Criscuolo, F., & Massemin, S. (2015). Maternal telomere length inheritance in the king penguin. *Heredity*, *114*, 10–16. https://doi.org/10.1038/hdy.2014.60

Reichert, S., & Stier, A. (2017). Does oxidative stress shorten telomeres in vivo? A review. *Biology Letters*, *13*, 20170463.

Richter, T., & von Zglinicki, T. (2007). A continuous correlation between oxidative stress and telomere shortening in fibroblasts. *Experimental Gerontology*, *42*, 1039–1042. https://doi.org/10.1016/j.exger.2007.08.005

Rollings, N., Friesen, C. R., Whittington, C. M., Johansson, R., Shine, R., & Olsson, M. (2019). Sex- and tissue-specific differences in telomere length in a reptile. *Ecology and Evolution*, *9*, 6211–6219. https://doi.org/10.1002/ece3.5164

Rollings, N., Waye, H. L., Krohmer, R. W., Uhrig, E. J., Mason, R. T., Olsson, M., … Friesen, C. R. (2020). Sperm telomere length correlates with blood telomeres and body size in red-sided garter snakes, *Thamnophis sirtalis parietalis*. *Journal of Zoology*, in press. https://doi.org/10.1111/jzo.12789

Ruthsatz, K., Peck, M. A., Dausmann, K. H., Sabatino, N. M., & Glos, J. (2018). Patterns of temperature induced developmental plasticity in anuran larvae. *Journal of Thermal Biology*, *74*, 123–132. https://doi.org/10.1016/j.jtherbio.2018.03.005

Sabharwal, S., Verhulst, S., Guirguis, G., Kark, J. D., Labat, C., Roche, N. E., … Aviv, A. (2018). Telomere length dynamics in early life: The blood-and-muscle model. *The FASEB Journal*, *32*, 529–534. https://doi.org/10.1096/fj.201700630r

Salin, K., Auer, S. K., Rey, B., Selman, C., & Metcalfe, N. B. (2015). Variation in the link between oxygen consumption and ATP production, and its relevance for animal performance. *Proceedings of the Royal Society B: Biological Sciences*, *282*, 20151028. https://doi.org/10.1098/rspb.2015.1028

Salin, K., Villasevil, E. M., Anderson, G. J., Lamarre, S. G., Melanson, C. A., McCarthy, I., … Metcalfe, N. B. (2019). Differences in mitochondrial efficiency explain individual variation in growth performance. *Proceedings of the Royal Society B: Biological Sciences*, *286*, 20191466. https://doi.org/10.1098/rspb.2019.1466

Seebacher, F., White, C. R., & Franklin, C. E. (2015). Physiological plasticity increases resilience of ectothermic animals to climate change. *Nature Climate Change*, *5*, 61. https://doi.org/10.1038/nclimate2457

Shine, R., Barrott, E. G., & Elphick, M. J. (2002). Some like it hot: Effects of forest clearing on nest temperatures of montane reptiles. *Ecology*, *83*, 2808–2815. https://doi.org/10.1890/0012-9658(2002)083[2808:SLIHEO]2.0.CO;2

Shoo, L. P., Olson, D. H., McMenamin, S. K., Murray, K. A., Van Sluys, M., Donnelly, M. A., … Hero, J.-M. (2011). Engineering a future for amphibians under climate change. *Journal of Applied Ecology*, *48*, 487–492. https://doi.org/10.1111/j.1365-2664.2010.01942.x

Simide, R., Angelier, F., Gaillard, S., & Stier, A. (2016). Age and heat stress as determinants of telomere length in a long-lived fish, the Siberian sturgeon. *Physiological and Biochemical Zoology*, *89*, 441–447. https://doi.org/10.1086/687378

Smith, S. M., Nager, R. G., & Costantini, D. (2016). Meta-analysis indicates that oxidative stress is both a constraint on and a cost of growth. *Ecology and Evolution*, *6*, 2833–2842. https://doi.org/10.1002/ece3.2080

Somero, G. N. (2010). The physiology of climate change: How potentials for acclimatization and genetic adaptation will determine 'winners' and 'losers'. *Journal of Experimental Biology*, *213*, 912–920. https://doi.org/10.1242/jeb.037473

Speakman, J. R. (2005). Body size, energy metabolism and lifespan. *Journal of Experimental Biology*, *208*, 1717–1730. https://doi.org/10.1242/jeb.01556

Stahlschmidt, Z. R., French, S. S., Ahn, A., Webb, A., & Butler, M. W. (2017). A simulated heat wave has diverse effects on immune function and oxidative physiology in the corn snake (*Pantherophis guttatus*). *Physiological and Biochemical Zoology*, *90*, 434–444.

Stark, G., & Meiri, S. (2018). Cold and dark captivity: Drivers of amphibian longevity. *Global Ecology and Biogeography*, *27*, 1384–1397. https://doi.org/10.1111/geb.12804

Stark, G., Tamar, K., Itescu, Y., Feldman, A., & Meiri, S. (2018). Cold and isolated ectotherms: Drivers of reptilian longevity. *Biological Journal of the Linnean Society*, *125*, 730–740. https://doi.org/10.1093/biolinnean/bly153

Sunday, J. M., Bates, A. E., Kearney, M. R., Colwell, R. K., Dulvy, N. K., Longino, J. T., & Huey, R. B. (2014). Thermal-safety margins and the necessity of thermoregulatory behavior across latitude and elevation. *Proceedings of the National Academy of Sciences of the United States of America*, *111*, 5610–5615. https://doi.org/10.1073/pnas.1316145111

Tian, X., Seluanov, A., & Gorbunova, V. (2017). Molecular mechanisms determining lifespan in short-and long-lived species. *Trends in Endocrinology & Metabolism*, *28*, 722–734. https://doi.org/10.1016/j.tem.2017.07.004

Tricola, G. M., Simons, M. J. P., Atema, E., Boughton, R. K., Brown, J. L., Dearborn, D. C., … Haussmann, M. F. (2018). The rate of telomere loss is related to maximum lifespan in birds. *Philosophical Transactions of the Royal Society B*, *373*, 20160445. https://doi.org/10.1098/rstb.2016.0445

Turbill, C., Ruf, T., Smith, S., & Bieber, C. (2013). Seasonal variation in telomere length of a hibernating rodent. *Biology Letters*, *9*, 20121095. https://doi.org/10.1098/rsbl.2012.1095

Ujvari, B., Biro, P. A., Charters, J. E., Brown, G., Heasman, K., Beckmann, C., & Madsen, T. (2017). Curvilinear telomere length dynamics in a squamate reptile. *Functional Ecology*, *31*, 753–759. https://doi.org/10.1111/1365-2435.12764

Velando, A., Noguera, J. C., da Silva, A., & Kim, S. Y. (2019). Redox-regulation and life-history trade-offs: Scavenging mitochondrial ROS improves growth in a wild bird. *Scientific Reports*, *9*, 2203. https://doi.org/10.1038/s41598-019-38535-5

Wilbourn, R. V., Moatt, J. P., Froy, H., Walling, C. A., Nussey, D. H., & Boonekamp, J. J. (2018). The relationship between telomere length and mortality risk in non-model vertebrate systems: A meta-analysis. *Philosophical Transactions of the Royal Society B: Biological Sciences*, *373*, 20160447. https://doi.org/10.1098/rstb.2016.0447

Yang, L. H., Huang, H., & Wang, J. J. (2010). Antioxidant responses of citrus red mite, *Panonychus citri* (McGregor) (Acari: Tetranychidae), exposed to thermal stress. *Journal of Insect Physiology*, *56*, 1871–1876. https://doi.org/10.1016/j.jinsphys.2010.08.006

Young, A. J. (2018). The role of telomeres in the mechanisms and evolution of life-history trade-offs and ageing. *Philosophical Transactions of the Royal Society B: Biological Sciences*, *373*, 20160452.

Zhang, Q., Han, X., Hao, X., Ma, L., Li, S., Wang, Y., & Du, W. (2018). A simulated heat wave shortens the telomere length and lifespan of a desert lizard. *Journal of Thermal Biology*, *72*, 94–100. https://doi.org/10.1016/j.jtherbio.2018.01.004

Zhao, M., Klaassen, C. A., Lisovski, S., & Klaassen, M. (2019). The adequacy of aging techniques in vertebrates for rapid estimation of population mortality rates from age distributions. *Ecology and Evolution*, *9*, 1394–1402. https://doi.org/10.1002/ece3.4854

How to cite this article: Burraco P, Orizaola G, Monaghan P, Metcalfe NB. Climate change and ageing in ectotherms. *Glob Change Biol*. 2020;26:5371–5381. https://doi.org/10.1111/gcb.15305

ARTICLES FOR FACULTY MEMBERS

GLOBAL WARMING EFFECTS ON ECTOTHERM SPECIES

Title/Author	**Evidence of stronger range shift response to ongoing climate change by ectotherms and high-latitude species / Ramalho, Q., Vale, M. M., Manes, S., Diniz, P., Malecha, A., & Prevedello, J. A**
Source	***Biological Conservation*** **Volume 279 (2023) 109911 Pages 1-9** **https://doi.org/10.1016/j.biocon.2023.109911** **(Database: ScienceDirect)**

Biological Conservation 279 (2023) 109911

Contents lists available at ScienceDirect

Biological Conservation

journal homepage: www.elsevier.com/locate/biocon

Evidence of stronger range shift response to ongoing climate change by ectotherms and high-latitude species

Quezia Ramalho [a,*], Mariana M. Vale [b], Stella Manes [c], Paula Diniz [c], Artur Malecha [a], Jayme A. Prevedello [d]

[a] Programa de Pós-Graduação em Ecologia e Evolução (PPGEE), Universidade do Estado do Rio de Janeiro, Rio de Janeiro, RJ 20550900, Brazil
[b] Departamento de Ecologia, Universidade Federal do Rio de Janeiro (UFRJ), Rio de Janeiro, RJ, Brazil
[c] Programa de Pós-Graduação em Ecologia (PPGE), Universidade Federal do Rio de Janeiro (UFRJ), Rio de Janeiro, RJ, Brazil
[d] Departamento de Ecologia, Universidade do Estado do Rio de Janeiro, Rio de Janeiro, RJ 20550900, Brazil

ARTICLE INFO

Original content: Climate-induced range shifts description (Original data)

Keywords:
Climate change
Distributional shift
Endotherms
Global change
Observed change
Terrestrial vertebrates

ABSTRACT

A well-known response of biodiversity to ongoing climate change is range shifts towards cooler temperature areas. Still, a major gap remains in the understanding of the latitudinal component and the differences between ectotherms and endotherms in these responses. The accumulation of evidence of observed climate tracking over the years provides an opportunity to close these gaps. Here, we evaluate latitude and species' thermoregulation as explanatory variables in climate-induced range shifts. We conducted an extensive literature review, selecting empirical studies that provided information about the direction and/or magnitude of climate-induced latitudinal and altitudinal range shifts of almost 400 species. We built linear mixed models to analyze both categorical and continuous distribution data. We showed that many species consistently shifted their ranges towards the poles or higher altitudes. Most importantly, we found that the higher the latitude, the greater the latitudinal range shift, and that ectotherms show stronger range shift responses to ongoing climate change than endotherms. Our findings show that range shifts are already occurring as a result of mild global warming. As global warming intensifies, species might soon reach hard adaptation limits, where shifting ranges is no longer an option, especially for ectotherms and high-latitude species.

1. Introduction

Biodiversity has faced many challenges in the last century, which are likely to intensify in the future. Countless studies have focused on projecting the potential impacts of different human-induced environmental changes on biodiversity, providing worrisome risk estimates for the future of the planet (e.g. Manes and Vale, 2022; Ramalho et al., 2021; Segan et al., 2016; Tourinho et al., 2021; Warren et al., 2018). Among the main drivers of biodiversity change, climate change has received particular attention, as it is expected to become a major threat in the near future (Pörtner et al., 2021). Most studies have focused on the potential future changes to species' geographical distribution because, as climate shifts, so will species towards suitable climates, a phenomenon known as 'climate tracking'. These predictions indicate a likely severe shrinkage and displacement of species distributions (Chaudhary et al., 2021; e.g. Manes et al., 2021; Urban, 2018).

Although ongoing climate change is predicted to put biodiversity at risk in the future, there is strong evidence that the so-called future has already begun. The average global temperature has already increased ~1.1 °C as compared to pre-industrial times (Allan et al., 2021), and many impacts on biodiversity have already been observed and quantified (Lane et al., 2012; e.g. Pacifici et al., 2017; Parmesan et al., 2003). Studies focusing on ongoing climate change provide concrete empirical evidence of the impact that has already been inflicted upon species (Parmesan and Yohe, 2003). Observed impacts, however, are much harder to identify, in part due to the difficulty in attributing observed changes in biodiversity to climate change as opposed to other stressors such as overexploitation or habitat loss (Cramer et al., 2014). Still, there is growing evidence of adverse impacts of climate change on biodiversity, including changes in ecosystem structure, species' phenology and abundance, species range shifts, and the first climate change-driven species extinctions (Parmesan and Yohe, 2003; Pörtner et al., 2022). Here, we aim to gather evidence of species range shifts due to ongoing climate change. In general, we expect that species are shifting their

* Corresponding author.
E-mail address: queziaramalho@gmail.com (Q. Ramalho).

https://doi.org/10.1016/j.biocon.2023.109911
Received 28 September 2022; Received in revised form 6 January 2023; Accepted 13 January 2023
Available online 1 February 2023

distribution to the poles and to higher altitudes, to compensate for increasing temperatures (Fig. 1).

The impact of climate change is likely to vary among species. Whereas some species can physiologically alter their metabolic rates and body temperature to endure wider temperature fluctuations (i.e. endotherms, e.g. mammals; Boyles et al., 2011), others are exclusively limited to behavioral strategies to try to escape increasing temperatures (i.e. ectotherms, e.g. amphibians and reptiles; Walther et al., 2002). Thus, the need to change behavior or environments to reduce their body temperature renders ectotherms potentially more vulnerable to climate change (Dillon et al., 2010). Such differences in the ability to cope with climate change can influence their range shift responses (Deutsch et al., 2008; Khaliq et al., 2017). Therefore, it is reasonable to expect that ectotherms would have to track climate for farther distances than endotherms (Fig. 1). Only one study to date has assessed differences between endotherms and ectotherms in observed range shift response to climate change, not finding differences in response between the two (Lenoir et al., 2020). The study, however, was not focused on the difference in response between ectotherms and endotherms, but on marine and terrestrial species. The study grouped species from both environments in the ectotherms versus endotherms comparison, including both vertebrates and invertebrates. Here, we focused specifically on the differences between endotherms and ectotherms' response to climate change, narrowing our comparison to terrestrial vertebrates (amphibians, reptiles, and mammals).

Besides thermoregulation, ectotherms and endotherms in different latitudes may also display different responses because temperate and polar regions are experiencing higher warming than tropical ones (Allan et al., 2021). Thus, a stronger response to climate change can be expected for high-latitude species. However, the literature does not show a clear trend in that regard. Although there are a lot of studies on climate-induced phenological responses (MacLean and Beissinger, 2017 e.g. Parmesan, 2007; Root et al., 2003), the influence of latitude remains unambiguous. For example, whereas the global review of Root et al. (2003) found a stronger phenological response in high-latitude species, Parmesan (2007) did not find any latitudinal trend in species' phenology. However, few studies evaluated the influence of latitude on range shifts, although range shift responses are particularly well-studied (Urban, 2018), with species moving towards higher elevations and latitudes in search of cooler climates conditions (Urban, 2018). Most studies, however, focus on specific taxa (e.g. Chen et al., 2011 for insects; Kirchman and Van Keuren, 2017 for birds; Uher-Koch et al., 2021 for marine species). We know of only one global review addressing the influence of latitude on range shifts, focused on altitudinal shifts only, which showed a stronger response in tropical species (see Freeman et al., 2021). Surprisingly, there are no review studies to date addressing the influence of latitude on latitudinal range shifts themselves. Thus, although range shifts in response to climate change are well studied and documented, a major gap remains in the understanding of the latitudinal component of these responses.

The accumulation of evidence of observed range shift responses to ongoing climate change over the years provides an opportunity to close these knowledge gaps. Here, we present the result of a comprehensive effort to detect altitudinal and latitudinal range shifts in responses to climate change, splitting the analysis between endotherm and ectotherm terrestrial vertebrates, and testing, for the first time, the influence of latitude in both responses. This study has important implications for understanding how species distribution has already been impacted by ongoing climate changes, and what conservation strategies can be used to increase their resilience.

2. Material and methods

2.1. Data compilation, extraction, and standardization

We did an extensive literature search through the ISI Web of Science – Core Collection (Clarivate Analytics) database. We used terms such as "climate change", "range", and "distribution" to find studies that focused exclusively on the observed impacts of climate change on species distribution. However, due to their methodological and temporal limitations, such empirical studies are scarcer in the literature compared to studies that assess projected impacts for the future. Therefore, we excluded in our search terms referring to climate modeling studies, such as "species distribution modeling" or "ecological niche modeling" and "glacial periods" since these are also the result of modeling efforts. The search was performed on May 11th 2021, considering the "title, abstract, and keywords" search sections of published studies regardless of the year. Then, we refined the search considering only Article and Early

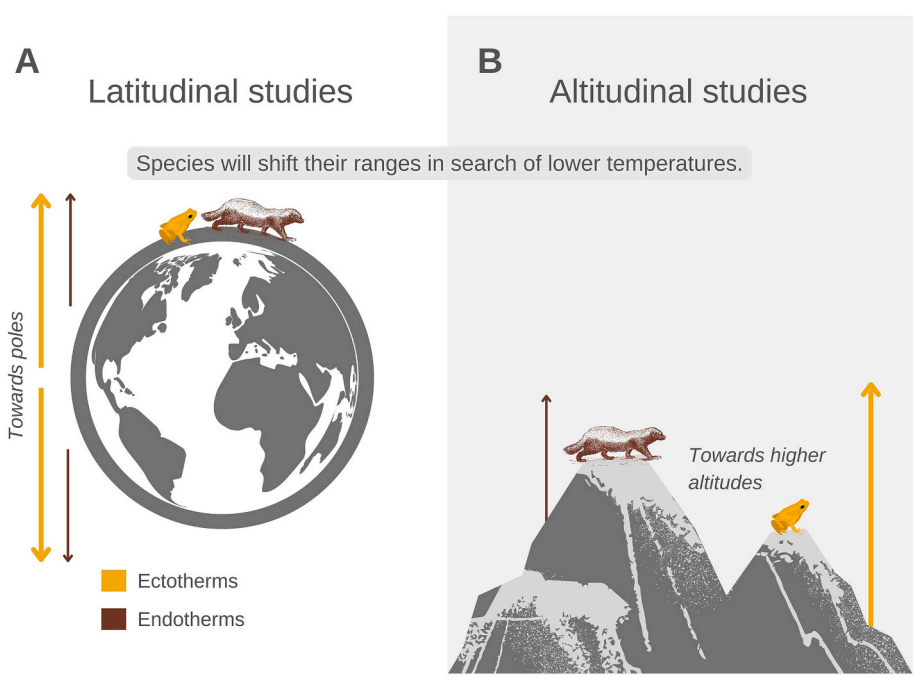

Fig. 1. Conceptual figure showing the expected direction of species climate-induced range shifts. The yellow arrows represent ectothermic species, and the brown arrows represent endothermic species. The thickness and size of the arrows illustrate the intensity of the expected changes. Thus, the greater the thickness and size, the greater the intensity of the shifts. A) Latitudinal range shifts. B) Altitudinal range shifts. (For interpretation of the references to color in this figure legend, the reader is referred to the web version of this article.)
©Macrovector, Canva Original Graphics, Color Vectors, and Vintage Illustrations via Canva.com

Access in the document type.

We included in our literature review studies that meet the following criteria: (1) explicitly assessed observed climatic changes; (2) assessed the impacts of climate change on the distribution of non-volant terrestrial vertebrates; (3) assessed species range shifts through the quantification of the displacement (in units of distance) for a given period; and (4) provided continuous or categorical data reporting range shifts, e.g. the species has moved 50 m/decade (continuous) or the species has expanded its occurrence, occupying higher altitudes (categorical). Additionally, we also included data about terrestrial non-volant vertebrates from the bibliographic review by Parmesan and Yohe (2003) and the articles used in the bibliographic review by Taheri et al. (2021). Of these, only the articles used in Taheri et al. (2021) provided data on species range shifts in response to climate change.

We defined two major categories to exclude articles during our search: (1) studies that did not have information about non-volant terrestrial vertebrates, and (2) studies that did not assess species range shifts in response to observed climate change. Therefore, we excluded: all Species Distribution Modeling (SDM) studies for the past and future; studies that only assessed changes in abundance and/or phenological characteristics but did not assess range shifts; studies that did not assess climate changes; studies that assessed range shifts but did not attribute it to climate change; and studies that did not present measurable results. We focused on non-volant terrestrial vertebrates because there are many more studies evaluating birds' distribution shifts than other terrestrial vertebrates, which could bias the analysis, and also because birds have large dispersal and migration ability, transiting among greater distances than non-volant terrestrial vertebrates. Indeed, the majority of studies evaluate migratory species, with large annual variation between their reproduction and winter sites (e.g. Curley et al., 2020; Easterling et al., 2000; Walther et al., 2002), which hampers differentiate them from changes in the long-term distribution.

To evaluate how species changed their distribution in response to climate change, we extracted observations from the articles considering the smallest possible taxonomic unit. The majority of studies provided data separately for each species (e.g. Botts et al., 2015; Enriquez-Urzelai et al., 2019), but some only provided data for groups of species, such as the taxonomic group (e.g. "Mammalia" or "Amphibia and Squamata" in Hickling et al., 2006) or family (e.g. Moreno-Rueda et al., 2012). Hereafter, we refer to the data obtained for the lowest taxonomic units available as "observations". We extracted the following information from the articles: a) Temperature regulation (ectothermic or endothermic species); b) Duration of the study (in years; when the study had two or more sampling periods, we considered the last year of the last period minus the last year of the first period); c) Direction of change (upward or downward for altitudinal studies and towards the poles or the equator for latitudinal studies); d) Variation in range extent (expansion, contraction or no change); and e) Magnitude of changes in distribution limits (in m/decade or km/decade).

We standardized the magnitude of changes in the distribution limits for all species to km/decade for latitudinal or m/decade for altitudinal studies, following Parmesan and Yohe (2003). We also considered changes polewards or upwards to be positive values and changes towards the equator or downwards to be negative values. In addition, to assess the distribution of studies across the globe, we extracted the approximate average geographic coordinates considering the location provided by the study, using Google Earth. We plotted a map with the distributions of the altitudinal studies and the latitudinal studies in QGIS (Fig. 2).

2.2. Data analysis

For all analyses, we transformed the latitude of each study into absolute latitude since the focus was to analyze the distance from the Equator regardless of the Hemisphere (North or South). For the analysis of categorical range shifts, we generated two binomial dependent variables, one representing the occurrence of a change in distribution (changed = 1, not changed = 0) and the other the type of change (expanded = 1, contracted = 0). Thus, we created two binomial models, one for each dependent variable:

Model 1. Occurrence of change (changed/not changed) ~ absolute latitude + thermoregulation (ectothermic/endothermic).

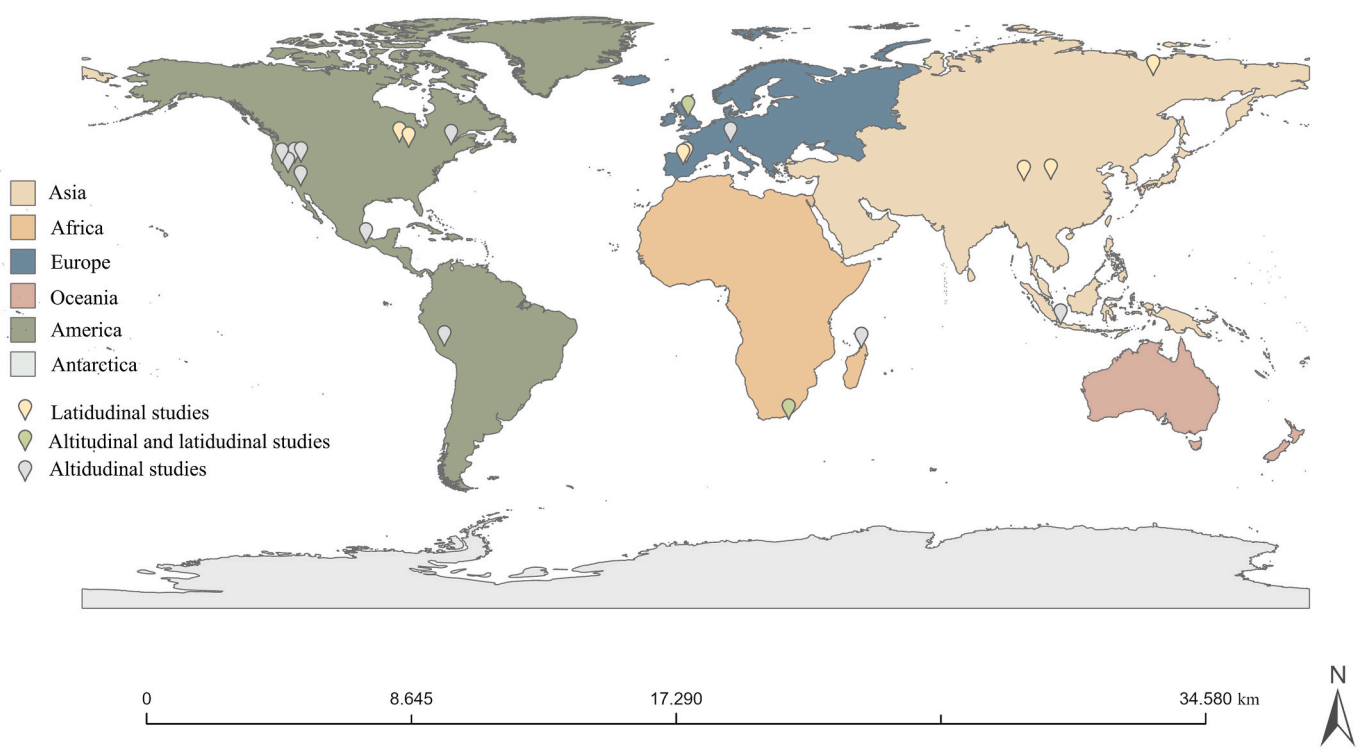

Fig. 2. Global distribution of altitudinal (n = 13) and latitudinal studies (n = 9).

Model 2. Type of change (expanded/contracted) ~ absolute latitude + thermoregulation (ectothermic/endothermic).

Both models included study identity (ID) as a random factor. This inclusion allowed controlling for the non-independence of multiple data from the same study and for the methodological variability among studies, which is known to affect range shift responses (Lenoir et al., 2020). Therefore, we fitted the two models to the data in the form of generalized linear mixed-effects models, with a binomial error distribution, using the 'nlme' package in the R 4.0.4 environment (Pinheiro et al., 2021; R. Core Team, 2021). We used these two models for both altitudinal and latitudinal analyses.

For the analysis of continuous range shifts, we used only the observations that presented numerical estimates (quantitative values) representing the magnitude of the range shift (403 altitudinal and 213 latitudinal observations). First, considering all values from all studies, we calculated the mean (+standard deviation; SD) range shift in km/decade (latitudinal studies) or m/decade (altitudinal studies). Then, we built a generalized linear mixed-effect model, assuming a normal error distribution (Gaussian), with the value of the change in the species' range (in m/decade for altitudinal data and km/decade for latitudinal data) as a function of absolute latitude and temperature regulation (ectothermic/endothermic) as fixed factors:

Model 3. Magnitude of change (numerical value) ~ absolute latitude + thermoregulation (ectothermic/endothermic).

Here, we also included ID as a random factor to control the non-independence of multiple data from the same study. Moreover, to test whether the patterns observed for ectothermic species were consistent for both amphibians and reptiles, we built an alternative version of Model 3, replacing thermoregulation (ectothermic/endothermic) by taxonomic group (amphibians, reptiles, or mammals). This alternative model showed that the two ectothermic groups do indeed respond similarly (compare Figs. 3 and 5 with Figs. A1, A2, and A3, respectively).

Finally, for all models, we also tested for a potential interaction between latitude and thermoregulation. The interaction terms, however, were always non-significant for all models. Therefore, we only kept the additive models. We performed all analyses in R 4.0.4 (R. Core Team, 2021).

3. Results

3.1. Literature search results

After our extensive literature review, we found 1916 articles (1888 from Web of Science, 4 from Parmesan and Yohe, 2003; and 24 from Taheri et al., 2021). Of these, 1279 were excluded for not assessing species range shifts, 130 for not addressing non-volant terrestrial vertebrates, and 209 were excluded for both reasons. At the end, only 20 studies were retained for the analysis, which is not surprising, given the difficulty in recording and attributing impacts of climate change on biodiversity (Pacifici et al., 2017). The studies, however, generated 669 range shift observations for almost 400 species (some species had more than one observation and some observations included more than one species; see Table A1). There was a clear geographic bias in the studies towards the Northern Hemisphere (Fig. 2). Eleven studies evaluated altitudinal range shifts in non-volant terrestrial vertebrates, seven evaluated latitudinal shifts, and two evaluated both altitudinal and latitudinal shifts (Table A1; Fig. 2). Eight assessed ectothermic species (amphibians and reptiles), 11 assessed endothermic species (non-volant terrestrial mammals), and one assessed both ectothermic and endothermic species. From these studies, we obtained a comparable number of observations between endotherms and ectotherms, but with a predominance of altitudinal range shift observations (Table A1, see Fig. A1 and Research Data). For endotherms, we found an expressive predominance of altitudinal shifts, whereas for ectotherms the amount of

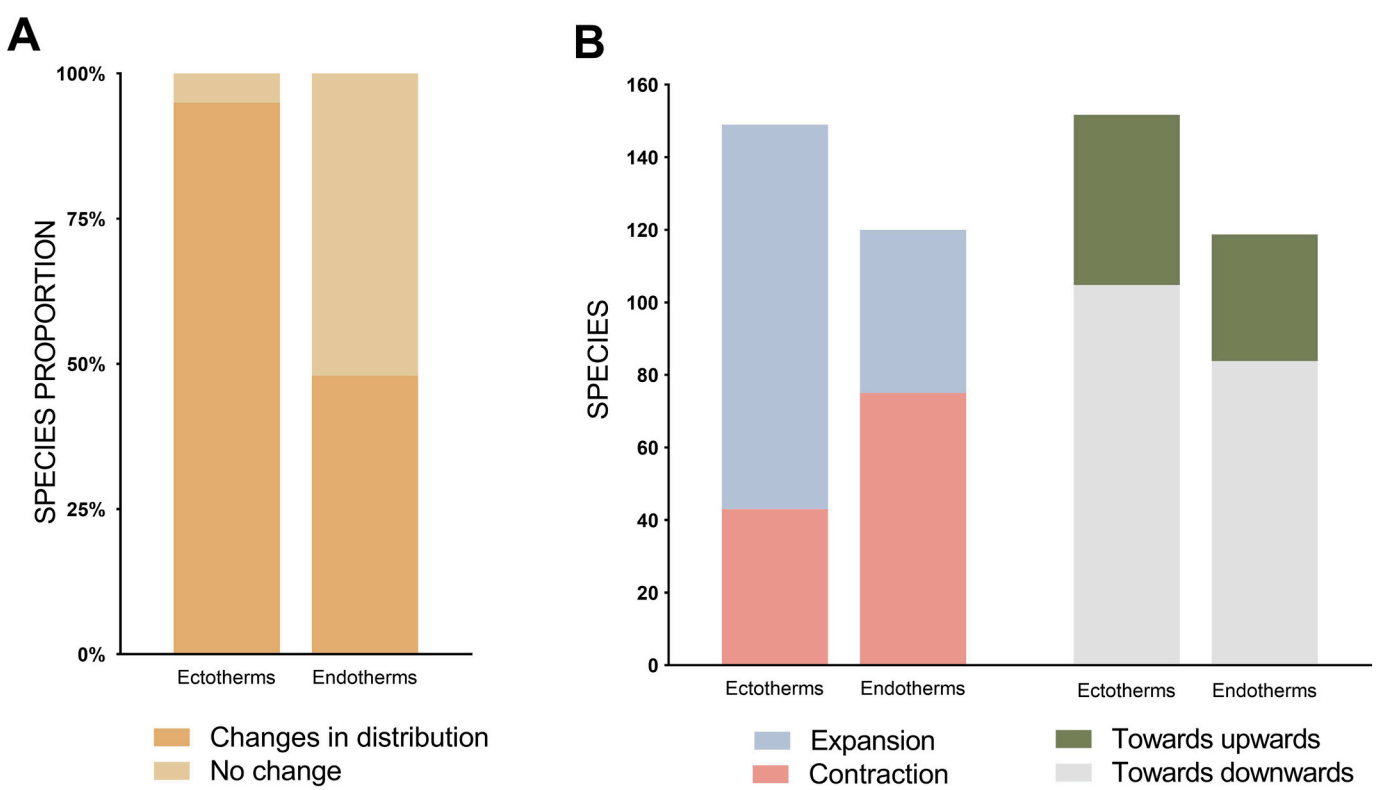

Fig. 3. Impact of climate change on the altitudinal range of species. A) Proportion of endothermic and ectothermic species that have undergone altitudinal range shifts. The number in parentheses indicates the total number of evaluated species. B) Number of endothermic and ectothermic species that have undergone altitudinal range shifts, indicating how many suffered expansions and how many suffered contractions in altitudinal range, as well as whose range displaced towards the top or base of the mountain.

altitudinal and latitudinal shifts was similar (Table A1; see Fig. A1 and Research Data).

3.2. Altitudinal studies

For the categorical data, the direction of altitudinal range shifts was predominantly upward, as expected (n = 189; Fig. 3B), although that movement did not produce a trend in terms of range extent, with 151 species expanding their range, 140 not showing any change and 118 contracting their range (Fig. 3B). Most ectotherms (65.6 %, n = 105) moved upwards, while most endotherms (45.4 %, n = 132) did not show range shifts (Fig. 3A). Altitudinal range shifts were influenced by thermoregulation (endotherms/ectotherms) but not by latitude (Table A2). The probability of altitudinal shifting was higher for ectotherms than for endotherms (Fig. 4A), and ectotherms were more likely to expand their altitudinal range (Fig. 4B).

The continuous data showed similar trends. The mean altitudinal range shift was 23.7 m/decade (±97.9 SD), with a large variability of responses among species. The magnitude of altitudinal change was significantly affected by thermoregulation (endotherms/ectotherms; p = 0.02; Table A3; Fig. 4C) but, again, not latitude (p = 0.29; Table A3). The mean altitudinal shift of ectotherms was 46.0 (±145.0) m/decade, but only 9.96 (±45.8) m/decade for endotherms.

3.3. Latitudinal studies

For the categorical data, the direction of latitudinal range shifts varied widely among species, but most moved poleward, as expected (Fig. 5B). Although the direction of the shift was similar between ectotherms and endotherms (Fig. 5B), latitudinal range shifts were more common in ectotherms (n = 168, 93.3 % of the species) than in endotherms (n = 24, 63.2 % of the species; Fig. 5A). Not surprisingly, therefore, latitudinal range shift probability was higher for ectothermic than endothermic species (Table A4; Fig. 6A). Considering range extent, however, the probability of species contracting or expanding their latitudinal ranges was similar for both groups (Table A4).

The continuous data showed a mean latitudinal shift of 4.0 km/decade (±46.1 SD), with a high variability of responses among species. The mean latitudinal changes were similar for ectothermic (3.9 ± 46.2 km/decade) and endothermic species (4.64 ± 45.9 km/decade). The magnitude of latitudinal shift increased significantly with latitude (Fig. 5B) but did not differ significantly between ectothermic and endothermic species (p = 0.83; Table A5). As there were few observations at latitudes >60°, we performed a bootstrap analysis to test the significance of the latitudinal effect further. This complementary analysis confirmed that the effect of latitude was statistically significant (mean slope for latitude = 3.13, 95 % CI = 0.51–4.94).

4. Discussion

After an extensive literature review, we compiled >600 observations for hundreds of species, with solid evidence that many are moving uphill and towards the poles in response to climate change. Although this is a well-known pattern, here, we provide, for the first time, a systematic review that supplies evidence of the difference in response between endotherms and ectotherms, showing that ectothermic species are more prone to shift their ranges than endotherms. Moreover, we tested, for the first time, latitude as an explanatory variable for species' latitudinal distribution shifts, and showed that high-latitude species are shifting their distribution faster. Despite the possible methodological differences among individual studies, we found clear trends in altitudinal and latitudinal range shifts of ectothermic and endothermic species in response to ongoing climate change. Our study reinforces the need for conservation strategies to safeguard species from the impacts of climate change, especially ectothermic and high-latitude species.

Through this review, we identified some geographic and taxonomic

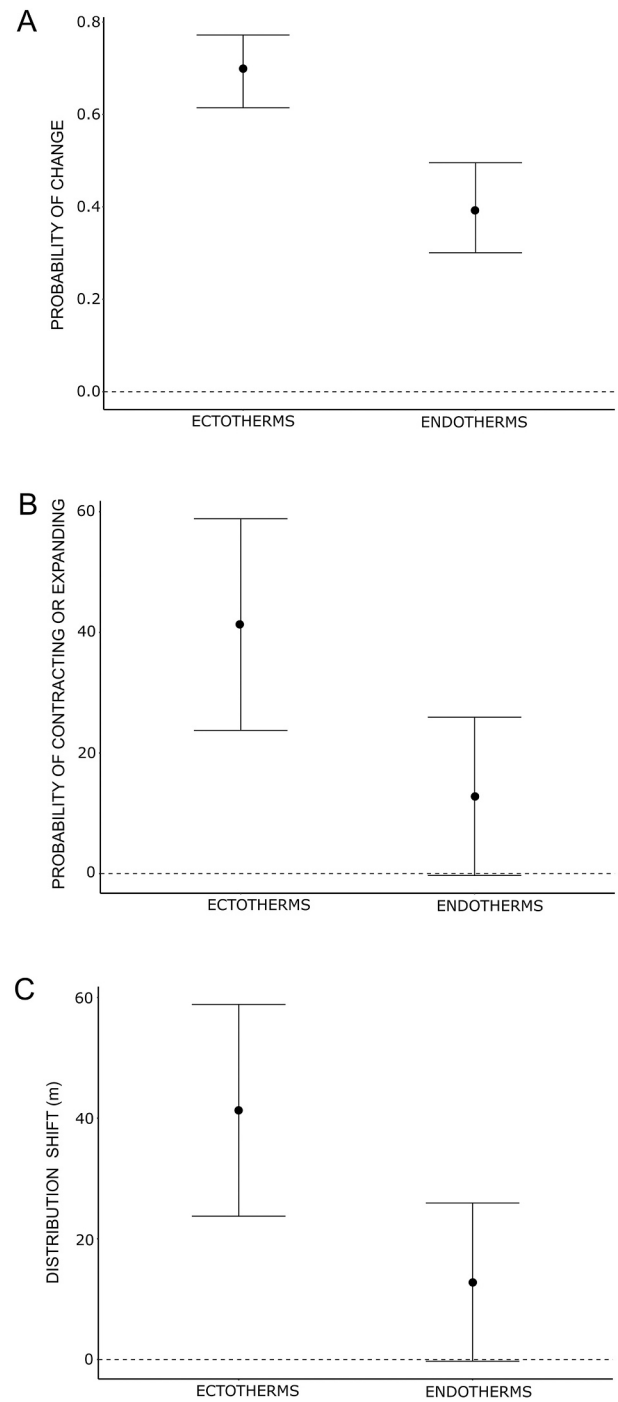

Fig. 4. Altitudinal range shifts. (A) Probability of endotherms and ectotherms shifting their altitudinal range. Positive values on the y-axis indicate the probability of the species' altitudinal range shift; the horizontal line shows the absence of probability of range shift (y = 0). (B) Probability of endotherms and ectotherms contracting or expanding their altitudinal range. Values on the y-axis indicate the probability that species will contract or expand their altitudinal range; the horizontal line shows the absence of probability range shift (y = 0). Both ectothermic and endothermic species showed significant results. There was a difference between the two groups, with a higher probability of expansion for the ectothermic species. (C) Response of endothermic and ectothermic species in altitudinal studies. Positive values on the y-axis indicate upward species displacements (in meters) and negative values indicate downward species displacements; the horizontal line shows no range shift (y = 0). The points represent mean changes between ectothermic and endothermic species and bars represent the 95 % confidence intervals. There was a significant response when comparing ectothermic and endothermic species.

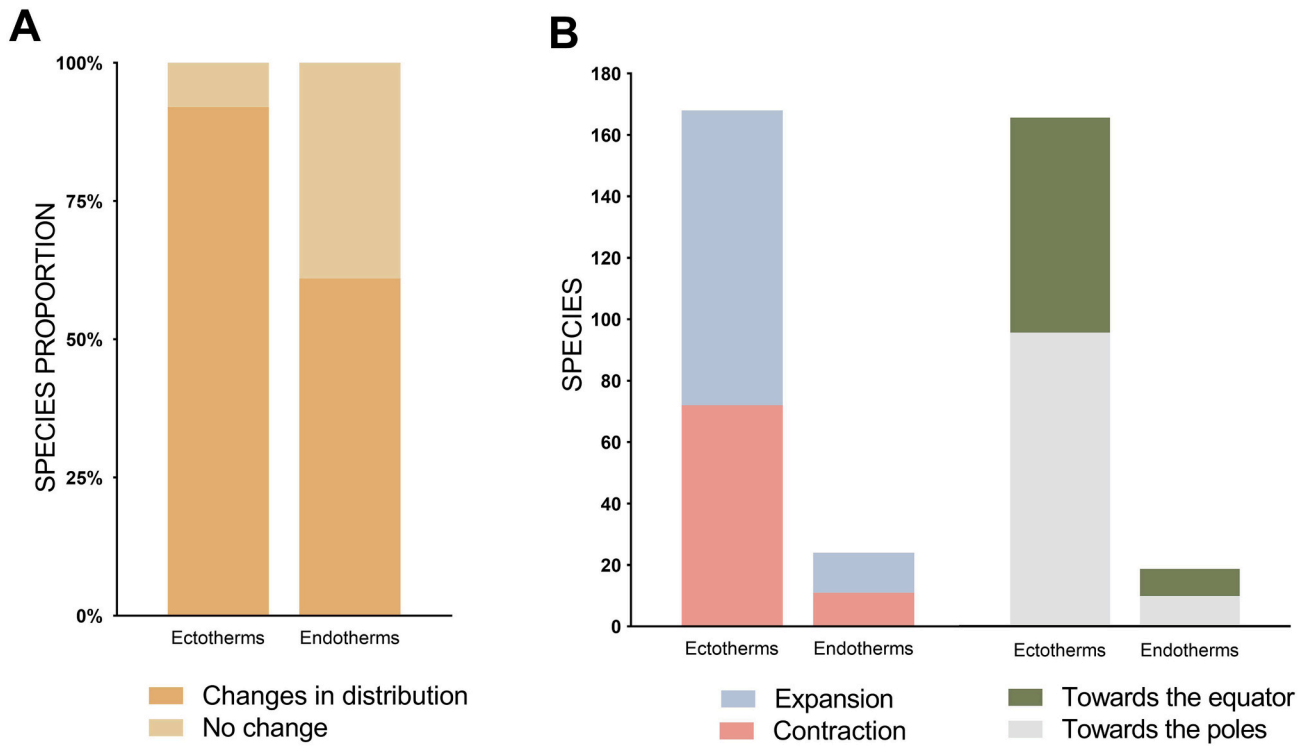

Fig. 5. Impact of climate change on the latitudinal range of species. A) Proportion of endothermic and ectothermic species that had undergone latitudinal range shifts. The number in parentheses indicates the total number of evaluated species. B) Number of endothermic and ectothermic species that have undergone latitudinal range shifts, indicating how many suffered expansions and how many suffered contractions in the range and whose range was displaced towards the equator or the poles.

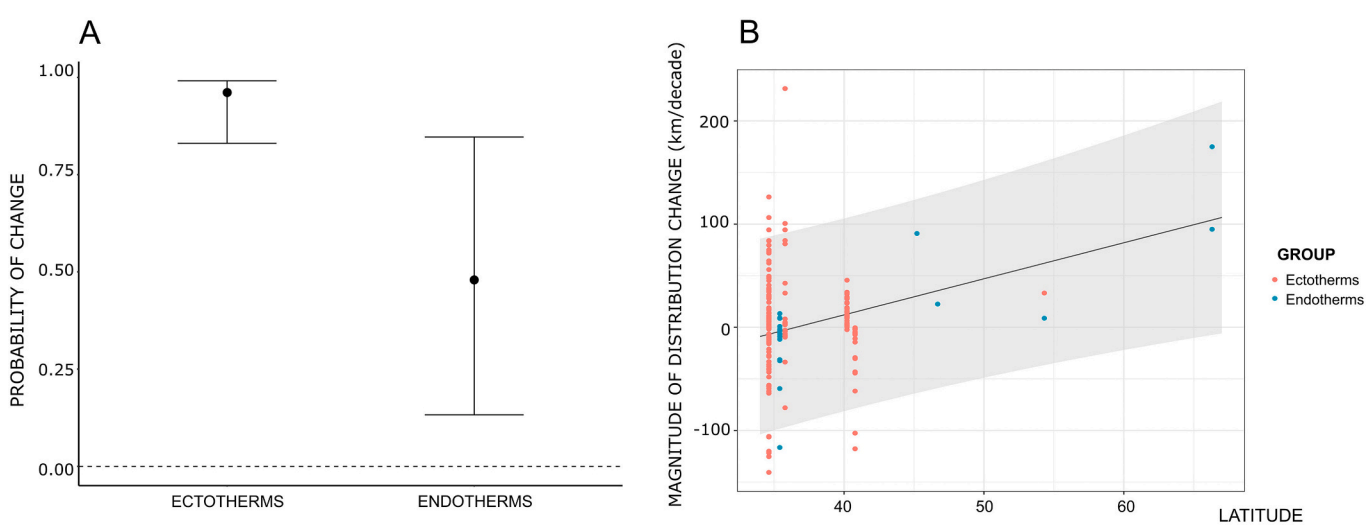

Fig. 6. Latitudinal range shifts. (A) Probability of ectotherms and endotherms shifting their latitudinal range in response to climate change. (B) Latitude effect on the magnitude of latitudinal range shift (in km/decade). Positive values in the y-axis indicate species displacements towards the poles in kilometers, and the negative values indicate species displacements towards the equator. The x-axis corresponds to the absolute latitude. Lines show the mean and the 95 % confidence interval.

biases and gaps. First, there is a strong geographical bias in studies towards the Northern Hemisphere, a pattern already identified in other studies (Feeley et al., 2017; Lenoir and Svenning, 2015). The geographical bias can be masking trends in tropical regions and interfering in the evaluation of the latitudinal component of range shift responses. This bias is worrisome given that most biodiversity is concentrated in the Tropics (Manes and Vale, 2022; Pacifici et al., 2017). We also found a taxonomic bias as most studies evaluating range shifts as a consequence of climate change focus on birds, leaving trends in non-volant terrestrial vertebrates poorly understood (e.g. Chen et al., 2011; Uher-Koch et al., 2021). In general, ectothermic terrestrial vertebrates are rarely present in literature reviews on climate-induced range shifts (e.g. Chen et al., 2011; Feeley et al., 2017; Freeman et al., 2021), and when present, they are underrepresented. Lenoir et al. (2020), the most comprehensive effort to summarize data on species' range shifts to date, shows taxonomic bias. Of the >15,000 observations of animals' range shifts in the study, only about 5 % of endotherms were mammals (369 mammals out of 7494 endotherms), and only about 6.5 % were herptiles (531 herptiles out of 8246 ectotherms). Thus, the specific responses of mammals and herptiles could be masked by the overrepresentation of

other taxa in Lenoir et al. (2020). That might explain why we found a difference in the response of ectotherms and endotherms to climate change, while Lenoir et al. (2020) did not.

We found that the magnitude of altitudinal range shifts was greater for ectotherms, showing that the same amount of warming triggers a stronger response in ectotherms, which is in tune with claims that ectothermic species are more susceptible to climate changes than endotherms (e.g. Deutsch et al., 2008; Nemesházi et al., 2022) because of their limited thermoregulation (Burraco et al., 2020). Tropical species are expected to show a stronger response to climate change than temperate ones because they are already closer to their maximum thermal limits and can endure fewer temperature fluctuations compared to temperate species (e.g. Deutsch et al., 2008; Dillon et al., 2010 but see Diele-Viegas and Rocha, 2018), a pattern that was not found in our study. This suggests that although mountains might be 'escalators to extinction' where species lose area by shifting ranges uphill (Urban, 2018), they might act as climate refugees compared to lowland areas in both low and high latitudes. The refuge provided by the mountains makes them essential environments for the conservation of tropical and temperate species alike.

We also found a trend in latitudinal range shifts, as the closer a species is to the poles, the greater its latitudinal range shift, for both endothermic and ectothermic species. This pattern may be explained by the fact that temperatures in temperate and polar regions are the ones enduring the greatest warming (Parmesan, 2007; Pörtner et al., 2022). Additionally, temperate regions experienced past glacial retreats (Willig et al., 2003), and temperate species could have behavioral or physiological adaptations that can be allowing or, at least, facilitating their dispersal in response to climate change (Feeley et al., 2017). Despite the fact that our result is sensitive to four outliers (observations at latitudes >60°), these outliers contain valuable information for different species and groups because they are real and valid data from two separate studies. Additionally, we made a complementary analysis that confirmed the significance of the latitude effect. So, our result shows an interesting ecological trend that deserves attention. This is the first review study to address the influence of latitude on latitudinal range shifts themselves and, therefore, more studies are needed to confirm the generality of our findings.

Here, we confirmed that climate change is already affecting the range of many species around the world. Although shifting ranges are often understood as a sign that the species is being harmed by climate change, they can also be understood as a sign that the species is able to cope with it. After all, shifting ranges can be considered climate change adaptations (sensu IPCC, 2018), i.e. the process of adjustment to reduce or avoid potential risks of climate change. It is important to note, however, that the range shifts compiled in our study are a result of mild global warming, as currently, the global temperature is ~1.1 °C above pre-industrial levels (Allan et al., 2021). Global warming, however, is likely to intensify in the coming years, reaching >4 °C by 2100 under the most drastic scenarios (Allan et al., 2021). Thus, species might soon reach hard adaptation limits (i.e. the change in climate where no additional adaptation is possible to prevent damaging impacts Allen et al., 2018; Pörtner et al., 2022). Thus, first and foremost, we recommend climate mitigation strategies to slow down climate change, keeping global warming within the Paris Agreement goals, greatly reducing species' vulnerability (Costello et al., 2022; Manes and Vale, 2022; Pörtner et al., 2022). We also recommend implementing adaptation strategies that can help species cope with ongoing climate change. We know that climate change operates together, and often in synergy, with other anthropogenic stressors such as habitat loss, invasive species, and overexploitation (e.g. Bellard et al., 2014; Mantyka-Pringle et al., 2015). Thus, we recommend actions focused on the conservation and restoration of natural habitats, especially within the range of high-latitude species and already threatened ectothermic, to increase species' resilience to climate change.

5. Conclusions and recommendations

We provide important new information for understanding how climate change impacts species ranges worldwide. On top of providing additional evidence that species are already shifting their ranges in response to climate change, we demonstrated for the first time that ectotherms and high-latitude species show a stronger response, suggesting greater susceptibility of these species to ongoing climate change. Thus, we recommend focusing on conservation efforts to increase the resilience of ectotherms to ongoing climate change, essentially by reducing other human-induced non-climatic stressors (Pörtner et al., 2022). We also reinforce that high-latitude species will be likely more impacted by global warming, as previously suggested (e.g. Cordier et al., 2020; Raxworthy et al., 2008; Rowe et al., 2015). Furthermore, as ectotherms and tropical species are underrepresented in global studies (Feeley et al., 2017), we also recommend more field research targeting those species to better understand how ongoing climate changes may already be impacting them.

CRediT authorship contribution statement

Quezia Ramalho: Conceptualization; Methodology; Formal analysis; Data Curation; Writing-Original draft preparation; Writing-Reviewing and Editing; Visualization; Project administration. **Mariana M. Vale:** Conceptualization; Methodology; Writing-Original draft preparation; Writing-Reviewing and Editing; Supervision. **Stella Manes:** Data Curation; Writing-Original draft preparation; Writing-Reviewing and Editing; Visualization. **Paula Diniz:** Data Curation; Writing-Original draft preparation; Writing-Reviewing and Editing; Visualization. **Artur Malecha:** Data Curation; Writing-Original draft preparation; Writing-Reviewing and Editing. **Jayme A. Prevedello:** Conceptualization; Methodology; Software; Formal analysis; Writing-Original draft preparation; Writing-Reviewing and Editing; Supervision.

Declaration of competing interest

The authors declare that they have no known competing financial interests or personal relationships that could have appeared to influence the work reported in this paper.

Data availability

I have shared the link to my data at the "Attach File" step.

Climate-induced range shifts description (Original data) (Google Sheets)

Acknowledgments

This study was financed in part by the Coordenação de Aperfeiçoamento de Pessoal de Nível Superior – Brazil (CAPES) – Finance Code 001. SM also received the Grant 'Doutorado Nota 10' from Fundação Carlos Chagas Filho de Amparo à Pesquisa do Estado do Rio de Janeiro (FAPERJ, Grant no. E-26/200.611/2021). MMV and AM received fellowships from the National Council for Scientific and Technological Development (CNPq, Grant ID: 304309/2018-4, 154243/2020-5, 202284/2020-4, and 304908/2021-5). MMV also received the Grant 'Cientista do Nosso Estado' from the Fundação Carlos Chagas Filho de Amparo à Pesquisa do Estado do Rio de Janeiro (FAPERJ, Grant no. E-26/202.647/2019). This paper was developed in the context of the Brazilian Research Network on Climate Change supported by FINEP (Grant ID: 01.13.0353-00) and the National Institutes for Science and Technology in Ecology, Evolution and Biodiversity Conservation, supported by CNPq (Grant ID: 465610/2014-5) and Fundação de Amparo à Pesquisa do Estado de Goiás (FAPEG, Grant ID: 201810267000023). We are grateful to Carlos Frederico Duarte Rocha, Luciana Fusinatto, Aliny

Pires, and the members of the Landscape Ecology Lab for constructive comments and revisions.

Appendix A. Supplementary data

Supplementary data to this article can be found online at https://doi.org/10.1016/j.biocon.2023.109911.

References

Allan, R.P., Arias, P.A., Berger, S., Canadell, J.G., Cassou, C., Chen, D., Cherchi, A., Connors, S.L., Coppola, E., Abigail Cruz, F., Doblas-Reyes, F.J., Douville, H., Driouech, F., Edwards, T.L., Engelbrecht, F., Eyring, V., Diongue-Niang, A., Fischer, E., Flato, G.M., Forster, P., Fox-Kemper, B., Fuglestvedt, J.S., Fyfe, J.C., Gillett, N.P., Gomis, M.I., Gulev, S.K., Gutiérrez, J.M., Hamdi, R., Harold, J., Hauser, M., Hawkins, E., Hewitt, H.T., Johansen, T.G., Jones, C., Jones, R.G., Kaufman, D.S., Klimont, Z., Kopp, R.E., Koven, C., Krinner, G., Lee, J.-Y., Lorenzoni, I., Marotzke, J., Masson-Delmotte, V., Maycock, T.K., Meinshausen, M., Monteiro, P.M.S., Morelli, A., Naik, V., Notz, D., Otto, F., Palmer, M.D., Pinto, I., Pirani, A., Plattner, G.-K., Raghavan, K., Ranasinghe, R., Rogelj, J., Rojas, M., Ruane, A.C., Sallée, J.-B., Samset, B.H., Seneviratne, S.I., Sillmann, J., Sörensson, A. A., Stephenson, T.S., Storelvmo, T., Szopa, S., Thorne, P.W., Trewin, B., Vautard, R., Vera, C., Yassaa, N., Zaehle, S., Zhai, P., Zhang, X., Zickfeld, K., 2021. Summary for Policymakers, Climate Change 2021: The Physical Science Basis. Contribution of Working Group I to the Sixth Assessment Report of the Intergovernmental Panel on Climate Change. IPCC.

Allen, M., Babiker, M., Chen, Yang, de Coninck, H., Connors, Sarah, van Diemen, R., Pauline Dube, O., Ebi, K.L., Engelbrecht, Francois Ferrat, M., Ford, J., Forster, P., Fuss, S., Bolaños, Guillén, Tania Harold, J., Hoegh-Guldberg, Ove Hourcade, Jean-Charles Huppmann, D., Jacob, D., Jiang, K., Johansen, Tom Gabriel Kainuma, M., de Kleijne, K., Kriegler, E., Ley, D., Liverman, D., Mahowald, N., Masson-Delmotte, Valérie, Robin Matthews, J.B., Millar, R., Mintenbeck, K., Morelli, A., Moufouma-Okia, Wilfran, Mundaca, L., Nicolai, M., Okereke, Chukwumerije Pathak, M., Payne, A., Pidcock, Roz, Pirani, Anna, Poloczanska, E., Pörtner, Hans-Otto, Revi, A., Riahi, K., Roberts, D.C., Rogelj, J., Roy, J., Seneviratne, S.I., Shukla, Priyadarshi, R., Skea, James, Slade, R., Shindell, D., Singh, C., Solecki, W., Steg, L., Taylor, M., Tschakert, P., Waisman, H., Warren, R., Zhai, Panmao, Zickfeld, K., 2018. Summary for policymakers. In: Masson-Delmotte, V., Zhai, P., Pörtner, H.-O., Roberts, D., Skea, J., Shukla, P.R., Pirani, A., Moufouma-Okia, W., Péan, C., Pidcock, R., Connors, S., Matthews, J.B.R., Chen, Y., Zhou, X., Gomis, M.I., Lonnoy, E., Maycock, T., Tignor, M., Waterfield, T. (Eds.), Global Warming of 1.5°C. An IPCC Special Report on the Impacts of Global Warming of 1.5°C above Pre-Industrial Levels and Related Global Greenhouse Gas Emission Pathways, in the Context of Strengthening the Global Response to the Threat of Climate Change. IPCC - The Intergovernmental Panel on Climate Change.

Bellard, C., Leclerc, C., Leroy, B., Bakkenes, M., Veloz, S., Thuiller, W., Courchamp, F., 2014. Vulnerability of biodiversity hotspots to global change. Glob. Ecol. Biogeogr. 23, 1376–1386. https://doi.org/10.1111/geb.12228.

Botts, E.A., Erasmus, B.F., Alexander, G.J., 2015. Observed range dynamics of South African amphibians under conditions of global change. Austral Ecol. 40, 309–317. https://doi.org/10.1111/aec.12215.

Boyles, J.G., Seebacher, F., Smit, B., McKechnie, A.E., 2011. Adaptive thermoregulation in endotherms may alter responses to climate change. Integr. Comp. Biol. https://doi.org/10.1093/icb/icr053.

Burraco, P., Orizaola, G., Monaghan, P., Metcalfe, N.B., 2020. Climate change and ageing in ectotherms. Glob. Chang. Biol. 26, 5371–5381. https://doi.org/10.1111/gcb.15305.

Chaudhary, C., Richardson, A.J., Schoeman, D.S., Costello, M.J., 2021. Global warming is causing a more pronounced dip in marine species richness around the equator. Proc. Natl. Acad. Sci. 118, e2015094118.

Chen, I.C., Hill, J.K., Shiu, H.J., Holloway, J.D., Benedick, S., Chey, V.K., Barlow, H.S., Thomas, C.D., 2011. Asymmetric boundary shifts of tropical montane Lepidoptera over four decades of climate warming. Glob. Ecol. Biogeogr. 20, 34–45. https://doi.org/10.1111/j.1466-8238.2010.00594.x.

Cordier, J.M., Lescano, J.N., Rios, N.E., Leynaud, G.C., Nori, J., 2020. Climate change threatens micro-endemic amphibians of an important South American high-altitude center of endemism. Amphib. Reptil. 41, 233–243. https://doi.org/10.1163/15685381-20191235.

Costello, M.J., Vale, M.M., Kiessling, W., Maharaj, S., Price, J., Talukdar, G.H., 2022. Cross-chapter paper 1: biodiversity hotspots. In: Pörtner, H.-O., Roberts, D.C., Tignor, M., Poloczanska, E.S., Mintenbeck, K., Alegría, A., Craig, M., Langsdorf, S., Löschke, S., Möller, V., Okem, A., Rama, B. (Eds.), Climate Change 2022: Impacts, Adaptation and Vulnerability. Contribution of Working Group II to the Sixth Assessment Report of the Intergovernmental Panel on Climate Change. Cambridge University Press, Cambridge, UK and New York, NY, USA, pp. 2123–2161. https://doi.org/10.1017/9781009325844.018.

Cramer, W., Yohe, G.W., Auffhammer, M., Huggel, C., Molau, U., da Silva Dias, M.A.F., Solow, A., Stone, D.A., Tibig, L., 2014. Detection and attribution of observed impacts. In: Climate Change, 2014: Impacts, Adaptation and Vulnerability: Part A: Global and Sectoral Aspects. Contribution of Working Group II to the Fifth Assessment Report of the Intergovernmental Panel on Climate Change. Cambridge University Press, pp. 979–1037. https://doi.org/10.1017/CBO9781107415379.005.

Curley, S.R., Manne, L.L., Veit, R.R., 2020. Differential winter and breeding range shifts: implications for avian migration distances. Divers. Distrib. 26, 415–425. https://doi.org/10.1111/ddi.13036.

Deutsch, C.A., Tewksbury, J.J., Huey, R.B., Sheldon, K.S., Ghalambor, C.K., Haak, D.C., Martin, P.R., 2008. Impacts of climate warming on terrestrial ectotherms across latitude. Proc. Natl. Acad. Sci. U. S. A. 105, 6668–6672. https://doi.org/10.1073/pnas.0709472105.

Diele-Viegas, L.M., Rocha, C.F.D., 2018. Unraveling the influences of climate change in Lepidosauria (Reptilia). J. Therm. Biol. 78, 401–414.

Dillon, M.E., Wang, G., Huey, R.B., 2010. Global metabolic impacts of recent climate warming. Nature 467, 704–706. https://doi.org/10.1038/nature09407.

Easterling, D.R., Meehl, G.A., Parmesan, C., Changnon, S.A., Karl, T.R., Mearns, L.O., 2000. Climate extremes: observations, modeling, and impacts. Science 289, 2068–2074. https://doi.org/10.1126/science.289.5487.2068.

Enriquez-Urzelai, U., Bernardo, N., Moreno-Rueda, G., Montori, A., Llorente, G., 2019. Are amphibians tracking their climatic niches in response to climate warming? A test with Iberian amphibians. Climatic Change 154, 289–301. https://doi.org/10.1007/s10584-019-02422-9.

Feeley, K.J., Stroud, J.T., Perez, T.M., 2017. Most 'global' reviews of species' responses to climate change are not truly global. Divers. Distrib. 23, 231–234. https://doi.org/10.1111/ddi.12517.

Freeman, B.G., Song, Y., Feeley, K.J., Zhu, K., 2021. Montane species track rising temperatures better in the tropics than in the temperate zone. Ecol. Lett. 24, 1697–1708.

Hickling, R., Roy, D.B., Hill, J.K., Fox, R., Thomas, C.D., 2006. The distributions of a wide range of taxonomic groups are expanding polewards. Glob. Chang. Biol. 12, 450–455. https://doi.org/10.1111/j.1365-2486.2006.01116.x.

IPCC, 2018: Global warming of 1.5°C. An IPCC Special Report on the impacts of global warming of 1.5°C above pre-industrial levels and related global greenhouse gas emission pathways, in the context of strengthening the global response to the threat of climate change, sustainable development, and efforts to eradicate poverty [V. Masson-Delmotte, P. Zhai, H. O. Pörtner, D. Roberts, J. Skea, P.R. Shukla, A. Pirani, W. Moufouma-Okia, C. Péan, R. Pidcock, S. Connors, J. B. R. Matthews, Y. Chen, X. Zhou, M. I. Gomis, E. Lonnoy, T. Maycock, M. Tignor, T. Waterfield (eds.)]. In Press.

Khaliq, I., Böhning-Gaese, K., Prinzinger, R., Pfenninger, M., Hof, C., 2017. The influence of thermal tolerances on geographical ranges of endotherms. Glob. Ecol. Biogeogr. 26, 650–668. https://doi.org/10.1111/geb.12575.

Kirchman, J.J., Van Keuren, A.E., 2017. Altitudinal range shifts of birds at the southern periphery of the boreal forest: 40 years of change in the Adirondack Mountains. Wilson J. Ornithol. 129, 742–753. https://doi.org/10.1676/16-164.1.

Lane, J.E., Kruuk, L.E.B., Charmantier, A., Murie, J.O., Dobson, F.S., 2012. Delayed phenology and reduced fitness associated with climate change in a wild hibernator. Nature 489, 554–557. https://doi.org/10.1038/nature11335.

Lenoir, J., Bertrand, R., Comte, L., Bourgeaud, L., Hattab, T., Murienne, J., Grenouillet, G., 2020. Species better track climate warming in the oceans than on land. Nat. Ecol. Evol. 4, 1044–1059. https://doi.org/10.1038/s41559-020-1198-2.

Lenoir, J., Svenning, J., 2015. Climate-related range shifts–a global multidimensional synthesis and new research directions. Ecography (Cop.) 38, 15–28.

MacLean, S.A., Beissinger, S.R., 2017. Species'traits as predictors of range shifts under contemporary climate change: a review and meta-analysis. Glob. Chang. Biol. 23, 4094–4105. https://doi.org/10.1111/gcb.13736.

Mantyka-Pringle, C.S., Visconti, P., Di Marco, M., Martin, T.G., Rondinini, C., Rhodes, J. R., 2015. Climate change modifies risk of global biodiversity loss due to land-cover change. Biol. Conserv. 187, 103–111. https://doi.org/10.1016/j.biocon.2015.04.016.

Manes, S., Costello, M.J., Beckett, H., Debnath, A., Devenish-Nelson, E., Grey, K.-A., Jenkins, R., Ming Khan, T., Kiessling, W., Krause, C., Maharaj, S.S., Midgley, G.F., Price, J., Talukdar, G., Vale, M.M., 2021. Endemism increases species'risk to climate change in areas of global biodiversity importance. Biol. Conserv. 257, 109070 https://doi.org/10.1016/j.biocon.2021.109070.

Manes, S., Vale, M.M., 2022. Achieving the Paris Agreement would substantially reduce climate change risks to biodiversity in Central and South America. Reg. Environ. Chang. 22, 1–11. https://doi.org/10.1007/s10113-022-01904-4.

Moreno-Rueda, G., Pleguezuelos, J.M., Pizarro, M., Montori, A., 2012. Northward shifts of the distributions of Spanish reptiles in association with climate change. Conserv. Biol. 26, 278–283. https://doi.org/10.1111/j.1523-1739.2011.01793.x.

Nemesházi, E., Sramkó, G., Laczkó, L., Balogh, E., Szatmári, L., Vili, N., Ujhegyi, N., Üveges, B., Bókony, V., 2022. Novel genetic sex markers reveal unexpected lack of, and similar susceptibility to, sex reversal in free-living common toads in both natural and anthropogenic habitats. Mol. Ecol. 31, 2032–2043. https://doi.org/10.1111/mec.16388.

Pacifici, M., Visconti, P., Butchart, S.H.M., Watson, J.E.M., Cassola, F.M., Rondinini, C., 2017. Species'traits influenced their response to recent climate change. Nat. Clim. Chang. 7, 205–208. https://doi.org/10.1038/nclimate3223.

Parmesan, C., 2007. Influences of species, latitudes and methodologies on estimates of phenological response to global warming. Glob. Chang. Biol. 13, 1860–1872. https://doi.org/10.1111/j.1365-2486.2007.01404.x.

Parmesan, C., Yohe, G., 2003. A globally coherent fingerprint of climate change impacts across natural systems. Nature 421, 37–42. https://doi.org/10.1038/nature01286.

Parmesan, C., Yohe, G., Andrus, J.E., 2003. A Globally Coherent Fingerprint of Climate Change Impacts Across Natural Systems.

Pinheiro, J., Bates, D., DebRoy, S., Sarkar, D., Core Team, R., 2021. nlme: Linear and Nonlinear Mixed Effects Models.

Pörtner, H.O., Scholes, R.J., Agard, J., Archer, E., Arneth, A., Bai, X., Barnes, D., Burrows, M., Chan, L., Cheung, W.L., Diamond, S., Donatti, C., Duarte, C., Eisenhauer, N., Foden, W., Gasalla, M.A., Handa, C., Hickler, T., Hoegh-

Guldberg, O., Ichii, H., 2021. IPBES-IPCC Co-Sponsored Workshop Report on Biodiversity and Climate Change. https://doi.org/10.5281/zenodo.4659158.IPBES. Bonn, Germany.

Pörtner, Hans-O., Roberts, D.C., Adams, H., Adler, C., Aldunce, P., Ali, E., Begum, R.A., Betts, R., Kerr, R.B., Biesbroek, R., Birkmann, J., Bowen, K., Castellanos, E., Cissé, G., Constable, A., Cramer, W., Dodman, D., Eriksen, S.H., Fischlin, A., Garschagen, M., Glavovic, B., Gilmore, E., Haasnoot, M., Harper, S., Hasegawa, T., Hayward, B., Hirabayashi, Y., Howden, M., Kalaba, K., Kiessling, W., Lasco, R., Lawrence, J., Lemos, M.F., Lempert, R., Ley, D., Lissner, T., Lluch-Cota, S., Loeschke, S., Lucatello, S., Luo, Y., Mackey, B., Maharaj, S., Mendaz, C., Mintenbeck, K., Vale, M. M., Morecroft, M.D., Mukherji, A., Mycoo, M., Mustonen, T., Nalau, J., Okem, A., Ometto, J.P., Parmesan, C., Pelling, M., Pinho, P., Poloczanska, E., Racault, M.F., Reckien, D., Pereira, J., Revi, A., Rose, S., Sanchez-Rodriguez, R., Schipper, E.L.F., Schmidt, D., Schoeman, D., Shaw, R., Singh, C., Solecki, W., Stringer, L., Thomas, A., Totin, E., Trisos, C., Aalst, M., Viner, D., Wairiu, M., Warren, R., Yanda, P., Ibrahim, Z.Z., 2022. Summary for policymakers. In: Climate Change 2022: Impacts, Adaptation, and Vulnerability. Contribution of Working Group II to the Sixth Assessment Report of the Intergovernmental Panel on Climate Change. IPCC, UN, p. 37.

R. Core Team, 2021. R: A Language and Environmental for Statistical Computing. R Found. Stat. Comput, Vienna, Austria.

Ramalho, Q., Tourinho, L., Almeida-Gomes, M., Vale, M.M., Prevedello, J.A., 2021. Reforestation can compensate negative effects of climate change on amphibians. Biol. Conserv. 260, 109187 https://doi.org/10.1016/j.biocon.2021.109187.

Raxworthy, C.J., Pearson, R.G., Rabibisoa, N., Rakotondrazafy, A.M., Ramanamanjato, J. B., Raselimanana, A.P., Wu, S., Nussbaum, R.A., Stone, D.A., 2008. Extinction vulnerability of tropical montane endemism from warming and upslope displacement: a preliminary appraisal for the highest massif in Madagascar. Glob. Chang. Biol. 14, 1703–1720. https://doi.org/10.1111/j.1365-2486.2008.01596.x.

Root, T.L., Price, J.T., Hall, K.R., Schneider, S.H., Rosenzweig, C., Pounds, A., 2003. Fingerprints of global warming on wild animals and plants. Nature 421, 57–60. https://doi.org/10.1142/9781848162044_0011.

Rowe, K.C., Rowe, K.M.C., Tingley, M.W., Koo, M.S., Patton, J.L., Conroy, C.J., Perrine, J.D., Beissinger, S.R., Moritz, C., 2015. Spatially heterogeneous impact of climate change on small mammals of montane California. Proc. R. Soc. B Biol. Sci. 282 https://doi.org/10.1098/rspb.2014.1857.

Segan, D.B., Murray, K.A., Watson, J.E.M., 2016. A global assessment of current and future biodiversity vulnerability to habitat loss–climate change interactions. Glob. Ecol. Conserv. 5, 12–21.

Taheri, S., Naimi, B., Rahbek, C., Araújo, M.B., 2021. Improvements in reports of species redistribution under climate change are required. Sci. Adv. 7, 1–12. https://doi.org/10.1126/SCIADV.ABE1110.

Tourinho, L., Prevedello, J., Carvalho, B., Rocha, D., Vale, M., 2021. Macroscale climate change predictions have little influence on landscape-scale habitat suitability. Perspect. Ecol. Conserv. https://doi.org/10.1016/j.pecon.2021.10.003.

Uher-Koch, B.D., Buchheit, R.M., Eldermire, C.R., Wilson, H.M., Schmutz, J.A., 2021. Shifts in the wintering distribution and abundance of emperor geese in Alaska. Glob. Ecol. Conserv. 25 https://doi.org/10.1016/j.gecco.2020.e01397.

Urban, M.C., 2018. Escalator to extinction. Proc. Natl. Acad. Sci. U. S. A. 115, 11871–11873. https://doi.org/10.1073/pnas.1817416115.

Walther, G.-R., Post, E., Convey, P., Menzel, A., Parmesank, C., Beebee, T.J.C., Fromentin, J.-M., Hoegh-Guldberg, O., Bairlein, F., 2002. Ecological responses to recent climate change. Nature 416, 389–395. https://doi.org/10.1038/416389a.

Warren, R., Price, J., VanDerWal, J., Cornelius, S., Sohl, H., 2018. The implications of the United Nations Paris Agreement on climate change for globally significant biodiversity areas. Clim. Chang. 147, 395–409. https://doi.org/10.1007/s10584-018-2158-6.

Willig, M.R., Kaufman, D.M., Stevens, R.D., 2003. Latitudinal gradients of biodiversity: pattern, process, scale, and synthesis. Annu. Rev. Ecol. Evol. Syst. 34, 273–309. https://doi.org/10.1146/annurev.ecolsys.34.012103.144032.

ARTICLES FOR FACULTY MEMBERS

GLOBAL WARMING EFFECTS ON ECTOTHERM SPECIES

Title/Author	**Extreme escalation of heat failure rates in ectotherms with global warming / Jørgensen, L. B., Ørsted, M., Malte, H., Wang, T., & Overgaard, J.**
Source	***Nature*** **Volume 611 Issue 7934 (2022) Pages 93–98** **https://doi.org/10.1038/s41586-022-05334-4** **(Database: Nature Portfolio)**

Extreme escalation of heat failure rates in ectotherms with global warming

https://doi.org/10.1038/s41586-022-05334-4

Received: 14 December 2021

Accepted: 9 September 2022

Published online: 26 October 2022

Check for updates

Lisa Bjerregaard Jørgensen[1], Michael Ørsted[1], Hans Malte[1], Tobias Wang[1] & Johannes Overgaard[1]✉

Temperature affects the rate of all biochemical processes in ectotherms[1,2] and is therefore critical for determining their current and future distribution under global climate change[3–5]. Here we show that the rate of biological processes maintaining growth, homeostasis and ageing in the permissive temperature range increases by 7% per degree Celsius (median activation energy E_a = 0.48 eV from 1,351 rates across 314 species). By contrast, the processes underlying heat failure rate within the stressful temperature range are extremely temperature sensitive, such that heat failure increases by more than 100% per degree Celsius across a broad range of taxa (median E_a = 6.13 eV from 123 rates across 112 species). The extreme thermal sensitivity of heat failure rates implies that the projected increase in the frequency and intensity of heatwaves can exacerbate heat mortality for many ectothermic species with severe and disproportionate consequences. Combining the extreme thermal sensitivities with projected increases in maximum temperatures globally[6], we predict that moderate warming scenarios can increase heat failure rates by 774% (terrestrial) and 180% (aquatic) by 2100. This finding suggests that we are likely to underestimate the potential impact of even a modest global warming scenario.

Temperature has a profound influence on processes at all levels of biological organization, ranging from the simple catalytic rates of enzymes to the complex biological interactions that underlie metabolism, growth and reproduction of ectothermic animals[1,2]. The interactions between multiple temperature-sensitive biological rates ultimately shape thermal performance and determine the thermal limits for life and death in ectotherms[1,7,8]. Accordingly, thermal tolerance limits are robust predictors of the geographical distribution of ectothermic animals[3,9,10], and climate change beyond tolerance limits can explain their current redistributions[4,11].

Thermal sensitivity of life and death

Temperature effects on biological rates are often described using Q_{10} (the factorial change in biological rate resulting from a 10 °C increase) but are more appropriately expressed by the Arrhenius activation energy E_a (ref. [2]). When rates are measured within permissive temperatures, defined as temperatures that allow for long-term survival, E_a typically ranges from 0.5 to 0.8 eV (equivalent to $Q_{10} \approx 2$–3) corresponding to a 7–12% rate increase per degree Celcius[12–14]. The consequences of global warming on the rate of energy metabolism in ectotherms are already implemented in contemporary analyses of ecosystems and agriculture[14–16]. However, temperature also affects biological rate functions at stressful temperatures, defined here as the temperature range causing acute heat injury and mortality. The temperature sensitivity of these processes is much more potent in ectothermic animals[17–19] but has received little attention in the context of global warming.

The disparate temperature sensitivities in the permissive and stressful temperature range can be exemplified through a combined analysis of temperature effects on the population growth capacity[20] and lifespan[18] of adult fruit flies (*Drosophila subobscura*; Fig. 1a). Within the permissive temperature range for this species (3–28 °C), warming increases the rates of biological processes in a manner that initially enhances fitness, that is, the product of egg laying rate, developmental viability and developmental speed[20]. However, as temperature increases further, the balance between catabolic and anabolic rates shifts and net fitness decreases[1,7,8,21] even if it remains positive. This declining fitness occurs even though many biological rates—such as feeding rate, heart rate, metabolic rate and ageing/mortality rate—continue to increase with the same thermal sensitivity throughout the permissive range[22]. Accordingly, when lifespan is analysed across the permissive temperature range, the increased rates of biological activities coincide with an acceleration of senescence and ageing[23,24]. In this example, the thermal sensitivity, Q_{10} = 2.5 for ageing/mortality rate (1/lifespan) (Fig. 1a), corresponds to an Arrhenius activation energy E_a of 0.66 eV (Fig. 1b). Similar moderate thermal sensitivities of ageing/mortality rate (1/lifespan) at permissive temperatures have been documented in a variety of ectothermic species (E_a = 0.56 ± 1 eV (mean ± s.d.) across 97 field and laboratory populations[24]).

There is a substantial shift in the influence of temperature on lifespan above a critical temperature T_c, defined as the temperature or narrow temperature zone that separates the permissive and stressful temperature range (Fig. 1). Although T_c is rarely parametrized experimentally (see the discussion in ref. [22]), it represents a temperature at which biological processes dictating the 'rate of death' become dominant over those determining the 'rate of life'. Heat failure rate above T_c is also calculated as 1/lifespan, and the Arrhenius breakpoint[1,2] at T_c indicates

[1]Section for Zoophysiology, Department of Biology, Aarhus University, Aarhus, Denmark. ✉e-mail: johannes.overgaard@bio.au.dk

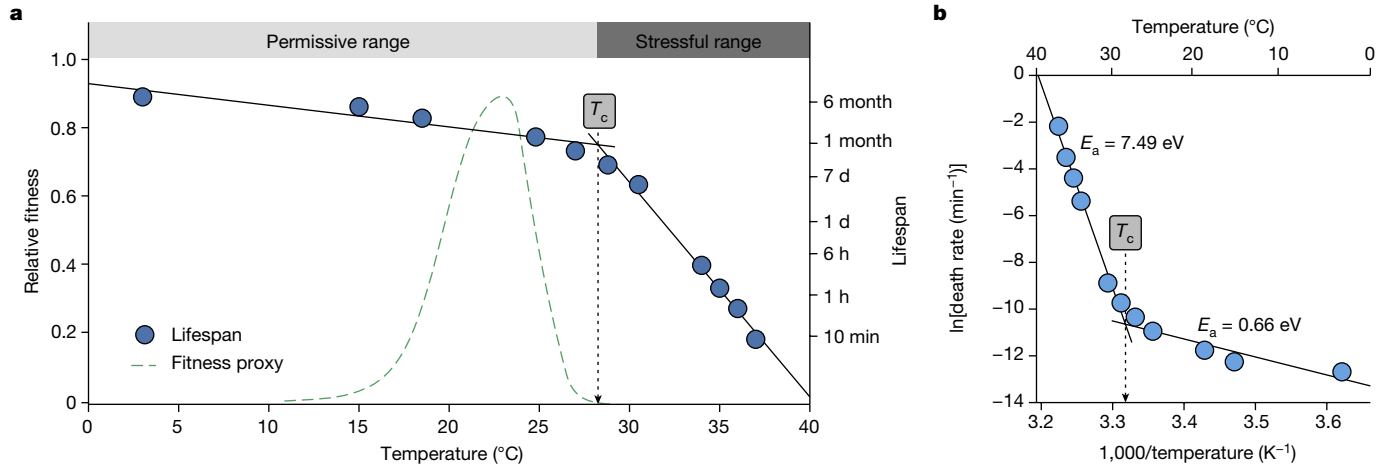

Fig. 1 | Disparate temperature sensitivities for the lifespan of an ectotherm reveal permissive and stressful temperature domains. a, Lifespan of adult fruit flies (*D. subobscura*) depicted on a $\log_{10}$ scale to indicate the exponential relationship between temperature and lifespan (right *y* axis; data are from ref. [18]). The critical temperature (T_c) indicates the transition at which the temperature effect on lifespan (slope) diverts from that of biological processes in the permissive temperature range to become extremely high in the stressful temperature range. A thermal performance curve for reproductive fitness in *D. subobscura* in the permissive temperature range illustrates that this is the range of temperatures that permits completion of the life cycle (dashed green curve on the left *y* axis; data are from ref. [20]). **b**, Temperature-specific death rates calculated as 1/lifespan from **a** were analysed in an Arrhenius plot. Activation energies E_a are indicated for the permissive (E_a = 0.66 eV) and stressful (E_a = 7.49 eV) temperature ranges separated at a breakpoint temperature T_c (28.2 °C) found using Davies' test for a change in slope (P < 0.001).

that the heat failure rate is dictated by different biological processes that are extremely sensitive to temperature (Q_{10} = 8,726 (Fig. 1a) and E_a = 7.49 eV (Fig. 1b)). For *D. subobscura*, heat death occurs after 6 h at 33 °C, while 4 °C further warming reduces its lifespan to less than 10 min (Fig. 1a). Similar extreme thermal sensitivities of heat failure have been described in thermal death time curves for many other ectotherms[19,25,26].

Analysis of activation energies

The fundamentally different thermal sensitivities for processes associated with life (permissive range) and death (stressful range) are not unique for *D. subobscura* (Fig. 1). Data compiled on 1,351 rates across different temperatures from 314 species show that the E_a of biological processes within the permissive temperature range (median E_a = 0.48 eV; interquartile range (IQR) = 0.28–0.71 eV; Fig. 2a,b) are indeed consistent with textbook values of $E_a \approx 0.5$–0.8 eV ($Q_{10} \approx 2$–3) for most ectothermic animals[12–14]. As previously discussed[13,14], these thermal sensitivities mirror most biological processes, including enzyme catalytic rates and integrated biological functions, such as feeding rate and metabolic rate (Fig. 2a,b and Extended Data Table 1). However, note that the integrated effect of many underlying biological rates causes a decline in 'fitness' in the warmer part of the permissive temperature range. As a consequence, the population growth rate (fitness) is associated with $E_a < 0$ or $Q_{10} < 1$ at the warmest permissive temperatures (Box 1) even though many underlying biological rates continue to increase after fitness has peaked at the optimal temperature (T_{opt})[22].

In contrast to the modest temperature sensitivity of biological rates in the permissive temperature range, the rate of heat failure is extraordinarily temperature sensitive in the stressful temperature range (Fig. 2c,d). We compiled data on the thermal sensitivity of heat failure for 112 species (123 datasets in total) with the criteria that time to heat failure was measured at three or more constant test temperatures. Heat failure rates (min^{-1}) were calculated as 1/time to heat failure (min) and the activation energy was subsequently calculated using an Arrhenius analysis (Fig. 2c). Heat failure rate has extreme thermal sensitivity across all of the ectotherms examined (Fig. 2d) with a median E_a = 6.13 eV (IQR = 4.42–8.82 eV) corresponding to a median Q_{10} > 1,500 and more than a doubling of heat failure rate per 1 °C of warming (median increase = 110%, IQR = 71–190%). The median duration of the heat failure experiments was 125 min (IQR = 31.5–422 min), with 122 out of 123 median durations less than 2.5 days, emphasizing that our estimates of heat failure rate are relevant for the acute heat exposures experienced during daily fluctuations and heatwaves[25]. All five ectothermic groups (fishes, crustaceans, molluscs, amphibians and insects) have a median E_a > 4.63 eV, but vertebrates are particularly sensitive to warming (median E_a = 10.06 eV and 10.30 eV for fishes and amphibians, respectively). This analysis also shows that E_a is high for both terrestrial (E_a = 5.53 eV; IQR = 4.13–6.42 eV) and aquatic species (E_a = 6.69 eV; IQR = 4.61–10.38 eV). Given the extraordinarily high thermal sensitivities in all taxonomic groups, we suggest that the extreme thermal sensitivity of heat failure rate is a general characteristic of all ectothermic animals.

The physiological causes of heat death in ectotherms are still poorly understood, but have been associated with protein denaturation, oxygen limitation, loss of cellular excitability and membrane dysfunction[2,7,8,12,21,27]. It is also unclear why the rates of these processes accelerate so substantially at extreme temperatures above T_c. Nevertheless, it is likely the same physiological dysfunctions that underlie chronic (hours) and acute (minutes) heat stress as exposure to different temperatures above T_c is additive in both fish[19] and insects[25]. Furthermore, the absence of Arrhenius breakpoints[2] above T_c suggests that heat failure is caused by a common heat stress syndrome that accelerates in intensity with an extreme thermal sensitivity. Importantly, many underlying biological rates typically begin to decrease within the stressful temperature range. Thus, metabolic rate, movement rate and heart rate, which typically increase throughout the permissive range[22], will eventually decline as temperatures become acutely stressful. The thermal sensitivity of this rate decline in the stressful temperature range is typically higher than the thermal sensitivity of the rate increase occurring in the permissive temperature range[13,22,28,29]. However, it remains difficult to pinpoint whether the extreme increase in death rate at stressful temperatures substantially limits heart rate, metabolic rate and movement rate or vice versa, as the causalities of the physiological heat stress syndrome are currently poorly understood[2,8,22,27].

Implications of global warming

In their active season, ectothermic animals are mostly confined to habitats with permissive temperatures that enable reproduction and

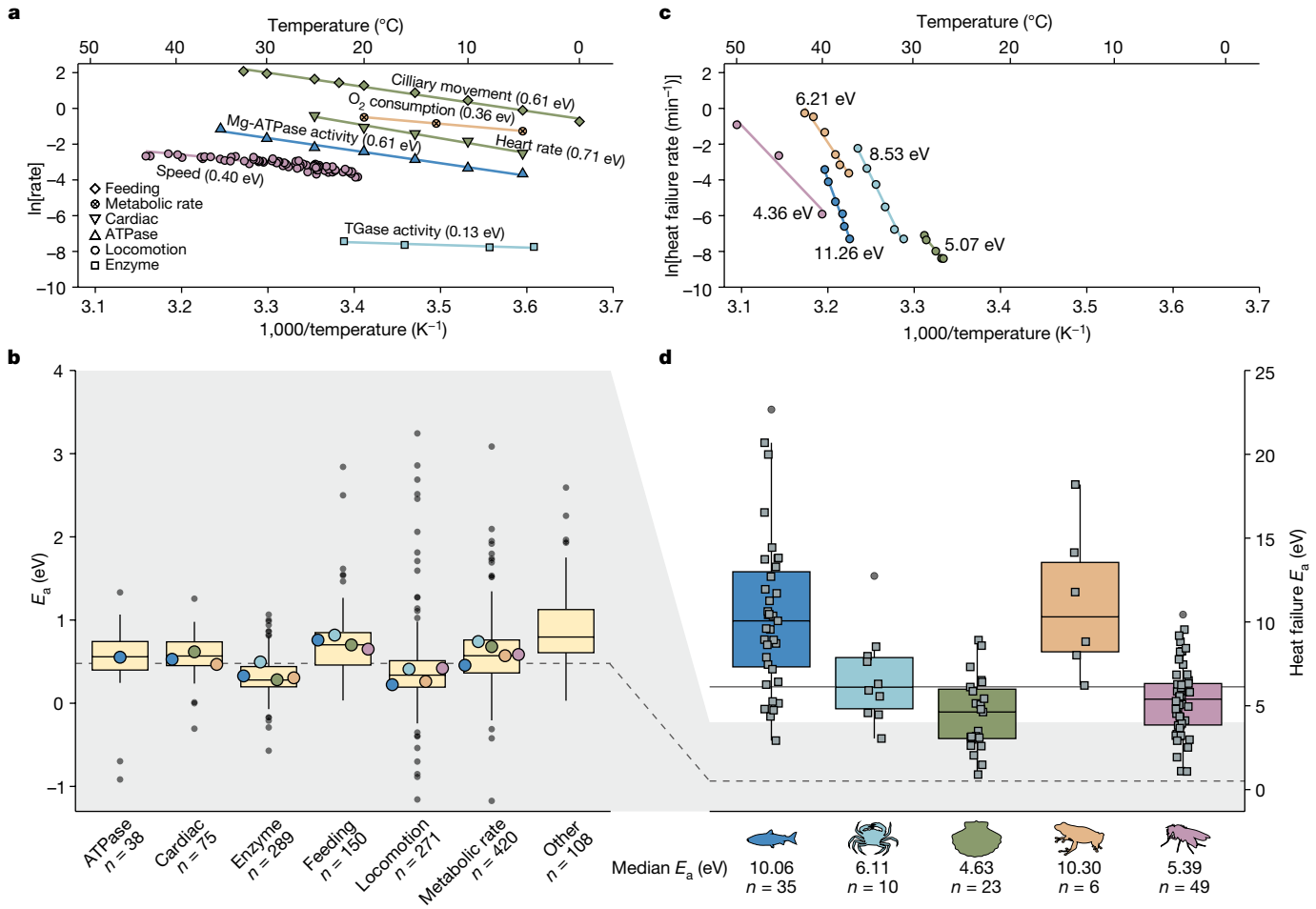

Fig. 2 | Thermal sensitivity of biological processes sustaining life in the permissive temperature range or causing heat death in the stressful temperature range. Data are organized in five ectotherm groups (fishes, crustaceans, molluscs, amphibians and insects) for which the most published data exist. **a**, Six representative examples of temperature sensitivity of biological processes measured within the permissive (non-stressful) temperature range (colour refers to the animal group and symbols to the trait; details are provided in Extended Data Table 1). **b**, Data from 1,351 literature estimates of E_a measured in the permissive temperature range from 314 species grouped by biological process. Coloured points represent averages in cases in which $n \geq 8$ for that animal group. Data from ectotherms not belonging to the five groups are also included in the box plots. The dashed line indicates the global median ($E_a = 0.48$ eV, corresponding to $Q_{10} = 1.9$). The box plots summarize each categorized biological process; the centre line shows the median, the box limits represent the first and third quartiles, the whiskers extend to 1.5 × IQR and the grey points show outliers. **c**, Representative examples of heat failure rates and their activation energy (E_a) measured in the stressful temperature range (the same or closely related species as in **a**). **d**, Activation energies of heat failure rate organized by ectothermic group with all 123 E_a values shown (squares, from 112 unique species). The full line indicates the global median ($E_a = 6.13$ eV, corresponding to $Q_{10} > 1{,}500$). For reference to **b**, the grey area denotes the E_a range −1.3–4 eV, and the dashed line indicates the median E_a for processes in the permissive range.

population growth[1,2,7]. Even so, ectotherms may experience stressful temperatures (exceeding T_c) during heatwaves or diurnal/seasonal temperature extremes. Tolerance to extremes is therefore an important determinant of species distributions[3,9], and thermal tolerance limits (CT_{min} and CT_{max}) often correlate stronger with distribution than the thermal optimum for population growth (T_{opt}), a performance measure within the permissive temperature range[20,30].

The severity of stressful temperatures depends on both the intensity (that is, the actual temperature) and the duration of the exposure[17,19,22,25,26]. The considerable thermal sensitivity of ectothermic heat failure rates more than doubles heat stress with every degree Celsius of warming. Accordingly, even modest increases in maximal exposure temperature—for example, as a result of moderate global warming—can substantially exacerbate the severity of heat injury. The potential magnitude of this problem was assessed by associating the median E_a for terrestrial and aquatic ectotherms with projected increases in maximum temperature for three IPCC warming scenarios (Fig. 3a and Extended Data Table 2). This analysis represents a worst-case scenario based on the assumption that species under current climate conditions experience temperatures equal to or above T_c on the warmest days within their distribution range. Terrestrial environments are projected to warm considerably more than aquatic environments[6] (Fig. 3 and Extended Data Fig. 1), but median thermal sensitivity is higher for aquatic ectotherms implying that both aquatic and terrestrial ecosystems will experience substantial increases in heat failure rate (median percentage increase, 180% and 774%, respectively, under the SSP2–4.5 scenario[6]; Fig. 3a). Furthermore, the more homogenous thermal conditions in aquatic habitats leave considerably fewer options for behavioural mitigation to avoid stressful temperature exposure[31]. These increases in heat failure rate are much more substantial than the projected 6% and 32% increases in permissive biological rates estimated for aquatic and terrestrial ectotherms, respectively, in association with increases in mean temperature (Fig. 3a and Extended Data Fig. 2).

Box 1

The impact of global warming on biological rates of life and death

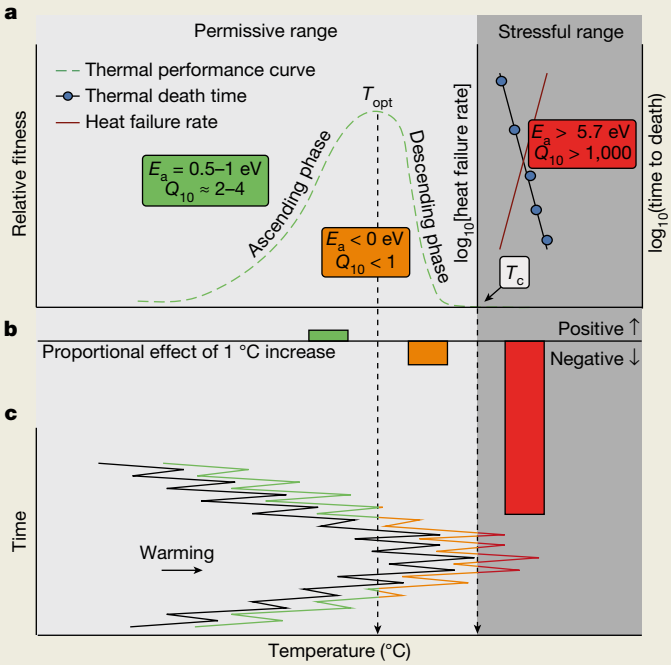

Increases in environmental temperature represent a substantial challenge for ectothermic animals in the Anthropocene[6,36] and there is an urgent need to understand how elevated temperature affects their fitness and survival[3,11,30,37–40]. A stylistic road map to assess this problem is shown in the figure with an idealized thermal performance curve for population growth in the permissive temperature range (green curve in **a**) and a thermal death time curve in the stressful temperature range (blue curve in **a**). When global warming increases temperature in the lower permissive range, below the optimal temperature (T_{opt}), it increases performance and population growth as discussed for both agricultural and natural ecosystems[15,16,40] (ascending phase in the figure; Q_{10} for positive fitness, ~2–4). However, population growth rate is progressively reduced when temperature exceeds T_{opt} along the descending part of the thermal performance curve (descending phase in the figure; Q_{10} for positive fitness < 1). Although population growth persists in this part of the permissive temperature range, the decline in performance is typically more sensitive to temperature change than on the ascending part of the thermal performance curve[1,13,29,41,42]. The negative effects of increased exposure to permissive temperatures beyond T_{opt} for population growth have been suggested to challenge particularly tropical species[40,43].

Exposure to stressful temperatures beyond T_c is associated with negative fitness (mortality) and inclusion of such extreme temperature exposures instead suggests that mid-latitude species are at risk[5,30,44]. As shown in this study, exposure to increased temperature in the stressful range is associated with a substantial acceleration of heat mortality as temperature effects on survival are characterized by an extreme thermal sensitivity in the stressful range (red curve in **a**, note the logarithmic axis for heat failure rate; Q_{10} for heat failure rate, >1,000). Accordingly, small increases in maximal temperature exposure can have severe consequences. Together, this schematic illustrates how different temperature ranges have positive or negative effects on performance or survival, but it also shows that these effects have very different temperature sensitivities (summarized in **b**).

To integrate the positive and negative temperature effects of global warming, we argue that models should consider how global warming alters the duration and intensity of exposures within both the permissive and stressful temperature ranges[25,45–47]. Such an approach is shown in **c**, where warming across daily and seasonal temperature variations changes the dynamics of positive and negative temperature effects. The pursuit of these integrative models is complicated by many factors—including acclimatization, behaviour, local adaptation and life stage—but, even so, it will be pivotal to consider the proportional exposure duration in these different temperature ranges. It is therefore critical to establish general methods to determine the T_c, which is central for risk assessment[22], but also to understand how the availability of suitable microhabitats and use of behavioural thermoregulation affects operative temperature, which ultimately determines the effect of temperature and climate warming on ectotherms[33,35,48].

To demonstrate that the risk of exposure to temperatures above T_c in current and future climate varies within the species distribution, Fig. 3b presents an analysis of two species (*Girella nigricans* and *Pheidole megacephala*). These species-level examples were generated by contrasting current and future (SSP2–4.5 scenario) estimates of maximal environmental temperature against a conservative approximation of T_c (here calculated as the temperature that causes heat failure in 24 h). Although some populations already experience temperatures above T_c in their current distribution, climate warming will result in more populations experiencing temperatures exceeding T_c (Fig. 3b and Extended Data Fig. 3). As evident from Fig. 3c, the consequences of future warming will depend on the current climate and the projected warming but, for some populations, projected warming will exacerbate the heat failure rate relative to current conditions by up to 2,100% and 690% for *G. nigricans* and *P. megacephala*, respectively (Fig. 3c). To put this into context, a 1,000% (tenfold) increase in heat failure rate entails that an ectotherm accumulating 15% of its lethal thermal injury on a very hot day under current climate conditions, will instead experience 150% of its lethal dose over the same duration under the future warming scenario. As a corollary, a 1,000% increase in failure rate implies that an ectotherm currently surviving for 5 h during a hot day will instead succumb to heat death within 30 min under the future warming scenario.

The general risk analysis for ectotherms in Fig. 3a suggests that both terrestrial and aquatic species may experience substantial increases in the intensity of injurious heat stress. Although terrestrial ectotherms can often escape short-term heat exposures by seeking permissive microhabitats (<T_c)[3,31–35], warming may reduce the availability of such microhabitats. In both terrestrial and aquatic environments, there is considerable spatial variation in regional climate warming with projected increases in maximum temperature greater than 8 °C in some regions even in the SSP2–4.5 scenario[6] (Extended Data Fig. 1). As a consequence, the potential increase in heat failure rate for species living close to their T_c can be even more extreme locally, particularly across

a

Warming scenario	Percentage increase in permissive biological rates: Terrestrial ΔT (°C)	Terrestrial Median E_a = 0.57 eV (IQR = 0.39–0.76 eV)	Aquatic ΔT (°C)	Aquatic Median E_a = 0.44 eV (IQR = 0.24–0.67 eV)	Percentage increase in heat failure rates: Terrestrial ΔT (°C)	Terrestrial Median E_a = 5.53 eV (IQR = 4.13–6.42 eV)	Aquatic ΔT (°C)	Aquatic Median E_a = 6.69 eV (IQR = 4.61–10.38 eV)
SSP1–2.6 (1.8 °C)	2.29	19% (12–26%)	0.50	3% (2–5%)	2.16	291% (177–387%)	0.67	75% (47–138%)
SSP2–4.5 (2.7 °C)	3.73	32% (21–45%)	0.96	6% (3–9%)	3.45	774% (405–1,141%)	1.24	180% (104–395%)
SSP5–8.5 (4.4 °C)	6.57	62% (39–91%)	2.53	17% (9–26%)	6.18	4,604% (1,678–8,661%)	3.25	1,363% (537–6,337%)
Baseline temperature		23.2 °C		16.5 °C		44.6 °C		31.8 °C

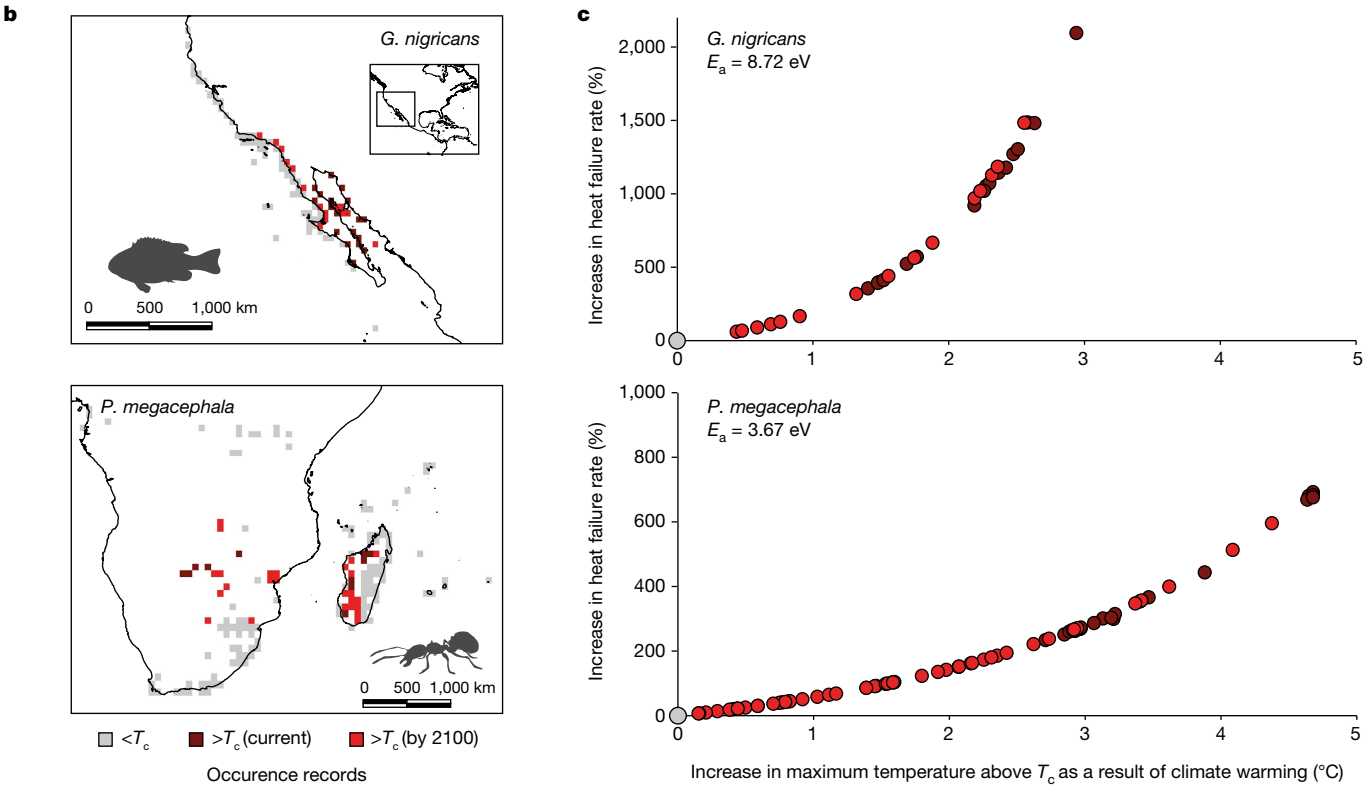

Fig. 3 | Projected increase in heat failure rate with climate warming. **a**, Percentage increases in biological rates associated with future climate change in terrestrial and aquatic environments (in 2081–2100 and 2090–2100, respectively). The temperature change ΔT for three warming scenarios[6] corresponds to changes in the mean and maximum temperature for the permissive and stressful range, respectively. SSP1–2.6 is within the limits of the Paris Agreement, whereas SSP2–4.5 and SSP5–8.5 represent intermediate and severe emission scenarios, respectively. Percentage increases in rates (median and IQR) are based on the baseline temperature, ΔT and environment-specific E_a for the permissive and stressful temperature range (Methods; see Extended Data Figs. 2 and 4 for global maps). **b**, Analysis evaluating the risk of exposure to temperatures above the critical temperature T_c (estimated as the temperature resulting in heat failure in 24 h) for two example species, *G. nigricans* and *P. megacephala*, in current and future (SSP2–4.5) climates. Occurrence locations are coloured according to the comparison between T_c and maximal environmental temperature ($T_{env\,max}$). Grey, $T_c > T_{env\,max}$ in both current and future climates; maroon, $T_c < T_{env\,max}$ in the current climate; red, $T_c < T_{env\,max}$ in future climates. The global distribution of *P. megacephala* is shown in Extended Data Fig. 3. **c**, Increases in heat failure rate resulting from SSP2–4.5-projected increase in maximal temperature above T_c using global occurrences and thermal sensitivities for *G. nigricans* and *P. megacephala* (Methods). Colours are as described in **b**. For occurrences in red, the increase in maximal temperature is the difference between future maximum temperature and T_c. For occurrences in maroon (which already experiences temperatures of $>T_c$), the additional increase in temperature between current and future maximum temperature was used.

temperate terrestrial environments in the Northern Hemisphere and in aquatic environments across the Arctic (Extended Data Figs. 4 and 5).

Using air and sea surface maximum temperatures may further underestimate the exposure to stressful temperature as it does not account for temperatures experienced in particular warm microclimates, nor does it consider that solar radiation and convective heat transfer[3,31,33] can increase the operative temperature considerably above air temperature. By contrast, the risk estimate presented here does not directly account for mitigation through behavioural selection of permissive microhabitats[32–35] or for acclimation/adaptive responses that could alter thermal tolerance[2,7]. Species-specific implications of future heatwaves should therefore consider the local risk of exposure to extreme events beyond T_c (Fig. 3b). Nevertheless, most ecosystems will probably include species that are at risk of exposure to temperatures beyond T_c (ref. [3]).

The risk analysis presented here is mainly relevant for species that experience temperatures above T_c in their current or future environment (Fig. 3b), and the notable implications primarily pertain to the periods during which environmental temperature is highest. The effect of global warming on processes of life and death should therefore ideally integrate positive and negative warming effects within both the permissive and stressful temperatures (Box 1). Even so, our analysis highlights that heat stress is likely to escalate substantially with even a modest degree of global warming (Fig. 3). The effects of warming on

heat failure rates are several magnitudes greater than the temperature effects previously considered when analysing warming of permissive biological processes. As a consequence, both aquatic and terrestrial ectotherms risk considerable increases in heat stress with global warming and this increase will be accentuated markedly on the regional scale and with each degree of further global warming.

Online content

Any methods, additional references, Nature Research reporting summaries, source data, extended data, supplementary information, acknowledgements, peer review information; details of author contributions and competing interests; and statements of data and code availability are available at https://doi.org/10.1038/s41586-022-05334-4.

1. Angilletta, M. J. *Thermal Adaptation: A Theoretical and Empirical Synthesis* (Oxford Univ. Press, 2009).
2. Cossins, A. R. & Bowler, K. *Temperature Biology of Animals* (Chapman and Hall, 1987).
3. Sunday, J. M. et al. Thermal-safety margins and the necessity of thermoregulatory behavior across latitude and elevation. *Proc. Natl Acad. Sci. USA* **111**, 5610–5615 (2014).
4. Perry, A. L., Low, P. J., Ellis, J. R. & Reynolds, J. D. Climate change and distribution shifts in marine fishes. *Science* **308**, 1912–1915 (2005).
5. Kellermann, V. et al. Upper thermal limits of *Drosophila* are linked to species distributions and strongly constrained phylogenetically. *Proc. Natl Acad. Sci. USA* **109**, 16228–16233 (2012).
6. IPCC. *Climate Change 2021: The Physical Science Basis* (eds Masson-Delmotte, V. et al.) (Cambridge Univ. Press, 2021).
7. Hofmann, G. E. & Todgham, A. E. Living in the now: physiological mechanisms to tolerate a rapidly changing environment. *Annu. Rev. Physiol.* **72**, 127–145 (2010).
8. Schulte, P. M. The effects of temperature on aerobic metabolism: towards a mechanistic understanding of the responses of ectotherms to a changing environment. *J. Exp. Biol.* **218**, 1856–1866 (2015).
9. Sunday, J. et al. Thermal tolerance patterns across latitude and elevation. *Philos. Trans. R. Soc. B* **374**, 20190036 (2019).
10. Parratt, S. R. et al. Temperatures that sterilize males better match global species distributions than lethal temperatures. *Nat. Clim. Change* **11**, 481–484 (2021).
11. Sunday, J. M., Bates, A. E. & Dulvy, N. K. Thermal tolerance and the global redistribution of animals. *Nat. Clim. Change* **2**, 686–690 (2012).
12. Schmidt-Nielsen, K. *Animal physiology: Adaptation and Environment* 5th edn (Cambridge Univ. Press, 1997).
13. Dell, A. I., Pawar, S. & Savage, V. M. Systematic variation in the temperature dependence of physiological and ecological traits. *Proc. Natl Acad. Sci. USA* **108**, 10591–10596 (2011).
14. Seebacher, F., White, C. R. & Franklin, C. E. Physiological plasticity increases resilience of ectothermic animals to climate change. *Nat. Clim. Change* **5**, 61–66 (2014).
15. Dillon, M. E., Wang, G. & Huey, R. B. Global metabolic impacts of recent climate warming. *Nature* **467**, 704–706 (2010).
16. Deutsch, C. A. et al. Increase in crop losses to insect pests in a warming climate. *Science* **361**, 916–919 (2018).
17. Jørgensen, L. B., Malte, H. & Overgaard, J. How to assess *Drosophila* heat tolerance: unifying static and dynamic tolerance assays to predict heat distribution limits. *Funct. Ecol.* **33**, 629–642 (2019).
18. Hollingsworth, M. J. Temperature and length of life in *Drosophila*. *Exp. Gerontol.* **4**, 49–55 (1969).
19. Fry, F. E. J., Hart, J. S. & Walker, K. F. *Lethal Temperature Relations for a Sample of Young Speckled Trout*, Salvelinus fontinalis 9–35 (Univ. Toronto, 1946).
20. MacLean, H. J. et al. Evolution and plasticity of thermal performance: an analysis of variation in thermal tolerance and fitness in 22 *Drosophila* species. *Philos. Trans. R. Soc. B* **374**, 20180548 (2019).
21. Pörtner, H.-O. & Farrell, A. P. Physiology and climate change. *Science* **322**, 690–692 (2008).
22. Ørsted, M., Jørgensen, L. B. & Overgaard, J. Finding the right thermal limit: a framework to reconcile ecological, physiological, and methodological aspects of CT_{max} in ectotherms. *J. Exp. Biol.* **225**, jeb244514 (2022).
23. Brown, J. H., Gillooly, J. F., Alle, A. P., Savage, V. M. & West, G. B. Toward a metabolic theory of ecology. *Ecology* **85**, 1771–1789 (2004).
24. Munch, S. B. & Salinas, S. Latitudinal variation in lifespan within species is explained by the metabolic theory of ecology. *Proc. Natl Acad. Sci. USA* **106**, 13860–13864 (2009).
25. Jørgensen, L. B., Malte, H., Ørsted, M., Klahn, N. A. & Overgaard, J. A unifying model to estimate thermal tolerance limits in ectotherms across static, dynamic and fluctuating exposures to thermal stress. *Sci. Rep.* **11**, 12840 (2021).
26. Rezende, E. L., Castañeda, L. E. & Santos, M. Tolerance landscapes in thermal ecology. *Funct. Ecol.* **28**, 799–809 (2014).
27. Bowler, K. Heat death in poikilotherms: is there a common cause? *J. Therm. Biol.* **76**, 77–79 (2018).
28. Somero, G. N. The physiology of climate change: how potentials for acclimatization and genetic adaptation will determine 'winners' and 'losers'. *J. Exp. Biol.* **213**, 912–920 (2010).
29. Buckley, L. B., Huey, R. B. & Kingsolver, J. G. Asymmetry of thermal sensitivity and the thermal risk of climate change. *Glob. Ecol. Biogeogr.* **31**, 2231–2244 (2022).
30. Overgaard, J., Kearney, M. R. & Hoffmann, A. A. Sensitivity to thermal extremes in Australian *Drosophila* implies similar impacts of climate change on the distribution of widespread and tropical species. *Glob. Change Biol.* **20**, 1738–1750 (2014).
31. Pinsky, M. L., Eikeset, A. M., McCauley, D. J., Payne, J. L. & Sunday, J. M. Greater vulnerability to warming of marine versus terrestrial ectotherms. *Nature* **569**, 108–111 (2019).
32. Huey, R. B. et al. Predicting organismal vulnerability to climate warming: roles of behaviour, physiology and adaptation. *Philos. Trans. R. Soc. B* **367**, 1665–1679 (2012).
33. Kearney, M., Shine, R. & Porter, W. P. The potential for behavioral thermoregulation to buffer 'cold-blooded' animals against climate warming. *Proc. Natl Acad. Sci. USA* **106**, 3835–3840 (2009).
34. Woods, H. A., Dillon, M. E. & Pincebourde, S. The roles of microclimatic diversity and of behavior in mediating the responses of ectotherms to climate change. *J. Therm. Biol* **54**, 86–97 (2015).
35. Stevenson, R. D. The relative importance of behavioral and physiological adjustments controlling body temperature in terrestrial ectotherms. *Am. Nat.* **126**, 362–386 (1985).
36. Chen, I., Hill, J. K., Ohlemüller, R., Roy, D. B. & Thomas, C. D. Rapid range shifts of species associated with high levels of climate warming. *Science* **333**, 1024–1026 (2011).
37. Buckley, L. B. & Kingsolver, J. G. Functional and phylogenetic approaches to forecasting species' responses to climate change. *Annu. Rev. Ecol. Evol. Syst.* **43**, 205–226 (2012).
38. Roeder, K. A., Bujan, J., de Beurs, K. M., Weiser, M. D. & Kaspari, M. Thermal traits predict the winners and losers under climate change: an example from North American ant communities. *Ecosphere* **12**, e03645 (2021).
39. Penick, C. A., Diamond, S. E., Sanders, N. J. & Dunn, R. R. Beyond thermal limits: comprehensive metrics of performance identify key axes of thermal adaptation in ants. *Funct. Ecol.* **31**, 1091–1100 (2017).
40. Deutsch, C. A. et al. Impacts of climate warming on terrestrial ectotherms across latitude. *Proc. Natl Acad. Sci. USA* **105**, 6668–6672 (2008).
41. Huey, R. B. & Stevenson, R. D. Integrating thermal physiology and ecology of ectotherms: a discussion of approaches. *Integr. Comp. Biol.* **19**, 357–366 (1979).
42. Sinclair, B. J. et al. Can we predict ectotherm responses to climate change using thermal performance curves and body temperatures? *Ecol. Lett.* **19**, 1372–1385 (2016).
43. Tewksbury, J. J., Huey, R. B. & Deutsch, C. A. Putting the heat on tropical animals the scale of prediction. *Science* **320**, 1296–1297 (2008).
44. Kingsolver, J. G., Diamond, S. E. & Buckley, L. B. Heat stress and the fitness consequences of climate change for terrestrial ectotherms. *Funct. Ecol.* **27**, 1415–1423 (2013).
45. Kingsolver, J. G. & Woods, H. A. Beyond thermal performance curves: modeling time-dependent effects of thermal stress on ectotherm growth rates. *Am. Nat.* **187**, 283–294 (2016).
46. Kingsolver, J. G., Higgins, J. K. & Augustine, K. E. Fluctuating temperatures and ectotherm growth: distinguishing non-linear and time-dependent effects. *J. Exp. Biol.* **218**, 2218–2225 (2015).
47. Clusella-Trullas, S., Garcia, R. A., Terblanche, J. S. & Hoffmann, A. A. How useful are thermal vulnerability indices? *Trends Ecol. Evol.* **36**, 1000–1010 (2021).
48. Pincebourde, S. & Casas, J. Narrow safety margin in the phyllosphere during thermal extremes. *Proc. Natl Acad. Sci. USA* **116**, 5588–5596 (2019).

Methods

Data collection for the meta-analysis

To estimate the thermal sensitivity of permissive biological rates, we collected data for a meta-analysis of processes covering enzyme activity, heart rate, locomotion, feeding and metabolic rate for a wide range of ectothermic animal species. The dataset includes 1,351 entries of biological rates measured at two temperatures and represents 314 species examined in 304 original publications. Data were mostly sourced from two large collections of published data compiled by Dell et al. (see Supporting Information in ref. [13]) (here we used only E_a of the ascending rates derived from trait performance curves) and by Seebacher et al. (see Supplementary Information in ref. [14]), and overlapping entries were removed. A few (n = 4) additional entries were included as they were used as examples in Fig. 2a.

To estimate the thermal sensitivity of heat failure rates in the highly stressful temperature range, we compiled data on time to heat failure with associated test temperatures. This dataset includes 123 thermal sensitivities for 112 species. Data were compiled from 69 individual studies and an additional 54 studies sourced from references reported by Rezende et al. (see Supporting Information in ref. [26]), and were included only if heat failure times were available for at least three temperatures.

Calculation of E_a

The Arrhenius activation energy E_a was calculated to quantify the thermal sensitivity of rates related to either permissive or stressful biological processes. The E_a values of ascending rates (in the permissive temperature range) originating from Supporting Information in ref. [13] were available from the publication, whereas E_a values for all other rates were calculated using a linear regression in an Arrhenius analysis. The Arrhenius analysis was performed by regressing the natural logarithm to the rate against the reciprocal temperature (1/temperature (K^{-1})). The regression slope was then used to calculate the activation energy E_a

$$E_a = \frac{-R \times \text{slope}}{N_A \times C} \tag{1}$$

Where R is the gas constant (8.31 J K^{-1} mol^{-1}), N_A is the Avogadro constant (6.022×10^{23} mol^{-1}), and C is a conversion factor to report E_a in eV (1.602×10^{-19} J eV^{-1}).

To estimate activation energy E_a for heat failure rates in the stressful temperature range, we calculated heat failure rates (min^{-1}) by converting the collected heat failure times (min) as

$$\text{Heat failure rate} = 1/\text{heat failure time} \tag{2}$$

Accordingly, heat failure rate represents the incremental heat stress that accumulates per minute at a specific constant temperature and, once the increments sum to 1, heat failure occurs (that is, the number of increments (time) to sum to 1 equals the heat failure time). For example, if heat failure time is 100 min at 38 °C, then the corresponding heat failure rate at 38 °C is 1/100 min = 0.01 min^{-1} and, therefore, accumulating these increments of heat stress over a 100 min exposure to 38 °C results in summation to 1 = heat failure.

The median heat failure times used to calculate E_a vary between studies (median = 125 min, IQR = 31.5–422 min) but a linear regression of $\log_{10}$[median duration] against E_a did not reveal any significant correlation ($F_{1,121} = 0.36$, $P = 0.55$, $R^2 < 0.01$), and we therefore conclude that high E_a is not an artefact of test duration.

Converting E_a to estimates of Q_{10}

In mainstream literature, thermal sensitivities are often presented using the thermal sensitivity quotient Q_{10} (that is, the factorial change in rate associated with a 10 °C temperature change). To discuss thermal sensitivities using the more commonplace Q_{10}, we converted activation energy E_a using

$$Q_{10} = e^{\frac{10\text{K} \times E_a}{k_B \times T^2}} \tag{3}$$

Where E_a is the activation energy (eV), k_B is the Boltzmann constant (8.617×10^{-5} eV K^{-1}) and T is the temperature (K). This conversion is sensitive to temperature and here we used the temperature T = 18.3 °C (291.5 K) for conversion to permissive Q_{10} and T = 36.3 °C (309.5 K) for stressful Q_{10}. These temperatures were chosen as they represent the mean temperature used to measure the rates in the permissive and stressful temperature range, respectively.

Modelling projected temperature change

To model the impact of increased intensity of heatwaves, we associated the predicted rise in future temperature with the thermal sensitivity E_a in terrestrial and aquatic environments. To make this change spatially and temporally explicit, we used projected global changes in mean and maximum temperature for three different emission scenarios (see below) towards the end of the twenty-first century compared with present-day conditions (Extended Data Fig. 1).

For terrestrial areas, we used the WorldClim v.2.1 climate database (https://worldclim.org)[49], based on monthly averages, using the bioclimatic variables 'mean annual temperature' (BIO1) and 'maximum temperature of the warmest month' (BIO5). In WorldClim, present conditions are produced with monthly averages for the latest climate period 1970–2000. Future layers of mean and maximum temperature (BIO1 and BIO5, respectively) were produced by averaging data from eight general circulation models (GCMs) (Extended Data Table 2) for the period 2081–2100. We used projected changes for three future Shared Socioeconomic Pathways (SSP) scenarios[6]: (1) the optimistic SSP1–2.6, a peak-and-decline scenario ending with low greenhouse gas concentration levels by the end of the twenty-first century; (2) the SSP2–4.5 'middle of the road' scenario where trends do not shift markedly from historical patterns; and (3) the pessimistic and perhaps unrealistic SSP5–8.5, where fossil-fuelled development increases emissions over time leading to high greenhouse gas concentrations (for discussions on the use and misuse of emission scenarios, see refs. [50–52]).

For aquatic areas, we used the Bio-ORACLE v.2.0 database (https://bio-oracle.org/)[53,54], based on monthly averages, using the variables average and maximum sea surface water temperature (SST). In Bio-ORACLE, present conditions are produced with monthly averages for the period 2000–2014. Future layers of mean and maximum SST were produced by averaging data from three atmosphere–ocean coupled GCMs (AO-GCMs) (Extended Data Table 2) for the period 2090–2100. The SSPs are not yet available for aquatic environments, so we used the corresponding Representative Concentration Pathway (RCP) scenarios (RCP2.6, RCP4.5, and RCP8.5, respectively) that precede the SSP scenarios (hereafter, we refer to all scenarios by the corresponding SSP). In terms of temperature change by the end of the twenty-first century, the SSPs and RCPs yield practically identical predictions[52]. All spatial data were used at a 5 arcmin resolution in a Behrmann equal area cylindrical projection (approximately 9.2 km) with the WGS84 datum.

Exposure to temperatures above T_c

In two example species (*G. nigricans* and *P. megacephala*), we estimated exposure to environmental temperatures above the critical temperature T_c separating the permissive and stressful temperature range. In this analysis we first established a proxy of T_c representing the temperature above which heat stress accumulates. Specifically, T_c (K) is estimated as the temperature causing heat failure after 24 h, using the slope and intercept from the linear regression in the Arrhenius analysis

$$T_c = \frac{\text{slope}}{\ln(R') - \text{intercept}} \quad (4)$$

Where R' is the rate calculated to result in heat failure after 24 h (that is, $R' = 1/1{,}440$ min, compare with equation (2)). This approximation of T_c is conservative as the linearity of heat failure rates often extends beyond 24 h (for example, Fig. 1a), suggesting that we may underestimate the risk of exposure to temperatures above T_c. However, the potent nature of heat failure versus temperature discourages excessive extrapolation of such data (see the discussions in refs. [17,25]).

For the species-level risk assessment, we then obtained occurrence records from the Global Biodiversity Information Facility (GBIF; https://www.gbif.org/; downloaded 20 March 2022). After removal of faulty records, we found 647 and 2,063 occurrences for *G. nigricans* and *P. megacephala*, respectively, from which we extracted the maximum temperature in the current climate and from the SSP2–4.5 future warming scenario (BIO5 (terrestrial) and maximum SST (aquatic) for *P. megacephala* and *G. nigricans*, respectively). Temperature data were aggregated within 46 × 46 km and 92 × 92 km cells for *G. nigricans* and *P. megacephala*, respectively, to avoid sampling bias, resulting in 93 and 403 cells for *G. nigricans* and *P. megacephala*, respectively. The maximum environmental temperatures at these locations were evaluated against the species-specific estimates of T_c to determine which of the occurrence locations experience temperatures $\geq T_c$ now and under future warming. The increase in maximal environmental temperature above T_c was associated with the resulting increase in heat failure rates using species-specific E_a estimates (8.72 eV and 3.67 eV for *G. nigricans* and *P. megacephala*, respectively), and T_c (31.5 °C and 34.4 °C for *G. nigricans* and *P. megacephala*, respectively). For the parts of the species-distribution ranges in which populations experience temperatures above T_c only after future climate warming, the increase in maximal temperature was calculated as the difference between the future maximum temperature and T_c. For the populations in which maximal temperature already exceeds T_c, the increase in temperature was calculated from the increase between current and projected future maximum temperatures.

Associating temperature change with E_a

The projections on future percentage increases in biological rates in the permissive temperature range were based on the mean annual temperature, whereas projections for increases in heat failure rates were based on the maximum temperatures (Extended Data Fig. 1a,b, respectively). The projected change in local temperature (ΔT) for the three future scenarios (SSP1–2.6, SSP2–4.5 and SSP5–8.5) was determined as follows:

$$\Delta T = T_{\text{future}} - T_{\text{present}} \quad (5)$$

Where T_{future} is the mean annual or maximum temperature for the specific future climate scenario, and T_{present} is the current mean annual or maximum temperature, and both were calculated separately for the terrestrial and aquatic environment. The current mean annual temperature was described by BIO1 or SST_{mean} for terrestrial and aquatic environments, respectively, and the current maximum temperature was described by BIO5 or SST_{max} for terrestrial and aquatic environments, respectively (see the 'Modelling projected temperature change' section; Extended Data Fig. 1c–h).

Subsequently, the projected change in temperature ΔT (mean and maximum for terrestrial and aquatic environments separately) was associated with the activation energy E_a (median and first–third quartile) for the specific group to calculate the increase in rate, for example, E_a for heat failure rate in terrestrial ectotherms was associated with ΔT based on the maximum temperature in the terrestrial environment. The projected percentage increase in rates (in the permissive and stressful range) was calculated as follows:

$$\Delta\text{Rate (\%)} = \left(e^{\frac{E_a}{k_B} \times \frac{\Delta T}{T_2 \times T_1}} - 1\right) \times 100\% \quad (6)$$

Where E_a is the activation energy (eV), k_B is the Boltzmann constant (8.617×10^{-5} eV K^{-1}), ΔT is the projected change in temperature (K) between the current and future climate scenario, and T_2 and T_1 are the future and current temperature [K], respectively. The following values of E_a were used for rates in the permissive temperature range: $E_a = 0.56839$ eV (terrestrial) and $E_a = 0.44329$ eV (aquatic); and for heat failure rates: $E_a = 5.52589$ eV (terrestrial) and $E_a = 6.68649$ eV (aquatic). These values are also presented in Fig. 3a, and the projected percentage increases in rates resulting from all three future scenarios are shown in Extended Data Fig. 2 (biological rates in the permissive temperature range) and in Extended Data Fig. 4 (heat failure rates in the stressful temperature range).

Equation (6) was also used to calculate the percentage increase in rates from a 1 °C temperature increase, using the median E_a for the permissive biological rates ($E_a = 0.48$ eV) or heat failure rates ($E_a = 6.13$ eV) disregarding the specific environment and using the temperatures listed in the 'Converting E_a to estimates of Q_{10}' section.

Reporting summary

Further information on research design is available in the Nature Research Reporting Summary linked to this article.

Data availability

The data supporting the findings of this study are available online[55].

49. Fick, S. E. & Hijmans, R. J. WorldClim 2: new 1-km spatial resolution climate surfaces for global land areas. *Int. J. Climatol.* **37**, 4302–4315 (2017).
50. Moss, R. H. et al. The next generation of scenarios for climate change research and assessment. *Nature* **463**, 747–756 (2010).
51. Hausfather, Z. & Peters, G. P. Emissions—the 'business as usual' story is misleading. *Nature* **577**, 618–620 (2020).
52. Tollefson, J. How hot will Earth get by 2100? *Nature* **580**, 443–445 (2020).
53. Assis, J. et al. Bio-ORACLE v2.0: extending marine data layers for bioclimatic modelling. *Glob. Ecol. Biogeogr.* **27**, 277–284 (2018).
54. Tyberghein, L. et al. Bio-ORACLE: a global environmental dataset for marine species distribution modelling. *Glob. Ecol. Biogeogr.* **21**, 272–281 (2012).
55. Jørgensen, L. B., Ørsted, M., Malte, H., Wang, T. & Overgaard, J. Data from: Extreme escalation of heat failure rates in ectotherms with global warming. *Zenodo* https://doi.org/10.5281/zenodo.6979789 (2022).
56. Grove, T. J., McFadden, L. A., Chase, P. B. & Moerland, T. S. Effects of temperature, ionic strength and pH on the function of skeletal muscle myosin from a eurythermal fish, *Fundulus heteroclitus*. *J. Muscle Res. Cell Motil.* **26**, 191–197 (2005).
57. Doudoroff, P. The resistance and acclimatization of marine fishes to temperature changes. II. Experiments with *Fundulus* and *Atherinops*. *Biol. Bull.* **88**, 194–206 (1945).
58. Sirikharin, R., Söderhäll, I. & Söderhäll, K. Characterization of a cold-active transglutaminase from a crayfish, *Pacifastacus leniusculus*. *Fish Shellfish Immunol.* **80**, 546–549 (2018).
59. Becker, C. D. & Genoway, R. G. Resistance of crayfish to acute thermal shock: preliminary studies. in *Proc. Thermal Ecology NTIS Conf. 730505* (eds Gibbons, J. W. & Sharitz, R. R.) 146–150 (NTIS, 1974).
60. Widdows, J. Effect of temperature and food on the heart beat, ventilation rate and oxygen uptake of *Mytilus edulis*. *Mar. Biol.* **20**, 269–276 (1973).
61. Wallis, R. L. Thermal tolerance of *Mytilus edulis* of eastern Australia. *Mar. Biol.* **30**, 183–191 (1975).
62. Gray, J. The mechanism of ciliary movement. III. The effect of temperature. *Proc. R. Soc. B* **95**, 6–15 (1923).
63. Shertzer, R. H., Hart, R. G. & Pavlick, F. M. Thermal acclimation in selected tissues of the leopard frog *Rana pipiens*. *Comp. Biochem. Physiol. A* **51**, 327–334 (1975).
64. Orr, P. R. Heat death. II. Differential response of entire animal (*Rana pipiens*) and several organ systems. *Physiol. Zool.* **28**, 294–302 (1955).
65. Lighton, J. R. B. & Duncan, F. D. Energy cost of locomotion: validation of laboratory data by in situ respirometry. *Ecology* **83**, 3517–3522 (2002).
66. Heatwole, H. & Harrington, S. Heat tolerances of some ants and beetles from the pre-Saharan steppe of Tunisia. *J. Arid Environ.* **16**, 69–77 (1989).

Acknowledgements We thank our colleagues at the Section for Zoophysiology, Aarhus University for the many discussions on temperature biology of animals. This work was funded by The Danish Council for Independent Research—Natural Sciences (to J.O.) and The Danish Council for Independent Research—Technology and Production Sciences (to M.Ø.).

Author contributions L.B.J., M.Ø. and J.O. conceptualized the study and all of the authors participated in its design. L.B.J., M.Ø., H.M. and J.O. collected the data and performed the analysis. L.B.J. curated the data. L.B.J., M.Ø., T.W. and J.O. wrote and visualized the original draft, and all of the authors contributed to the review and editing of the final manuscript.

Competing interests The authors declare no competing interests.

Additional information

Supplementary information The online version contains supplementary material available at https://doi.org/10.1038/s41586-022-05334-4.

Correspondence and requests for materials should be addressed to Johannes Overgaard.

Peer review information *Nature* thanks Raymond Huey, David Vasseur and the other, anonymous, reviewer(s) for their contribution to the peer review of this work. Peer reviewer reports are available.

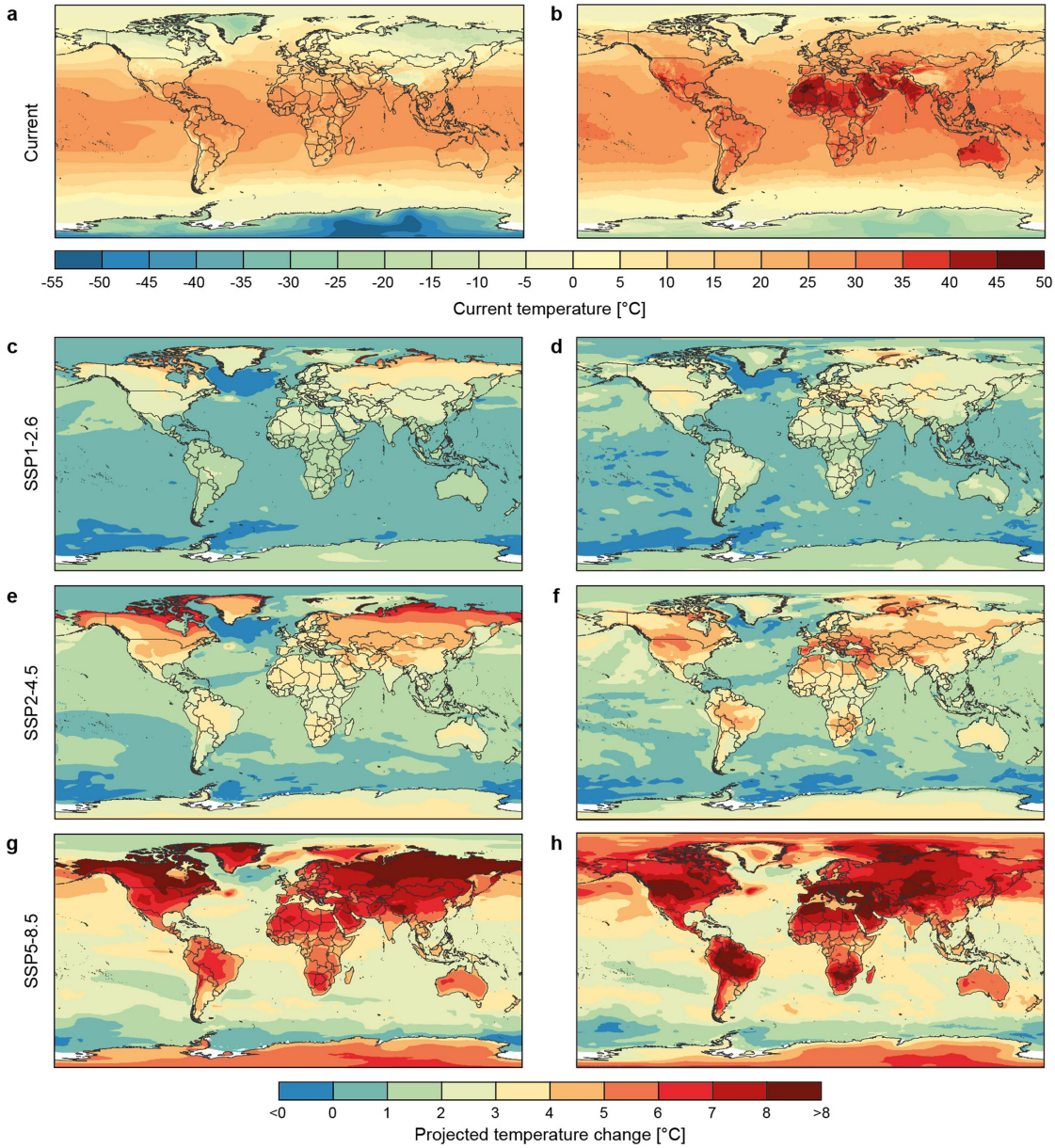

Extended Data Fig. 1 | Current and projected change in mean and maximum temperature under climate warming. a, Current mean annual temperature described by BIO1 or SST_{mean} for terrestrial and aquatic environments, respectively. **b**, Current maximum temperature described by BIO5 or SST_{max} for terrestrial and aquatic environments, respectively. (**a**, **b**) share the legend immediately below. **c**–**d**, Projected change in (**c**) mean annual temperature and (**d**) maximum temperature under the SSP1-2.6 scenario. **e**–**f**, Projected change in (**e**) mean annual temperature and (**f**) maximum temperature under the SSP2-4.5 scenario. **g**–**h**, Projected change in (**g**) mean annual temperature and (**h**) maximum temperature under the SSP5-8.5 scenarios. (**c**–**h**) share the bottom legend and the future period is 2081-2100 for terrestrial environments and 2090-2100 for aquatic environments, as they appear in WorldClim 2.1[49] and Bio-ORACLE 2.0[53,54], respectively. White areas indicate that temperature data were not available.

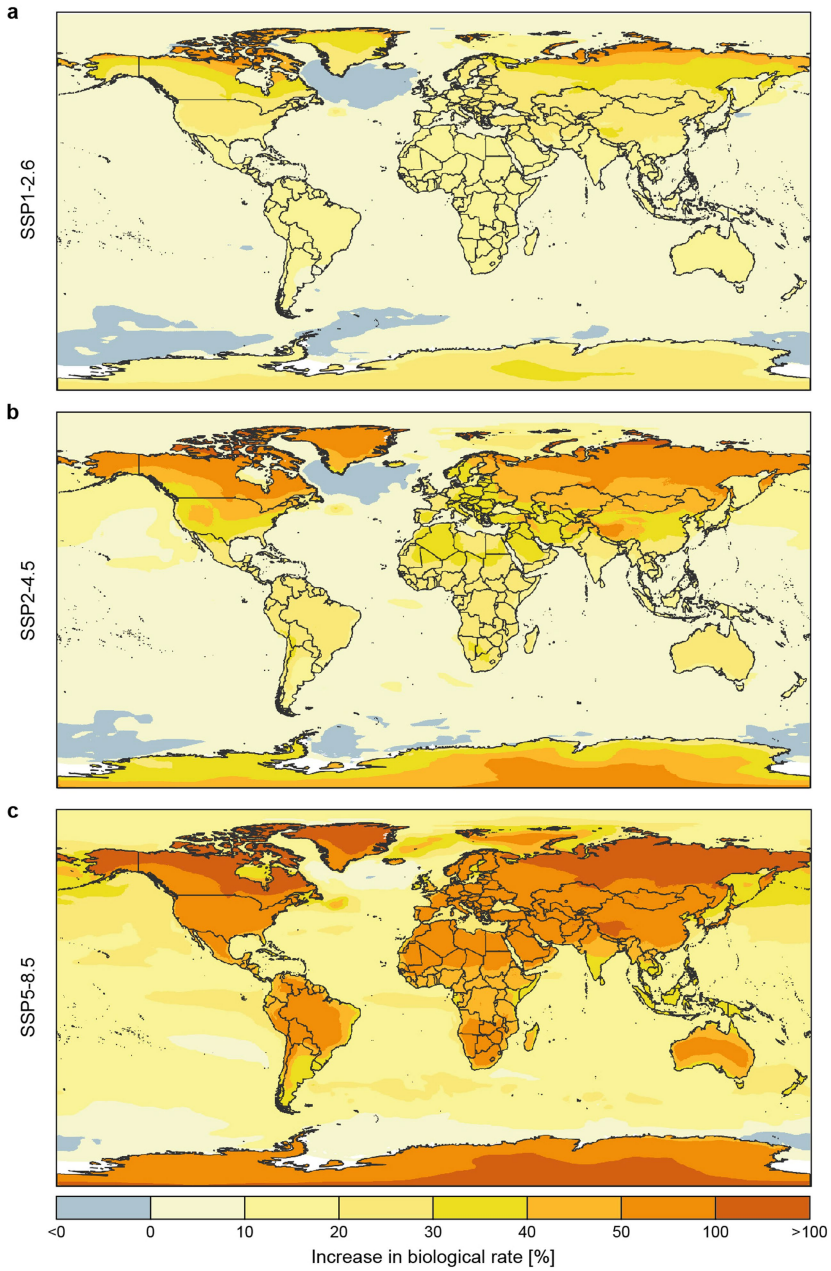

Extended Data Fig. 2 | Projected increase in biological rates of permissive processes under climate warming. Increase in biological rates (in %) of permissive processes for both terrestrial (E_a = 0.57 eV) and aquatic species (E_a = 0.44 eV) resulting from changes in annual mean temperature under the (**a**) SSP1-2.6, (**b**) SSP2-4.5 and (**c**) SSP5-8.5 scenario. The future period is 2081-2100 for terrestrial environments and 2090-2100 for aquatic environments, as they appear in WorldClim 2.1[49] and Bio-ORACLE 2.0[53,54], respectively. White areas indicate that temperature data were not available to calculate the increase in biological rate.

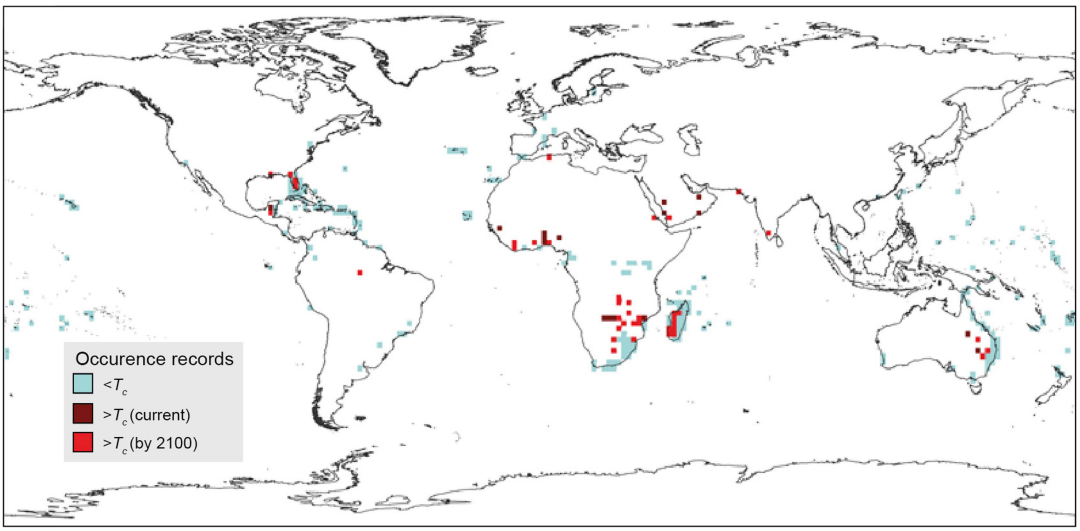

Extended Data Fig. 3 | Risk of exposure to environmental temperatures above T_c for *Pheidole megacephala*. Global risk analysis evaluating exposure to environmental (air) temperatures beyond the critical temperature T_c (separating the permissive and stressful temperature range, here calculated as the temperature causing heat failure in 24 h) in current and future climates (2081-2100, SSP2-4.5). Occurrence locations in the global distribution of *P. megacephala* are coloured according to the comparison of T_c to maximal air temperature (T_{airmax}). Grey, $T_c > T_{airmax}$ in current and future climates; red, $T_c < T_{airmax}$ in the future climate scenarios; maroon, $T_c < T_{airmax}$ in the current climate. Occurrence records were aggregated to 184 km cells for increased visibility, and a section of the distribution found in Southern Africa is shown in Fig. 3b, with slight discrepancies due to different spatial resolutions of occupied cells.

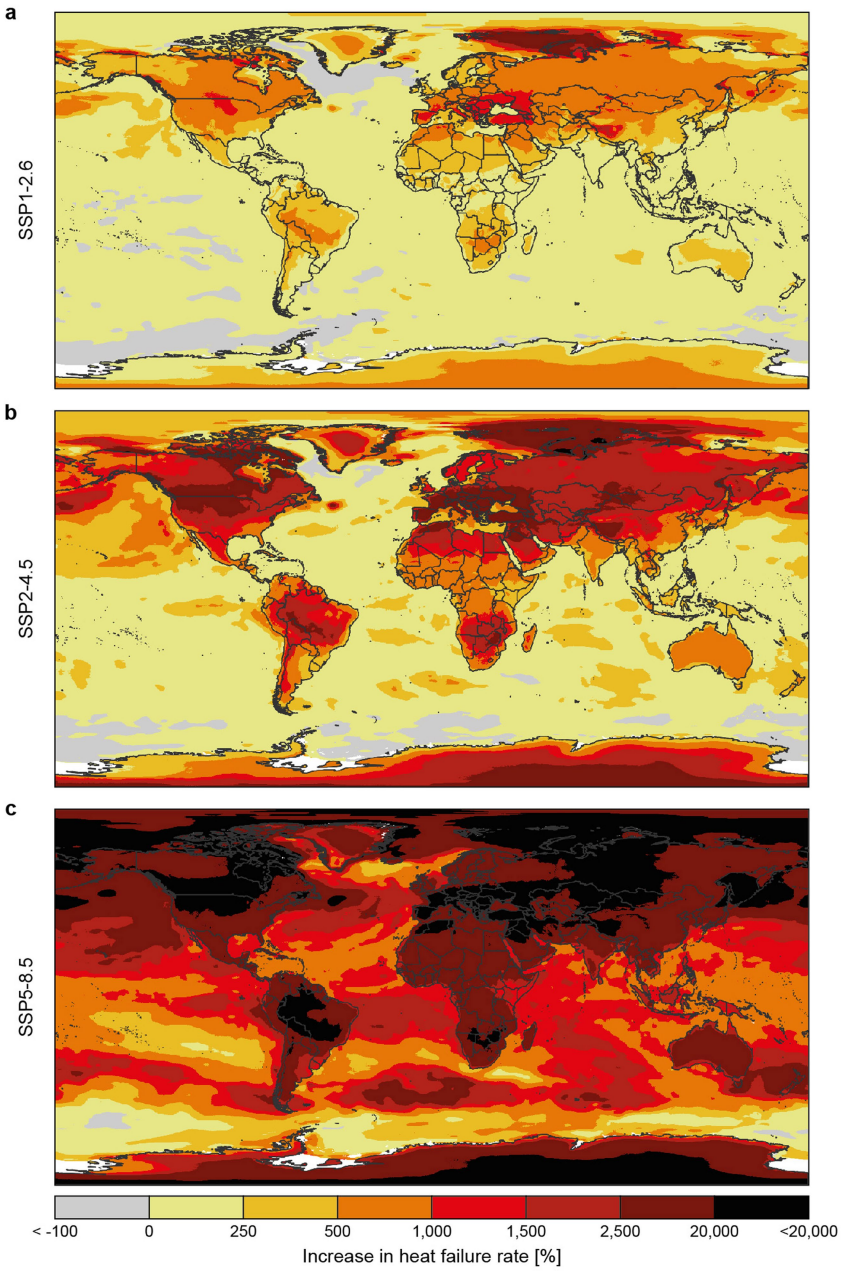

Extended Data Fig. 4 | Projected increase in heat failure rates under climate warming. Increase in heat failure rates (in %) for both terrestrial (E_a = 5.53 eV) and aquatic species (E_a = 6.69 eV) resulting from changes in maximum temperature under the (**a**) SSP1-2.6, (**b**) SSP2-4.5 and (**c**) SSP5-8.5 scenario. The future period is 2081-2100 for terrestrial environments and 2090-2100 for aquatic environments, as they appear in WorldClim 2.1[49] and Bio-ORACLE 2.0[53,54], respectively. White areas indicate that temperature data were not available to calculate the heat failure rate increase.

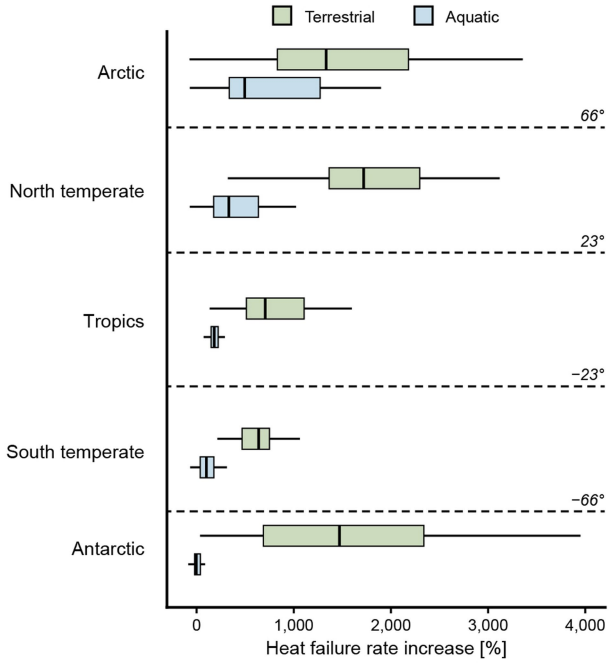

Extended Data Fig. 5 | Summary of increases in heat failure rate across latitudes. Boxplots of terrestrial and aquatic heat failure rates under the SSP2-4.5 warming scenario across five latitudinal clines summarizing the results reported in Extended Data Fig. 4b. The boxplot midline represents the median, the lower and upper line of the box represents the 1st and 3rd quartile, respectively (with whiskers extending up to 1.5 times this range), outliers not shown.

Extended Data Table 1 | Overview of the species used for the representative rates in Fig. 2a,c

		Species[reference]	
Group	Biological process [unit]	Permissive biological rate	Heat failure rate
Fishes	*ATPase* Actin activated Mg-ATPase [P_i s^{-1} $myosin^{-1}$]	*Fundulus heteroclitus*[56]	*Fundulus parvipinnis*[57]
Crustaceans	*Enzyme* Transglutaminase activity [ΔOD_{450} s^{-1}]	*Pacifastacus leniusculus*[58]	*Pacifastacus leniusculus*[59]
Molluscs	*Cardiac* Heart rate [beats s^{-1}]	*Mytilus edulis*[60]	*Mytilus edulis*[61]
	Feeding Ciliary movement [cm min^{-1}]	*Mytilus edulis*[62]	
Amphibians	*Metabolic rate* Muscle O_2 consumption rate [µL O_2 mg^{-1} h^{-1}]	*Rana pipiens*[63]	*Rana pipiens*[64]
Insects	*Locomotion* Running speed [m s^{-1}]	*Messor pergandei*[65]	*Messor collingwoodi*[66]

Overview of the species used to represent the biological processes and their [units] in the permissive temperature range and the heat failure rates in the stressful temperature range. Species were chosen based on the availability of heat failure rates and matched with measurements of permissive biological rates preferably from the same species but at least within the genus[56–66]. For each ectothermic group it was aimed that the biological process should represent the most frequent category within this group.

Extended Data Table 2 | Source of spatial data in the terrestrial and aquatic environment

Environment (source)	GCMs/AO-GCMs	Period	Future scenarios
Terrestrial (WorldClim v2.1)[49]	BCC-CSM2-MR CNRM-CM6-1 CNRM-ESM2-1 CanESM5 IPSL-CM6A-LR MIROC-ES2L MIROC6 MRI-ESM2-0	2081-2100	SSP1-2.6 SSP2-4.5 SSP5-8.5
Aquatic (Bio-ORACLE v2.0)[53,54]	CCSM4 HadGEM2-ES MIROC5	2090-2100	RCP2.6 RCP4.5 RCP8.5

Eight General Circulation Models (GCMs) were used for the terrestrial environment and three Atmosphere–Ocean coupled GCMs (AO-GCMs) were used for the aquatic environment to build consensus models (as the average of mean and max temperature projections). Terrestrial GCMs are from the Coupled Model Intercomparison Project v6, CMIP6, while AO-GCMs are from CMIPv5. The future Shared Socioeconomic Pathways (SSP) used for terrestrial environments[6] are not yet available for aquatic environments, so here we used the corresponding Representative Concentration Pathways (RCPs) scenarios (RCP2.6, RCP4.5, and RCP8.5, respectively) as used in the Bio-ORACLE 2.0 database.

nature portfolio

Corresponding author(s): Johannes Overgaard

Last updated by author(s): Aug 11, 2022

Reporting Summary

Nature Portfolio wishes to improve the reproducibility of the work that we publish. This form provides structure for consistency and transparency in reporting. For further information on Nature Portfolio policies, see our Editorial Policies and the Editorial Policy Checklist.

Statistics

For all statistical analyses, confirm that the following items are present in the figure legend, table legend, main text, or Methods section.

n/a	Confirmed	
☐	☒	The exact sample size (*n*) for each experimental group/condition, given as a discrete number and unit of measurement
☐	☒	A statement on whether measurements were taken from distinct samples or whether the same sample was measured repeatedly
☐	☒	The statistical test(s) used AND whether they are one- or two-sided *Only common tests should be described solely by name; describe more complex techniques in the Methods section.*
☒	☐	A description of all covariates tested
☒	☐	A description of any assumptions or corrections, such as tests of normality and adjustment for multiple comparisons
☐	☒	A full description of the statistical parameters including central tendency (e.g. means) or other basic estimates (e.g. regression coefficient) AND variation (e.g. standard deviation) or associated estimates of uncertainty (e.g. confidence intervals)
☐	☒	For null hypothesis testing, the test statistic (e.g. *F*, *t*, *r*) with confidence intervals, effect sizes, degrees of freedom and *P* value noted *Give P values as exact values whenever suitable.*
☒	☐	For Bayesian analysis, information on the choice of priors and Markov chain Monte Carlo settings
☒	☐	For hierarchical and complex designs, identification of the appropriate level for tests and full reporting of outcomes
☒	☐	Estimates of effect sizes (e.g. Cohen's *d*, Pearson's *r*), indicating how they were calculated

Our web collection on statistics for biologists contains articles on many of the points above.

Software and code

Policy information about availability of computer code

Data collection	*Provide a description of all commercial, open source and custom code used to collect the data in this study, specifying the version used OR state that no software was used.*
Data analysis	R version 4.4.1

For manuscripts utilizing custom algorithms or software that are central to the research but not yet described in published literature, software must be made available to editors and reviewers. We strongly encourage code deposition in a community repository (e.g. GitHub). See the Nature Portfolio guidelines for submitting code & software for further information.

Data

Policy information about availability of data

All manuscripts must include a data availability statement. This statement should provide the following information, where applicable:

- Accession codes, unique identifiers, or web links for publicly available datasets
- A description of any restrictions on data availability
- For clinical datasets or third party data, please ensure that the statement adheres to our policy

Provide your data availability statement here.

Human research participants

Policy information about studies involving human research participants and Sex and Gender in Research.

Reporting on sex and gender	n/a
Population characteristics	n/a
Recruitment	n/a
Ethics oversight	n/a

Note that full information on the approval of the study protocol must also be provided in the manuscript.

Field-specific reporting

Please select the one below that is the best fit for your research. If you are not sure, read the appropriate sections before making your selection.

☐ Life sciences ☐ Behavioural & social sciences ☒ Ecological, evolutionary & environmental sciences

For a reference copy of the document with all sections, see nature.com/documents/nr-reporting-summary-flat.pdf

Ecological, evolutionary & environmental sciences study design

All studies must disclose on these points even when the disclosure is negative.

Study description	Data were collected from the litterature of heat tolerance measurements (a minimum of 3 test temperatures with corresponding heat failure times/rates per species within a single study to create a thermal death time curve) and from these data the activation energy (Ea) was calculated for each entry (species in an individual study). Here n = 123 thermal death time curves representing 112 unique species. The rate of "normal" biological processes (e.g. metabolism, enzyme rates and locomotion) at two temperatures were also collected and the activation energy was calculated, here n = 1,351 rates from 314 unique species. Activation energies of both types were then combined with climate data projections of average and maximum temperature using three different future emission scenarios, and the projected change in heat failure rates were calculated. Specific examples for two species were demonstrated by combining distribution data with local temperature (sites n=647 and 2063) and use the calculated species-specific activation energy for heat failure to indicate the percent increase in heat failure rate with climate warming.
Research sample	Data on "normal" biological rates (e.g. metabolism, enzyme rates and locomotion) measured at two temperatures were compiled from Dell et al (2011, PNAS) and Seebacher et al (2014, Nature Climate Change), and a few additional entries (n = 4, rates measured at >4 temperatures) were added as they were used in a figure. Heat failure data were collected in a litterature search, and the criterium for selection was that for a specific species heat failure time was measured at at least 3 temperatures, to allow for a linear regression. Both the "normal rate" and heat failure data set includes a wide range of ectothermic species with major groups like fishes, insects, crustaceans, amphibians and molluscs represented.
Sampling strategy	No sample size calculation was performed; we collected as many entries as we could find for the heat failure data and used the available "normal" rates from Dell et al (2011, PNAS) and Seebacher et al (2014, Nature Climate Change). A few additional "normal rate" entries (n = 4, rates measured at >4 temperatures) were added as they were used in a figure.
Data collection	Heat failure data were collected in a literature search (Google Scholar) performed by LBJ, and the data found in Dell et al (2011, PNAS) and Seebacher et al (2014, Nature Climate Change) was curated to the needs of this study by LBJ. Current and projected future mean annual temperature and maximum monthly temperature was obtained for terrestrial and aquatic environments from the WorldClim v2.1 and Bio-ORACLE v2.0 databases, respectively. In these databases, current conditions represent 1970-2000 or 2000-2014 for terrestrial and aquatic environments, respectively. Future climate conditions were predicted for three future emission scenarios (SSP1-2.6, SSP2-4.5, and SSP5-8.5), from eight General Circulation Models (GCMs) for the period 2081-2100 for the terrestrial environments or three Atmosphere-Ocean coupled GCMs (AO-GCMs) for the period 2090-2100 for the aquatic environments. All climate data was used in a 5 arc minute resolution with the WGS84 datum. All climate data was analyzed and curated by MØ.
Timing and spatial scale	The litterature search was performed in the fall of 2021. The spatial scale of the climate association analysis is global.
Data exclusions	No data were excluded, except overlapping entries in the data sets from Dell et al (2011, PNAS) and Seebacher et al (2014, Nature Climate Change).
Reproducibility	Not applicable to this literature data analysis.
Randomization	Data were not randomized as only litterature data were used.
Blinding	Blinding was not used as only litterature data were used.

Did the study involve field work? ☐ Yes ☒ No

Reporting for specific materials, systems and methods

We require information from authors about some types of materials, experimental systems and methods used in many studies. Here, indicate whether each material, system or method listed is relevant to your study. If you are not sure if a list item applies to your research, read the appropriate section before selecting a response.

Materials & experimental systems

n/a	Involved in the study
☒	☐ Antibodies
☒	☐ Eukaryotic cell lines
☒	☐ Palaeontology and archaeology
☒	☐ Animals and other organisms
☒	☐ Clinical data
☒	☐ Dual use research of concern

Methods

n/a	Involved in the study
☒	☐ ChIP-seq
☒	☐ Flow cytometry
☒	☐ MRI-based neuroimaging

ARTICLES FOR FACULTY MEMBERS

GLOBAL WARMING EFFECTS ON ECTOTHERM SPECIES

Title/Author	**Fish shrinking, energy balance and climate change / Queiros, Q., McKenzie, D. J., Dutto, G., Killen, S., Saraux, C., & Schull, Q.**
Source	***Science of the Total Environment*** **Volume 906 (2024) 167310 Pages 1-12** **https://doi.org/10.1016/j.scitotenv.2023.167310** **(Database: Science Direct)**

Science of the Total Environment 906 (2024) 167310

Contents lists available at ScienceDirect

Science of the Total Environment

journal homepage: www.elsevier.com/locate/scitotenv

Fish shrinking, energy balance and climate change

Quentin Queiros [a,b,*], David J. McKenzie [a], Gilbert Dutto [a], Shaun Killen [c], Claire Saraux [d], Quentin Schull [a]

[a] MARBEC, Univ Montpellier, IFREMER, CNRS, IRD, Montpellier, Sète, Palavas-les-Flots, France
[b] DECOD (Ecosystem Dynamics and Sustainability), INRAE, Institut Agro, IFREMER, Rennes, France
[c] Institute of Biodiversity, Animal Health and Comparative Medicine, University of Glasgow, Graham Kerr Building, Glasgow G12 8QQ, UK
[d] IPHC UMR 7178, Université de Strasbourg, CNRS, Strasbourg, France

HIGHLIGHTS

- Size decline in fish may be a universal response to global change.
- Global change can disturb energy balance of consumers feeding at low trophic levels.
- Prey shrinking raised the energetic costs of feeding and daily energy expenditure.
- Warmer waters with smaller prey dramatically increase energy expenditure.

GRAPHICAL ABSTRACT

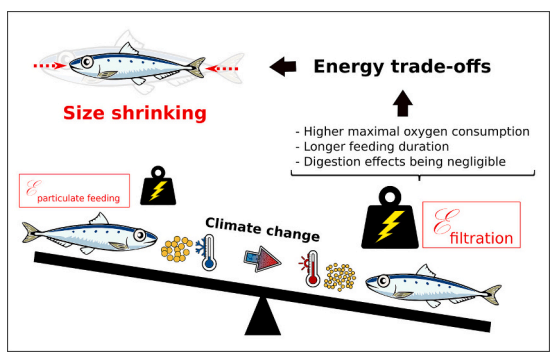

ARTICLE INFO

Editor: Martin Drews

Keywords:
Size decline
Energy expenditure
Feeding behaviour
Temperature
Small pelagic fish
Respirometry
Experiments

ABSTRACT

A decline in size is increasingly recognised as a major response by ectothermic species to global warming. Mechanisms underlying this phenomenon are poorly understood but could include changes in energy balance of consumers, driven by declines in prey size coupled with increased energy demands due to warming. The sardine *Sardina pilchardus* is a prime example of animal shrinking, European populations of this planktivorous fish are undergoing profound decreases in body condition and adult size. This is apparently a bottom-up effect coincident with a shift towards increased reliance on smaller planktonic prey. We investigated the hypothesis that foraging on smaller prey would lead to increased rates of energy expenditure by sardines, and that such expenditures would be exacerbated by warming temperature. Using group respirometry we measured rates of energy expenditure indirectly, as oxygen uptake, by captive adult sardines offered food of two different sizes (0.2 or 1.2 mm items) when acclimated to two temperatures (16 °C or 21 °C). Energy expenditure during feeding on small items was tripled at 16 °C and doubled at 21 °C compared to large items, linked to a change in foraging mode between filter feeding on small or direct capture of large. This caused daily energy expenditure to increase by ~10 % at 16 °C and ~40 % at 21 °C on small items, compared to large items at 16 °C. These results support that declines in prey size coupled with warming could influence energy allocation towards life-history traits in wild populations. This bottom-up effect could partially explain the shrinking and declining condition of many small pelagic fish populations and may be contributing to the shrinking of other fish species throughout the marine

* Corresponding author at: MARBEC, Univ Montpellier, IFREMER, CNRS, IRD, Montpellier, Sète, Palavas-les-Flots, France.
E-mail address: quentin.queiros@slu.se (Q. Queiros).

https://doi.org/10.1016/j.scitotenv.2023.167310
Received 3 March 2023; Received in revised form 1 September 2023; Accepted 21 September 2023
Available online 23 September 2023

food web. Understanding how declines in prey size can couple with warming to affect consumers is a crucial element of projecting the consequences for marine fauna of ongoing anthropogenic global change.

1. Introduction

Ongoing global warming constitutes a major threat for biodiversity, especially in marine ecosystems, with some scenarios of future temperature increases reaching +5 °C in 2100 (IPCC, 2013, 2014; Orr et al., 2005). For ectotherms such as fishes, warming results in large increases in their physiological rates (Clarke and Fraser, 2004; Seebacher et al., 2015). While ongoing global warming might therefore be expected to boost growth rates in ectotherms (Morrongiello et al., 2019; Seebacher et al., 2015), it has in fact been correlated with a progressive decline in adult body size of many fish species in the wild (e.g. in Baudron et al., 2014; Gardner et al., 2011; Sheridan and Bickford, 2011, but see Audzijonyte et al., 2020). The factors that contribute to this shrinking of fishes are poorly understood; it is coherent with how warming might affect macroecological phenomena such as Bergmann's rule and James' rule, and is associated with a significantly higher proportion of younger age classes and a generalised decline in individual size-at-age in populations (Daufresne et al., 2009). Shrinking of fishes may also be linked to the Temperature-Size rule (TSR), the phenomenon whereby warm temperatures cause more rapid early growth of ectotherms but a decline in their final adult size, when compared to conspecifics reared in a cooler regime (Atkinson, 1994). The mechanisms involved in the TSR remain to be elucidated, it is observed in wild populations but can also be reproduced under controlled conditions in the laboratory (Forster et al., 2012; Horne et al., 2015).

Although there has been recent theoretical focus on whether the TSR relates to respiratory physiology (Verberk et al., 2021), early work focussed upon whether changes in energy budget and allocation may be a major driver of fish shrinking with warming (Gardner et al., 2011; Pauly et al., 2010). The availability and quality of food resources can affect individual growth rates and adult body size through energy trade-offs among growth, survival and reproduction (Stearns, 1989, 1992), and such effects may be exacerbated if energy requirements are increased by warming. That is, it is unlikely that temperature per se is the only variable involved in the size decline in wild populations, since few exceptions to this rule are spreading across years, in particular studies that investigated food resources as a driver explaining the TSR (e.g. in Diamond and Kingsolver, 2010; Lee et al., 2015; Ljungström et al., 2020; Millien et al., 2006).

Temperature and food resources are both environmental variables whose variations can challenge an individual's energy balance and that can drive fish life-history traits through physiological processes. Thus, while the higher physiological rates due to warming cause an increase in energy demands, energy availability for marine fishes is predicted to decline due to climatic stressors that affect primary production and marine animal biomass (Ariza et al., 2022; Bopp et al., 2005; Daufresne et al., 2009; Lotze et al., 2019). Ocean warming can amplify vertical stratification and limit nutrient mixing (Roemmich and McGowan, 1995) which causes declines in plankton abundance at the base of the food web and leads to communities dominated by smaller-sized species and individuals (Bopp et al., 2005, 2013; Daufresne et al., 2009; Richardson and Schoeman, 2004; Ward et al., 2012).

The first impacts of such changes at low trophic levels could be observed on planktivorous species, such as small pelagic fishes (e.g. Brosset et al., 2017; van Beveren et al., 2014). These species represent about 25 % of worldwide fishery landings by weight (FAO, 2018), supporting the economy of several countries (Alheit et al., 2009; Fréon et al., 2005). Fluctuations of their populations can have critical economic and social consequences, as observed following the collapse of the Peruvian anchovy in the early 1970s (Alheit et al., 2009; Allison et al., 2009; Schwartzlose et al., 1999). Population fluctuations of small pelagics are being exacerbated by ongoing global change (Brochier et al., 2013; Shannon et al., 2009), so these species represent key models to evaluate energetic mechanisms underlying shrinking of adult fish size.

In fact, small pelagic planktivorous fishes in the Mediterranean Sea are a major example of shrinking (Albo-Puigserver et al., 2021; Brosset et al., 2017). There is an ongoing and profound decrease in individual body size and condition of sardine (*Sardina pilchardus*) and anchovy (*Engraulis encrasicolus*), which appears to be a consequence of bottom-up control mediated by changes in plankton composition and abundance (Brosset et al., 2016; Saraux et al., 2019). This was associated with a major regime change in the mid-2000s, with shifts of nutrient inputs, water mixing and plankton production (Feuilloley et al., 2020). Since 2008, these species' diet has shifted progressively from large prey (> 1 mm, especially cladocerans) to increased reliance on smaller prey (< 1 mm, especially copepods), which indicates changes in the plankton community towards smaller species (Brosset et al., 2016). Smaller zooplankton can be less nutritious (Zarubin et al., 2014), so a decline in zooplankton size could entrain a decrease in rates of energy acquisition by their predators. Identifying a clear mechanistic link between a decrease in plankton size and fish growth, and ultimately population dynamics, is crucial since fish shrinking is spreading to new ecosystems and species (see Bensebaini et al., 2022; Véron et al., 2020).

Challenges to energy balance when prey become smaller could be further exacerbated in fishes if prey size also influences foraging behaviour. Here, the sardine is also an interesting model species. Sardines spontaneously modify their feeding behaviour according to the size of their prey, using diffuse filter-feeding when prey is small but direct capture when prey is large (Garrido et al., 2007, 2008). A recent long-term experiment on captive sardines showed that, for the same food ration, a reduction in food size could significantly impair growth and body condition (Queiros et al., 2019). Sardines filter feeding on small particles had to consume twice as much as those capturing large particles to achieve the same growth and body condition (Queiros et al., 2019). We suspected that the two foraging modes had different energetic costs for the same degree of resource acquisition, with costs being higher for sustained aerobic swimming during filter-feeding compared to brief bursts of swimming to capture prey (Costalago and Palomera, 2014; Queiros et al., 2019). At the same time, food availability could be highly significant in the wild, filtration could be effective in very rich areas such as upwellings whereas particulate feeding might be more advantageous in areas with lower prey density (Costalago et al., 2015).

The current study focused on this complex predator-prey interaction in a captive population of adult sardines. We investigated the hypothesis that foraging on smaller prey would lead to increased rates of energy expenditure by sardines, and that these energy requirements would be exacerbated with warming temperature. To assess the energetic consequences of feeding sardines on prey of different sizes and at different abundances, we used group respirometry to measure rates of oxygen uptake and provided prey as commercial pellets of two different sizes at a range of ration levels. We compared animals acclimated to two temperatures within the species' thermal range, either a cool 16 °C or warm 21 °C. Thus, the effects on oxygen consumption of particle size and temperature were investigated according to 5 scenarios: (1) change from large to small particles at cool temperature; (2) change from large to small particles at warm temperature; (3) rise in temperature with fish fed on large particles; (4) rise in temperature with fish fed on small particles, and (5) change from large to small particles while also increasing temperature. To that end, we focussed on overall daily energetic costs but also a careful comparison of energetic costs incurred during and after feeding for each scenario.

2. Material and methods

2.1. Animal capture and husbandry

Sardines were captured by commercial purse-seiner and transferred to the IFREMER Palavas-les-Flots research station, with the same fishing and husbandry procedures as described tailed in Queiros et al. (2019). Over the first week, sardines were acclimated to tanks and weaned onto commercial aquaculture pellets. They were fed with a mixture of Artemia nauplii and commercial aquaculture pellets (mix of 0.2 and 1.2 mm diameter), with increasing proportions of pellets and decreasing proportions of Artemia throughout the week, concluding exclusively with pellets. After 2–3 weeks, sardines were transferred into indoor 1 m^3 holding tanks, until experimentation. Water temperature was not set during this period but followed natural fluctuations from 15 to 20 °C (SST at the time of capture was 14 °C).

2.2. Experimental design

Eighty sardines were distributed among 8 experimental tanks in groups of 10 animals (volume 50 L), to ensure similar distributions of body mass and condition among tanks (Fig. S1), and fish densities comparable to those of Queiros et al. (2019). Fish were acclimated to the new tanks while temperature was gradually changed from 19 °C to either 16 °C or 21 °C over one week. Before the experiments began, fish were fed with commercial pellets twice a day, a mix of 0.2 and 1.2 mm to avoid preference bias for pellet size. These eighty sardines were used for both experiments 1 and 2, described below, and these two experiments were performed sequentially in the same setup.

The tanks were modified to function as open automated respirometers (McKenzie et al., 2007, 2012; Queiros et al., 2021) using the principles of cyclical intermittent stopped flow (Steffensen, 1989), as described below. Four tanks were held at each of the two temperatures, each set of four was supplied by water from a single reservoir where water temperature was regulated by an Ice 3000 (Aquavie) at 16 °C or by a Red Line heater (Zodiac) at 21 °C. Water in the reservoir was vigorously aerated, to maintain oxygen saturation and ensure thorough mixing. Water was delivered to tank respirometers by submersible pumps (Eheim 3400); within each respirometer the water was also gently but thoroughly mixed by a submersible pump (Newa Maxi 500) to avoid any thermal or oxygen gradients (see Supplementary Material and Fig. S2).

All respirometers were exposed to a 12L:12D photoperiod (L: light, D: darkness) with a natural sunlight spectrum and 30 min progressive dawns and sunsets. Individual total length and body mass was measured every two weeks under anaesthesia (140 mg L^{-1} benzocaine). To estimate total tank biomass each day, body mass gain (or loss) was assumed to be linear between successive bi-weekly measures. Total biomass was then used to adjust rations and to calculate oxygen consumption. No mortality was observed during the experiments.

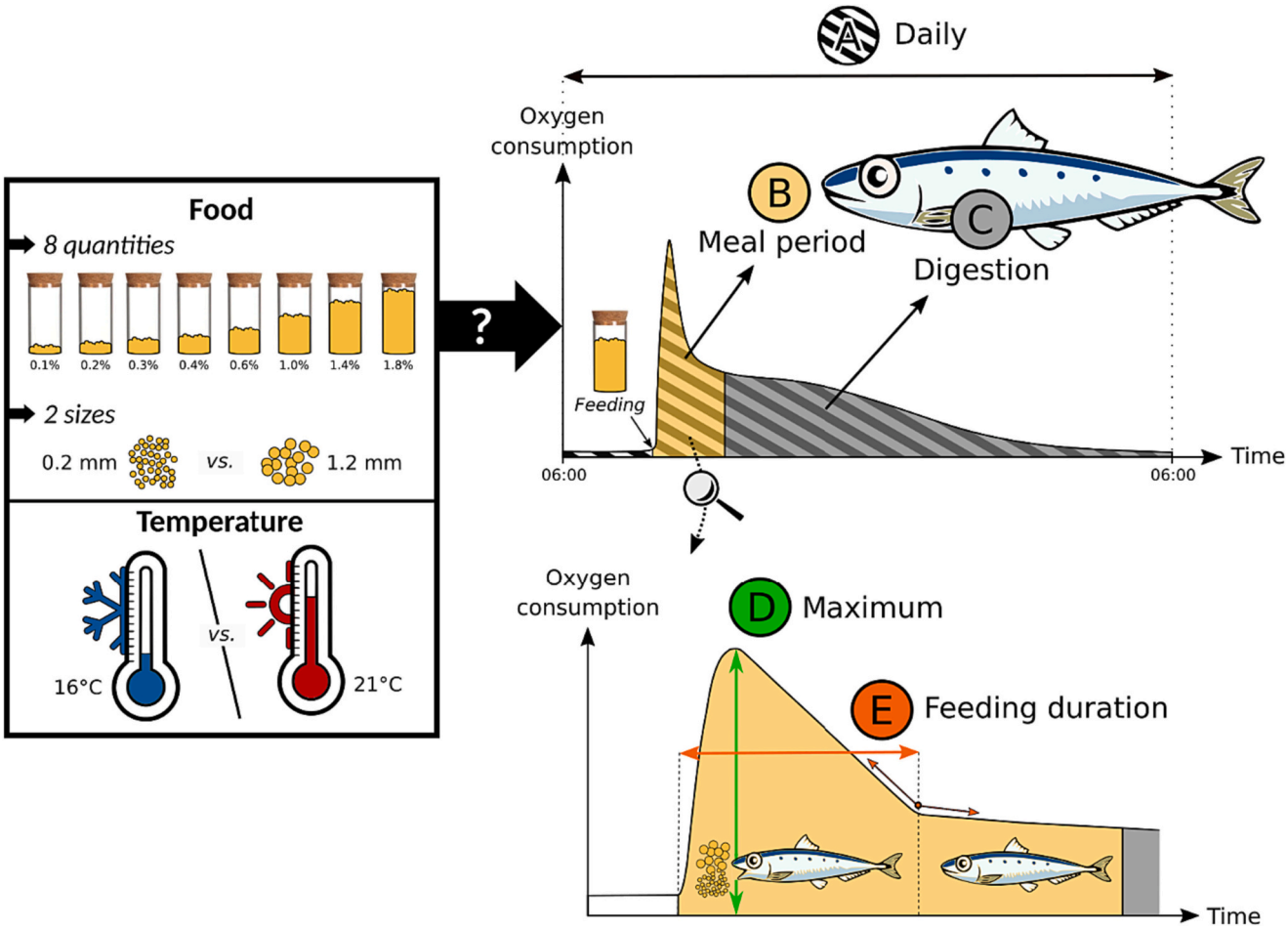

Fig. 1. Conceptual framework of the two experiments on cocktail effects of food size (0.2 and 1.2 mm), food rations (between 0.1 % and 1.8 % of the total biomass in tank) and temperature (16 °C and 21 °C) on energy expenditure of sardines (daily [A], during the meal period [B], during digestion [C], on the maximal intensity during feeding [D]) and on the duration of the feeding activity [E].

2.3. Protocols

2.3.1. Experiment 1: effects of prey size, prey abundance and temperature on daily energy expenditure

To investigate effects of prey size, we offered sardines one of two commercial pellets that had similar composition in terms of lipids and proteins but differed in size, being either 0.2 mm or 1.2 mm in diameter, for a period of six weeks. These sizes fall within the natural range of sardine prey (Nikolioudakis et al., 2012), but elicit two markedly different foraging modes, being either filtering on 0.2 mm pellets or particulate capture of 1.2 mm pellets (Queiros et al., 2019). Eight prey abundances were studied, as pellet rations ranging from 0.1 to 1.8 % of the total fish mass per tank: 0.1 %, 0.2 %, 0.3 %, 0.4 %, 0.6 %, 1.0 %, 1.4 %, 1.8 %. The combination of two sizes and eight rations resulted in 16 feeding treatments for each of the 2 temperatures (Fig. 1). Sardines were fed once a day at 09:00 in the morning. Daily feeding treatment for a tank was randomly assigned but comprised 2 replicates of each feeding treatment per tank over the entire experiment (i.e. 8 replicates per feeding treatment × temperature).

The cyclical measures of oxygen uptake rate (MO2 in mg kg^{-1} h^{-1}) provided an indirect estimate of metabolic rate and, therefore, energy use, while the sardines fed, digested and exhibited diurnal patterns of spontaneous activity. Methodological details are provided below. A continual cycle of 15 min stopped flow to measure MO2 alternated with 15 min flush with aerated water was used, except at feeding when flow was stopped for 30 min (at rations of 0.1 %, 0.2 %, 0.3 % and 0.4 %) or 60 min (at rations of 0.6 %, 1.0 %, 1.4 % and 1.8 %), to ensure the entire ration was consumed before flushing. Food was distributed 5 min after flow was stopped, when water level had stabilized in all respirometers.

Bias due to behavioural responses to the act of feeding (e.g. anticipation caused by human presence near tanks at the typical feeding time) was controlled for by sham-feeding events, where the typical feeding gestures were performed but no food was provided. These shams were performed twice a day (9:00 am and 2:00 pm) for 2 days in all tanks, in the middle and at the end of experiment 1.

2.3.2. Experiment 2: effects of prey size, prey abundance and temperature on features of foraging behaviour

In this experiment we studied features of the foraging modes, filtration or particulate capture, in more detail, considering duration and maximum intensity (Fig. 1). To this end, sardines were fed twice a day (9:00 am and 2:00 pm) for 3 weeks with 8 treatments: one of two food sizes (0.2 and 1.2 mm) at four rations (0.1, 0.2, 0.3 and 0.4 % of tank biomass). The combination of two sizes and four rations resulted in 8 feeding treatments for each of the 2 temperatures (16 °C and 21 °C). Based on the results of Experiment 1, rations were chosen not to cause satiety. Similar to Experiment 1, MO2 was measured throughout and for 30 min during feeding (food distributed after 5 min). Combining these data with those of Experiment 1 (Fig. S3), we obtained a total of 24 replicates per feeding treatment × temperature for food rations between 0.1 % and 0.4 %. Any bias due to behavioural responses to the act of feeding was assessed by two sham events, as described above.

2.4. Respirometry

Water oxygen levels were recorded every 5 s in the tank respirometers, with an O_2 optode (Oxy-10 mini; PreSens Precision Sensing GmbH, /www.presens.de) and associated software (Pre-Sens Oxy 4v2). Water O_2 saturation never fell below 70 % during the 15 min of stopped flow and never below 60 % after feeding. Saturation was rapidly restored when the tanks were flushed with a flow of aerated water from the reservoir.

Oxygen uptake by the sardines caused a linear decline in water O_2 concentration over time during each stopped flow phase ('closed phase'). The MO2 was calculated in mg O_2 kg^{-1} h^{-1}, using least-square regression of the slope, considering oxygen solubility at the appropriate temperature (measured continuously) and salinity (measured daily); tank volume (50 L), and fish biomass (McKenzie et al., 2007). Only slopes with $R^2 \geq 0.95$ were kept for further analyses (<5 % of slopes were removed from analyses). Gas exchange across the water surface being negligible, no correction was applied when estimating sardine oxygen consumption (McKenzie et al., 2007; Queiros et al., 2021).

2.5. Respirometry data analyses

2.5.1. Basal and daily oxygen consumption

Basal O_2 uptake rate of day_i was expressed as the lowest 15 %-quantile (Chabot et al., 2016a) of the daily O_2 consumption of the previous day (from 06:00 a.m. day_{i-1} to 06:00 a.m. day_i). This rate of oxygen uptake was then used as a baseline for calculating daily oxygen consumption on day_i, expressed in mg O_2 kg^{-1} d^{-1}, as an increase from this basal rate. This normalisation avoided bias linked to a change in fish biomass during experiments, short-term effects of a previous meal, or a small change in temperature, salinity, minor human disturbance, etc. Daily MO2 was calculated as the area under the curve (AUC) of MO2 over time, from 06:00 a.m. and for 24 h (Fig. 1, point A) using the '*DescTools*' package in R (Signorell, 2023). The AUC was calculated over two periods: (i) raw data from 06:00 a.m. until noon, to catch the peak of oxygen consumption observed during the meal period and (ii) smoothed values of the oxygen consumption after 12:00 a.m. (oxygen consumption smoothed using *lowess* function) to avoid outliers due to, for example, minor disturbance in the room, that might distort daily estimations (Fig. S3).

2.5.2. Oxygen consumption during feeding

When focusing on effects of a meal on MO2, these were calculated relative to a control baseline that was estimated as the mean of the preceding 2.5 h. This was done to avoid bias when either lights were turned on 1.5 h before the 1st daily meal, or there were remnant effects of digestion of that 1st meal for the 2nd meal period. Since it took up to 2 min to feed all tanks (i.e. between 5 and 7 min after the beginning of the closed phase), we first needed to establish the start of the feeding event for each tank. To do so, we identified a break in the rate of oxygen decline in the water during the initial minutes of the 'closed phase', using the '*segmented*' package (Muggeo, 2008). Once this was identified, oxygen consumption was calculated, in mg O_2 kg^{-1} h^{-1}, as the linear decline of oxygen concentration from there until 2 min before the end of the 'closed phase' (Fig. 1, point B).

2.5.3. Oxygen consumption during digestion

The start of the digestion period was considered to begin 90 min after the start of the meal period, this being the maximal duration of the feeding and then flush periods across the different rations. Thus, with feeding at 09:00, the oxygen consumption during digestion was calculated, in mg O_2 kg^{-1} d^{-1}, as the AUC of the oxygen consumption over time between 10:30 a.m. of day_i and 06:00 a.m. of day_{i+1} (Fig. 1, point C). This oxygen consumption was expressed as an increase from the basal O_2 uptake of day_i as estimated above.

2.5.4. Maximal oxygen consumption during feeding

To reveal dynamics of metabolic rate after feeding (Fig. S5), MO2 was estimated as a moving average at 30 s intervals during the closed feeding period, using linear regressions over 1 min on smoothed data for 12 measures of tank oxygen concentration. This revealed the maximum oxygen consumption, in mg O_2 kg^{-1} h^{-1}, achieved during each meal period (Fig. 1, point D).

2.5.5. Duration of the feeding period

To estimate feeding duration, in minutes, we identified the end of the meal as the breakpoint when oxygen concentration stopped decreasing severely after feeding, taken to indicate the end of feeding-related activity (Fig. 1, point E). That is, a broken-line regression was performed

on oxygen consumption values calculated every 30 s (also every 30 s over 1 min), starting at the peak of oxygen consumption as estimated above.

2.6. Statistical analyses

Effects of food rations, prey (particle) size and temperature, on oxygen consumption and feeding duration, were assessed using linear mixed-effects models. We built a series of models including three fixed effects (food size, food ration and temperature), as well as their interactions. Because of variability among tanks within each food ration × food size × temperature treatment, we also introduced a random tank intercept effect. The best-fitting model was selected based on the lowest AIC_c values (Burnham and Anderson, 2002) following Zuur et al. (2009). When the difference between these models in AIC_c (ΔAIC_c) was lower than two, the most parsimonious model was selected (Burnham and Anderson, 2002). Food ration was log-transformed for models of MO2 during feeding and maximal MO2 during feeding. Then, food ration was second order polynomial transformed to model feeding activity.

Finally, the effects of prey (particle) size and temperature on oxygen consumption were investigated according to 5 scenarios: (1) a change from large to small particles at cool temperature; (2) a change from large to small particles at warm temperature; (3) a rise in temperature with fish fed on large particles; (4) a rise in temperature with fish fed on small particles, and (5) a change from large to small particles while also increasing temperature (see arrows in Fig. 2). As such effects also depend on the food ration when the interaction with food ration was significant, we performed pairwise comparison to test significance of scenarios using selected best-fitting models as previously described. Results of scenarios over food ration are expressed as absolute and relative increases. Results are indicated as mean [95 % CI]. Upper and lower 95 % CI values of relative differences over food ration were calculated following Kohavi et al. (2009).

All data analyses were performed under R (R Core Team, 2020) and linear mixed-effects models were built using the 'lme4' package (Bates et al., 2015). All statistical tests were considered significant at p-values <0.05.

3. Results

When fasted, MO2 was low and statistically similar throughout the day (black curve in Fig. 2). When sardines were fed, MO2 peaked during the feeding period after 09:00, then decreased for the rest of the day for all feeding treatments and both temperatures. Oxygen consumption increased with food ration and rearing temperature but, during feeding at both temperatures, MO2 was higher when feeding on the small particles (Fig. 2).

3.1. Daily oxygen consumption

During fasting days, median daily MO2 (i.e. the AUC relative to basal daily oxygen consumption) was the lowest, demonstrating the clear effects that feeding and/or digestion exerted on daily energy expenditure (Fig. 2, Fig. S6).

The best linear mixed-effect model included double interactions between food ration and food size and between food ration and temperature (Tables S1 and S2, Fig. S6, S7). An increase in ration consistently caused a significant increase in daily oxygen consumption when

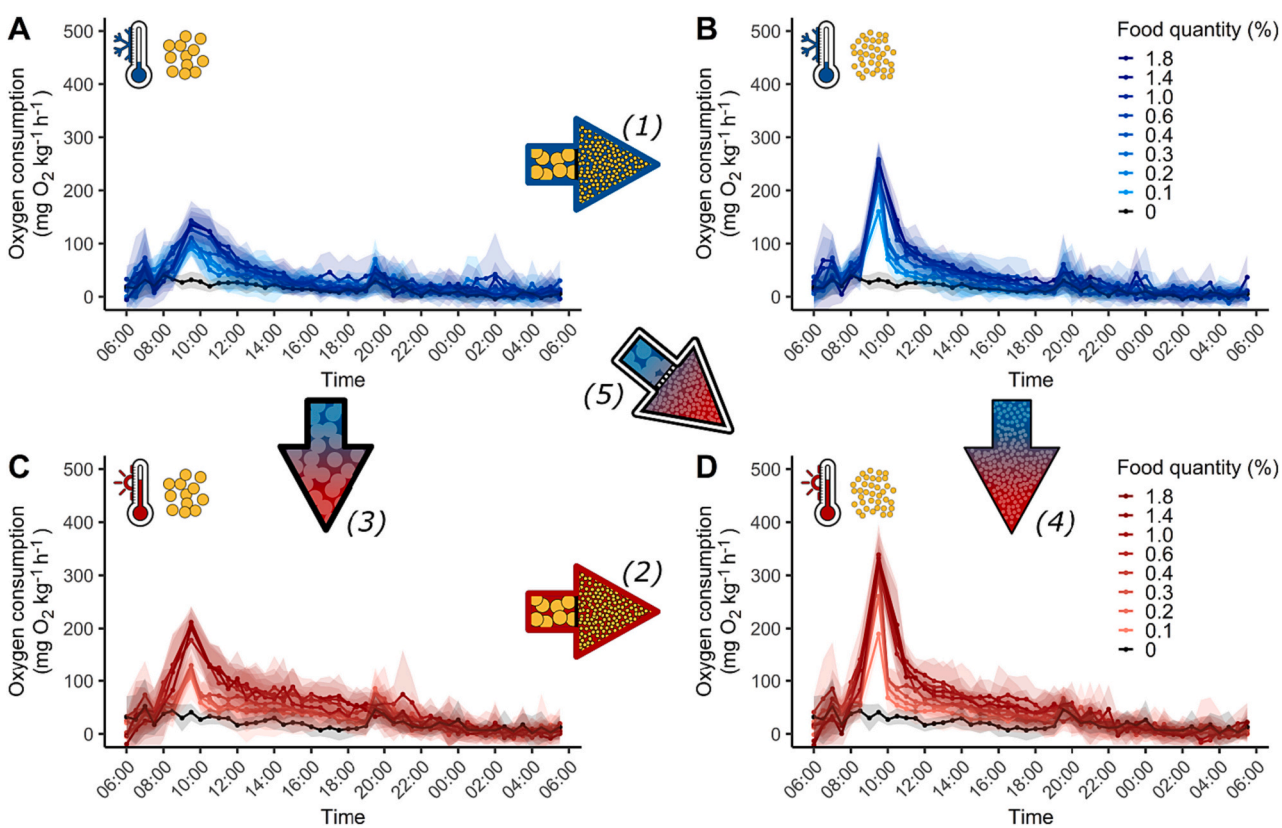

Fig. 2. Median oxygen consumption over time according to food ration for the 4 experimental treatments: cool temperature and large particles (A), cool temperature and small particles (B), warm temperature and large particles (C) warm temperature and small particles (D). Black lines are for days of fasting, blue and red represent cool (16 °C) and warm (21 °C) temperatures, respectively. Darker lines represent higher rations of food. Arrows represent the 5 scenarios for which oxygen consumption were compared: (1) change from large particles to small particles at cool temperature; (2) change from large particles to small particles at warm temperature; (3) rise in temperature for fish fed on large particles; (4) rise in temperature for fish fed on small particles, and (5) change from large particles to small particles while also increasing temperature.

considering either food size or temperature. When considering only food size effects, slopes were significantly different ($p < 0.001$) and the increase was smaller for large particles (slope [95 % CI]; 420 [324;515] mg of O_2 kg^{-1} d^{-1}) than for small particles (714 [618;810] mg of O2/kg/d, graph *Daily* in Fig. 3, Table S3).

When comparing large to small particles over all food rations, scenarios (1) and (2) were not significant since food size × temperature interaction was not retained during model selection. Daily MO2 exhibited a mean [95 % CI] relative increase of 13 [1;37]% for small particles at 16 °C, while this increase was 10 [3;22]% at 21 °C (graph *Daily* in Fig. 3, Table 1).

3.2. Oxygen consumption during feeding

During fasting days, median MO2 at the time of sham feeding was centered on zero (Fig. S8), indicating that the increase in MO2 observed during all true feeding events resulted from actual energy expenditure to feed and not from behavioural responses by the sardines to feeding gestures.

The MO2 during feeding was significantly related to the three double interactions (food ration × food size, food ration × temperature and food size × temperature, Tables S4 and S5, Fig. S8, S9). When considering only food size effects, slopes were significantly different ($p < 0.001$) and the increase was smaller for large particles (slope [95 % CI]; 95 [85;105] mg of O_2 kg^{-1} h^{-1}) than for small particles (129 [119;139] mg of O_2 kg^{-1} h^{-1}, Table S3).

Food size had a strong and significant effect on MO2 during feeding. When sardines fed on small particles at 16 °C, their mean [95 % CI] MO2 was almost multiplied by 2.5 by comparison to large particles (p-value <0.001), rising by 155 [46;397]%, while it doubled in sardines feeding on small particles, rising by 116 [59;209]% compared to large particles at 21 °C (p-value <0.001, graph *Meal period* in Fig. 3, Table 1).

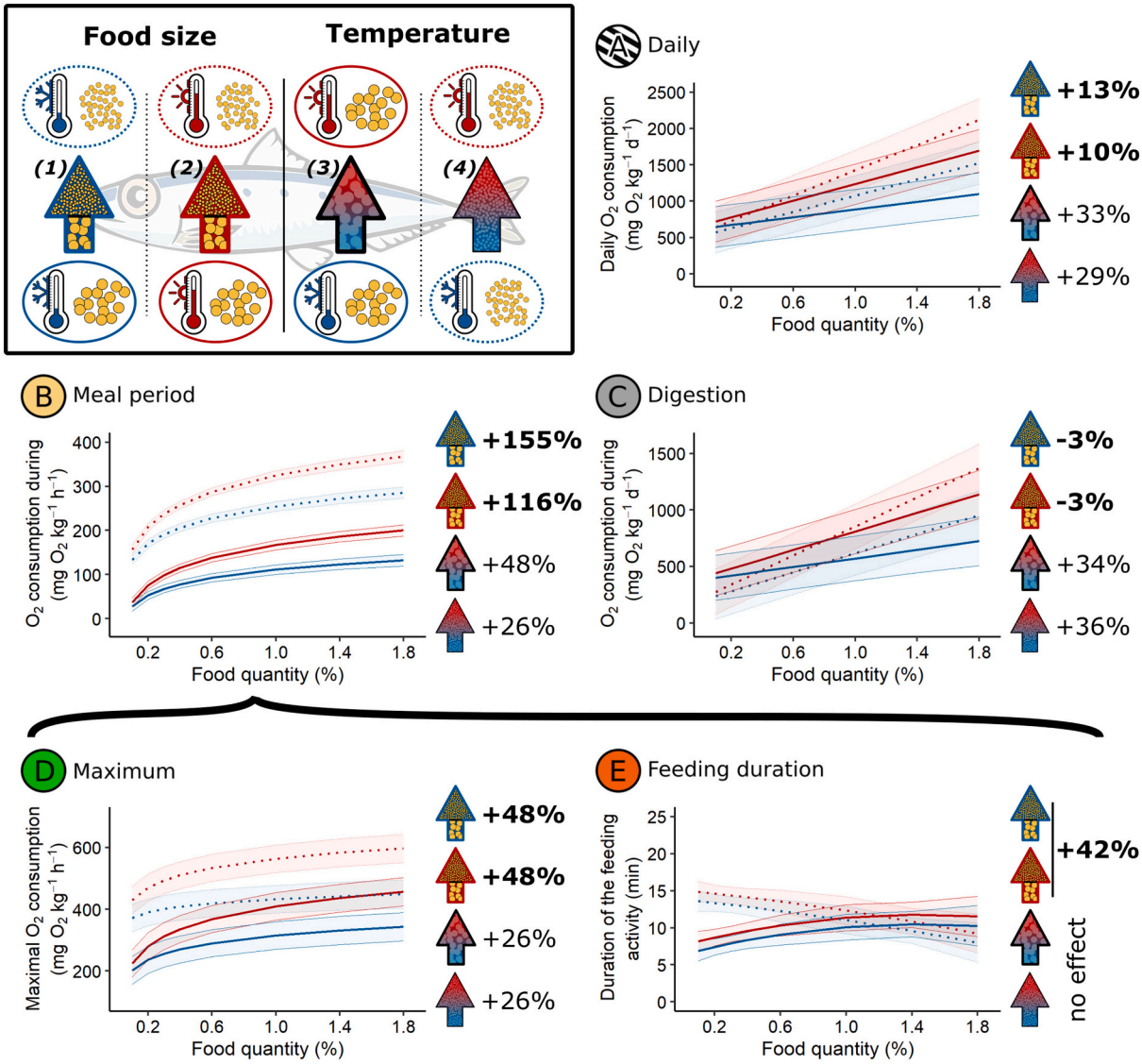

Fig. 3. Smooth functions of [A] daily, [B] while feeding, [C] while digesting, [D] maximal oxygen consumptions (relative to basal oxygen consumption, see details in Material and Methods) and [E] feeding duration according to the food ration for the 4 experimental treatments: cool temperature and large particles (solid blue lines), cool temperature and small particles (dotted blue lines), warm temperature and large particles (solid red lines) and warm temperature and small particles (dotted red lines). Arrows represent the mean relative increase of the oxygen consumption/feeding duration according to 4 scenarios summarized in top-left panel: scenario 1 = meal modification from large particles to small particles at cool temperature, (2) meal modification from large particles to small particles at warm temperature, (3) increasing temperature when fish fed on large particles and (4) increasing temperature when fish fed on small particles. Only food size × food ration had a significant effect on feeding duration.

Table 1
Absolute and relative differences (estimates and 95 % confidence intervals) for the 5 scenarios for which oxygen consumption were compared: (1) change from large particles to small particles at cool temperature; (2) change from large particles to small particles at warm temperature; (3) rise in temperature for fish fed on large particles; (4) rise in temperature for fish fed on small particles, and (5) change from large particles to small particles while also increasing temperature. Scenarios were tested using pairwise comparisons. Both differences were calculated by pairwise comparisons and 95 % CI of relative differences were estimated following Kohavi et al., 2009. Absolute differences are given in mg of O_2 kg^{-1} d^{-1} for daily and during digestion, in mg of O_2 kg^{-1} h^{-1} for maximal and during feeding, and in minutes for feeding duration.

Period	Scenario	Relative change (%)	Absolute change
Daily	**Scenario (1):** 16°C | Large ⇨ Small	13 [1;37]	108 [6;211]
	Scenario (2): 21°C | Large ⇨ Small	10 [3;22]	108 [6;211]
	Scenario (3): Large | 16°C ⇨ 21°C	33 [6;87]	265 [-290;821]
	Scenario (4): Small | 16°C ⇨ 21°C	29 [8;68]	265 [-265;821]
	Scenario (5): 16°C + Large ⇨ 21°C + Small	46 [10;121]	373 [-179;926]
Meal period	**Scenario (1):** 16°C | Large ⇨ Small	155 [46;397]	132 [120;143]
	Scenario (2): 21°C | Large ⇨ Small	116 [59;209]	146 [135;157]
	Scenario (3): Large | 16°C ⇨ 21°C	48 [11;128]	41 [24;58]
	Scenario (4): Small | 16°C ⇨ 21°C	26 [16;37]	56 [38;73]
	Scenario (5): 16°C + Large ⇨ 21°C + Small	220 [68;561]	187 [170;205]
Digestion	**Scenario (1):** 16°C | Large ⇨ Small	-3 [-13;-1]	-18 [-112;76]
	Scenario (2): 21°C | Large ⇨ Small	-3 [-6;-1]	-18 [-112;76]
	Scenario (3): Large | 16°C ⇨ 21°C	34 [-4;183]	178 [-212;569]
	Scenario (4): Small | 16°C ⇨ 21°C	36 [-5;214]	178 [-212;569]
	Scenario (5): 16°C + Large ⇨ 21°C + Small	31 [-3;164]	160 [-228;548]
Maximal	**Scenario (1):** 16°C | Large ⇨ Small	48 [24;84]	134 [111;157]
	Scenario (2): 21°C | Large ⇨ Small	48 [29;75]	170 [148;193]
	Scenario (3): Large | 16°C ⇨ 21°C	26 [12;46]	72 [-15;159]
	Scenario (4): Small | 16°C ⇨ 21°C	26 [16;39]	108 [21;195]
	Scenario (5): 16°C + Large ⇨ 21°C + Small	87 [47;148]	242 [155;329]
Duration	Large ⇨ Small	42 [-11;339]	4 [2;6]

3.3. Oxygen consumption during digestion

Similar to the daily MO2, best linear mixed-effect model for MO2 during digestion included double interactions between food ration and food size and between food ration and temperature (Tables S6 and S7, Fig. S10, S11). Slopes differed significantly ($p < 0.001$); the lowest slope was estimated for sardines on large particles (slope [95 % CI]; 300 [213;388] mg of O_2 kg^{-1} d^{-1}) while the highest slope was obtained for sardines on small particles (533 [445;621] mg of O_2 kg^{-1} d^{-1}, graph *Digestion* in Fig. 3).

When comparing large to small particles averaged over all food rations, scenarios (1) and (2) were not significant since interaction between food size and temperature was not retained in the selected model. Indeed, mean [95 % CI] MO2 during digestion decreased by 3 [−13,−1]% at 16 °C, while this decrease was 3 [−6;-1]% at 21 °C (graph *Digestion* in Fig. 3, Table 1).

3.4. Maximal consumption during feeding

Similar to the MO2 during feeding, maximal MO2 during feeding was significantly correlated with the three double interactions (Tables S8 and S9, Fig. S12, S13). Slopes differed significantly ($p = 0.001$); the lowest slope was estimated for sardines on small particles (slope [95 % CI]; 87 [67;106] mg of O_2 kg^{-1} h^{-1}) while the highest slope was obtained for sardines on large particles (132 [113;152] mg of O_2 kg^{-1} h^{-1}, graph *Maximum* in Fig. 3, Table S3).

Food size had a strong and significant effect on maximal MO2 during feeding since food size × temperature interaction was retained during model processing. When sardines fed on small particles at 16 °C, their mean [95 % CI] maximal MO2 rose by 48 [24;84]% by comparison to large particles, while such increase was 48 [29;75]% at 21 °C (graph *Maximum* in Fig. 3, Table 1).

3.5. Feeding duration

Contrary to the previous MO2 features, the selected model for the feeding duration included interaction between food ration and food size but not with temperature since food ration × temperature and food size × temperature interaction were not retained (Tables S10 and S11, Fig. S14, S15). Slopes differed significantly between the two food sizes ($p = 0.004$). Indeed, the feeding duration decreased with increasing food ration when sardines fed on small particles (slope [95 % CI]; −3 [−6;0] min) while it increased when sardines fed on large particles (4 [1;7] min, Table S3).

When comparing large to small particles averaged over all food rations, scenarios (1) and (2) were not significant since interaction between food size and temperature was not retained in the selected model. Mean [95 % CI] feeding duration increased by 42 [−11;339]% (graph *Feeding duration* in Fig. 3, Table 1).

3.6. Temperature effects

Temperature had significant effects on all oxygen consumptions and on the feeding duration (Tables S1 to S11). Indeed, food ration × temperature interaction was included in all selected models on MO2 and food size × temperature interaction was included in models on MO2 during feeding and maximal MO2 during feeding. Moreover, in the model on feeding duration, temperature was retained without its interactions (Tables S10).

When studying interaction of food ration and temperature, slopes were significant different between the two temperatures in all MO2 models and they were always smaller at cool than at warm temperature. Thus, slopes were smaller at 16 °C than at 21 °C for daily MO2, MO2 during digestion, MO2 during feeding, and maximal MO2 during feeding (Table S3). Surprisingly, slopes were very similar when considering either large particles or cool temperature effects (e.g. slopes [95 % CI] for daily MO2, 420 [324;515] and 413 [317;509], respectively) and either small particles or warm temperature effects (for daily MO2, 714 [618;810] and 721 [626;817], respectively, suggesting similar effects of prey shrinking and temperature warming over food ration on MO2 (see Table S3).

When comparing cool to warm conditions, in scenarios (3) and (4) there was no significant effect of temperature on daily MO2, MO2 during digestion or on feeding duration, because food size × temperature interaction was not retained within selected models. On the other hand, warming effects were significant on MO2 during feeding (p-values <0.001) but only scenario (4) was significant on maximal MO2 during feeding (p-value = 0.02). Thus, the temperature change from 16 °C to 21 °C caused mean MO2 during feeding to increase by 26 [16;37]% in fish fed on small particles, and by 49 [11;129]% in fish fed on large particles. This temperature change caused mean maximal MO2 during feeding to increase by 26 [16;39]% in sardines fed with small particles (Fig. 3, Table 1).

3.7. Cocktail effects of the global warming

Smaller particle size and higher temperature resulted in a mean [95 % CI] daily MO2 increase of 46 [10;121]%, representing an increase of 373 [−179;926] mg of O_2 kg^{-1} d^{-1}. This increase was caused by the significant multiplication by 3 of the MO2 during the meal period (220 [68;561]%, representing 187 [170;205] mg of O_2 kg^{-1} h^{-1}) and higher MO2 during the digestion (31 [−3;163]%, representing 160 [−228;548] mg of O_2 kg^{-1} d^{-1}). Moreover, such change caused an increase of the maximal MO2 during feeding by 87 [47;148]%, representing an increase of 242 [155;329] mg of O_2 kg^{-1} h^{-1}, and a longer feeding period (42 [−11;339]%, representing 4 [2;6] min without temperature effect, Fig. 4, Table 1).

4. Discussion

This study investigated how a modification of food resources under climate warming might jeopardize energy balance of small pelagic species, using sardines in the Mediterranean Sea as a case study. To do so, we used in-vivo group respirometry to investigate the effects of prey (food) size and availability (ration) on sardine energy expenditure, and how this was influenced by temperature. Our results demonstrate that both food size and temperature had significant effects on multiple measures of energy expenditures, over daily and hourly timescales. While temperature significantly increased expenditures overall, food size had a major impact on energy expenditure for activity during feeding itself. That is, the results indicate that food resources and temperature are major environmental drivers that can dramatically increase energy expenditures of fishes and disturb their energy balance in a scenario of future climate change, in warmer waters with smaller prey. As such, the results also provide experimental evidence that such challenges to energy balance may contribute to the ongoing shrinking of fish populations.

Daily oxygen consumption measured in this study was corrected against a baseline of standard metabolism (Chabot et al., 2016a), so represents daily energy expenditure on activity. The results suggested greater expenditure for days where sardines fed on small particles, due to higher oxygen consumption during either feeding and/or digestion. The very marked increase in oxygen consumption during actual feeding on small items must reflect different costs of foraging mode, with filtering being more expensive than particulate feeding. While this confirms our hypothesis and helps explain the decreased growth and body condition of sardines fed for an extended period on small items (Queiros et al., 2019), the magnitude of the effect is quite remarkable. Both MO2 and duration of the meals provide a more detailed understanding of the widely different energy costs of the two foraging modes. First, the higher maximal MO2 when fish fed on small particles indicates greater energy requirements for the continuous aerobic swimming in filter-feeding compared to rapid bursts to capture large particles (Costalago and Palomera, 2014). Queiros et al. (2019) had already noted that the duration of feeding activity was longer when sardines fed on small particles, it presumably represents the time needed to filter the entire tank volume and, therefore, might not be expected to change much with ration. It is interesting therefore that feeding duration on small particles was in fact lower at low or high rations than at intermediate ones. Low duration at low ration might suggest rapid loss of interest if food acquisition was very poor, while at high ration it might indicate satiation. For particulate feeding, more particles to catch should translate into longer duration, which was observed until a ration threshold where a plateau would indicate satiation. Overall, we expected feeding duration to be longer on small particles at low ration but longer on large particles, but this was only true for rations below 0.6 %, after which duration was similar for both particle sizes. Finally, all these results indicate that higher energy expenditure by sardines filter feeding on small particles can explain why they would have to eat twice as much as when feeding on large pellets to achieve similar growth or body condition (Queiros et al., 2019).

Our finding that oxygen consumption during the digestion increased with the food ration, for both particle sizes, presumably reflects the so-called specific dynamic action of feeding (SDA) response (McCue, 2006). This reflects the energy needed for the digestion, absorption and assimilation of a meal (Chabot et al., 2016b), hence the energetic 'costs of growth'. Therefore, larger meals require greater energy investment but then provide a great return in terms of tissue accretion and growth

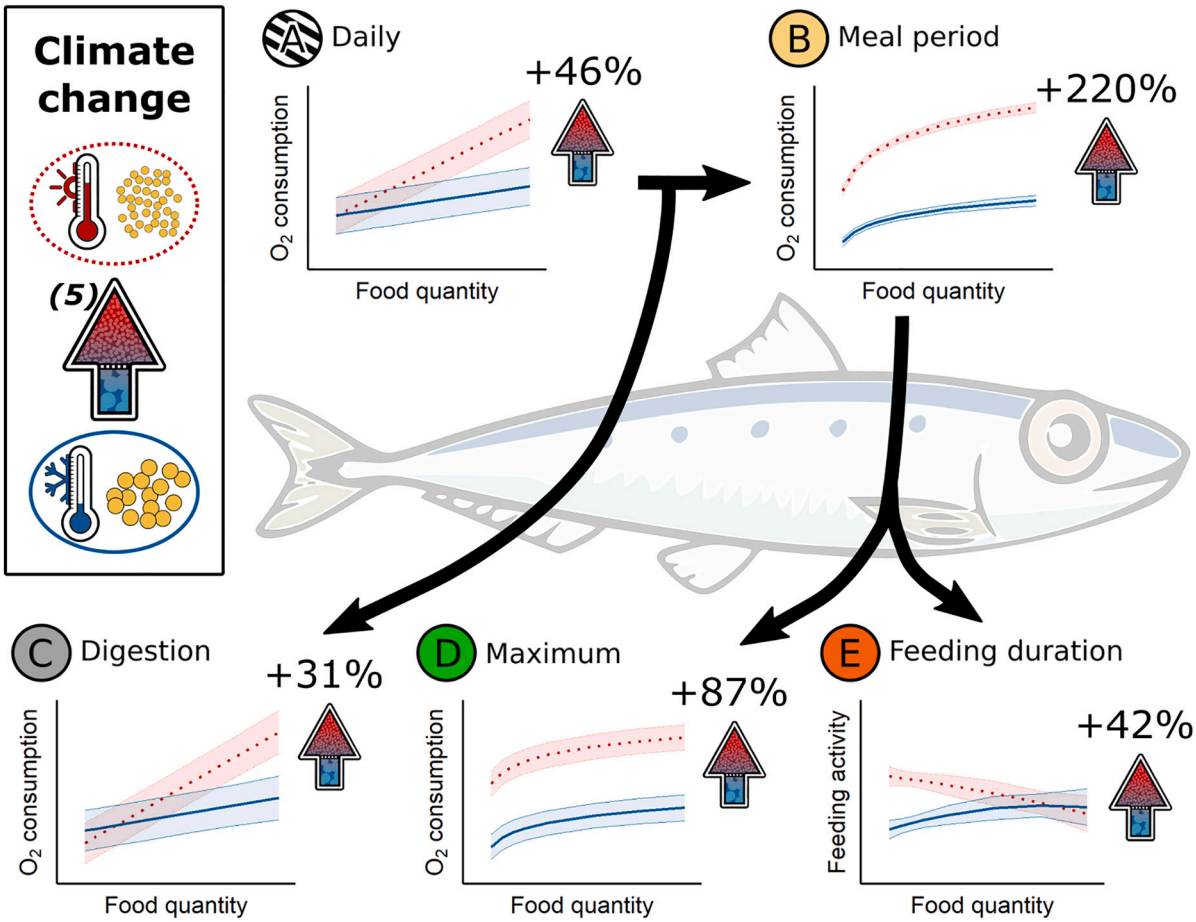

Fig. 4. Smooth functions of [A] daily, [B] while feeding, [C] while digesting, [D] maximal oxygen consumptions and [E] feeding duration according to the food ration for the 2 experimental treatments representing past and future environmental conditions, i.e. cool temperature and large particles (solid blue lines) and warm temperature and small particles (dotted red lines), respectively. Arrows represent the mean relative increase of the oxygen consumption/feeding duration according to the global warming (scenario 5), i.e. meal modification from large particles to small particles with increasing temperature, and summarized in top-left panel (feeding duration is not significantly affected by temperature increase, see Results).

(Fu et al., 2005a, 2005b; Jordan and Steffensen, 2007; Norin and Clark, 2017). The fact that a doubling of ration from 0.4 % to 0.8 % only caused a 17 % or 55 % increase in apparent SDA (based on estimated slopes), in fish fed large items at 16 °C or small items at 21 °C, respectively, might seem limited. This increase with doubling of ration is low compared to other fish species (see Secor, 2009). Furthermore, the high surface area to volume ratio of small particles should speed up digestion by promoting enzymatic processes and, thereby, reduce a part of digestion costs (discussed in Legler et al., 2010). On the other hand, a large SDA response can indicate that lots of nutrients were assimilated, notably amino acids for protein synthesis, with high costs of turning these into tissues but that reflect robust growth (Fraser and Rogers, 2007; McCue, 2006; Secor, 2009). That is, a large SDA would imply good growth, which is coherent with the fact that sardines fed on large particles exhibited higher growth and greater condition in previous studies (see Queiros et al., 2019).

There is another mechanism that might increase energy expenditure during 'digestion' of large particles, being the costs of recovery from rapid bursts of anaerobic swimming used for prey capture. The metabolic cost of such recovery, so-called 'excess post-exercise oxygen consumption' (EPOC) can be divided into 3 phases in fishes: rapid, plateau, slow (Zhang et al., 2018). While the rapid phase is very short (< 1 h), both plateau and slow phases can require several hours to return to standard metabolism. This can be more than 10 h for salmon although the duration is certainly species dependent (C. G. Lee et al., 2003; Li et al., 2020; Plambech et al., 2013; Svendsen et al., 2012; Zhang et al., 2018). Considering that we estimated energy expenditure of digestion starting at 1.5 h after providing the meal, this would omit the rapid phase of EPOC, although the phenomenon may have contributed to the final phases of metabolic costs of feeding. A potential role for EPOC in costs of feeding on large prey remains to be proven, since studies on individual sardines are technically extremely challenging. Overall, oxygen consumption due to digestion was lower for small compared to large particles, but the magnitude of the difference was much less than for the activity costs of feeding. Therefore, daily energy expenditure was mostly affected by what happened during the meal. The benefit of digesting small prey (in terms of energy expenditure for a same food ration) remained too weak to counterbalance the increased energy to capture shrinking plankton in the wild. Furthermore, the warm temperature also significantly increased metabolic rates, leading to overall higher energy expenditure during both meals and digestion (Clarke and Fraser, 2004; Seebacher et al., 2015), whatever the food size or ration. Higher energetic cost for digestion at warm temperatures has been reported for tunas, another species that swims continuously (Klinger et al., 2016) although relationships between costs of digestion and temperature are not necessarily linear (McKenzie et al., 2013; Tirsgaard et al., 2015).

Our study applied relatively short thermal acclimation times, which might tend to overestimate temperature effects. When natural populations are allowed to acclimatise over generations, baseline metabolism may show a much less marked effect of temperature (e.g. Wootton et al., 2022). Such intergenerational experiments are not

feasible for the Mediterranean sardine because their life cycle cannot be completed in captivity. Our experimental temperatures (16 °C and 21 °C) were well within the range that sardines have experienced in the Gulf of Lions over the last 40 years (12–24 °C; Feuilloley et al., 2020) and our rate of temperature change was slow (< 0.5 °C/day) allowing acclimation at an ecologically realistic pace. Furthermore, by expressing oxygen consumption as a relative increase from MO2 baseline (the baseline was estimated daily as the lowest 15 %-quantile rate for daily MO2 and MO2 during digestion, and as the mean of the preceding 2.5 h for MO2 while feeding), effects of temperature on baseline metabolism were been taken into account in our study. Finally, although the effects of temperature were significant, potential acclimation across a few generations leading to similar baseline metabolism between generations would reinforce our results on the effects of food size.

Although food size had only quite minor effects on daily energy use, increasing it by 10 [3;22]% in fish fed on small particles at 21 °C, long-term effects may be significant. Furthermore, sardines may feed continuously in the wild, not only once or twice a day, which would increase consequences of differences in energy expenditure during feeding. In the wild, sardines face predation and pathogens that require energy expenditure. Therefore, higher daily energy expenditure for feeding may well impair energy balance in the wild, resulting in less energy allocated towards survival and growth. For instance, lower swimming performance due to low energy reserves (e.g. swimming endurance (Martínez et al., 2003, 2004)) could isolate leaner individuals from schools, leading to a vicious circle, with lower food foraging and thus reinforcing lower energy reserves. Nonetheless, calorie-restricted sardines display better phenotypic plasticity to face fasting, which improves their ability to reduce their metabolic energy expenditures during long-term fasting (Queiros et al., 2021). Further, mitochondria from sardines fed with small particles exhibited lower basal oxidative activity but higher efficiency of ATP production than those fed with large particles, a mechanism that should help them spare energy (Thoral et al., 2021). Nevertheless, although sardines may display plasticity or adaptation that ameliorates the energetic consequences of smaller prey and warmer temperatures, the situation of sardine populations in the Gulf of Lions remains very concerning.

5. Conclusion

This study supports the hypothesis of bottom-up control to explain the profound shrinking of small pelagic fish communities in the Gulf of Lions and is a hypothesis worth exploring to explain the spread of this phenomenon throughout the Mediterranean (Albo-Puigserver et al., 2021; Brosset et al., 2017) to new ecosystems, and to species higher in the food web (Bensebaini et al., 2022; Véron et al., 2020). Altogether, the results indicate that energy balance can be a major mechanism explaining shrinking of fish populations globally. Declines in prey size could impact the energy balance of individuals when their energy expenditures are increased by warmer temperatures, with future projections of prey resources predicting a decline of prey biomass and quality.

Funding

The study was funded by the MUSE Key Initiative Sea and Coast.

CRediT authorship contribution statement

Quentin Queiros: Conceptualization, Formal analysis, Investigation, Writing – original draft, Visualization. **David J. McKenzie:** Conceptualization, Investigation, Resources, Writing – review & editing, Supervision. **Gilbert Dutto:** Conceptualization, Investigation, Writing – review & editing. **Shaun Killen:** Conceptualization, Funding acquisition. **Claire Saraux:** Conceptualization, Writing – review & editing. **Quentin Schull:** Conceptualization, Writing – review & editing, Supervision, Funding acquisition.

Declaration of competing interest

The authors declare that they have no known competing financial interests or personal relationships that could have appeared to influence the work reported in this paper.

Data availability

Data and scripts are now available here: https://zenodo.org/record/8413664.

Acknowledgments

We would like to thank colleagues at the IFREMER experimental station for their welcome and their fruitful advice during the conceptualization of the experiments. We would also like to express our thanks to the two anonymous reviewers for their comments that helped us improve the manuscript.

Appendix A. Supplementary data

Supplementary data to this article can be found online at https://doi.org/10.1016/j.scitotenv.2023.167310.

References

Albo-Puigserver, M., Pennino, M.G., Bellido, J.M., Colmenero, A.I., Giráldez, A., Hidalgo, M., Gabriel Ramírez, J., Steenbeek, J., Torres, P., Cousido-Rocha, M., Coll, M., 2021. Changes in life history traits of small pelagic fish in the Western Mediterranean Sea. Front. Mar. Sci. 8, 1197. https://doi.org/10.3389/FMARS.2021.570354/BIBTEX.

Alheit, J., Roy, C., Kifani, S., 2009. Decadal-scale variability in populations. In: Checkley, D., Alheit, J., Oozeki, Y., Roy, C. (Eds.), Climate Change and Small Pelagic Fish. Cambridge University Press, pp. 64–87.

Allison, E.H., Perry, A.L., Badjeck, M.C., Neil Adger, W., Brown, K., Conway, D., Halls, A. S., Pilling, G.M., Reynolds, J.D., Andrew, N.L., Dulvy, N.K., 2009. Vulnerability of national economies to the impacts of climate change on fisheries. Fish Fish. 10 (2), 173–196. https://doi.org/10.1111/j.1467-2979.2008.00310.x.

Ariza, A., Lengaigne, M., Menkes, C., Lebourges-Dhaussy, A., Receveur, A., Gorgues, T., Habasque, J., Gutiérrez, M., Maury, O., Bertrand, A., 2022. Global decline of pelagic fauna in a warmer ocean. Nat. Clim. Chang. https://doi.org/10.1038/S41558-022-01479-2.

Atkinson, D., 1994. Temperature and organism size—a biological law for ectotherms?. In: Advances in Ecological Research, vol. 25, issue C, pp. 1–58. https://doi.org/10.1016/S0065-2504(08)60212-3.

Audzijonyte, A., Richards, S.A., Stuart-Smith, R.D., Pecl, G., Edgar, G.J., Barrett, N.S., Payne, N., Blanchard, J.L., 2020. Fish body sizes change with temperature but not all species shrink with warming. Nat. Ecol. Evol. 4 (6), 809–814. https://doi.org/10.1038/s41559-020-1171-0.

Bates, D., Mächler, M., Bolker, B., Walker, S., 2015. Fitting linear mixed-effects models using lme4. J. Stat. Softw. https://doi.org/10.18637/jss.v067.i01.

Baudron, A.R., Needle, C.L., Rijnsdorp, A.D., Tara Marshall, C., 2014. Warming temperatures and smaller body sizes: synchronous changes in growth of {North}{Sea} fishes. Glob. Chang. Biol. 20 (4), 1023–1031. https://doi.org/10.1111/gcb.12514.

Bensebaini, C.M., Certain, G., Billet, N., Jadaud, A., Gourguet, S., Hattab, T., Fromentin, J.M., 2022. Interactions between demersal fish body condition and density during the regime shift of the Gulf of Lions. ICES J. Mar. Sci. https://doi.org/10.1093/icesjms/fsac106.

Bopp, L., Aumont, O., Cadule, P., Alvain, S., Gehlen, M., 2005. Response of diatoms distribution to global warming and potential implications: a global model study. Geophys. Res. Lett. 32, L19606 https://doi.org/10.1029/2005GL023653.

Bopp, L., Resplandy, L., Orr, J.C., Doney, S.C., Dunne, J.P., Gehlen, M., Halloran, P., Heinze, C., Ilyina, T., Séférian, R., Tjiputra, J., Vichi, M., 2013. Multiple stressors of ocean ecosystems in the 21st century: projections with CMIP5 models. Biogeosciences 10 (10), 6225–6245. https://doi.org/10.5194/bg-10-6225-2013.

Brochier, T., Echevin, V., Tam, J., Chaigneau, A., Goubanova, K., Bertrand, A., 2013. Climate change scenarios experiments predict a future reduction in small pelagic fish recruitment in the Humboldt Current system. Glob. Chang. Biol. 19 (6), 1841–1853. https://doi.org/10.1111/gcb.12184.

Brosset, P., le Bourg, B., Costalago, D., Bănaru, D., van Beveren, E., Bourdeix, J., Fromentin, J., Ménard, F., Saraux, C., 2016. Linking small pelagic dietary shifts with ecosystem changes in the Gulf of Lions. Mar. Ecol. Prog. Ser. 554, 157–171. https://doi.org/10.3354/meps11796.

Brosset, P., Fromentin, J.-M., van Beveren, E., Lloret, J., Marques, V., Basilone, G., Bonanno, A., Carpi, P., Donato, F., Čikeš Keč, V., de Felice, A., Ferreri, R., Gašparević, D., Giráldez, A., Gücü, A., Iglesias, M., Leonori, I., Palomera, I., Somarakis, S., Saraux, C., 2017. Spatio-temporal patterns and environmental controls of small pelagic fish body condition from contrasted Mediterranean areas. Prog. Oceanogr. 151, 149–162. https://doi.org/10.1016/j.pocean.2016.12.002.

Burnham, K.P., Anderson, D.R., 2002. Model Selection and Multimodel Inference, 2nd ed. Springer New York, New York, NY. https://doi.org/10.1007/b97636.

Chabot, D., Steffensen, J.F., Farrell, A.P., 2016a. The determination of standard metabolic rate in fishes. J. Fish Biol. 88 (1), 81–121. https://doi.org/10.1111/jfb.12845.

Chabot, D., Koenker, R., Farrell, A.P., 2016b. The measurement of specific dynamic action in fishes. J. Fish Biol. 88 (1), 152–172. https://doi.org/10.1111/JFB.12836.

Clarke, A., Fraser, K.P.P., 2004. Why does metabolism scale with temperature? Funct. Ecol. 18 (2), 243–251. https://doi.org/10.1111/j.0269-8463.2004.00841.x.

Costalago, D., Palomera, I., 2014. Feeding of European pilchard (Sardina pilchardus) in the northwestern Mediterranean: from late larvae to adults. Sci. Mar. 78 (1), 41–54. https://doi.org/10.3989/scimar.03898.06D.

Costalago, D., Garrido, S., Palomera, I., 2015. Comparison of the feeding apparatus and diet of European sardines Sardina pilchardus of Atlantic and Mediterranean waters: ecological implications. J. Fish Biol. 86 (4), 1348–1362. https://doi.org/10.1111/jfb.12645.

Daufresne, M., Lengfellner, K., Sommer, U., 2009. Global warming benefits the small in aquatic ecosystems. Proc. Natl. Acad. Sci. 106 (31), 12788–12793. https://doi.org/10.1073/pnas.0902080106.

Diamond, S.E., Kingsolver, J.G., 2010. Environmental dependence of thermal reaction norms: host plant quality can reverse the temperature-size rule. Am. Nat. 175 (1), 1–10. https://doi.org/10.1086/648602.

FAO, 2018. The State of World Fisheries and Aquaculture 2018 - Meeting the Sustainable Development Goals, 210 pp.

Feuilloley, G., Fromentin, J.M., Stemmann, L., Demarcq, H., Estournel, C., Saraux, C., 2020. Concomitant changes in the environment and small pelagic fish community of the Gulf of Lions. Prog. Oceanogr. 186, 102375. https://doi.org/10.1016/j.pocean.2020.102375.

Forster, J., Hirst, A.G., Atkinson, D., 2012. Warming-induced reductions in body size are greater in aquatic than terrestrial species. Proc. Natl. Acad. Sci. 109 (47), 19310–19314. https://doi.org/10.1073/pnas.1210460109.

Fraser, K.P.P., Rogers, A.D., 2007. Protein metabolism in marine animals: the underlying mechanism of growth. Adv. Mar. Biol. 52, 267–362. https://doi.org/10.1016/S0065-2881(06)52003-6.

Fréon, P., Cury, P.M., Shannon, L.J., Roy, C., 2005. Sustainable exploitation of small pelagic fish stocks challenged by environmental and ecosystem changes: a review. Bull. Mar. Sci. 76 (2), 385–462.

Fu, S.J., Xie, X.J., Cao, Z.D., 2005a. Effect of meal size on postprandial metabolic response in southern catfish (Silurus meridionalis). Comp. Biochem. Physiol. A Mol. Integr. Physiol. 140 (4), 445–451. https://doi.org/10.1016/j.cbpb.2005.02.008.

Fu, S.J., Xie, X.J., Cao, Z.D., 2005b. Effect of feeding level and feeding frequency on specific dynamic action in Silurus meridionalis. J. Fish Biol. 67 (1), 171–181. https://doi.org/10.1111/j.0022-1112.2005.00722.x.

Gardner, J.L., Peters, A., Kearney, M.R., Joseph, L., Heinsohn, R., 2011. Declining body size: a third universal response to warming? Trends Ecol. Evol. 26 (6), 285–291. https://doi.org/10.1016/j.tree.2011.03.005.

Garrido, S., Marçalo, A., Zwolinski, J., van der Lingen, C., 2007. Laboratory investigations on the effect of prey size and concentration on the feeding behaviour of Sardina pilchardus. Mar. Ecol. Prog. Ser. 330, 189–199. https://doi.org/10.3354/meps330189.

Garrido, S., Ben-Hamadou, R., Oliveira, P.B., Cunha, M.E., Chícharo, M.A., van der Lingen, C.D., 2008. Diet and feeding intensity of sardine Sardina pilchardus: correlation with satellite-derived chlorophyll data. Mar. Ecol. Prog. Ser. 354, 245–256. https://doi.org/10.3354/meps07201.

Horne, C.R., Hirst, Andrew G., Atkinson, D., 2015. Temperature-size responses match latitudinal-size clines in arthropods, revealing critical differences between aquatic and terrestrial species. Ecol. Lett. 18 (4), 327–335. https://doi.org/10.1111/ele.12413.

IPCC, 2013. Climate change 2013: the physical science basis. In: B, V., P. M. M. Stocker, T.F., Qin, D., Plattner, G.-K., Tignor, M., Allen, S.K., Boschung, J., Nauels, A., Xia, Y. (Eds.), Contribution of Working Group I to the Fifth Assessment Report of the Intergovernmental Panel on Climate Change. Cambridge University Press.

IPCC, 2014. Climate change 2014: synthesis report. In: Contribution of Working Groups I, II and III to the Fifth Assessment Report of the Intergovernmental Panel on Climate Change. https://www.ipcc.ch/report/ar5/syr/.

Jordan, A.D., Steffensen, J.F., 2007. Effects of ration size and hypoxia on specific dynamic action in the cod, 80 (2), 178–185. https://doi.org/10.1086/510565.

Klinger, D.H., Dale, J.J., Gleiss, A.C., Brandt, T., Estess, E.E., Gardner, L., Machado, B., Norton, A., Rodriguez, L., Stiltner, J., Farwell, C., Block, B.A., 2016. The effect of temperature on postprandial metabolism of yellowfin tuna (Thunnus albacares). Comp. Biochem. Physiol. A Mol. Integr. Physiol. 195, 32–38. https://doi.org/10.1016/J.CBPA.2016.01.005.

Kohavi, R., Longbotham, R., Sommerfield, D., Henne, R.M., 2009. Controlled experiments on the web: survey and practical guide. Data Min. Knowl. Disc. 18, 140–181. https://doi.org/10.1007/s10618-008-0114-1.

Lee, C.G., Farrell, A.P., Lotto, A., Hinch, S.G., Healey, M.C., 2003. Excess post-exercise oxygen consumption in adult sockeye (Oncorhynchus nerka) and coho (O. kisutch) salmon following critical speed swimming. J. Exp. Biol. 206 (18), 3253–3260. https://doi.org/10.1242/JEB.00548.

Lee, K.P., Jang, T., Ravzanaadii, N., Rho, M.S., 2015. Macronutrient balance modulates the temperature-size rule in an ectotherm. Am. Nat. 186 (2), 212–222. https://doi.org/10.1086/682072.

Legler, N.D., Johnson, T.B., Heath, D.D., Ludsin, S.A., 2010. Water temperature and prey size effects on the rate of digestion of larval and early juvenile fish. Trans. Am. Fish. Soc. 139 (3), 868–875. https://doi.org/10.1577/T09-212.1.

Li, X., Zhang, Y., Fu, S., 2020. Effects of short-term fasting on spontaneous activity and excess post-exercise oxygen consumption in four juvenile fish species with different foraging strategies. Biol. Open 9 (9). https://doi.org/10.1242/BIO.051755/225755.

Ljungström, G., Claireaux, M., Fiksen, Ø., Jørgensen, C., 2020. Body size adaptions under climate change: zooplankton community more important than temperature or food abundance in model of a zooplanktivorous fish. Mar. Ecol. Prog. Ser. 636, 1–18. https://doi.org/10.3354/meps13241.

Lotze, H.K., Tittensor, D.P., Bryndum-Buchholz, A., Eddy, T.D., Cheung, W.W.L., Galbraith, E.D., Barange, M., Barrier, N., Bianchi, D., Blanchard, J.L., Bopp, L., Büchner, M., Bulman, C.M., Carozza, D.A., Christensen, V., Coll, M., Dunne, J.P., Fulton, E.A., Jennings, S., Worm, B., 2019. Global ensemble projections reveal trophic amplification of ocean biomass declines with climate change. Proc. Natl. Acad. Sci. 116 (26), 12907–12912. https://doi.org/10.1073/pnas.1900194116.

Martínez, M., Guderley, H., Dutil, J.D., Winger, P.D., He, P., Walsh, S.J., 2003. Condition, prolonged swimming performance and muscle metabolic capacities of cod Gadus morhua. J. Exp. Biol. 206 (3), 503–511. https://doi.org/10.1242/JEB.00098.

Martínez, M., Bédard, M., Dutil, J.-D., Guderley, H., 2004. Does condition of Atlantic cod (Gadus morhua) have a greater impact upon swimming performance at Ucrit or sprint speeds? J. Exp. Biol. 207 (17), 2979–2990. https://doi.org/10.1242/jeb.01142.

McCue, M.D., 2006. Specific dynamic action: a century of investigation. Comp. Biochem. Physiol. A Mol. Integr. Physiol. 144 (4), 381–394. https://doi.org/10.1016/J.CBPA.2006.03.011.

McKenzie, D.J., Pedersen, P.B., Jokumsen, A., 2007. Aspects of respiratory physiology and energetics in rainbow trout (Oncorhynchus mykiss) families with different size-at-age and condition factor. Aquaculture 263 (1–4), 280–294. https://doi.org/10.1016/j.aquaculture.2006.10.022.

McKenzie, D.J., Höglund, E., Dupont-Prinet, A., Larsen, B.K., Skov, P.V., Pedersen, P.B., Jokumsen, A., 2012. Effects of stocking density and sustained aerobic exercise on growth, energetics and welfare of rainbow trout. Aquaculture 338–341, 216–222. https://doi.org/10.1016/j.aquaculture.2012.01.020.

McKenzie, D.J., Estivales, G., Svendsen, J.C., Steffensen, J.F., Agnèse, J.F., 2013. Local adaptation to altitude underlies divergent thermal physiology in tropical killifishes of the genus Aphyosemion. PLoS One 8 (1). https://doi.org/10.1371/JOURNAL.PONE.0054345.

Millien, V., Kathleen Lyons, S., Olson, L., Smith, F.A., Wilson, A.B., Yom-Tov, Y., 2006. Ecotypic variation in the context of global climate change: revisiting the rules. Ecol. Lett. 9 (7), 853–869. https://doi.org/10.1111/J.1461-0248.2006.00928.X.

Morrongiello, J.R., Sweetman, P.C., Thresher, R.E., 2019. Fishing constrains phenotypic responses of marine fish to climate variability. J. Anim. Ecol. 88 (11), 1645–1656. https://doi.org/10.1111/1365-2656.12999.

Muggeo, V.M.R., 2008. Segmented: an R package to fit regression models with broken-line relationships. R News 8 (1), 20–25. https://cran.r-project.org/doc/Rnews/.

Nikolioudakis, N., Isari, S., Pitta, P., Somarakis, S., 2012. Diet of sardine Sardina pilchardus: an "end-to-end" field study. Mar. Ecol. Prog. Ser. 453, 173–188. https://doi.org/10.3354/meps09656.

Norin, T., Clark, T.D., 2017. Fish face a trade-off between 'eating big' for growth efficiency and 'eating small' to retain aerobic capacity. Biol. Lett. 13 (9) https://doi.org/10.1098/RSBL.2017.0298.

Orr, J.C., Fabry, V.J., Aumont, O., Bopp, L., Doney, S.C., Feely, R.A., Gnanadesikan, A., Gruber, N., Ishida, A., Joos, F., Key, R.M., Lindsay, K., Maier-Reimer, E., Matear, R., Monfray, P., Mouchet, A., Najjar, R.G., Plattner, G.-K., Rodgers, K.B., Yool, A., 2005. Anthropogenic ocean acidification over the twenty-first century and its impact on calcifying organisms. Nature 437 (7059), 681–686. https://doi.org/10.1038/nature04095.

Pauly, D., International Ecology Inst, Kinne, O., Jorgensen, B.B., 2010. Gasping Fish and Panting Squids: Oxygen, Temperature and the Growth of Water-breathing Animals doi: 10.3/JQUERY-UI.JS.

Plambech, M., van Deurs, M., Steffensen, J.F., Tirsgaard, B., Behrens, J.W., 2013. Excess post-hypoxic oxygen consumption in Atlantic cod *Gadus morhua*. J. Fish Biol. 83 (2), 396–403. https://doi.org/10.1111/jfb.12171.

Queiros, Q., Fromentin, J.-M., Gasset, E., Dutto, G., Huiban, C., Metral, L., Leclerc, L., Schull, Q., McKenzie, D.J., Saraux, C., 2019. Food in the sea: size also matters for pelagic fish. Front. Mar. Sci. 6 https://doi.org/10.3389/fmars.2019.00385.

Queiros, Q., Saraux, C., Dutto, G., Gasset, E., Marguerite, A., Brosset, P., Fromentin, J.-M. M., McKenzie, D.J., 2021. Is starvation a cause of overmortality of the Mediterranean sardine? Mar. Environ. Res. 170, 105441. https://doi.org/10.1016/j.marenvres.2021.105441.

R Core Team, 2020. R: A Language and Environment for Statistical Computing. https://www.r-project.org/.

Richardson, A.J., Schoeman, D.S., 2004. Climate impact on plankton ecosystems in the Northeast Atlantic. Science 305 (5690), 1609–1612. https://doi.org/10.1126/science.1100958.

Roemmich, D., McGowan, J., 1995. Climatic warming and the decline of zooplankton in the California current. Science 267 (5202), 1324–1326. https://doi.org/10.1126/science.267.5202.1324.

Saraux, C., van Beveren, E., Brosset, P., Queiros, Q., Bourdeix, J.-H., Dutto, G., Gasset, E., Jac, C., Bonhommeau, S., Fromentin, J.-M., 2019. Small pelagic fish dynamics: a review of mechanisms in the Gulf of Lions. Deep-Sea Res. II Top. Stud. Oceanogr. 159, 52–61. https://doi.org/10.1016/j.dsr2.2018.02.010.

Schwartzlose, R.A., Alheit, J., Bakun, A., Baumgartner, T.R., Cloete, R., Crawford, R.J.M., Fletcher, W.J., Green-Ruiz, Y., Hagen, E., Kawasaki, T., Lluch-Belda, D., Lluch-Cota, S.E., MacCall, A.D., Matsuura, Y., Nevárez-Martínez, M.O., Parrish, R.H., Roy, C., Serra, R., Shust, K.v., Zuzunaga, J.Z., 1999. Worldwide large-scale fluctuations of sardine and anchovy populations. S. Afr. J. Mar. Sci. 21 (1), 289–347. https://doi.org/10.2989/025776199784125962.

Secor, S.M., 2009. Specific dynamic action: a review of the postprandial metabolic response. J. Comp. Physiol. B: Biochem. Syst. Environ. Physiol. 179 (1), 1–56. https://doi.org/10.1007/s00360-008-0283-7.

Seebacher, F., White, C.R., Franklin, C.E., 2015. Physiological plasticity increases resilience of ectothermic animals to climate change. Nat. Clim. Chang. 5 (1), 61–66. https://doi.org/10.1038/nclimate2457.

Shannon, L.J., Coll, M., Neira, S., Cury, P.M., Roux, J.-P., 2009. Impacts of fishing and climate change explored using trophic models. In: Checkley, D., Alheit, J., Oozeki, Y., Roy, C. (Eds.), Climate Change and Small Pelagic Fish. Cambridge University Press, pp. 158–190.

Sheridan, J.A., Bickford, D., 2011. Shrinking body size as an ecological response to climate change. Nat. Clim. Chang. 1 (8), 401–406. https://doi.org/10.1038/nclimate1259.

Signorell, Andri, 2023. DescTools: Tools for Descriptive Statistics (R Package Version 0.99.49). https://cran.r-project.org/package=DescTools.

Stearns, S.C., 1989. Trade-offs in life-history evolution. Funct. Ecol. 3 (3), 259. https://doi.org/10.2307/2389364.

Stearns, S.C., 1992. The Evolution of Life Histories. Oxford University Press. http://www.sidalc.net/cgi-bin/wxis.exe/?IsisScript=sibe01.xis&method=post&formato=2&cantidad=1&expresion=mfn=007580.

Steffensen, J.F., 1989. Some errors in respirometry of aquatic breathers: how to avoid and correct for them. Fish Physiol. Biochem. 6 (1), 49–59. https://doi.org/10.1007/BF02995809.

Svendsen, J.C., Steffensen, J.F., Aarestrup, K., Frisk, M., Etzerodt, A., Jyde, M., 2012. Excess posthypoxic oxygen consumption in rainbow trout (Oncorhynchus mykiss): recovery in normoxia and hypoxia. Can. J. Zool. 90 (1), 1–11. https://doi.org/10.1139/Z11-095/ASSET/IMAGES/Z11-095TAB1.GIF.

Thoral, E., Queiros, Q., Roussel, D., Dutto, G., Gasset, E., McKenzie, D.J., Romestaing, C., Fromentin, J., Saraux, C., Teulier, L., 2021. Changes in foraging mode caused by a decline in prey size have major bioenergetic consequences for a small pelagic fish. J. Anim. Ecol. 1365-2656, 13535. https://doi.org/10.1111/1365-2656.13535.

Tirsgaard, B., Svendsen, J.C., Steffensen, J.F., 2015. Effects of temperature on specific dynamic action in Atlantic cod Gadus morhua. Fish Physiol. Biochem. 41 (1), 41–50. https://doi.org/10.1007/s10695-014-0004-y.

van Beveren, E., Bonhommeau, S., Fromentin, J.-M., Bigot, J.-L., Bourdeix, J.-H., Brosset, P., Roos, D., Saraux, C., 2014. Rapid changes in growth, condition, size and age of small pelagic fish in the Mediterranean. Mar. Biol. 161 (8), 1809–1822. https://doi.org/10.1007/s00227-014-2463-1.

Verberk, W.C.E.P., Atkinson, D., Hoefnagel, K.N., Hirst, A.G., Horne, C.R., Siepel, H., 2021. Shrinking body sizes in response to warming: explanations for the temperature–size rule with special emphasis on the role of oxygen. Biol. Rev. 96 (1), 247–268. https://doi.org/10.1111/brv.12653.

Véron, M., Duhamel, E., Bertignac, M., Pawlowski, L., Huret, M., 2020. Major changes in sardine growth and body condition in the Bay of Biscay between 2003 and 2016: temporal trends and drivers. Prog. Oceanogr. 182, 102274. https://doi.org/10.1016/j.pocean.2020.102274.

Ward, B.A., Dutkiewicz, S., Jahn, O., Follows, M.J., 2012. A size-structured food-web model for the global ocean. Limnol. Oceanogr. 57 (6), 1877–1891. https://doi.org/10.4319/lo.2012.57.6.1877.

Wootton, H.F., Morrongiello, J.R., Schmitt, T., Audzijonyte, A., 2022. Smaller adult fish size in warmer water is not explained by elevated metabolism. Ecol. Lett. 25, 1177–1188. https://doi.org/10.1111/ele.13989.

Zarubin, M., Farstey, V., Wold, A., Falk-Petersen, S., Genin, A., 2014. Intraspecific differences in lipid content of calanoid copepods across fine-scale depth ranges within the photic layer. PLoS One 9 (3), 1–10. https://doi.org/10.1371/journal.pone.0092935.

Zhang, Y., Claireaux, G., Takle, H., Jørgensen, S.M., Farrell, A.P., 2018. A three-phase excess post-exercise oxygen consumption in Atlantic salmon Salmo salar and its response to exercise training. J. Fish Biol. 92 (5), 1385–1403. https://doi.org/10.1111/JFB.13593.

Zuur, A.F., Ieno, E.N., Walker, N., Saveliev, A.A., Smith, G.M., 2009. Mixed effects models and extensions in ecology with R. In: Statistics for Biology and Health. Springer New York, New York, NY. https://doi.org/10.1007/978-0-387-87458-6.

ARTICLES FOR FACULTY MEMBERS

GLOBAL WARMING EFFECTS ON ECTOTHERM SPECIES

Title/Author	**Global warming is projected to lead to increased freshwater growth potential and changes in pace of life in Atlantic salmon Salmo salar / Rinaldo, A., de Eyto, E., Reed, T., Gjelland, K. Ø., & McGinnity, P.**
Source	***Journal of Fish Biology*** **Volume 104 Issue 3 (2024) Pages 647–661** **https://doi.org/10.1111/jfb.15603** **(Database: Wiley Online Library)**

Received: 8 September 2023 | Revised: 24 October 2023 | Accepted: 29 October 2023

DOI: 10.1111/jfb.15603

REGULAR ARTICLE

JOURNAL OF FISH BIOLOGY fsbi

Global warming is projected to lead to increased freshwater growth potential and changes in pace of life in Atlantic salmon *Salmo salar*

Adrian Rinaldo[1,2,3] | Elvira de Eyto[2] | Thomas Reed[1,3] | Karl Øystein Gjelland[4] | Philip McGinnity[1,3]

[1]School of Biological, Earth and Environmental Sciences, University College Cork, Cork, Ireland

[2]Fisheries Ecosystems Advisory Services, Marine Institute, Newport, Ireland

[3]Environmental Research Institute, University College Cork, Cork, Ireland

[4]Norwegian Institute for Nature Research, Tromsø, Norway

Correspondence
Adrian Rinaldo, School of Biological, Earth and Environmental Sciences, University College Cork, Distillery Fields, North Mall Campus, University College Cork, T23 N73K Cork, Ireland.
Email: ARinaldo@ucc.ie

Funding information
HORIZON EUROPE Marie Sklodowska-Curie Actions, Grant/Award Number: 956623; Marine Institute Grant-in-Aid, Grant/Award Number: RESPI/BIO/21/01; Science Foundation Ireland, Grant/Award Numbers: 15/IA/3028, 16/BBSRC/3316

Abstract

Global warming has been implicated in widespread demographic changes in Atlantic salmon *Salmo salar* populations, but projections of life-history responses to future climate change are lacking. Here, we first exploit multiple decades of climate and biological data from the Burrishoole catchment in the west of Ireland to model statistical relationships between atmospheric variables, water temperature, and freshwater growth of juvenile Atlantic salmon. We then use this information to project potential changes in juvenile growth and life-history scheduling under three shared socioeconomic pathway and representative concentration pathway scenarios from 1961 to 2100, based on an ensemble of five climate models. Historical water temperatures were well predicted with a recurrent neural network, using observation-based atmospheric forcing data. Length-at-age was in turn also well predicted by cumulative growing degree days calculated from these water temperatures. Most juveniles in the Burrishoole population migrated to sea as 2-year-old smolts, but our future projections indicate that the system should start producing a greater proportion of 1-year-old smolts, as increasingly more juveniles cross a size-based threshold in their first summer for smoltification the following spring. Those failing to cross the size-based threshold will instead become 2-year-old smolts, but at a larger length relative to 2-year-old smolts observed currently, owing to greater overall freshwater growth opportunity. These changes in age- and size-at-seaward migration could have cascading effects on age- and size-at-maturity and reproductive output. Consequently, the seemingly small changes that our results demonstrate have the potential to cause significant shifts in population dynamics over the full life cycle. This workflow is highly applicable across the range of the Atlantic salmon, as well as to other anadromous species, as it uses openly accessible climate data and a length-at-age model with minimal input requirements, fostering improved general understanding of phenotypic and demographic responses to climate change and management implications.

KEYWORDS
aquatic ectotherms, growing degree days, ISIMIP, life history, population dynamics

1 | INTRODUCTION

The Earth's climate is warming (IPCC, 2022), leading to changes in near-surface air temperature, humidity, air pressure, wind, and precipitation, which in turn influences ecosystems across multiple levels (i.e., individual, population, and community) (Woodward et al., 2010). Species may respond to changes in their environment by phenotypic plasticity, evolutionary adaptation, or migration (Sears & Angilletta, 2011). However, changes are happening at an unprecedented rate, and many species may be unable to adapt quickly enough to avoid population decline and possible extinction (Radchuk et al., 2019; Reed, Schindler, & Waples, 2011). This is particularly the case for species that undertake seasonal migrations, as successful migration relies on fine-tuned responses to environmental cues (Crozier et al., 2008). The adaptation of migratory individuals to their surroundings manifests in their life-history traits such as growth pattern, age- and size-at-migration, and reproduction timing. Juvenile Atlantic salmon *Salmo salar* L. 1758 typically spend 1–5 years in fresh water before undergoing the physiological smoltification process and migrating to sea as smolts. They then spend between one and three winters at sea, before completing the life cycle by returning to spawn. A decrease in the age-at-smoltification with increasing temperatures has already been observed in some populations (Russell et al., 2012; Thorstad et al., 2021). Widespread recent declines in Atlantic salmon stocks appear to be driven predominantly by declines in marine survival, possibly related to climate change (ICES, 2022). Climate-driven impacts in fresh water can also directly affect population dynamics via reductions in smolt numbers, or indirectly via carry-over effects on marine survival and growth, and the number of years spent at sea (Mobley et al., 2021). It is, therefore, crucial to quantify and understand how juvenile Atlantic salmon will respond to climate change across their native range in the coming decades.

The Atlantic salmon is native to river systems draining into the North Atlantic Ocean, the Baltic Sea, and the Barents Sea (Klemetsen et al., 2003; MacCrimmon & Gots, 1979; Thorstad et al., 2011, 2021). Atlantic salmon that occur in linked river and ocean systems are within their physiological requirements for temperature (see Bennett et al., 2021). Lower and upper thermal limits are 0 and 27°C, respectively, for juvenile life stages (Elliott, 1991; Elliott & Elliott, 2010; Jensen et al., 1991; Thorstad et al., 2021), with growth occurring between 7 and 23°C with an optimum of 15.9°C (Elliott & Hurley, 1997). The effects of climate change are expected to be most prominent for the populations at or close to the edges of the distribution range (Thorstad et al., 2021), with the southernmost populations disappearing, and the northernmost populations experiencing significant changes in life-history and, consequently, population dynamics.

Physiological processes in ectotherms are dependent on ambient temperatures (Atkinson, 1994; Hazel & Prosser, 1974; Van Der Have & De Jong, 1996), but the precise relationship between temperature and growth in ectotherms is uncertain (Sears & Angilletta, 2011). Cumulative growing degree days (CGDD) is the accumulation of ambient temperatures over time relevant for growth and development in ectotherms, and this metric of physiological time is widely applied in agronomy and entomology (Neuheimer & Taggart, 2007). The use of CGDD in fish ecology is increasing, and several studies show strong linear correlations between CGDD and growth in immature fish (Chezik et al., 2014; Neuheimer & Taggart, 2007; Venturelli et al., 2010). Growth in juvenile Atlantic salmon is controlled by both intrinsic and extrinsic factors. Temperature and photoperiod are key determinants of both internal (e.g., physiological processes) and external (e.g., resource availability) processes, varying substantially across seasons. Because CGDD integrates time and temperature, the method offers good possibilities for investigating the effects of climate change on growth, and subsequent changes in life history of juvenile Atlantic salmon.

Recent reviews of climate change effects on Atlantic salmon suggest that changes in water temperature and hydrology will cause significant shifts in life-history traits such as growth and age- and size-at-smoltification with cascading effects on age- and size-at-maturity, pace of life and ultimately reproductive output (Jonsson & Jonsson, 2009; Thorstad et al., 2021). Consequently, seemingly small changes in the life history of juvenile Atlantic salmon may cause significant changes in population dynamics. Moving from qualitative explorations to quantitative projections can be supported by the development and validation of models that can then be driven by future climate projections.

Quantitative approaches have been developed to investigate climate change impacts on Atlantic salmon. For example, Hedger et al. (2013), Piou and Prévost (2012) and Sundt-Hansen et al. (2018) have used individual-based models to quantify individual and population-level responses to changes in climate. However, these studies build on large amounts of observational data (e.g., discharges, fish density estimates, genetics), to calibrate and parameterize the models to specific populations. The data requirements of these approaches make them difficult to apply to broad spatial scales such that they are applicable to populations across the distribution range of the species. We sought to design a model workflow quantifying the impact of global warming on a key life-history trait in the Atlantic salmon, which would be applicable across the distribution range for both data-poor and data-rich populations. The Intersectoral Impact Model Intercomparison Project (ISIMIP) offers a framework for consistently projecting the impacts of climate change across affected sectors and spatial scales (Frieler et al., 2017), which is well suited to the Atlantic salmon as it inhabits a wide geographic area and several distinct habitats (e.g., freshwater, coastal, and marine).

The overarching aim of this study is to develop a modeling workflow that ties atmospheric climate data to the key life-history traits size- and age-at-smoltification via freshwater growth. Specifically, we (1) statistically model a relationship between atmospheric data ISIMIP phase 3a and in-situ water temperature using a neural network approach; (2) establish a statistical relationship between length-at-age and CGDD using a generalized linear model; (3) couple the water temperature model with the length-at-age model, and future climate projections from ISIMIP phase 3b; and (4) analyse the life-history response using a calibrated reaction norm for smoltification.

2 | MATERIALS AND METHODS

2.1 | Study site

The Burrishoole catchment (53°56′ N, 9°35′ W) is situated in the west of Ireland. The catchment is ~100 km^2 in size and consists of lakes and streams draining into the northeast Atlantic Ocean through Clew Bay (Figure 1). Due to the temperate oceanic climate, air temperatures historically rarely exceed 20°C, and the minimum water temperature is typically between 2 and 4°C (de Eyto et al., 2022).

Monitoring of diadromous fish in the Burrishoole catchment began in the late 1950s. Complete monitoring of migrating diadromous fish has been in place since 1970, with sea-entry traps on the Mill Race and Salmon Leap (Figure 1). Atlantic salmon in the Burrishoole catchment migrate as 1- to 3-year-old smolts from March to June, with more than 90% migrating as 2-year-olds (Piggins & Mills, 1985). The annual number of smolts declined from ~16,000 in the 1970s to around 5500 in the mid-to-late 2010s (Marine Institute, 2020).

2.2 | Model workflow

To investigate the effects of climate change on juvenile Atlantic salmon in the Burrishoole, a multistep workflow was developed using Python (Van Rossum & Drake, 2010). The multistep workflow consists of four main steps: (1) statistical modeling of water temperatures from atmospheric data; (2) statistical modeling of length-at-age from CGDD calculated from modeled water temperature; (3) coupling of the water temperature model, the length-at-age model, and future climate projections; and (4) analysis of life-history response (Figure 2). Multiple substeps to the workflow are only briefly described, but more detailed descriptions are found in the supplementary material S1a, S1b, S2, S3, S4 and S5.

This study uses climate data from the ISIMIP as it provides a framework to assess the effects of climate change by offering openly accessible historical and current data, and future climate projections (Frieler et al., 2017). The ISIMIP consists of several phases: phase 3a provides climate reanalysis data from the historical to contemporary climate, and phase 3b provides historical, current, and three future climate scenarios based on the combination of three shared socioeconomic pathways and representative concentration pathways (i.e., SSP-RCPs) (https://www.isimip.org/). In short, the three SSP-RCP scenarios denote the socioeconomic trends in combination with the level of greenhouse gas (GHG) emissions, with SSP1-RCP2.6 being a low emission scenario, SSP3-RCP7.0 a medium to high emission scenario, and SSP5-RCP8.5 a high emission scenario (see Meinshausen et al., 2011; Riahi et al., 2017). The ISIMIP phase 3a and 3b data applied in this study have a daily temporal and 0.5°latitude × longitude spatial resolution and comprise near-surface air temperature (°C), near-surface wind speed (m s^{-1}), precipitation (kg m^{-2}s^{-1}), snowfall flux (kg m^{-2}s^{-1}), surface downwelling shortwave radiation (W m^{-2}), surface downwelling longwave radiation (W m^{-2}), near-surface specific humidity (unitless), and near-surface relative humidity (%).

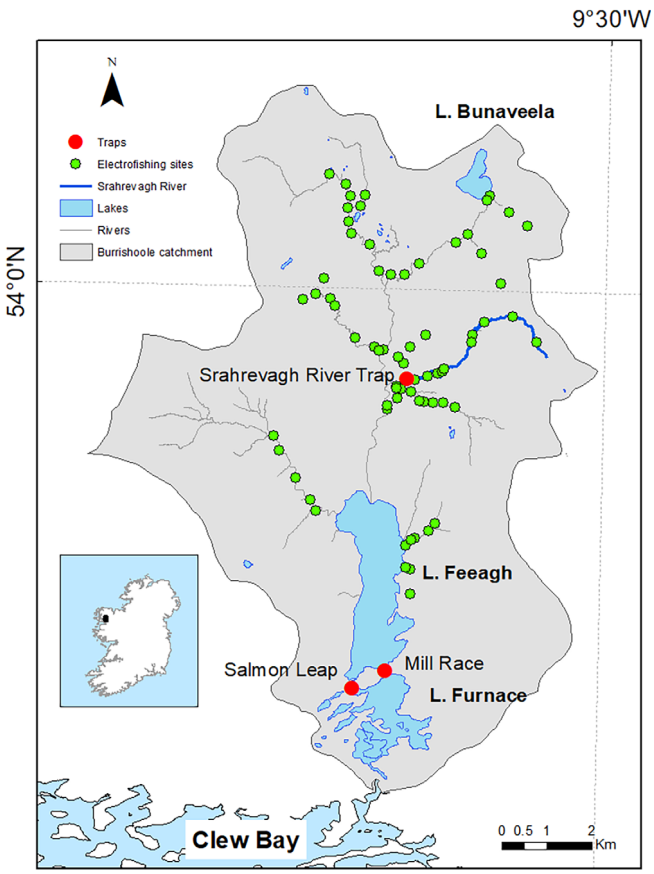

FIGURE 1 Location of electrofishing sites (green circles) and fish traps (red circles) in the Burrishoole catchment, Co. Mayo, Ireland.

2.2.1 | Step 1: Water temperature model

To establish a link between atmospheric conditions and water temperatures, daily average in-situ water temperatures (1961–2019) from the Burrishoole catchment were obtained from the Marine Institute Ireland (Marine Institute Ireland, doi: 10/cvft), measured in the Mill Race (Figure 1). Historical to concurrent climate reanalysis data (i.e., GSWP3-W5E5 observation-based, climate-related forcing data) were obtained from ISIMIP phase 3a (1961–2019). To retain as much data as possible, missing values in the Mill Race time series were linearly interpolated if the consecutive number of missing values was less than 30 days. If the number of consecutive missing values was more than 30 days, the entire year was removed from the time series. The years 1965, 1967, 1974, 1991, 2012, 2013, and 2017 were excluded due to extended periods of missing data, and 1990 and 2005 were removed due to calibration and sensor issues (E. de Eyto, pers. comm.).

The in-situ water temperature and modeled atmospheric data were merged, centered, and scaled according to quantile range scaling using RobustScaler from the scikit-learn module (Pedregosa et al., 2011). Information on seasonality was encoded using sine and cosine transformations of the day of year, which results in equal

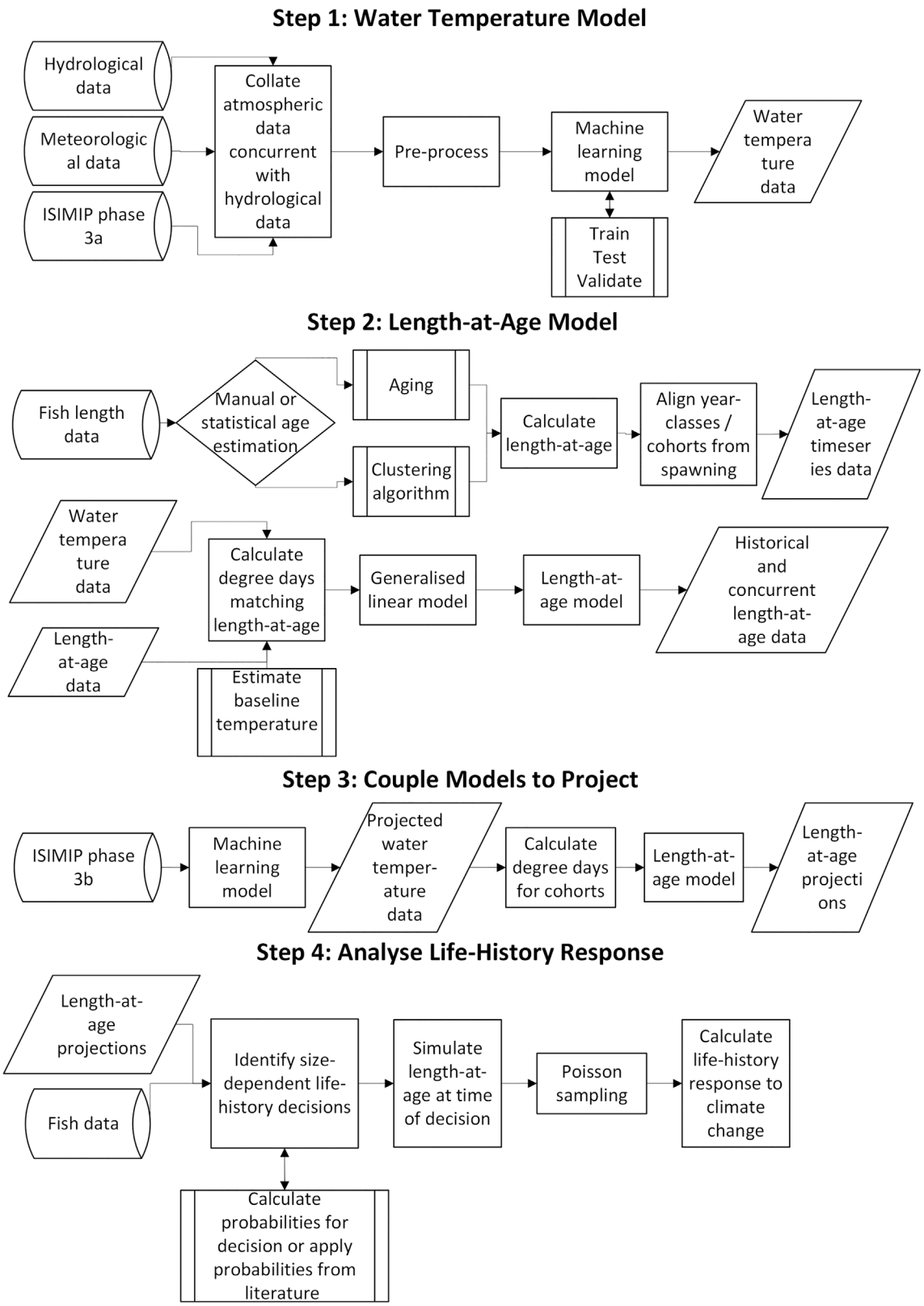

FIGURE 2 The four-step model workflow for quantitatively estimating length-at-age and life history of juvenile Atlantic salmon in response to climate change. Step 1 describes the collation of necessary data and construction of the water temperature model. Step 2 details the data preparation and construction of the length-at-age model for juvenile Atlantic salmon. Step 3 shows the coupling of the ISIMIP phase 3B projections to the water temperature model, and the subsequent coupling with the length-at-age model. Step 4 shows the post-processing of length-at-age projections to estimate smoltification probability and proportion of 1-, 2- and 3-year-old smolts. Shapes are according to ISO 5807 standard.

spacing between every date (e.g., day 365 is as close to day 1 as day 1 is to day 2). The merged dataset was then split into a training (1961–1994) subset and a validation (1995–2019) subset. A long short-term memory neural network (i.e., LSTM) was selected based on fidelity of multiple approaches measured by mean absolute error (i.e., MAE) and mean root squared error (i.e., RMSE) (see supplementary material S1a).

The LSTM neural network allows for modeling of nonlinear relationships and was constructed of a masking layer, an LSTM layer with 16 nodes and a tanh activation function, a dropout layer with a dropout rate of 0.2 to prevent overfitting, and a dense layer with a single node using a linear activation function. Additionally, a call-back function based on the validation RMSE and patience of 10 epochs was specified to prevent overfitting (see supplementary material S1b). The LSTM neural network was set up using the TensorFlow and Keras modules (Abadi et al., 2016; Chollet, 2013).

2.2.2 | Step 2: Length-at-age model

To assess the effect of water temperature on juvenile Atlantic salmon, fish length data from three sources within the Burrishoole catchment were obtained (Figure 1). First, annual catchment-wide electrofishing surveys are carried out every year between July and October at approximately 40 sites distributed across the catchment. Body lengths of 30,912 wild juvenile Atlantic salmon belonging to 20 cohorts from these surveys were extracted from 2000 to 2019. Second, high-resolution monitoring is carried out in the Srahrevagh River using a fish trap to capture all life-history stages from swim-up fry to sea-migrating smolts (McGinnity et al., 1997). These records include measured body lengths of 2999 wild juvenile Atlantic salmon belonging to nine cohorts sampled between 1998 and 2017. Finally, a subsample of migrating smolts that is killed for biometric sampling each year at the Mill Race and Salmon Leap Traps, and body lengths from 3366 Atlantic salmon smolts belonging to 20 cohorts sampled between 2000 and 2019 were included. In total, information on 37,277 individual fish was collated, but after the removal of outliers and observations with missing values, the number of fish in the analysis was reduced to 37,258 juvenile Atlantic salmon. A further reduction to the sample number was undertaken due to missing water temperature data for years after 2019, and so the final number of fish in the analysis was brought down to 35,719. In all cases, body length is expressed as the fork length.

After amalgamation of fish body length data, age classification was performed based on body length and time of capture using a Gaussian mixture model (with the expectation-maximization algorithm) from the scikit-learn module (Pedregosa et al., 2011). A sliding window technique was used to subdivide the year into shorter time periods accounting for growth. Backcalculation of age in days for each fish was done using a 2-year smolt trajectory and a fixed date for egg deposition in the riverbed substrate, allowing for alignment of cohorts consistent with Gregorian calendar years. The fixed egg deposition was set as the date of winter solstice (i.e., 21st of December), which falls well within the spawning window of adult Atlantic salmon in the Burrishoole (see supplementary material S2).

The CGDD for each cohort was calculated from the date of fixed egg deposition and for the entire freshwater residency using Equation (1),

$$\mathrm{CGDD} = \sum_{i=1}^{n} T_{\mathrm{d}} - T_{\mathrm{b}}, \tag{1}$$

where T_{d} is the daily mean water temperature obtained from the LSTM neural network predictions using climate reanalysis data, and T_{b} is the lower threshold temperature for growth (i.e., baseline temperature). Based on repeated iterations of an ordinary least squares (OLS) model with varying baseline temperatures, T_{b} was set to 0°C based on the highest coefficient of determination and lowest AIC (see supplementary material S3).

Multiple length-at-age models were then parameterized linking body length (mm) to CGDD (°C·day) using the Statsmodels module (Seabold & Perktold, 2010). Based on model fidelity, a generalized linear model using the gamma distribution and natural logarithmic link function was selected (see supplementary material S4). The 95% prediction interval for the model was obtained by normal approximation of the sampling distribution of the coefficients with 50,000 random draws.

2.2.3 | Step 3: Coupling of models and projection

To generate future projections of water temperatures for the Mill Race, atmospheric data produced by five general circulation models (i.e., GFDL-ESM4, IPSL-CM6A-LR, MPI-ESM1-2-HR, MRI-ESM2-0, and UKESM1-0-LL) for the SSP-RCP 1–2.6, 3–7.0, and 5–8.5 climate scenarios (2020–2100) were obtained from ISIMIP phase 3b for the 0.5°latitude × longitude grid cell overlying the Burrishoole catchment.

These data were used to simulate future water temperatures by forcing the LSTM neural network derived in Step 1, and the ensemble mean was calculated and used to determine the number of CGDD experienced and body length achieved for every cohort from 2021 to 2098 using the length-at-age model derived in Step 2.

2.2.4 | Step 4: Analysis of life-history response

To investigate the response of juvenile Atlantic salmon to climate change, the body length distribution was simulated for a total of 10,000 fish per cohort using a normal approximation of the sample distribution of the coefficient (i.e., the prediction interval) at three key time points via the length CGDD model: (1) first decision window for smoltification; (2) time of seaward migration for 1-year-old smolts; and (3) time of seaward migration for 2-year-old smolts. We further assume no early maturation of male parr due to no available records. The probability for smoltification as a 1-year-old was calculated using Equation (2):

$$P(\text{will smolt next spring}) = 1 - P(\text{will not smolt next spring}) = 1 - \left(e^{52.321-0.862*FL}\right), \quad (2)$$

where FL is body length expressed as fork length (adapted from Metcalfe, 1998 [p. 99, Table 1]), and iteratively calibrated to the smolt run of 1983 reported in Piggins and Mills (1985). Using Poisson sampling (i.e., independent Bernoulli trials) and a uniform probability distribution, each fish was assigned to one of two alternative categories: "will smolt as a 1-year-old" (success) or "will not smolt as a 1-year-old" (failure). Subsequently, for fish in the "will not smolt as a 1-year-old" category the probability of being a smolt as a 2-year-old was calculated using Equation (3):

$$P(\text{immature fish is now smolt}) = e^{0.0823*FL-8.774}, \quad (3)$$

where FL is body length expressed as fork length and iteratively calibrated to the smolt run of 1983 reported in Piggins and Mills (1985). Again, using Poisson sampling and a uniform probability distribution, non-smolts were assigned to the either of two categories: "are now 2-year-old smolts" (success) or "will not smolt as a 2-year-old" (failure). The remaining fish that did not smolt as 1- or 2-year-olds were then considered to be 3-year-old smolts (more detail is contained in supplementary material S5).

The impact of climate change on smolt age composition was then calculated for each cohort, and the underlying trend was quantified using OLS regression. Lastly, the length distribution of 1-year- and 2-year-old smolts was visualized over time using the JoyPy module.

TABLE 1 Ordinary least squares regression of annual average water temperature as a function of year for observed and modeled water temperature in the Mill Race (Burrishoole Catchment, Co. Mayo, Ireland).

	Observed average water temperature (°C year^{-1})	Modeled average water temperature (°C year^{-1})
Intercept	−35.250*** (8.633)	−23.940*** (6.316)
Year	0.023 *** (0.004)	0.017*** (0.003)
R^2	0.368	0.344
R^2 adj.	0.355	0.333
N (DF)	50 (48)	58 (56)

Note: Water temperature was modeled using a long short-term memory neural network. Standard error in parentheses. *$p < 0.1$; **$p < 0.05$; ***$p < 0.01$.
Abbreviation: DF, degrees of freedom.

2.3 | Ethics statement

Ethical review and approval was not required for this study because the data used in this article were collected by the Irish Marine Institute for stock assessment purposes and therefore does not fall under the EU and Irish directives on animal welfare (2010/63/EU, SI No 543 of 2012). The sampling infrastructure (fish traps) operates under license (Fisheries Acts 1959–2003) from the Department of Agriculture, Food and Marine and by permission of the Minister of Agriculture, Food and Marine.

3 | RESULTS

3.1 | Historic to contemporary

3.1.1 | LSTM neural network

Comparison of in-situ and statistically modeled water temperature in the Mill Race showed close agreement for the training period (1961–1994) with an RMSE = 0.654°C and MAE = 0.488°C, and the validation period (1995–2019) with an RMSE = 0.844°C and MAE = 0.633°C (Figure 3). Due to the model setup, the year 1961 is

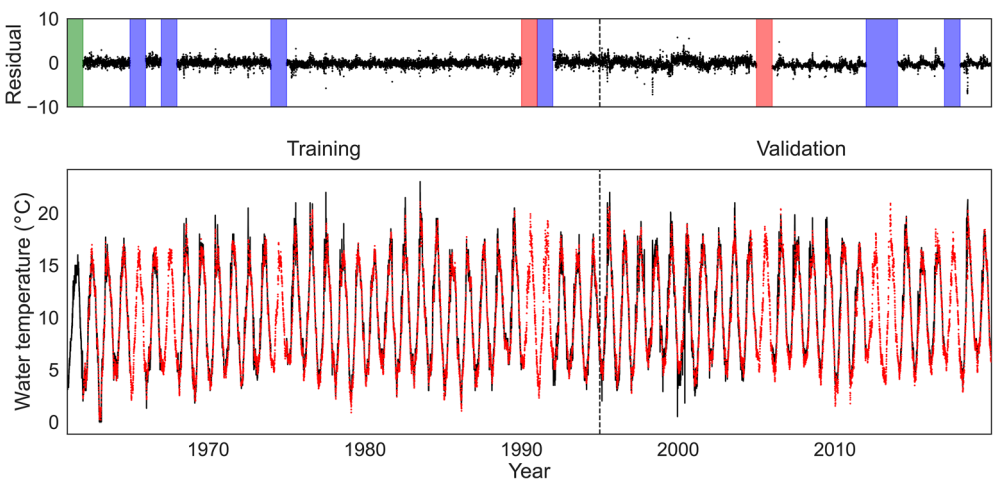

FIGURE 3 The residual error between observed and predicted water temperature (top panel), and the in-situ water temperature (black line) and long short-term memory neural network water temperature prediction (red crosses) for the training (1961–1994) and validation (1995–2019) dataset in the Mill Race (bottom panel). Years excluded due to accumulation of internal sate (green), prolonged periods of missing data (blue shaded), and measurement error (red shaded) are shown in the top panel, and the delineation of the training and validation period is shown by the vertical dashed line in both panels.

TABLE 2 Summary statistics describing the length of juvenile Atlantic salmon, measured in the Burrishoole catchment, Co. Mayo, Ireland.

Age class	Count	Mean	S.D.	Min	25%	50%	75%	Max
0	22,048	55.4	7.6	21	50	55	60	77
1	9021	98.7	14.7	48	89	98	108	164
2	1284	120.1	13.9	80	110	120	130	166
Smolt	3366	138.4	14.7	101	128	137	147	214

Note: Age-classes were determined using Gaussian mixture model classification.

omitted from the time series. The high fidelity of the LSTM neural network when driven by the 0.5°latitude × longitude ISIMIP phase 3a obsclim data was considered sufficient for the projection of water temperatures in the Mill Race.

From the historic to the contemporary period (1961–2019), a significant warming was found for the Mill Race. When quantified using the observed and modeled time series, the long-term increase in water temperature was ~ 0.023 and ~ 0.017°C year^{-1}, respectively (Table 1).

3.1.2 | Length-at-age

The juvenile Atlantic salmon observations from the historical and contemporary periods (1996–2019) were a mix of age classes, as determined by a Gaussian mixture model classification (Table 2). The relationship between body length (mm) of these fish and CGDD was positive and statistically significant using 35,719 observations belonging to 23 cohorts (Kendall rank correlation coefficient; $r_\tau = 0.61, p < 0.001$). A general linear model (GLM) with a gamma family, log link, and Newey-West HAC estimator found body length to increase by approximately $0.0146 \pm 0.0002\%$ ($p < 0.001$) degree day^{-1} (GLM : $\beta_1 = 1.46 * 10^{-4} \pm 0.02 * 10^{-4}, \beta_0 = 3.6463 \pm 0.010, R^2_{cs} = 0.99, p < 0.001$; Figure 4).

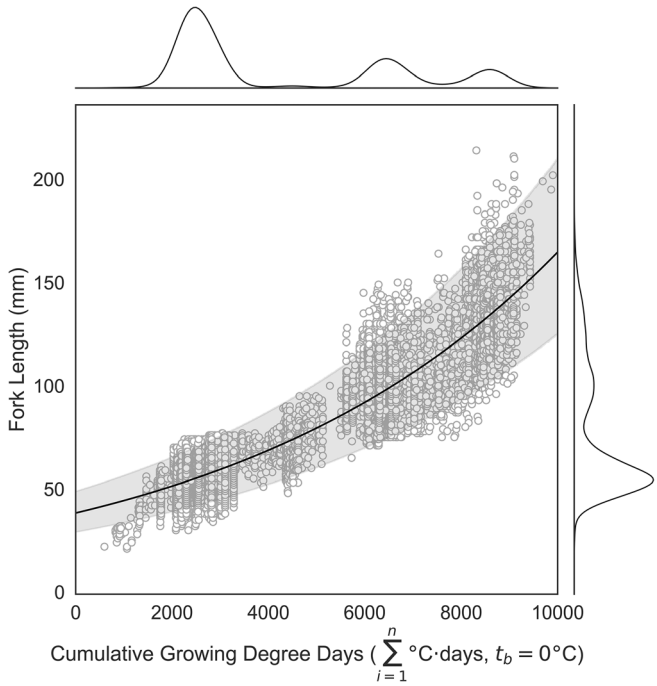

FIGURE 4 Generalized linear model of body length (mm) as a function of cumulative growing degree days (CGDD, °C day) for the 23 observed cohorts of juvenile Atlantic salmon in the Burrishoole watershed. The solid line represents the mean length, and the gray bands represent the 95% prediction interval. The outer lines represent the sample density.

3.2 | Future projections

3.2.1 | Water temperatures in the Mill Race

Future projections derived by coupling of the LSTM neural network and atmospheric data from the ISIMIP phase 3b climate forcing ensemble revealed warming of water temperatures in the Mill Race across the 80-year period (2020–2100) under two of the three SSP-RCP-scenarios (Figure 5). There was no significant linear long-term trend in water temperature for SSP1-RCP 2.6 ($p > 0.05$), whereas SSP3-RCP 7.0 increased by ~ 0.02°C year^{-1} ($p > 0.01$) and SSP5-RCP 8.5 increased by ~ 0.03°C year^{-1} ($p > 0.01$) ($OLS : R^2_{\text{adj}} = 0.89$).

3.2.2 | Life-history response

When the length-at-age model is driven by the LSTM water temperature projections to simulate (1) length-at-smoltification decision; (2) length-at-smoltification as 1-year-old smolts; and (3) length-at-smoltification as 2-year-old smolts, the response to temperature change, in terms of growth gain, differs between the three key moments of freshwater residency (Figure 6; Table 3).

The different response to temperature changes between the key life-history events results in diverging trends in the proportion of Atlantic salmon that chose to smolt as 1-year-olds between SSP1-RCP2.6 ($\beta = -0.0002\, cohort^{-1}, p < 0.01$), SSP3-RCP7.0 ($\beta = 0.0011\, cohort^{-1}, p < 0.01$) and SSP5-RCP8.5 ($\beta = 0.0017\, cohort^{-1}, p < 0.01$), when quantified using OLS regression ($R^2 = 0.830, F(5,228) = 222.4, p < 0.01$; Figure 7).

Using OLS regression ($R^2 = 0.825, F(5,228) = 220.1, p < 0.01$) to estimate the effects of changing smolt age proportion on population average age-at-smoltification (Figure 8), barring the effect of mortality, age-at-smoltification had an initial decrease before tending toward current age-at-smoltification under SSP1-RCP2.6 ($\beta = -0.0002, p < 0.01$), but decreased under SSP3-RCP7.0 ($\beta = -0.0011, p < 0.01$) and SSP-RCP8.5 ($\beta = -0.0017, p < 0.01$).

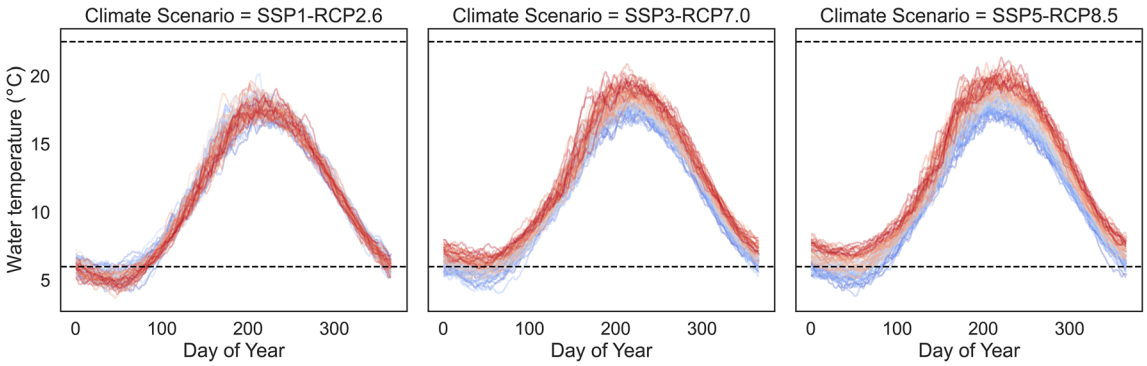

FIGURE 5 Ensemble average daily water temperature by day of year for the future projections under the three shared socioeconomic pathways and representative concentration pathways (SSP1-RCP2.6 left, SSP5-RCP7.0 middle, and SSP5-RCP8.5 right). Each line represents the day of year average temperature for the climate forcing ensemble with colors transitioning from blue to red toward the end of the century (starting with 2020 and ending with 2100). The lower dashed line represents the lower growth threshold temperature of 7°C, and the upper dashed line represents the upper growth threshold temperature for 23°C (Elliott & Hurley, 1997).

4 | DISCUSSION

This study provides a data-efficient approach to simulating length-at-age in ectotherms under historical, contemporary, and future climates using the ISIMIP framework. The potential of the approach is demonstrated by elucidating life-history responses of the migratory, cold-water-evolved Atlantic salmon under historical, contemporary, and three future climate warming scenarios.

As has been previously reported, growth in ectotherms follows thermal clines, with higher temperatures causing faster growth and earlier maturation (Angilletta et al., 2004). For the Atlantic salmon, this is ascribed to the combination of temperature and photoperiod (Metcalfe & Thorpe, 1990; Power, 1981, 1986). This study shows that water temperatures in the geographic area encompassing the Burrishoole catchment will shift closer to the optimal growth temperature of ~16°C for Atlantic salmon parr proposed by Elliott and Hurley (1997) under SSP3-RCP7.0 and SSP5-RCP8.5, whereas SSP1-RCP2.6 appears to remain close to contemporary conditions. Moreover, with respect to the two most severe warming scenarios, it shows a lengthening of the growth season by temperature (i.e., the period of time within which temperatures of 7 to 23°C are experienced) is expected, which effectively translates into an increase in growth potential for juvenile Atlantic salmon in the Burrishoole River system over the century.

An increase in growth potential will, if realized, cause increased growth rates, which is here shown as an increase in the length-at-age for juvenile Atlantic salmon in the Burrishoole. This finding is in line with Hedger et al. (2013), Piou and Prévost (2012), Sundt-Hansen et al. (2018), all showing faster growth during freshwater residency. For Atlantic salmon, growth rate will cause changes in life-history traits age- and size-at-smoltification, which will have carry-over effects on marine survival, age- and size-at-reproduction, and reproductive investment (Gregory et al., 2019; Jonsson & Jonsson, 2007; Mobley et al., 2020).

In Atlantic salmon, the decision to smoltify is made in late summer the year prior to spring migration and is based on energetic status and growth rate at that time and the likelihood of reaching a threshold length at the time of migration (Metcalfe, 1998; Thorpe et al., 1998). Our results show that the increase in growth rate caused by temperature will lead to an increase in the proportion of juveniles that satisfy the conditions for smoltification as 1-year-olds and a reduction in the proportion of juveniles that require 3 years to satisfy these conditions. In accordance with the findings of Russell et al. (2012), Piou & Prévost, 2012, Hedger et al., 2013, and Sundt-Hansen et al., 2018, we find a decrease in the age-at-smoltification measured at the population level in response to the temperature increase under SSP3-RCP7.0 and SSP5-RCP8.5, but for SSP1-RCP 2.6 the reversal of the GHG concentrations causes the initial decrease in age-at-smoltification, which is gradually reversed over the century.

Sundt-Hansen et al. (2018) associated this reduction in freshwater residency (implicit from a decrease in age-at-smoltification) with a shortening of the period subject to density-dependent mortality, which would result in an increased smolt abundance. However, ambient temperatures regulate metabolism, and thus resource requirements, and may potentially strengthen density-dependent mortality even if the period in which the density-dependent mortality occurs is shortened. Further, a decrease in age-at-smoltification is likely to entail a reduction in size-at-smoltification due to the migration window usually occurring once every year. Accordingly, when increasing temperatures push a growth rate previously resulting in a 2-year-smoltification trajectory into a 1-year-smoltification trajectory, it results in the loss of an entire year of freshwater growth. Consequently, the faster growth trajectories with a marginal improvement in growth will likely not compensate for this loss of freshwater growth. There will, however, be an increase in length-at-smoltification within smolt age groups as the total growth potential between migration windows increases.

The consequence of a reduction in age- and size-at-smoltification on population vital rates is unclear. Gregory et al. (2019) showed that marine survival, measured from time of smoltification to return as one sea-winter spawner, is positively correlated with body size at the time of smoltification, whereas Jonsson and Jonsson (2007) and Mobley

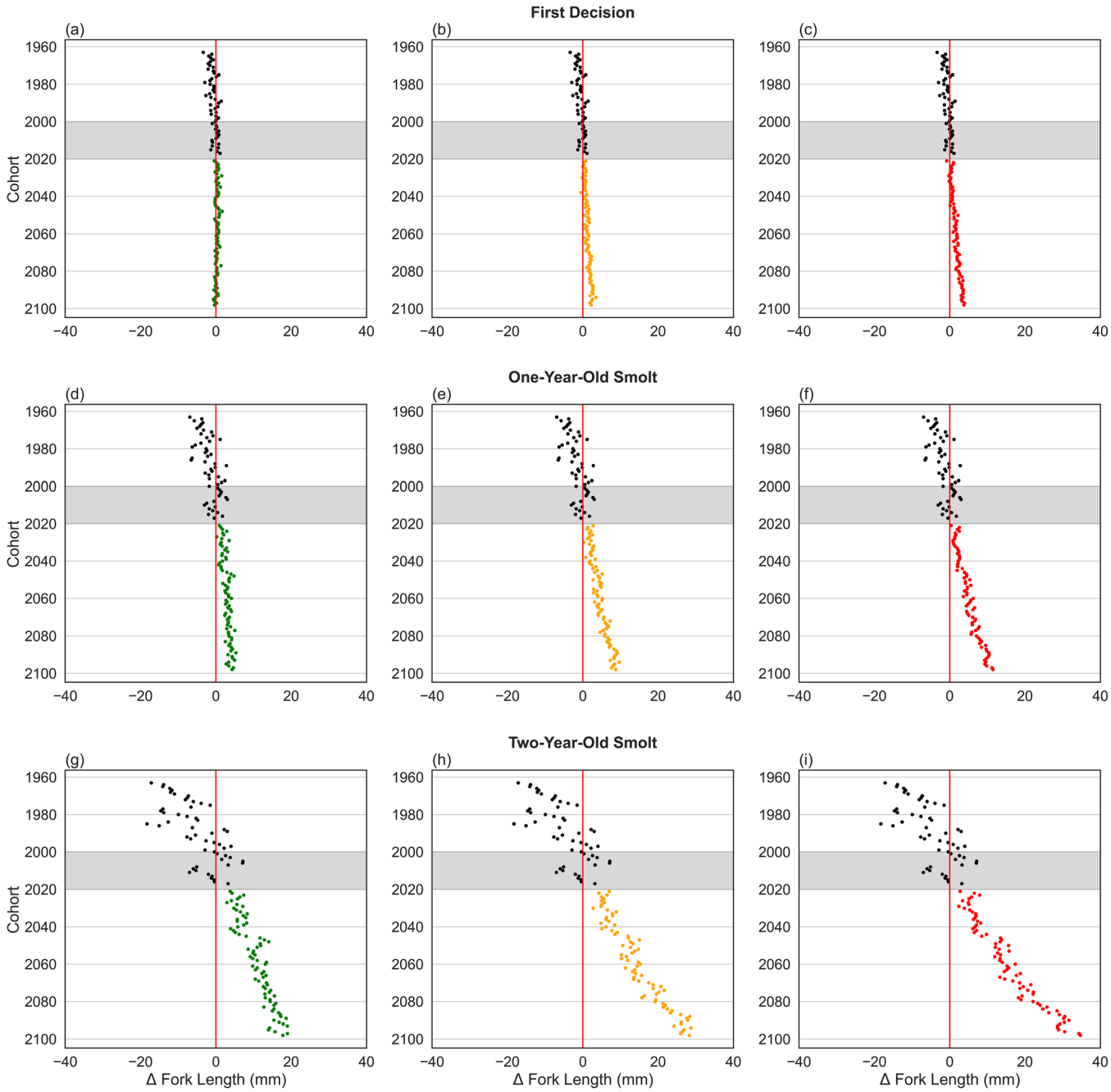

FIGURE 6 Projected change between 1960 and 2100 in length-at-smoltification decision (a, b, and c), length-at-smoltification as 1-year-olds (d, e, and f), and length-at-smoltification as 2-year-olds (g, h, and i) under the three shared socioeconomic pathways and representative concentration pathways: SSP1-RCP2.6 (green), SSP3-RCP7.0 (orange), and SSP5-RCP8.5 (red) for juvenile Atlantic salmon in the Burrishoole. The gray-shaded area represents the historical reference (2000 to 2020), and the red vertical line represents the historical average.

et al. (2020) showed that females migrating at a younger age had a higher propensity to return as multi sea-winter aged spawners (MSW). Jonsson and Jonsson (2007) attributed this increased propensity to return as MSW to an increased growth rate over the first sea-winter, but they also pointed out that the relationship between early marine growth and sea age is likely to be population-specific and might even vary in sign across regions. How this will play out when growth rates increase because of climate change is difficult to predict, as these younger migrants are likely to reach greater body size and therefore lower relative growth rates. If the consequences of temperature increases follow the temperature-size rule and the intraspecific formulation of Bergmann's rule (Angilletta et al., 2004; Ashton, 2004; Blackburn et al., 1999), then a decrease in body size of adult spawners in the Burrishoole is to be expected. Smaller body size in Atlantic salmon, and fish in general, typically corresponds to a disproportional decrease in reproductive output (Barneche et al., 2018). Further, the

TABLE 3 Ordinary least squares regression of change in length (mm) scaled to the 2000–2020 historical reference length at (1) length-at-smoltification decision, (2) length-at-smoltification (1-year-olds), and (3) length-at-smoltification (2-year-olds) under SSP1-RCP2.6, SSP3-RCP7.0, and SSP5-RCP8.5 for juvenile Atlantic salmon in the Burrishoole catchment, Co. Mayo, Ireland.

	Length at decision	Length at smoltification (1-year-old)	Length at smoltification (2-year-old)
SSP1-RCP2.6	65.21*** (4.47)	7.75*** (8.85)	−211.12*** (21.76)
SSP3-RCP7.0	−72.66*** (6.32)	−125.21*** (12.52)	−283.04*** (30.77)
SSP5-RCP8.5	−107.62*** (6.32)	−184.17*** (12.52)	−411.82*** (30.77)
Cohort * SSP1-RCP2.6	−0.01*** (0.00)	0.03*** (0.00)	0.17*** (0.01)
Cohort * SSP3-RCP7.0	0.04*** (0.00)	0.06*** (0.01)	0.14*** (0.01)
Cohort * SSP5-RCP8.5	0.05*** (0.00)	0.09*** (0.01)	0.20*** (0.01)
R^2	0.82	0.88	0.92
R^2 adj.	0.82	0.88	0.92
N (DF)	234 (228)	234 (228)	234 (228)

Note: Standard errors in parentheses. *$p < 0.1$, **$p < 0.05$, ***$p < 0.01$.
Abbreviation: SSP-RCPs, shared socioeconomic pathways and representative concentration pathways.

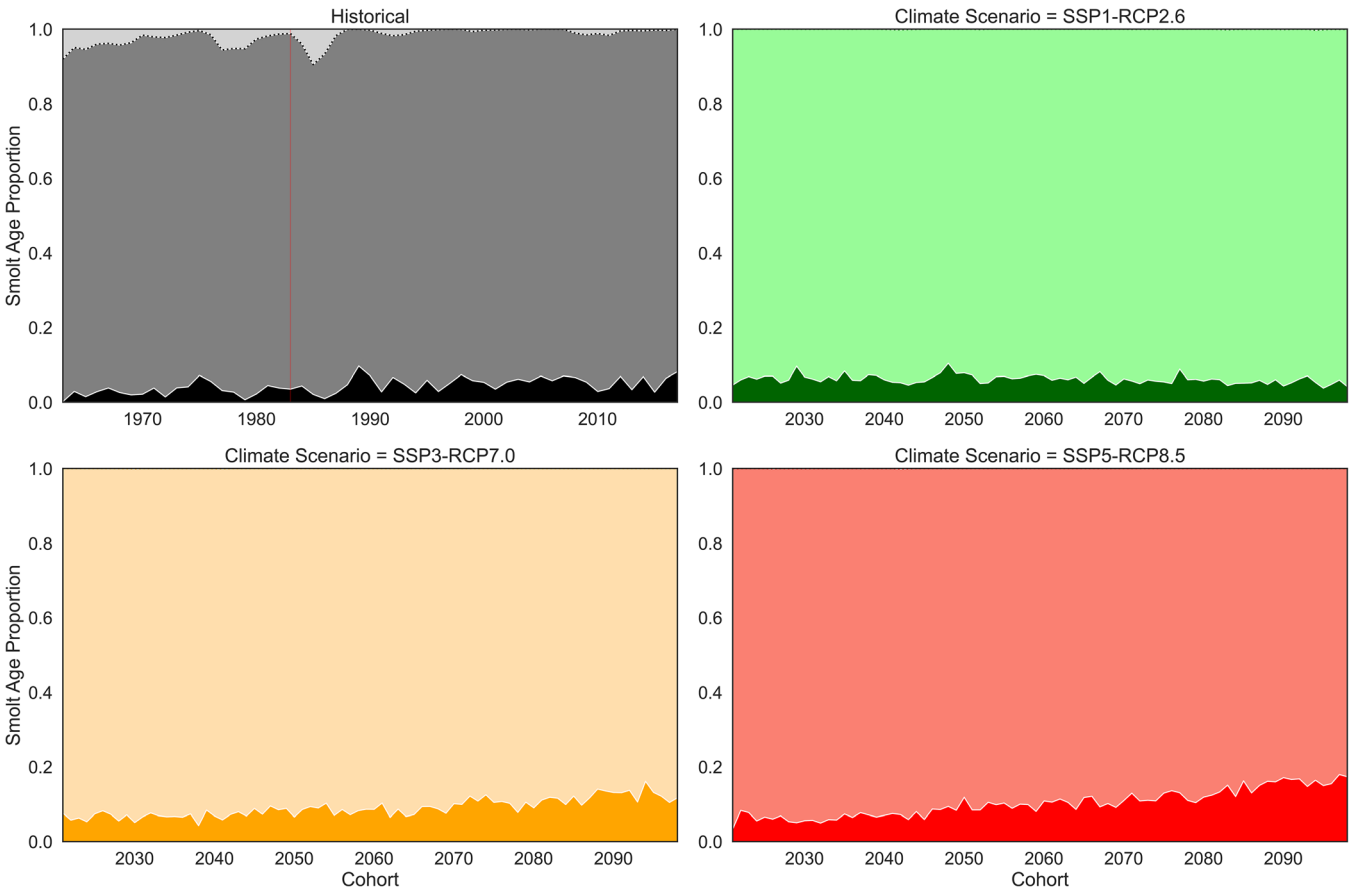

FIGURE 7 Model prediction of the proportion of juvenile Atlantic salmon choosing to smolt as 1-year-olds (full saturation, black = historical, green = SSP1-RCP2.6, orange = SSP3-RCP7.0, and red = SSP5-RCP8.5), 2-year-olds (medium saturation, black = historical, green = SSP1-RCP2.6, orange = SSP3-RCP7.0, and red = SSP5-RCP8.5), and 3-year-olds (low saturation, black = historical, green = SSP1-RCP2.6, orange = SSP3-RCP7.0, and red = SSP5-RCP8.5). The red line is the point of reaction norm calibration to Piggins and Mills (1985).

disappearance of 3-year-old smolts is also a direct loss of life-history diversity, which could then be associated with reductions in population stability (Greene et al., 2010; Schindler et al., 2010).

On the basis of the differing impacts projected under SSP1-RCP2.6, SSP3-RCP7.0, and SSP5-RCP8.5, it is evident that anthropogenic influence on climate will have major implications for the future

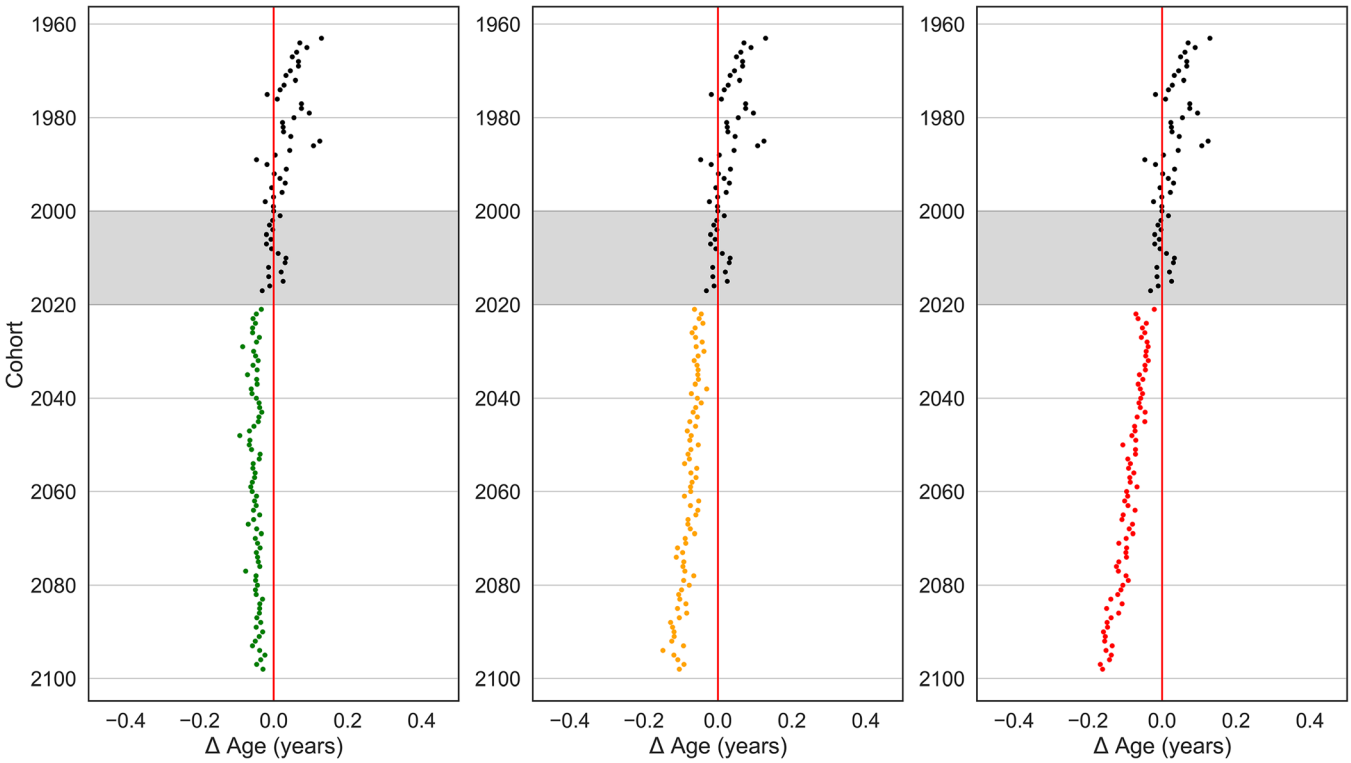

FIGURE 8 Projected change in age-at-smoltification under the three shared socioeconomic pathways and representative concentration pathways: (a) SSP1-RCP2.6 (green), (b) SSP3-RCP7.0 (orange), and (c) SSP5-RCP8.5 (red) for juvenile Atlantic salmon in the Burrishoole. The gray-shaded area represents the historical reference (2000 to 2020), and the red vertical line represents the historical average.

of Atlantic salmon in the Burrishoole. It is possible given the most optimistic response, as described in SSP1-RCP2.6, that climate change impacts on Atlantic salmon may be reversed by the end of the century. In stark contrast, gradually increasing impacts to the Atlantic salmon in the Burrishoole are projected under the SSP3-RCP7.0 and SSP5-RCP8.5 scenarios, potentially leading to reduced marine survival, reduced size- and age-at-reproduction, and reduced reproductive output. However, the prospects under SSP3-RCP7.0 are better than those for SSP5-RCP8.5 as the population is given a better opportunity to adapt to climate change (see Reed, Schindler, Hague, et al., 2011).

In this study, we demonstrated the ability of an LSTM neural network to accurately estimate water temperature from the atmospheric data available from ISIMIP phase 3a. The high accuracy of the neural network on validation data indicates that it is useful for hindcasting and forecasting water temperature in near, mid, and potentially distant time. Therefore, the method is a promising approach to studying effects on climate change on juvenile Atlantic salmon when data availability for systems is poor. However, the LSTM neural network does seem to struggle with extreme temperatures. This could be due to the lack of discharge data, although the issue appears to be common for machine learning models and may be a limitation of the approach (see Feigl et al., 2021). Nevertheless, in line with the findings of Feigl et al. (2021), we found that recurrent neural networks performed better than other machine learning and traditional regression approaches when long-term dependencies are relevant (i.e., temperature-buffering of an upstream lake relative to the temperature monitoring station; see supplementary material S1a).

The study shows that the CGDD, when calculated from water temperature, is an excellent general predictor of length-at-age in juvenile Atlantic salmon. However, several discontinuities in the relationship occur between size-at-age and CGDD at points in time that correspond to life-history stage transitions, notably alevin (i.e., endogenous energy source via the yolk sac) to fry, and potentially parr to smolt (Neuheimer & Taggart, 2007). These discontinuities may entail the need for a more complex model, or combination of several models, when quantifying the relationship between CGDD and length-at-age over the span of several life stages. Nevertheless, in this case, the use of a GLM with a gamma distribution and log-link successfully captured the growth trajectory of the juvenile Atlantic salmon in the Burrishoole catchment. However, we are aware that the underlying mechanisms for life-stage transition are dependent on genetics and growth, which again depends on temperature, photoperiod, productivity, and fish density, and that these interactions may become difficult to predict in future climates.

The first observed discontinuity in the length-at-age CGDD relationship occurred during the alevin-fry life-stage transition (i.e., fish < 38 mm). The transition between alevin and fry life-stage requires energy allocation into development of physical structures required for the ingestion and digestion of exogenous food (Skoglund et al., 2011). The transition is also characterized by a shift in behavior from passively hiding in the interstitial spaces of riverbed substrates to actively

foraging (Einum & Fleming, 2004). This shift from endogenous to exogenous nutrition also involves the start of intraspecific competition and territory establishment, after a period of higher densities sustained by the use of resources acquired by parental fish in the marine environment. Therefore, it is reasonable to assume that the relationship between length-at-age and CGDD may deviate from that found for other life stages. A potential second discontinuity in the relationship between length-at-age and CGDD occurs during the parr-smolt life-stage transition (i.e., apparent from fish ≥ 90 mm) due to the smoltification process. According to Kadri et al. (1996), Kristinsson et al. (1985), Metcalfe (1998), Saunders et al. (1994), and Skilbrei (1988), growth of juvenile Atlantic salmon accelerates when the life-history decision has been made.

The length-at-age CGDD relationship relies on the fact that growth is near-linear in the mid-range of temperatures (Neuheimer & Taggart, 2007). However, like other statistical methods, it does not have any track record under the extreme changes in water temperature that we may experience in the future. This study assumes that the growth response to temperature is close to a bell-shaped curve, and although our projected water temperatures do not exceed the maximum growth temperature, it may still be a shortcoming of the model. Nevertheless, it is possible that the current relationship between length-at-age and CGDD breaks down given larger shifts than observed over the validation period.

This study is limited by our desire for a data-efficient, geographically transferrable, approach using only abiotic and biotic variables available for a large proportion of Atlantic salmon populations across the native range. As datasets become available for modeling other aspects of climate change impacts on juvenile Atlantic salmon, these may be added to this workflow. We are aware that this limits the ability to accurately capture important underlying processes (e.g., evolutionary responses), which determine the overall response of juvenile Atlantic salmon in a climate change context. Although this paper focuses on the plastic response of juvenile Atlantic salmon to warming temperatures, potential evolutionary responses may add further complexity. For example, Debes et al. (2020) showed that there is a heritable genetic component to growth potential that contributes to determining the smoltification reaction norm across different temperatures and productivity regimes (feeding rates). Evolution and plasticity may, therefore, act either in the same direction or in opposite directions, regarding age-at-smoltification depending on whether higher or lower growth potential is selected at higher temperatures. Further work is needed to evaluate these alternatives.

One other aspect that is worth considering is the probability of an individual smolting in the following spring. It has been proposed that this decision is made in late July (Metcalfe, 1998; Metcalfe & Thorpe, 1992) and depends on an individual's phenotypic size and an assessment of its energetic status. Furthermore, Debes et al. (2020) suggest that there is also a genetic component to this decision. Those individuals that postpone smoltification, as an adaptive response to the expected local winter conditions, in the following spring are observed to downregulate metabolism, suspend feeding, and adopt an anorexic state despite adequate food availability (Metcalfe & Thorpe, 1992). Given that there will likely be changes to winter thermal regimes (i.e., warmer winters) in the future, it might be assumed that this contemporary adaptive response to overwintering could change. Although warmer winters might simplistically be presumed to be less harsh, it is more likely that they will be more severe due to heightened energetic demands and insufficient food to sustain higher metabolic demands. This has been shown in several important studies (Bradshaw & Holzapfel, 2006; Humphries et al., 2002; McGinnity et al., 2009). Warmer winter temperatures are therefore likely to select against the torpor strategy in the future as an effective strategy for overwinter survival and thus favor faster-growing individuals and result in an increased pace of life for the population overall.

However, these limitations do not imply that we cannot identify changes to existing large-scale trends, such as the ones driven by temperature. An example of this would be the underestimated length distribution of 1-year-old smolt, as we are unable to quantify growth for fish in the 1-year-smolt trajectory after the smoltification decision. Nevertheless, the growth response only causes a positive shift in the length distribution, and the mechanism remains the same, implying that it captures the large-scale trend. Moreover, the model may not be robust due to the inherent uncertainty tied to extrapolation, and the model chain has only been applied to one study system; the generalizability of the model workflow should be applied to several systems for validation. An improvement to the model workflow may be obtained by re-estimation of Equation (2) from Metcalfe (1998), which is derived from hatchery-reared fish, and does, most likely, overestimate the smoltification probability found in the Burrishoole River system due to differences in growth rates and resource limitations.

In conclusion, this study provides a data-efficient model workflow applicable to ectotherms, in particular aquatic ectotherms, for investigation of their life-history response to historical, contemporary, and future climates. The potential of the model, although simplistic relative to the underlying mechanisms, is shown by its ability to reproduce findings in line with more complex and data-demanding approaches, as well as expectations founded in best available knowledge on the Atlantic salmon. Although the geographical transferability of the model remains untested, the underlying data are commonly found throughout the native range of the Atlantic salmon. This enables the transfer of the model from data-rich to data-poor systems, allowing a range-wide examination of climate impacts on Atlantic salmon. More generally, our modeling work emphasizes how increased growth potential in ectotherms as a result of global warming can filter through the life cycle in complex ways, potentially speeding up the overall pace of life.

AUTHOR CONTRIBUTIONS

Conceptualization: Adrian Rinaldo, Elvira de Eyto, Philip McGinnity, Thomas Reed. Developing methods: Adrian Rinaldo, Elvira de Eyto, Philip McGinnity, Karl Øystein Gjelland. Data analysis: Adrian Rinaldo. Preparation of figures and tables: Adrian Rinaldo. Conducting the research, data interpretation, writing: Adrian Rinaldo, Elvira de Eyto, Philip McGinnity, Thomas Reed, Karl Øystein Gjelland.

ACKNOWLEDGMENTS

This project has received funding from the European Union's Horizon 2020 research and innovation programme under the Marie Skłodowska-Curie grant agreement no. 956623. MSCA-ITN-ETN-European Training Network, inventWater (https://inventwater.eu/). P. M. was supported in part by grants from Science Foundation Ireland (15/IA/3028 and 16/BBSRC/3316) and by grant-in-aid (RESPI/BIO/21/01) from the Marine Institute (Ireland) as part of the Marine Research Programme by the Irish Government. Further, we acknowledge the Inter-Sectoral Impact Model Intercomparison Project (ISIMIP) for their role as provider and coordinator of climate data. The in-situ data collection for this work was carried out by the many staff of the Marine Institute (formerly the Salmon Research Agency and the Salmon Research Trust of Ireland). Their contribution is gratefully acknowledged. Eva Bonsak Thorstad, Joshka Kaufmann, and Ian Jones provided helpful comments throughout this work. Open access funding provided by IReL.

DATA AVAILABILITY STATEMENT

The code, models, and projections used for this article are available at https://github.com/AdrianRinaldo/Size-at-Age-Juvenile-Atlantic-Salmon. The climatological (atmospheric) data are available at https://data.isimip.org/. Fish size data (lengths) from the Burrishoole catchment are openly accessible from https://data.marine.ie/geonetwork/srv/eng/catalog.search#/metadata/ie.marine.data:data.5125.

ORCID

Adrian Rinaldo https://orcid.org/0009-0007-4832-3684

REFERENCES

Abadi, M., Barham, P., Chen, J., Chen, Z., Davis, A., Dean, J., Devin, M., Ghemawat, S., Irving, G., Isard, M., Kudlur, M., Levenberg, J., Monga, R., Moore, S., Murray, D. G., Steiner, B., Tucker, P., Vasudevan, V., Warden, P., … Zheng, X. (2016). TensorFlow: A system for large-scale machine learning. *Proceedings of the 12th USENIX Symposium on Operating Systems Design and Implementation, OSDI 2016*.

Angilletta, M. J., Steury, T. D., & Sears, M. W. (2004). Temperature, growth rate, and body size in ectotherms: Fitting pieces of a life-history puzzle. *Integrative and Comparative Biology*, *44*(6), 498–509. https://doi.org/10.1093/icb/44.6.498

Ashton, K. G. (2004). Sensitivity of intraspecific latitudinal clines of body size for tetrapods to sampling, latitude and body size. *Integrative and Comparative Biology*, *44*(6), 403–412. https://doi.org/10.1093/icb/44.6.403

Atkinson, D. (1994). Temperature and organism size—A biological law for ectotherms? In M. Begon, & A. H. Fitter (Eds.), *Advances in ecological research* (Vol. 25, pp. 1–58). https://doi.org/10.1016/S0065-2504(08)60212-3

Barneche, D. R., Ross Robertson, D., White, C. R., & Marshall, D. J. (2018). Fish reproductive-energy output increases disproportionately with body size. *Science*, *360*, 642–645. https://doi.org/10.1126/science.aao6868

Bennett, J. M., Sunday, J., Calosi, P., Villalobos, F., Martínez, B., Molina-Venegas, R., Araújo, M. B., Algar, A. C., Clusella-Trullas, S., Hawkins, B. A., Keith, S. A., Kühn, I., Rahbek, C., Rodríguez, L., Singer, A., Morales-Castilla, I., & Olalla-Tárraga, M. Á. (2021). The evolution of critical thermal limits of life on earth. *Nature Communications*, *12*(1), 1198. https://doi.org/10.1038/s41467-021-21263-8

Blackburn, T. M., Gaston, K. J., & Loder, N. (1999). Geographic gradients in body size: A clarification of Bergmann's rule. *Diversity and Distributions*, *5*(4), 165–174. https://doi.org/10.1046/j.1472-4642.1999.00046.x

Bradshaw, W. E., & Holzapfel, C. M. (2006). Evolutionary response to rapid climate change. *Science*, *312*(5779), 1477–1478. https://doi.org/10.1126/science.1127000

Chezik, K. A., Lester, N. P., & Venturelli, P. A. (2014). Fish growth and degree-days I: Selecting a base temperature for a within-population study. *Canadian Journal of Fisheries and Aquatic Sciences*, *71*(1), 47–55. https://doi.org/10.1139/cjfas-2013-0295

Chollet, F. (2013). Keras. *Journal of Chemical Information and Modeling*, *53*(9). https://keras.io

Crozier, L. G., Hendry, A. P., Lawson, P. W., Quinn, T. P., Mantua, N. J., Battin, J., Shaw, R. G., & Huey, R. B. (2008). Potential responses to climate change in organisms with complex life histories: Evolution and plasticity in Pacific salmon. *Evolutionary Applications*, *1*(2), 252–270. https://doi.org/10.1111/j.1752-4571.2008.00033.x

de Eyto, E., Kelly, S., Rogan, G., French, A., Cooney, J., Murphy, M., Nixon, P., Hughes, P., Sweeney, D., & McGInnity, P. (2022). Decadal trends in the migration phenology of diadromous fishes native to the Burrishoole catchment, Ireland. *Frontiers in Ecology and Evolution*, *640*, 19. https://doi.org/10.3389/fevo.2022.915854

Debes, P. V., Piavchenko, N., Erkinaro, J., & Primmer, C. R. (2020). Genetic growth potential, rather than phenotypic size, predicts migration phenotype in Atlantic salmon. *Proceedings of the Royal Society B: Biological Sciences*, *287*(1931), 20200867. https://doi.org/10.1098/rspb.2020.0867

Einum, S., & Fleming, I. A. (2004). Does within-population variation in egg size reduce intraspecific competition in Atlantic Salmon, *Salmo salar*? *Functional Ecology*, *18*(1), 110–115. https://doi.org/10.1111/j.1365-2435.2004.00824.x

Elliott, J. M. (1991). Tolerance and resistance to thermal stress in juvenile Atlantic salmon, *Salmo salar*. *Freshwater Biology*, *25*(1), 61–70. https://doi.org/10.1111/j.1365-2427.1991.tb00473.x

Elliott, J. M., & Elliott, J. A. (2010). Temperature requirements of Atlantic salmon *Salmo salar*, brown trout Salmo trutta and Arctic charr Salvelinus alpinus: Predicting the effects of climate change. *Journal of Fish Biology*, *77*(8), 1793–1817. https://doi.org/10.1111/j.1095-8649.2010.02762.x

Elliott, J. M., & Hurley, M. A. (1997). A functional model for maximum growth of Atlantic Salmon parr, *Salmo salar*, from two populations in Northwest England. *Functional Ecology*, *11*(5), 592–603. https://doi.org/10.1046/j.1365-2435.1997.00130.x

Feigl, M., Lebiedzinski, K., Herrnegger, M., & Schulz, K. (2021). Machine-learning methods for stream water temperature prediction. *Hydrology and Earth System Sciences*, *25*(5), 2951–2977. https://doi.org/10.5194/hess-25-2951-2021

Frieler, K., Lange, S., Piontek, F., Reyer, C. P. O., Schewe, J., Warszawski, L., Zhao, F., Chini, L., Denvil, S., Emanuel, K., Geiger, T., Halladay, K., Hurtt, G., Mengel, M., Murakami, D., Ostberg, S., Popp, A., Riva, R., Stevanovic, M., … Yamagata, Y. (2017). Assessing the impacts of 1.5 C global warming – Simulation protocol of the inter-sectoral impact model Intercomparison project (ISIMIP2b). *Geoscientific Model Development*, *10*(12), 4321–4345. https://doi.org/10.5194/gmd-10-4321-2017

Greene, C. M., Hall, J. E., Guilbault, K. R., & Quinn, T. P. (2010). Improved viability of populations with diverse life-history portfolios. *Biology Letters*, *6*(3), 382–386. https://doi.org/10.1098/rsbl.2009.0780

Gregory, S. D., Ibbotson, A. T., Riley, W. D., Nevoux, M., Lauridsen, R. B., Russell, I. C., Britton, J. R., Gillingham, P. K., Simmons, O. M., Rivot, E., & Durif, C. (2019). Atlantic salmon return rate increases with smolt length. *ICES Journal of Marine Science*, *76*(6), 1702–1712. https://doi.org/10.1093/icesjms/fsz066

Hazel, J. R., & Prosser, C. L. (1974). Molecular mechanisms of temperature compensation in poikilotherms. *Physiological Reviews*, *54*(3), 620–677. https://doi.org/10.1152/physrev.1974.54.3.620

Hedger, R. D., Sundt-Hansen, L. E., Forseth, T., Ugedal, O., Diserud, O. H., Kvambekk, Å. S., & Finstad, A. G. (2013). Predicting climate change effects on subarctic-arctic populations of Atlantic salmon (*Salmo salar*). *Canadian Journal of Fisheries and Aquatic Sciences*, *70*(2), 159–168. https://doi.org/10.1139/cjfas-2012-0205

Humphries, M. M., Thomas, D. W., & Speakman, J. R. (2002). Climate-mediated energetic constraints on the distribution of hibernating mammals. *Nature*, *418*(6895), 313–316. https://doi.org/10.1038/nature00828

ICES. (2022). *Working Group on North Atlantic Salmon (WGNAS)*. https://doi.org/10.17895/ices.pub.7923

IPCC. (2022). IPCC, 2022: Summary for policy makers. In *Climate change 2022: Impacts, Adaptation and Vulnerability*. Intergovernmental Panel on Climate Change.

Jensen, A. J., Johnsen, B. O., & Heggberget, T. G. (1991). Initial feeding time of Atlantic salmon, *Salmo salar*, alevins compared to river flow and water temperature in Norwegian streams. *Environmental Biology of Fishes*, *30*(4), 379–385. https://doi.org/10.1007/BF02027981

Jonsson, B., & Jonsson, N. (2009). A review of the likely effects of climate change on anadromous Atlantic salmon *Salmo salar* and brown trout Salmo trutta, with particular reference to water temperature and flow. In. *Journal of Fish Biology*, *75*(10), 2381–2447. https://doi.org/10.1111/j.1095-8649.2009.02380.x

Jonsson, N., & Jonsson, B. (2007). Sea growth, smolt age and age at sexual maturation in Atlantic salmon. *Journal of Fish Biology*, *71*(1), 245–252. https://doi.org/10.1111/j.1095-8649.2007.01488.x

Kadri, S., Mitchell, D. F., Metcalfe, N. B., Huntingford, F. A., & Thorpe, J. E. (1996). Differential patterns of feeding and resource accumulation in maturing and immature Atlantic salmon, *Salmo salar*. *Aquaculture*, *142*(3–4), 245–257. https://doi.org/10.1016/0044-8486(96)01258-6

Klemetsen, A., Amundsen, P. A., Dempson, J. B., Jonsson, B., Jonsson, N., O'Connell, M. F., & Mortensen, E. (2003). Atlantic salmon *Salmo salar* L., brown trout Salmo trutta L. and Arctic charr Salvelinus alpinus (L.): A review of aspects of their life histories. *Wiley online. Library*, *12*(1), 1–59. https://doi.org/10.1034/j.1600-0633.2003.00010.x%4010.1111/%28ISSN%291600-0633.Editors-Choice-2011

Kristinsson, J. B., Saunders, R. L., & Wiggs, A. J. (1985). Growth dynamics during the development of bimodal length-frequency distribution in juvenile Atlantic salmon (*Salmo salar* L.). *Aquaculture*, *45*(1–4), 1–20. https://doi.org/10.1016/0044-8486(85)90254-6

MacCrimmon, H. R., & Gots, B. L. (1979). World distribution of Atlantic Salmon, *Salmo salar*. *Journal of the Fisheries Research Board of Canada*, *36*(4), 422–457. https://doi.org/10.1139/f79-062

Marine Institute. (2020). *Newport research facility, annual report No. 65, 2020*. Marine Institute https://oar.marine.ie/bitstream/handle/10793/1672/Newport%20Annual%20Report%202019.pdf?sequence=1&isAllowed=y.

McGinnity, P., Jennings, E., DeEyto, E., Allott, N., Samuelsson, P., Rogan, G., Whelan, K., & Cross, T. (2009). Impact of naturally spawning captive-bred Atlantic salmon on wild populations: Depressed recruitment and increased risk of climate-mediated extinction. *Proceedings of the Royal Society B: Biological Sciences*, *276*(1673), 3601–3610. https://doi.org/10.1098/rspb.2009.0799

McGinnity, P., Stone, C., Taggart, J. B., Cooke, D., Cotter, D., Hynes, R., McCamley, C., Cross, T., & Ferguson, A. (1997). Genetic impact of escaped farmed Atlantic salmon (*Salmo salar* L.) on native populations: Use of DNA profiling to assess freshwater performance of wild, farmed, and hybrid progeny in a natural river environment. *ICES Journal of Marine Science*, *54*(6), 998–1008. https://doi.org/10.1016/s1054-3139(97)80004-5

Meinshausen, M., Smith, S. J., Calvin, K., Daniel, J. S., Kainuma, M. L. T., Lamarque, J., Matsumoto, K., Montzka, S. A., Raper, S. C. B., Riahi, K., Thomson, A., Velders, G. J. M., & van Vuuren, D. P. P. (2011). The RCP greenhouse gas concentrations and their extensions from 1765 to 2300. *Climatic Change*, *109*(1), 213–241. https://doi.org/10.1007/s10584-011-0156-z

Metcalfe, N. B. (1998). The interaction between behavior and physiology in determining life history patterns in Atlantic salmon (*Salmo salar*). *Canadian Journal of Fisheries and Aquatic Sciences*, *55*(S1), 93–103. https://doi.org/10.1139/cjfas-55-s1-93

Metcalfe, N. B., & Thorpe, J. E. (1990). Determinants of geographical variation in the age of seaward-migrating Salmon, *Salmo salar*. *The Journal of Animal Ecology*, *59*(1), 135. https://doi.org/10.2307/5163

Metcalfe, N. B., & Thorpe, J. E. (1992). Anorexia and defended energy levels in over-wintering juvenile Salmon. *The Journal of Animal Ecology*, *61*(1), 175. https://doi.org/10.2307/5520

Mobley, K. B., Aykanat, T., Czorlich, Y., House, A., Kurko, J., Miettinen, A., Moustakas-Verho, J., Salgado, A., Sinclair-Waters, M., Verta, J. P., & Primmer, C. R. (2021). Maturation in Atlantic salmon (*Salmo salar*, Salmonidae): A synthesis of ecological, genetic, and molecular processes. In. *Reviews in Fish Biology and Fisheries*, *31*(3), 523–571. https://doi.org/10.1007/s11160-021-09656-w

Mobley, K. B., Granroth-Wilding, H., Ellmén, M., Orell, P., Erkinaro, J., & Primmer, C. R. (2020). Time spent in distinct life history stages has sex-specific effects on reproductive fitness in wild Atlantic salmon. *Molecular Ecology*, *29*(6), 1173–1184. https://doi.org/10.1111/mec.15390

Neuheimer, A. B., & Taggart, C. T. (2007). The growing degree-day and fish size-at-age: The overlooked metric. *Canadian Journal of Fisheries and Aquatic Sciences*, *64*(2), 375–385. https://doi.org/10.1139/F07-003

Pedregosa, F., Varoquaux, G., Gramfort, A., Michel, V., Thirion, B., Grisel, O., Blondel, M., Prettenhofer, P., Weiss, R., Dubourg, V., Vanderplas, J., Passos, A., Cournapeau, D., Brucher, M., Perrot, M., & Duchesnay, É. (2011). Scikit-learn: Machine learning in python. *Journal of Machine Learning Research*, *12*, 2825–2830.

Piggins, D. J., & Mills, C. P. R. (1985). Comparative aspects of the biology of naturally produced and hatchery-reared Atlantic salmon smolts (*Salmo salar* L.). *Aquaculture*, *45*(1–4), 321–333. https://doi.org/10.1016/0044-8486(85)90278-9

Piou, C., & Prévost, E. (2012). A demo-genetic individual-based model for Atlantic salmon populations: Model structure, parameterization and sensitivity. *Ecological Modelling*, *231*, 37–52. https://doi.org/10.1016/j.ecolmodel.2012.01.025

Power, G. (1981). Stock characteristics and catches of Atlantic Salmon (*Salmo salar*) in Quebec, and Newfoundland and Labrador in relation to environmental variables. *Canadian Journal of Fisheries and Aquatic Sciences*, *38*(12), 1601–1611. https://doi.org/10.1139/f81-210

Power, G. (1986). Physical influences on age at maturity of Atlantic salmon (*Salmo salar*): A synthesis of ideas and questions. In D. J. Meerburg (Ed.), *Salmonid age at maturity*. *Canadian Special Publication of Fisheries and Aquatic Sciences* (Vol. 89, pp. 97–101).

Radchuk, V., Reed, T., Teplitsky, C., van de Pol, M., Charmantier, A., Hassall, C., Adamík, P., Adriaensen, F., Ahola, M. P., Arcese, P., Miguel Avilés, J., Balbontin, J., Berg, K. S., Borras, A., Burthe, S., Clobert, J., Dehnhard, N., de Lope, F., Dhondt, A. A., … Kramer-Schadt, S. (2019). Adaptive responses of animals to climate change are most likely insufficient. *Nature Communications*, *10*(1), 14. https://doi.org/10.1038/s41467-019-10924-4

Reed, T. E., Schindler, D. E., Hague, M. J., Patterson, D. A., Meir, E., Waples, R. S., & Hinch, S. G. (2011). Time to evolve? Potential evolutionary responses of Fraser river sockeye salmon to climate change and effects on persistence. *PLoS One*, *6*(6), e20380. https://doi.org/10.1371/journal.pone.0020380

Reed, T. E., Schindler, D. E., & Waples, R. S. (2011). Interacting effects of phenotypic plasticity and evolution on population persistence in a changing climate. *Conservation Biology*, *25*(1), 56–63. https://doi.org/10.1111/j.1523-1739.2010.01552.x

Riahi, K., van Vuuren, D. P., Kriegler, E., Edmonds, J., O'Neill, B. C., Fujimori, S., Bauer, N., Calvin, K., Dellink, R., Fricko, O., Lutz, W., Popp, A., Cuaresma, J. C., Kc, S., Leimbach, M., Jiang, L., Kram, T., Rao, S., Emmerling, J., … Tavoni, M. (2017). The shared socioeconomic pathways and their energy, land use, and greenhouse gas emissions

implications: An overview. *Global Environmental Change*, *42*, 153–168. https://doi.org/10.1016/j.gloenvcha.2016.05.009

Russell, I. C., Aprahamian, M. W., Barry, J., Davidson, I. C., Fiske, P., Ibbotson, A. T., Kennedy, R. J., MacLean, J. C., Moore, A., Otero, J., Potter, T., & Todd, C. D. (2012). The influence of the freshwater environment and the biological characteristics of Atlantic salmon smolts on their subsequent marine survival. *ICES Journal of Marine Science*, *69*(9), 1563–1573. https://doi.org/10.1093/icesjms/fsr208

Saunders, R. L., Duston, J., & Benfey, T. J. (1994). Environmental and biological factors affecting growth dynamics in relation to smolting of Atlantic salmon, *Salmo salar* L. *Aquaculture Research*, *25*(1), 9–20. https://doi.org/10.1111/j.1365-2109.1994.tb00662.x

Schindler, D. E., Hilborn, R., Chasco, B., Boatright, C. P., Quinn, T. P., Rogers, L. A., & Webster, M. S. (2010). Population diversity and the portfolio effect in an exploited species. *Nature*, *465*(7298), 609–612. https://doi.org/10.1038/nature09060

Seabold, S., & Perktold, J. (2010). Statsmodels: Econometric and statistical modeling with python. *SciPy*. https://doi.org/10.25080/majora-92bf1922-011

Sears, M. W., & Angilletta, M. J. (2011). Introduction to the symposium: Responses of organisms to climate change: A synthetic approach to the role of thermal adaptation. *Integrative and Comparative Biology*, *51*(5), 662–665. https://doi.org/10.1093/icb/icr113

Skilbrei, O. T. (1988). Growth pattern of pre-smolt Atlantic salmon (*Salmo salar* L.): The percentile increment method (PIM) as a new method to estimate length-dependent growth. *Aquaculture*, *69*(1–2), 129–143. https://doi.org/10.1016/0044-8486(88)90192-5

Skoglund, H., Einum, S., Forseth, T., & Barlaup, B. T. (2011). Phenotypic plasticity in physiological status at emergence from nests as a response to temperature in Atlantic salmon (*Salmo salar*). *Canadian Journal of Fisheries and Aquatic Sciences*, *68*(8), 1470–1479. https://doi.org/10.1139/f2011-056

Sundt-Hansen, L. E., Hedger, R. D., Ugedal, O., Diserud, O. H., Finstad, A. G., Sauterleute, J. F., Tøfte, L., Alfredsen, K., & Forseth, T. (2018). Modelling climate change effects on Atlantic salmon: Implications for mitigation in regulated rivers. *Science of the Total Environment*, *631–632*, 1005–1017. https://doi.org/10.1016/j.scitotenv.2018.03.058

Thorpe, J. E., Mangel, M., Metcalfe, N. B., & Huntingford, F. A. (1998). Modelling the proximate basis of salmonid life-history variation, with application to Atlantic salmon, *Salmo salar* L. *Evolutionary Ecology*, *12*(5), 581–599. https://doi.org/10.1023/A:1022351814644

Thorstad, E. B., Bliss, D., Breau, C., Damon-Randall, K., Sundt-Hansen, L. E., Hatfield, E. M. C., Horsburgh, G., Hansen, H., Maoiléidigh, N., Sheehan, T., & Sutton, S. G. (2021). Atlantic salmon in a rapidly changing environment—Facing the challenges of reduced marine survival and climate change. *Aquatic Conservation: Marine and Freshwater Ecosystems*, *31*(9), 2654–2665. https://doi.org/10.1002/aqc.3624

Thorstad, E. B., Whoriskey, F., Rikardsen, A. H., & Aarestrup, K. (2011). Aquatic nomads: The life and migrations of the Atlantic Salmon. In *Atlantic Salmon ecology*. Blackwell Publishing Ltd. https://doi.org/10.1002/9781444327755.ch1

Van Der Have, T. M., & De Jong, G. (1996). Adult size in ectotherms: Temperature effects on growth and differentiation. *Journal of Theoretical Biology*, *183*(3), 329–340. https://doi.org/10.1006/jtbi.1996.0224

van Rossum, G., & Drake, F. L. (2010). The Python Library Reference. *October*.

Venturelli, P. A., Lester, N. P., Marshall, T. R., & Shuter, B. J. (2010). Consistent patterns of maturity and density-dependent growth among populations of walleye (Sander vitreus): Application of the growing degree-day metric. *Canadian Journal of Fisheries and Aquatic Sciences*, *67*(7), 1057–1067. https://doi.org/10.1139/F10-041

Woodward, G., Perkins, D. M., & Brown, L. E. (2010). Climate change and freshwater ecosystems: Impacts across multiple levels of organization. *Philosophical Transactions of the Royal Society B: Biological Sciences*, *365*(1549), 2093–2106. https://doi.org/10.1098/rstb.2010.0055

SUPPORTING INFORMATION

Additional supporting information can be found online in the Supporting Information section at the end of this article.

How to cite this article: Rinaldo, A., de Eyto, E., Reed, T., Gjelland, K. Ø., & McGinnity, P. (2024). Global warming is projected to lead to increased freshwater growth potential and changes in pace of life in Atlantic salmon *Salmo salar*. *Journal of Fish Biology*, *104*(3), 647–661. https://doi.org/10.1111/jfb.15603

ARTICLES FOR FACULTY MEMBERS

GLOBAL WARMING EFFECTS ON ECTOTHERM SPECIES

Title/Author	**Predicting the fundamental thermal niche of ectotherms / Simon, M. W., & Amarasekare, P.**
Source	***Ecology*** **Volume 105, Issue 5 (2024) e4289 Pages 1-18** **https://doi.org/10.1002/ecy.4289** **(Database: Wiley Online Library)**

Received: 13 August 2023 | Revised: 4 December 2023 | Accepted: 1 February 2024

DOI: 10.1002/ecy.4289

ARTICLE

ECOLOGY
ECOLOGICAL SOCIETY OF AMERICA

Predicting the fundamental thermal niche of ectotherms

Margaret W. Simon | **Priyanga Amarasekare**

Department of Ecology and Evolutionary Biology, University of California, Los Angeles, California, Los Angeles, USA

Correspondence
Margaret W. Simon
Email: mwsimon@ku.edu

Present address
Margaret W. Simon, Department of Ecology and Evolutionary Biology, University of Kansas, Lawrence, Kansas, USA.

Funding information
National Institute of General Medical Sciences, Grant/Award Number: T32GM008185; National Science Foundation, Grant/Award Numbers: DDIG DEB-1502071, DEB-1949796

Handling Editor: Kathryn L. Cottingham

Abstract

Climate warming is predicted to increase mean temperatures and thermal extremes on a global scale. Because their body temperature depends on the environmental temperature, ectotherms bear the full brunt of climate warming. Predicting the impact of climate warming on ectotherm diversity and distributions requires a framework that can translate temperature effects on ectotherm life-history traits into population- and community-level outcomes. Here we present a mechanistic theoretical framework that can predict the fundamental thermal niche and climate envelope of ectotherm species based on how temperature affects the underlying life-history traits. The advantage of this framework is twofold. First, it can translate temperature effects on the phenotypic traits of individual organisms to population-level patterns observed in nature. Second, it can predict thermal niches and climate envelopes based solely on trait response data and, hence, completely independently of any population-level information. We find that the temperature at which the intrinsic growth rate is maximized exceeds the temperature at which abundance is maximized under density-dependent growth. As a result, the temperature at which a species will increase the fastest when rare is lower than the temperature at which it will recover from a perturbation the fastest when abundant. We test model predictions using data from a naturalized–invasive interaction to identify the temperatures at which the invasive can most easily invade the naturalized's habitat and the naturalized is most likely to resist the invasive. The framework is sufficiently mechanistic to yield reliable predictions for individual species and sufficiently broad to apply across a range of ectothermic taxa. This ability to predict the thermal niche before a species encounters a new thermal environment is essential to mitigating some of the major effects of climate change on ectotherm populations around the globe.

KEYWORDS
climate envelope, conditions for population viability, delay differential equation population model, density-independent abundance, temperature response of abundance, temperature response of life-history traits

INTRODUCTION

Climate change is predicted to increase global temperatures and generate more extreme temperature fluctuations (IPCC, 2018; Sherwood et al., 2020). There is increasing evidence that warming facilitates the invasion success of exotic species (Dukes & Mooney, 1999; Sorte et al., 2013; Stachowicz et al., 2002), predisposes native biota to extinction (Parmesan, 2006; Pereira et al., 2010; Root et al., 2003; Walther et al., 2002, 2009), and increases outbreaks of pests and pathogens (Bebber et al., 2013; Harvey et al., 2020; Lehmann et al., 2020). Ameliorating the joint effects of climate warming and invasive species is one of the major environmental challenges of this century (Hellmann et al., 2008; Sala et al., 2000).

The vast majority of biodiversity on the planet consists of ectotherms, species that cannot physiologically regulate their body temperature (e.g., microbes, invertebrates, fish, amphibians and reptiles). Nearly all pests and pathogens are also ectotherms. Temperature variation directly affects the physiology, behavior, and population dynamics of such species. Ectotherm life-history traits (e.g., fecundity, development, survivorship) exhibit responses to temperature variation that are plastic, that is, when the temperature changes the response changes accordingly (Figure 1a–d). Population- and community-level responses to climate change—shifting of species' ranges, competitive displacement of native species by invasive species, emergence of new pathogens—ultimately arise from these plastic responses that occur at the level of individual organisms. For example, thermal plasticity in ectotherm development rates allow for population-level phenological changes such as earlier or later emergence (CaraDonna et al., 2014; Forrest, 2016; Miller-Rushing et al., 2010; Post et al., 2018; Scranton & Amarasekare, 2017; Vitasse et al., 2022). It is these individual-level responses on which we need to focus if we are to predict the impact of warming on biodiversity and invasive species. The challenge is to determine how these individual-level responses translate into population- and community-level patterns.

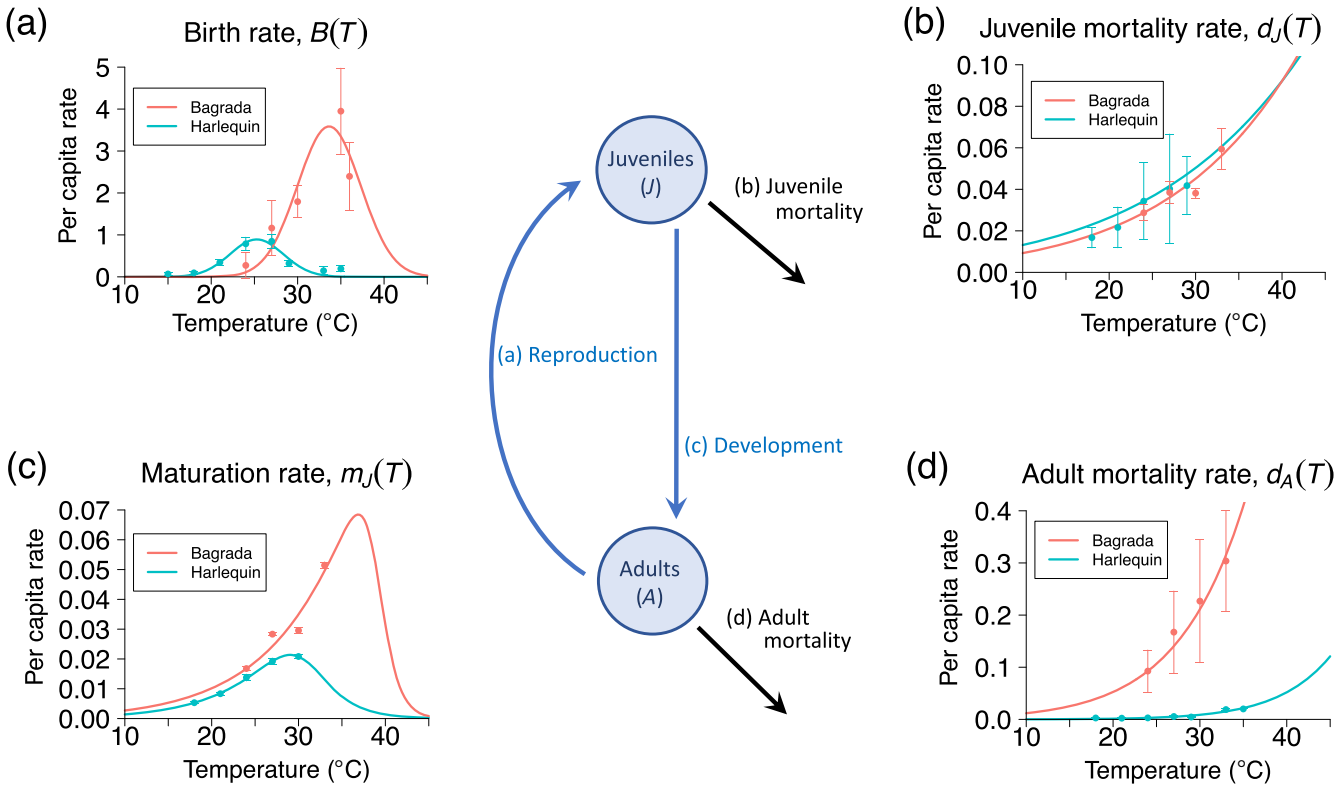

FIGURE 1 Conceptual diagram of typical ectotherm life cycle and temperature responses of life-history traits for bagrada (red curves) and harlequin bug (blue curves) in absence of density dependence (representing Equations 1–4). Juveniles develop into adults over a temperature-dependent duration (T) $\left(\tau(T) = \frac{1}{m_J(T)}\right)$, and adults produce new juveniles at birth rate $B(T)$. Mortality, $d_J(T)$, $d_A(T)$, can occur at either stage. Panels (a)–(d) depict, respectively, the temperature responses of birth, juvenile mortality, maturation, and adult mortality rates in units per day. Solid circles with error bars depict observed trait responses, and curves depict temperature responses predicted using parameterized response functions (Equations 10–12, Table 1). Density dependence can alter these rates in a fashion that is monotonically increasing or unimodal in response to temperature (Appendix S1: Figure S1).

The metric that makes this translation possible is the fundamental thermal niche, the range of temperatures over which a species can maintain a positive intrinsic growth rate. The typical approach is to use observed abundances across space to quantify a species' thermal niche, for example, by using maximum entropy approaches to relate species observations and the temperatures for which such observations occurred (Buckley et al., 2010). However, this has the drawback that the observed pattern is the result of both abiotic and biotic factors and, hence, represents a species' realized thermal niche, not the fundamental niche. A species might be abundant at a particular location simply because it is released from competitors or natural enemies and not because the temperature is optimal for population growth. Making reliable predictions of warming effects on population viability and species' distributions requires an alternative approach.

Here we present a mechanistic theoretical framework that allows us to predict a species' fundamental thermal niche based solely on how temperature affects the species' life-history traits, completely independently of any population-level information. We build on recent theory that predicts temperature effects on ectotherm fitness and population dynamics (Amarasekare & Coutinho, 2013, 2014; Amarasekare & Savage, 2012). We take advantage of large-scale data analyses showing that the qualitative nature (e.g., left-skewed, Gaussian) of trait responses to temperature (i.e., thermal reaction norms) is conserved across ectotherm taxa and that their parameter values are thermodynamically constrained to fall within a narrow range (Amarasekare & Savage, 2012; Brown et al., 2004; Dell et al., 2011; Englund et al., 2011; Gillooly et al., 2001, 2002; Savage et al., 2004). This allows us to build a general framework that applies broadly across ectotherm taxa, habitats, and latitudes.

Our framework incorporates temperature responses of ectotherm life-history traits into a stage-structured population model that realistically captures the complex life cycles of multicellular ectotherms (Figure 1). We use the model to derive a relationship between a species' temperature-dependent intrinsic growth rate and its abundance in the absence of population regulation. We also predict long-term abundance when population regulation is itself temperature-dependent. Since the trait-based framework allows us to calculate the intrinsic growth rate, long-term abundance, and the recovery time (time for a population to return to steady state following a disturbance in population dynamics) at any biologically relevant temperature, we can determine the temperature for which a species will (1) increase when rare at the fastest rate, (2) exhibit the greatest long-term abundance under resource limitation, and (3) recover from a perturbation to the steady state most quickly. Together, these metrics enhance predictive understanding of the response of native species under warming as well as potential outcomes (establishment or extinction) of species introductions into novel thermal environments. We apply these concepts to investigate the interaction between a naturalized insect species in the California coastal sage scrub and an exotic species that has recently invaded this habitat.

CONCEPTUAL FRAMEWORK

In the absence of density-dependent (DD) factors, a population will grow at its intrinsic growth rate, r. When $r > 0$, the population can increase from initially small numbers. We can define the fundamental niche as the range of abiotic conditions over which a species can maintain a positive intrinsic growth rate (Holt, 2009).

This characterization of the fundamental niche is straightforward in principle but difficult to estimate in practice. The prevailing approach is to measure abundance data in the field and calculate the intrinsic growth rate as the average rate of change in population size between consecutive sampling periods having similar abiotic conditions. However, abundance observed in the field is the outcome of both abiotic conditions and biotic interactions. A species may be absent from a given location simply because it has been excluded by a competitor, overexploited by a predator, or has not yet arrived there due to dispersal limitation. Thus, calculation of the intrinsic growth rate in the field using abundance data could unknowingly incorporate, for example, ongoing biotic interactions that impose DD feedbacks on the per-capita growth rate. We need a way to relate the intrinsic growth rate to abundance so that we can predict the range of temperatures over which a species attains nonzero abundance in the absence of competitors, natural enemies, and dispersal limitation.

We make this connection by developing a population model that incorporates the (1) stage-structured life cycle characteristic of all multicellular ectotherms and (2) mechanistic descriptions of life-history trait responses to temperature (Figure 1). We consider an ectotherm species whose life cycle consists of a nonreproductive juvenile stage (e.g., eggs, larvae, nymphs) and a reproductive adult stage. The juvenile stage transitions to the adult stage through the process of development, which involves both maturation and mortality. Maturation from juvenile to adult introduces a time delay between when the current adult population reproduces and when the resulting offspring become adults. Since some juveniles die during maturation, not all reproductive events lead to a new

adult. A biologically realistic model for ectotherm population dynamics requires incorporating both the developmental delay and mortality during maturation. We do this using delay differential equations (DDEs), which provide the analytical means of incorporating delays and their temperature dependence into a stage-structured population model. We use the DDE framework to derive necessary and sufficient conditions for population viability.

Necessary condition for viability

The necessary condition for viability is that a species be able to increase from initially small numbers, that is, its intrinsic growth rate should be positive (Chesson, 2000). We use a stage-structured model with density-independent (DI) population dynamics to derive the temperature response of the intrinsic growth rate:

$$\begin{aligned} \frac{dJ(t)}{dt} &= b[T(t)]A(t) - M_J(t) - d_J[T(t)]J(t) \\ \frac{dA(t)}{dt} &= M_J(t) - d_A[T(t)]A(t) \end{aligned}, \tag{1}$$

where J and A depict juvenile and adult abundances, and the functions $b[T(t)]$ and $d_X[T(t)]$ describe the temperature-dependent birth and mortality rates ($X = J, A$). Note that the temperature upon which these functions depend, $T(t)$, is itself a function of time. The function $M_J(t)$ depicts the total maturation rate of juveniles into adults and is given by

$$M_J(t) = b[T(t-\tau(t))]A(t-\tau(t))\frac{m_J[T(t)]}{m_J[T(t-\tau(t))]}S_J(t). \tag{2}$$

Juveniles maturing into adults at any given time t are those born at time $t-\tau(t)$ via adult reproduction at that time, where $\tau(t)$ is the length of the maturation period. The birth rate at time $t-\tau(t)$ is given by $b[T(t-\tau(t))]A(t-\tau(t))$. Not all births are successful, however, since some juveniles die during maturation at the DI rate $d_J[T(t)]$. Hence, the fraction of individuals surviving through the juvenile stage is $S_J(t) = e^{-d_J[T(t)]\tau(t)}$. The ratio $\frac{m_J[T(t)]}{m_J[T(t-\tau(t))]}$ depicts the temperature dependence of the per-capita maturation rate $m_J[T(t)]$ (see details below).

When temperature varies over time (e.g., due to diurnal and/or seasonal variation), all life-history traits become functions of time. This time dependence necessitates two additional equations to describe through-stage survivorship $S_J(t)$ and developmental delay $\tau(t)$ (Murdoch et al., 2003; Nisbet, 1997; Nisbet & Gurney, 1983).

When the developmental delay varies over time, we can assign each juvenile a maturation index M_{index} to describe its progression through the juvenile stage. Maturation to the adult stage occurs when $M_{\text{index}} = 1$ (Nisbet, 1997; Nisbet & Gurney, 1983). If $m_J(t)$ is the per-capita maturation rate, which varies with time in response to temperature variation, and $\tau(t)$ is the time spent in the juvenile stage by an individual maturing at time t, then $\int_{t-\tau(t)}^{t} m_J[T(t)]dx = 1$. By differentiating the integral and rearranging terms (Nisbet, 1997; Nisbet & Gurney, 1983), we obtain the following DDE for the developmental delay:

$$\frac{d\tau(t)}{dt} = 1 - \frac{m_J[T(t)]}{m_J[T(t-\tau(t))]}. \tag{3}$$

The ratio $\frac{m_J[T(t)]}{m_J[T(t-\tau(t))]}$ determines how temperature affects maturation. If temperature increases over the juvenile stage duration, the ratio exceeds one, stage duration is shorter, and more individuals survive through the stage; if temperature decreases over the stage duration, the ratio is less than one, stage duration is longer, and fewer individuals survive through the stage.

To describe the time variation in through-stage survivorship, $S_J(t)$, in response to temperature variation, we again replace the integral $S_J(t) = e^{-\int_{t-\tau(t)}^{t} S[T(t)]dx}$ with its time derivative to obtain a DDE (Nisbet, 1997; Nisbet & Gurney, 1983):

$$\frac{dS_J(t)}{dt} = S_J(t)\left[\frac{m_J[T(t)]\, d_J[T(t-\tau(t))]}{m_J[T(t-\tau(t))]} - d_J[T(t)]\right]. \tag{4}$$

In the absence of density dependence, the long-term growth rate of a population is its intrinsic growth rate. For stage-structured populations, the intrinsic growth rate is given by the dominant eigenvalue of the Jacobian matrix for the system of equations depicting population dynamics. For the stage-structured model given by Equation (1), the temperature-dependent intrinsic growth rate in a constant thermal environment, that is, $T(t) = T$, is given by

$$r(T) = -d_A(T) + \frac{1}{\tau(T)} W\left[b(T)\tau(T)e^{\tau(T)(d_A(T) - d_J(T))}\right], \tag{5}$$

where W is the positive branch of the Lambert W function (Corless et al., 1996). The detailed derivation is given in Amarasekare and Coutinho (2013).

Importantly, Equation (5) allows us to derive the key properties of the fundamental thermal niche. The lower ($T_{\min}$) and upper ($T_{\max}$) temperature limits at which $r(T) = 0$ constitute the lower and upper limits beyond

which the population goes extinct. The temperature at which $r(T)$ is maximized (T_{opt_r}) is the temperature at which the species increases most quickly from low abundance.

Sufficient condition for viability

The sufficient condition for viability is that the population be able to achieve a long-term (steady-state) abundance that is stable to perturbations. This requires population regulation via a DD feedback mechanism such as self-limitation (intraspecific competition).

Temperature dependence of self-limitation

There are two hypotheses regarding the temperature dependence of self-limitation. The first is based on temperature effects on activity levels. Because increasing activity levels increase the per individual demand for resources, and, assuming the resource supply remains approximately constant with temperature (Bernhardt et al., 2018; Savage et al., 2004), this hypothesis predicts that competition strength (quantified as per-capita competitive effect) should increase monotonically with increasing temperature according to the Boltzmann-Arrhenius relationship:

$$q(T) = q_{TR} e^{A_q\left(\frac{1}{T_R} - \frac{1}{T}\right)}, \tag{6}$$

where $q(T)$ is the self-limitation strength at temperature T, A_q is the Arrhenius constant, T_R is the reference temperature as described earlier, and q_{TR} is the self-limitation strength at the reference temperature (Appendix S1: Figure S1, red curve). Note that when T changes over time, as in Equations (1)–(4), the strength of self-limitation is also time dependent, given by $q[T(t)]$.

The second hypothesis predicts that self-limitation should be strongest at temperatures optimal for reproduction because the demand for resources is likely to be most intense during periods of peak reproductive activity (Gao et al., 2013; Johnson et al., 2016). Now $q(T)$ is unimodal and given by

$$q(T) = q_{T\mathrm{opt}} e^{-\frac{\left(T - T_{\mathrm{opt_q}}\right)^2}{2s_q^2}}, \tag{7}$$

where the strongest self-limitation ($q_{T_{\mathrm{opt}}}$) occurs at temperature $T_{\mathrm{opt_q}}$, and s_q depicts the temperature range over which self-limitation operates (Appendix S1: Figure S1, black curve).

Temperature-dependent population model with density dependence

Given these hypotheses, we can use a DD version of the DDE model given by Equations (1)–(4) to derive the sufficient condition for viability:

$$\begin{aligned}
\frac{dJ(t)}{dt} &= B[T(t),A(t)]A(t) - M_J(t) - D_J[T(t),J(t)]J(t)\\
\frac{dA(t)}{dt} &= M_J(t) - D_A[T(t),A(t)]A(t)\\
M_J(t) &= B[T(t-\tau(t)),A(t-\tau(t))]\\
&\quad \times A(t-\tau(t))\frac{m_J[T(t)]}{m_J[T(t-\tau(t))]}S_J(t)\\
\frac{dS_J(t)}{dt} &= S_J(t)\left[\frac{m_J[T(t)]D_J[T(t-\tau(t)),J(t-\tau(t))]}{m_J[T(t-\tau(t))]}\right.\\
&\quad \left. - D_J[T(t),J(t)]\right]\\
\frac{d\tau(t)}{dt} &= 1 - \frac{m_J[T(t)]}{m_J[T(t-\tau(t))]},
\end{aligned} \tag{8}$$

where the terms and notation are the same as in the DI model, except that birth and mortality rates are now DD. The functions $B[T(t), A(t)]$ and $D_X[T(t), X(t)]$, $(X = J,A)$, describe the joint effects of temperature $T(t)$ and density on per-capita birth and mortality rates. We depict DD birth and death rates using functions that empirical data show to be the most commonly observed density responses (Murdoch et al., 2003), that is, $B[T(t), A(t)] = b[T(t)]\, e^{-q_b[T(t)]\,A(t)}$ and $D_X[T(t), X(t)] = d_X[T(t)]\left(1 + q_{d_X}[T(t)]\,X(t)\right)$, where $q_Y[T(t)]$ is the temperature-dependent per-capita competition coefficient for trait Y ($Y = b,d$, corresponding to birth or death rate).

Because we are interested in applying the model to a Hemipteran insect system in which juvenile mortality is low and densities are highest at the adult stage, we focus our analyses on intraspecific density dependence operating on birth and adult mortality rates. However, the model is general and can be applied to any system in which density dependence occurs at either juvenile or adult stages.

Time to recover following a perturbation to steady-state abundance

We can solve the dynamical model (Equation 8) to obtain analytical expressions for steady-state abundance in a constant thermal environment (Appendix S1). In nature,

populations are frequently perturbed from steady states by variation in the biotic and abiotic environment. It is therefore informative to also quantify how quickly a population might return to steady state following a perturbation. By computing the dominant eigenvalue of the Jacobian matrix of Equation (8), we can also obtain an analytical expression for the recovery time following a perturbation to the steady state:

$$t_{\text{recovery}}(T) = \frac{-\lambda(T)}{|\lambda(T)|} \cdot \frac{1}{|\lambda(T)|}, \tag{9}$$

where $\lambda(T)$ is the dominant eigenvalue and $|\lambda(T)|$ the absolute value of $\lambda(T)$ (or its modulus when $\lambda(T)$ is complex). Because a stable equilibrium occurs when the dominant eigenvalue has negative real parts, the negative sign in the numerator guarantees a positive recovery time when the equilibrium is stable. Analytical expressions for $\lambda(T)$ under DD birth and mortality rates are given in Appendix S1 (Equations S3 and S5).

By incorporating mechanistic descriptions of life-history trait responses to temperature into the steady-state solutions, we can derive an analytical expression for the climate envelope, the range of temperatures over which an ectotherm species can maintain a viable long-term population under DD population regulation. By doing the same for the recovery time, we can get a trait-based prediction of how long it would take an ectotherm population to recover from a perturbation. The novelty of our approach is that it allows us to make predictions about temperature effects on long-term abundance and recovery from perturbations based solely on trait response data, completely independently of any population-level information.

We compare the climate envelope obtained using Equation (8) with the fundamental thermal niche derived using Equation (5) to determine whether the temperature at which long-term abundance is maximized under population regulation is higher or lower than the temperature at which the intrinsic growth rate is maximized (which occurs in the absence of population regulation; see *Hypotheses and predictions* below). Making this comparison requires that we first elucidate the temperature responses of the underlying life-history traits. We do this next.

TEMPERATURE DEPENDENCE OF LIFE HISTORY

Phenotypic-level temperature responses of ectotherm life-history traits (per-capita birth, maturation, and mortality rates) are the result of temperature effects on the underlying biochemical processes (e.g., reaction kinetics and enzyme inactivation, hormonal regulation Johnson & Lewin, 1946; Kingsolver, 2009; Kingsolver et al., 2011; Nijhout, 1994; Ratkowsky et al., 2005; Schoolfield et al., 1981; Sharpe & DeMichele, 1977; van der Have, 2002; van der Have & de Jong, 1996). Temperature effects on rate-controlled processes such as reaction kinetics and enzyme inactivation yield phenotypic-level trait responses that are left-skewed or monotonically increasing/decreasing (Gillooly et al., 2001, 2002; Savage et al., 2004; van der Have, 2002; van der Have & de Jong, 1996). Mortality and maturation rates exhibit such responses (Amarasekare & Savage, 2012; Scranton & Amarasekare, 2017; Uszko et al., 2017). Temperature effects on regulatory processes such as neural and hormonal regulation (Hochachka & Somero, 2002; Long & Fee, 2008; Nijhout, 1994) yield symmetrically unimodal (e.g., Gaussian) trait responses at the phenotypic level. This is because regulatory processes are driven by negative feedbacks that push increasing and decreasing rate processes toward intermediate optima. Birth and attack rates exhibit such responses (Amarasekare & Savage, 2012; Englund et al., 2011; Scranton & Amarasekare, 2017; Uszko et al., 2017).

Temperature response of mortality rate

The per-capita mortality rate of all ectotherms increases monotonically with temperature above the low temperature threshold for viability (see references in Gillooly et al., 2002; Savage et al., 2004). This response is well described by the Boltzmann-Arrhenius function for reaction kinetics (Gillooly et al., 2002; Savage et al., 2004; van der Have & de Jong, 1996; as in Figure 1b,d):

$$d_X(T) = d_{X_{T_R}} e^{A_{d_X}\left(\frac{1}{T_R} - \frac{1}{T}\right)}, \tag{10}$$

where $d_X(T)\,(X = J, A)$ is the mortality rate at temperature T (in degrees Kelvin); A_{d_X} is the Arrhenius constant, which quantifies how fast the mortality rate increases with increasing temperature; and T_R is a reference (baseline) temperature at which mortality is equal to $d_{X_{T_R}}$. The reference temperature occurs within the range where enzymes are 100% active. This is typically between 20 and 30°C, with 24–25°C being the most common (Johnson & Lewin, 1946; Ratkowsky et al., 2005; Schoolfield et al., 1981; Sharpe & DeMichele, 1977). As with the temperature response of self-limitation (Equations 6 and 7), if temperature T changes in time, then so does the mortality rate: $d_X(T(t))$. This similarly holds for the birth and maturation rates explained below.

Temperature response of birth rate

A large number of studies spanning a range of ectothermic taxa show that the per-capita birth rate exhibits a unimodal response to temperature (Amarasekare, 2015; Amarasekare & Savage, 2012; Carriere & Boivin, 1997; Dannon et al., 2010; Dell et al., 2011; Dreyer & Baumgärtner, 1996; Englund et al., 2011; Hou & Weng, 2010; Jandricic et al., 2010; Morgan et al., 2001), which is well-described by a Gaussian function (as in Figure 1a):

$$b(T) = b_{T_{\text{opt}}} e^{-\frac{\left(T - T_{\text{opt}_b}\right)^2}{2 s_b^2}}, \tag{11}$$

where T_{opt_b} is the temperature at which the birth rate is maximal ($b_{T_{\text{opt}}}$), and s_b determines how quickly or slowly the response decays from the optimum. The latter provides a statistically quantifiable index of the response breadth (i.e., the temperature range over which the species can reproduce).

Temperature response of maturation rate

The maturation rate of ectotherms exhibits a left-skewed temperature response (Kingsolver, 2009; Kingsolver et al., 2011; Schoolfield et al., 1981; Sharpe & DeMichele, 1977; van der Have, 2002; van der Have & de Jong, 1996) that results from the reduction in reaction rates at low and high temperature extremes due to enzyme inactivation. This response is well described by a thermodynamic rate process model (Ratkowsky et al., 2005; Schoolfield et al., 1981; Sharpe & DeMichele, 1977; as in Figure 1c):

$$m_J(T) = \frac{\frac{T}{T_R} m_{TR} e^{A_m\left(\frac{1}{T_R} - \frac{1}{T}\right)}}{1 + e^{A_L\left(\frac{1}{T_{L/2}} - \frac{1}{T}\right)} + e^{A_H\left(\frac{1}{T_{H/2}} - \frac{1}{T}\right)}}, \tag{12}$$

where $m_J(T)$ is the maturation rate at temperature T (in degrees Kelvin); m_{TR} is the maturation rate at the reference temperature T_R at which the enzyme is 100% active; A_m, the enthalpy of activation divided by the universal gas constant R, quantifies temperature sensitivity; $T_{\text{L}/2}$ and $T_{\text{H}/2}$ are, respectively, the low and high temperatures at which the enzyme is 50% active; and A_{L} and A_{H} are the enthalpy changes associated with low- and high-temperature enzyme inactivation divided by R (Johnson & Lewin, 1946; Ratkowsky et al., 2005; Schoolfield et al., 1981; Sharpe & DeMichele, 1977; van der Have, 2002; van der Have & de Jong, 1996). When insufficient data exist to parameterize the full maturation function, alternative forms can be used. For example, when there are not enough data to fit the lower temperature limit of maturation, a form such as $m_{\text{alt}}(T)$, given in the note section of Table 1, can be used. If there is insufficient data at both the high and low ends of the maturation function, but maturation is expected to increase across the full range of temperatures for which reproduction occurs, an exponential function can be used such as

$$m_{\text{exp}}(T) = m_{T_R} e^{A_m\left(\frac{1}{T_R} - \frac{1}{T}\right)}. \tag{13}$$

We show an example using this form for a generic warm-adapted ectotherm species in Figure 2 (see Appendix S2 for details).

Several large-scale data analyses (Dell et al., 2011; Englund et al., 2011; Sunday et al., 2010) show that the qualitative nature of the trait responses described earlier (e.g., monotonic, left-skewed, Gaussian) is conserved across ectotherm taxa. This suggests that the trait-based models we develop here can be applied across a range of ectotherm species.

METHODS

Hypotheses and predictions

Temperature at which long-term abundance is maximized

We hypothesize that the temperature for which long-term abundance is maximized under DD population growth is lower than the temperature at which the intrinsic growth rate and abundance under DI growth are maximized. The rationale is as follows. Self-limitation should be strongest at temperatures for which abundance is maximized in the absence of competition (T_{opt_r}). When the strength of competition increases monotonically with increasing temperature, we expect strong competition at temperatures at and above T_{opt_r}. Therefore, a population under DD regulation should achieve maximal abundance at a temperature below T_{opt_r}. When competition strength is a unimodal function of temperature, maximum abundance cannot occur at a temperature above the optimal temperature for reproduction. This is because above the reproductive optimum, mortality rate increases and birth rate decreases with increasing temperature (Gillooly et al., 2002; Savage et al., 2004; van der Have & de Jong, 1996). Since $r(T)$ is a composite of the temperature response of fecundity (which is symmetric unimodal) and the temperature responses of maturation and mortality (left-skewed and exponential, respectively) it is maximized at a temperature above the optimal temperature

TABLE 1 Parameter estimates (±SE) for temperature responses of life-history traits of bagrada and harlequin bugs fitted from data.

	Species							
	Bagrada bug				Harlequin bug			
Life-history trait	**Estimate ± SE**	***t* value**	***p*-value**	**df**	**Estimate ± SE**	***t* value**	***p*-value**	**df**
Birth rate $b(T)$								
$b_{T_{\text{opt}}}$	3.586 ± 1.033	3.471	7.39×10^{-2}	2	0.8921 ± 0.1119	7.973	$p < 0.001$	5
T_{opt_b}	306.6 ± 1.29	238.24	$p < 0.001$	2	298.3 ± 0.41	722.292	$p < 0.001$	5
s	3.659 ± 1.617	2.264	0.152	2	3.085 ± 0.468	6.598	1.2×10^{-3}	5
Maturation rate $m(T)$								
m_{T_R}	0.0168[a] ($T_R = 297$)	NA	NA	NA	0.0138 ($T_R = 297$)	NA	NA	NA
A_m	$10{,}671.0 \pm 728.2$[a]	14.65	$p < 0.001$	3	$13{,}480 \pm 592.6$	22.75	1.93×10^{-3}	2
A_L	NA[a]	NA	NA	NA	$-100{,}000$[b]	NA	NA	NA
A_H	90,000[b]	NA	NA	NA	$48{,}150 \pm 4223$	11.40	7.6×10^{-3}	2
$T_{L/2}$	NA[a]	NA	NA	NA	273[b]	NA	NA	NA
$T_{H/2}$	312[b]	NA	NA	NA	303.8 ± 0.197	1544.93	$p < 0.001$	2
Juvenile mortality rate $d_J(T)$								
d_{JT_R}	0.0287 ($T_R = 297$)	NA	NA	NA	0.0343 ($T_R = 297$)	NA	NA	NA
A_{d_J}	6779.1 ± 720.5	9.409	2.54×10^{-3}	3	5743 ± 1516	3.787	0.0193	4
Adult mortality rate $d_A(T)$								
$d_{A_{T_R}}$	0.0926 ($T_R = 297$)	NA	NA	NA	0.0029 ($T_R = 297$)	NA	NA	NA
A_{d_A}	$12{,}355.6 \pm 552.6$	22.36	$p < 0.001$	3	$16{,}824 \pm 705$	23.86	$p < 0.001$	6

Note: Estimates for life-history trait parameters were conducted using nonlinear least squares. Temperatures are in degrees Kelvin.
[a]Given insufficient data to quantify the low temperature decline, a simpler model, $m_{\text{alt}}(T)$, was used to fit the bagrada maturation rate data: $m_{\text{alt}}(T) = \frac{\frac{T}{T_R} m_{T_R} e^{A_m\left(\frac{1}{T_R} - \frac{1}{T}\right)}}{1 + e^{A_H\left(\frac{1}{T_{H/2}} - \frac{1}{T}\right)}}$.
[b]This was a biologically reasonable choice.

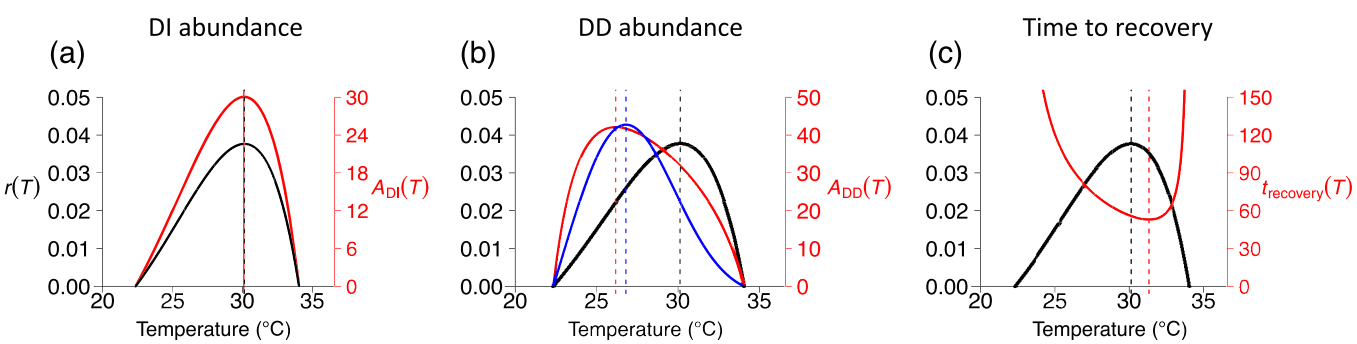

FIGURE 2 Model predictions for generic ectotherm species. (a) Temperature responses of intrinsic growth rate $r(T)$ (black curve in all panels) and adult abundance $A_{\text{DI}}(T)$ (red curve) calculated from DI model (Equation 1). Note that the $A_{\text{DI}}(T)$ axis is in units of Log(adult individuals). (b) Comparison of temperature response of intrinsic growth rate (black curve) with those of steady-state adult abundance calculated from density-dependent (DD) model (Equation 8) for when competition affects adult mortality and temperature response of competition is monotonically increasing (blue) versus unimodal (red). The $A_{\text{DD}}(T)$ axis is in units of adult individuals. Dashed vertical lines indicate temperature at which abundance (blue, red) and $r(T)$ (black) are maximized. (c) Comparison of intrinsic growth rate with recovery time to equilibrium calculated from DD model when density dependence operates on adult mortality. The strength of competition is monotonically increasing, but this does not affect stability (Appendix S1). Parameter values are realistic for warm-adapted species, such as those studied: $b_{T_{\text{opt}}} = 2.2$, $T_{\text{opt}_b} = 302$, $s = 3.4$, $T_R = 297$, $d_{JT_R} = 0.03$, $A_{d_J} = 6260$, $d_{AT_R} = 0.048$, $A_{d_A} = 14{,}600$, $q_{TR} = q_{T_{\text{opt}}} = 0.1$, $A_q = A_{d_A}$, $T_{\text{opt}_q} = T_{\text{opt}_b}$, $s_q = s$, $m_{T_R} = 0.015$, and $A_m = 11{,}500$. Maturation function Equation (13) was used.

for reproduction (Amarasekare & Coutinho, 2013; Amarasekare & Savage, 2012). The key point is that regardless of whether the temperature response of competition is monotonic or unimodal, maximum abundance under DD regulation should occur at a temperature below T_{opt_r}.

Testing this hypothesis requires comparing the temperature at which long-term abundance is maximized ($T_{\mathrm{opt}_{\mathrm{DD}}}$) with the temperature at which the intrinsic growth rate is maximized (T_{opt_r}). When the thermal environment is constant (i.e., the species experiences the same temperature, on average, with few or no fluctuations around the mean), Equation (1) converges to a stable equilibrium. We solve for the steady-state solution when density dependence operates through birth or death rates and generate the climate envelope for when the temperature response of competition is monotonic or unimodal (Appendix S1). We make the connection between the intrinsic growth rate and maximum abundance when life-history traits are DI by simulating the DI model (Equation 2) long enough to produce a smooth function of abundances (expected for a dynamical model) over the full range of temperatures constituting the niche. This makes it possible to quantify an ectotherm species' fundamental niche through measurements of its relative abundance.

Temperature effects on population recovery from perturbations

We expect the temperature at which the intrinsic growth rate is maximized to differ from the temperature at which the recovery time is minimized. We do so because the intrinsic growth rate (Equation 5) consists of the temperature responses of life-history traits only, while the dominant eigenvalue (Appendix S1: Equations S3 and S5) used to calculate the recovery time from a perturbation (Equation 7) includes temperature responses of life-history traits and competition.

Testing theory with data

Natural history of insect community

We tested model predictions using trait response data from a naturalized–invasive insect community inhabiting the California Coastal Sage Scrub (CSS) community of Southern California. Both insects are Hemiptera (family: Pentatomidae), and both undergo five nymphal instar (nonreproductive) stages before reaching adulthood. The harlequin bug (*Murgantia histrionica*) is a naturalized herbivore that has inhabited the CSS in southern California for likely well over a century (Blatchley, 1934; Wallingford et al., 2011) and is adapted to the Mediterranean climate. The bagrada bug (*Bagrada hilaris*) is a recent introduction to North America and is native to subtropical and tropical regions of Southeastern Africa and South Asia (Hill, 2008). First recorded in Los Angeles County, California, in June 2008, the bagrada has since expanded across the southwestern United States and Mexico (Palumbo et al., 2016). Like the harlequin bug, bagrada is a generalist herbivore that feeds on a variety of crucifers (e.g., mustard, broccoli, cabbage). In the field, egg parasites are common for the harlequin, but neither bagrada or harlequin juveniles or adults incur mortality from natural enemies (Ludwig & Kok, 1998; Palumbo et al., 2016).

These naturalized and invasive insects represent an ideal system for testing predictions about the thermal niche and climate envelope because the two species are phylogenetically closely related (both are members of the family Pentatomidae) and have the same feeding niche (both are sap-sucking insects that predominantly feed on plants in the Brassicae family) but are adapted to different thermal regimes (subtropical vs. Mediterranean). We therefore expect them to differ in the characteristics of their fundamental thermal niche (e.g., T_{min}, T_{max}, and T_{opt}).

Fitting mechanistic functions to trait response data: Experiments

We conducted laboratory experiments at different constant temperatures to quantify the two species' response of life-history traits (birth, maturation, mortality) to temperature. We used bagrada individuals laid by first- and second-generation wild-caught individuals originating from collection sites in New Mexico (Tome and Las Cruces) and California (Leo Carrillo State Park and Lake Perris State Recreation Area) during summer 2013 (NM) and fall 2015 (CA) under California Department of Food and Agriculture State Plant Pest Movement Permit 2979 and California Department of Fish and Wildlife Scientific Collecting Permit 12788. We measured trait responses in temperature-controlled growth chambers (40 ± 10% humidity; 12-h photoperiod) at the University of California, Los Angeles starting in fall 2013. Experiments were conducted at six temperatures (24, 27, 30, 33, 35, and 36°C) and were started with newly laid eggs checked daily for first instar nymphal emergence. Emerged first instar nymphs were placed in a plastic cylinder vial (9.5 cm in length by 2.8 cm in diameter) containing a piece of cabbage approximately 2.5 cm in diameter and sealed with a foam stopper. Individuals were checked daily for transition between each of the five juvenile life stages or death. Individuals who survived to the adult stage were put into mating pairs to measure lifetime fecundity. Cabbage was

replaced in both nymphal and adult containers every 48–72 h. Data for the harlequin bugs, collected at eight temperatures (15, 18, 21, 24, 27, 29, 33, and 35°C) using the same resource and similar protocols, are reported in Amarasekare and Savage (2012) and Amarasekare and Sifuentes (2012). Both bagrada and harlequin data are available in Simon and Amarasekare (2024a).

For both species, per-capita birth rate was measured as the number of eggs laid per adult life span of a given female and per-capita mortality rate, the inverse of time until death, where time until death is number of days from first instar nymph emergence until juvenile death (juvenile mortality) or from the date of adult emergence until death (adult mortality). Per-capita maturation rate was measured as the inverse of juvenile development duration (τ), which is the number of days from first instar emergence to fifth molt (the molt from which the adult emerges).

Fitting mechanistic functions to trait response data: Parameter estimation

We followed previous studies (e.g., Amarasekare & Savage, 2012; Lin et al., 2023; Scranton & Amarasekare, 2017) in quantifying the mean value of each trait by averaging over the number of replicates (individuals) at each experimental temperature. This approach allows one to estimate the standard error and probability associated with each parameter estimate and, hence, the reliability of the estimates. We fitted mechanistic temperature response functions (Equations 10–12) to these mean trait values using least-squares nonlinear regression. Fits were conducted with the "nls" function of the base stats package in R version 4.2.2 (R Core Team, 2017). This analysis assumes Gaussian error around predictions of population means, a reference trait value measured at a reference temperature typically determined by the investigator (given in Table 1 as "$T_R = \ldots$" for applicable parameters), and that parameter ranges are dictated by biological realism (i.e., the low temperature at which an enzyme is 50% active must be greater than the freezing temperature 273 K). Table 1 gives the resulting parameter estimates and Figure 1a–d depict the observed and fitted trait response functions for the two species. When the nls algorithm did not converge due to a lack of data at the extremes, as was the case with maturation data for the bagrada at high temperatures, biologically realistic values were assigned. However, comparison with an exponential function (Equation 13) that does not incorporate the high temperature decline shows a negligible difference in model predictions (Appendix S2). The code used for parameter estimation is available in Simon and Amarasekare (2024b).

Analysis of dynamical models

We conducted two analyses. First, we used DI (Equations 1–4) and DD (Equation 8) models with realistic parameter values for ectotherm species to test the general predictions made in *Hypotheses and predictions* above. We then parameterized the models with trait response data for the two insect species to test the validity of model predictions when applied to real species. In both cases, we used the DI model to quantify the temperature response of the intrinsic growth rate and climate envelope in a constant thermal environment. Since the DI model has no long-term equilibrium, we simulated exponential growth using the dde command of the PBSddesolve package (version 1.13.3; Couture-Beil et al., 2023) in R (R Core Team, 2017) and long-term abundance at the end of 5 years (long enough to achieve a stable-stage distribution across the thermal niche) for a range of mean habitat temperatures (see Simulation_FigureGeneration_Rcode.R in Simon & Amarasekare, 2024b). This gives the species' climate envelope in the absence of population regulation. We compared the temperature responses of intrinsic growth rate and DI climate envelope to test whether the prediction that when population growth is DI, the temperature at which abundance is maximized coincides with the temperature at which $r(T)$ is maximized.

We used the DD model to generate the climate envelope under population regulation for the same range of mean temperatures as for the DI model. We compared the temperature responses of intrinsic growth rate and DD climate envelope to test the prediction that the temperature at which abundance is maximized under DD growth is lower than that at which $r(T)$ is maximized. We calculated the recovery time following a perturbation under DD growth using Equation (7) to test the expectation that the temperature at which the intrinsic growth rate is maximized should be different from the temperature at which the recovery time is minimized.

We calculated the degree of thermal niche overlap between the two insect species by integrating $r(T)$ for each species at their respective thermal limits for viability:

$$\int_{T_{r_{\text{bagrada}_{\min}}}}^{T_{\text{intersect}}} r_{\text{bagrada}}(T)dT + \int_{T_{\text{intersect}}}^{T_{r_{\text{harlequin}_{\max}}}} r_{\text{harlequin}}(T)dT, \quad (14)$$

where $T_{r_{\text{bagrada}_{\min}}}$ and $T_{r_{\text{harlequin}_{\max}}}$ are, respectively, the lower and upper temperature limits for the viability of the bagrada and harlequin bugs ($T_{\min}$ and $T_{\max}$ in Table 2). The intersection of the thermal niches of the two species, $T_{\text{intersect}}$, occurs when $r_{\text{bagrada}}(T) - r_{\text{harlequin}}(T) \approx 0$ (equivalently, where $r_{\text{bagrada}}(T) \approx r_{\text{harlequin}}(T)$). We solved for the intersection with accuracy

TABLE 2 Parameters characterizing temperature dependence of intrinsic growth rate, long-term abundance, and recovery time for invasive bagrada bug and naturalized harlequin bug.

Metric	Species	
	Bagrada	Harlequin
Intrinsic growth rate $r(T)$		
T_{opt_r} (°C)	34.1	26.7
$r_{T_{\mathrm{opt}}}$ (per day)	0.058	0.023
$T_{\min}$ (°C)	26.8	18.2
$T_{\max}$ (°C)	37.7	30.9
Density-dependent fecundity		
$T_{\mathrm{opt}_{A_{\mathrm{DD}}}}$ (°C)	28.9	19.7
$A_{\mathrm{DD}}(T_{\mathrm{opt}})$ (adult individuals)	18.1	62.6
$T_{\mathrm{opt}_{t_{\mathrm{recovery}}}}$ (°C)	35.2	29.2
$t_{\mathrm{recovery}_{T_{\mathrm{opt}}}}$ (days)	0.451	0.029
Density-dependent mortality		
$T_{\mathrm{opt}_{A_{\mathrm{DD}}}}$ (°C)	31.3	23.7
$A_{\mathrm{DD}}(T_{\mathrm{opt}})$ (adult individuals)	8.98	213.2
$T_{\mathrm{opt}_{t_{\mathrm{recovery}}}}$ (°C)	35.0	27.7
$t_{\mathrm{recovery}_{T_{\mathrm{opt}}}}$ (days)	0.029	0.012

$r_{\mathrm{bagrada}}(T) - r_{\mathrm{harlequin}}(T) \leq 10^{-6}$ by calculating the difference at successively smaller T intervals. Equation (14) was calculated using the "Nintegrate" function in Mathematica (Wolfram Research, Inc, 2019). The code is available in Simon and Amarasekare (2024b).

RESULTS

General predictions from dynamical models

As expected, the temperature at which the intrinsic growth rate, $r(T)$, was maximized was indeed the same temperature at which abundance was maximized (Figure 2a). This suggests that, in the absence of intraspecific competition, the temperature at which an ectotherm species' ability to increase when rare is the one at which it also reaches the highest abundance. As also expected, the temperature at which equilibrium abundance was maximized was lower than the temperature at which the intrinsic growth rate was maximized (Figure 2b). We found that the temperature at which recovery time was minimized (the temperature at which recovery from a perturbation was the fastest) was higher than that at which the intrinsic growth rate was maximized (Figure 2c). The key point is that steady-state abundance is maximal at the cooler end of the thermal niche, while the fastest response to perturbation occurs at the warmer end of the niche. These outcomes ensue regardless of the life-history trait (fecundity, mortality) on which density dependence operates or the qualitative form of the temperature response of competition (monotonic vs. unimodal; Appendix S1: Figure S2).

Testing theory with data from a naturalized–invasive insect community

Analyses of the parameterized models confirm that our predictions hold when applied to insect species in the wild. When population growth is DI, the temperature of maximum abundance coincides with the temperature at which $r(T)$, and hence the ability to increase when rare, is maximized (Figure 3a,d). This occurs at 34.1°C in the warm-adapted bagrada and, almost 7°C degrees cooler, at 26.7°C in the cooler-adapted harlequin (Table 2).

As predicted, when population growth was DD, the temperature at which abundance was maximized was lower than that at which the intrinsic growth rate $r(T)$ was maximized (Figure 3b,e). Interestingly, we found that the temperature at which the bagrada achieved its maximum abundance (28.9 and 31.3°C, DD fecundity, mortality, respectively; Figure 3e) was very close to the temperature at which the harlequin's intrinsic growth rate was maximized (26.7°C Figure 3a). Additionally, bagrada's maximum abundance also occurred very close to the temperature for which harlequin's time to recovery was shortest (29.2 and 27.7°C, DD fecundity, mortality, respectively; Figure 3c).

Lower and upper thermal limits of the fundamental niche are greater for the bagrada, which is of subtropical origin ($T_{\min} =$ 26.8°C, $T_{\max} =$ 37.7°C), than for the Mediterranean-adapted harlequin bug ($T_{\min} =$ 18.2°C, $T_{\max} =$ 30.9°C). The two species' niches overlap within the temperature range 26.8–30.9°C (Figure 4, Table 2). This overlap constitutes ~25% of the harlequin's thermal niche but only ~10% of the bagrada bug's niche (see NicheOverlap_MathematicaCode_OUTPUT.pdf in Simon & Amarasekare, 2024b). Importantly, this temperature range of niche overlap includes the temperatures at which the harlequin bug's intrinsic growth rate (26.7°C) and recovery time are maximized (29.2 and 27.7°C for DD fecundity, mortality, respectively) and the temperature at which the bagrada's steady-state abundance is maximized when density dependence operates on fecundity (28.9°C; the maximum under DD mortality slightly exceeds niche overlap at 31.3°C).

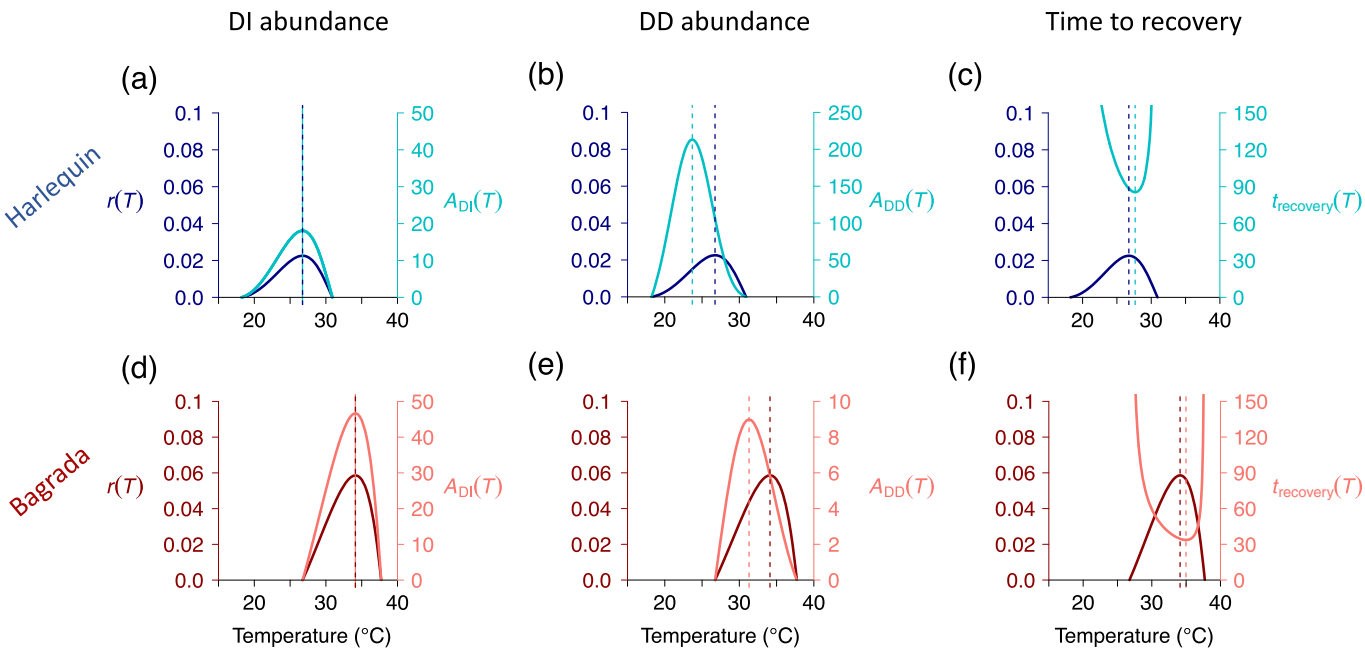

FIGURE 3 Temperature-dependent intrinsic growth rate, $r(T)$, and climate envelope under density-independent (DI), $A_{\mathrm{DI}}(T)$, and density-dependent (DD) population growth, $A_{\mathrm{DD}}(T)$, for the naturalized harlequin bug (top; blue) and invasive bagrada (bottom; red). Panels (a) and (d) depict the intrinsic growth rate (dark blue curve in [a], dark red curve in [d]) and adult abundance (in units Log[adult individuals]) under DI growth (light blue curve in [a], light red curve in [d]). Panels (b) and (e) compare $r(T)$ with $A_{\mathrm{DD}}(T)$ when competition affects adult mortality via a monotonic temperature response of competition. Units of $A_{\mathrm{DD}}(T)$ are adult individuals. Panels (c) and (f) depict $r(T)$ and the recovery time to equilibrium $t_{\mathrm{recovery}}(T)$ (in units of time). Parameters: $q_{TR} = 0.1$ for both bugs; $A_q = A_{d_A}$ for each respective bug; all other parameters are given in Table 1.

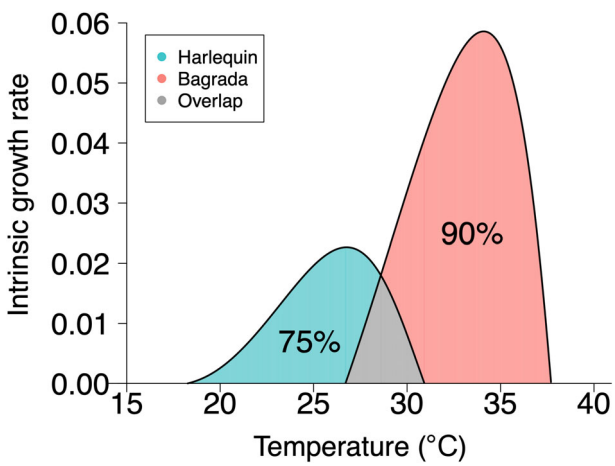

FIGURE 4 Fundamental thermal niches of naturalized harlequin (blue and gray regions) and invasive bagrada bugs (red and gray regions) as predicted from trait response data (Figure 1, Table 1). Niche overlap is shown in gray. Niche metrics are given in Table 2.

DISCUSSION

Climate warming is widely expected to shift species' distributions, enhance extinction risk, and increase the invasion of exotic pests and pathogens. Predicting the ecological impacts of climate warming requires that we understand how temperature effects on ectotherm species' life-history traits translate into population-level patterns of abundance and distributional changes through the shaping of species' thermal niches. Here we developed a mechanistic, trait-based framework for characterizing the fundamental thermal niche and, hence, a species' climate envelope (the range of temperatures over which a species maintains a viable population), based on how species' life-history traits and population regulatory mechanisms respond to temperature (Figure 1).

The particular strength of our framework is that it is sufficiently biologically realistic to apply to specific species but is, at the same time, sufficiently general to apply broadly across ectotherm taxa. Its novelty is that it generates testable predictions about species' abundances and distributions based solely on information on the temperature responses of the underlying life-history traits. The predictions are therefore completely independent of observed distribution and abundance patterns. This is important because, when a framework is used based on species' traits for which the temperature responses can be carefully measured in the laboratory, the thermal niche can be quantified in the absence of biotic filters that

generally plague measurements obtained from the field. This allows for more accurate predictions of climate envelopes of ectotherm species of interest. Further, several large-scale data analyses show that the qualitative nature of the temperature responses of life-history traits (e.g., monotonic, left-skewed, Gaussian) is conserved across ectotherm taxa (Kingsolver, 2009; Kingsolver et al., 2011; van der Have, 2002; van der Have & de Jong, 1996) and their parameters are thermodynamically constrained to lie within narrow limits (Brown et al., 2004; Dell et al., 2011; Gillooly et al., 2001, 2002; Savage et al., 2004). This affords the advantage of being able to use parameter values of related species from similar thermal environments when data are unavailable for a species for whom a climate envelope is required.

Data limitation is most likely to occur when quantifying the temperature response of the maturation rate. Most previous studies quantified only the rising portion of the maturation curve, that is, the temperature range within which the maturation rate increases exponentially with temperature (Equation 13; Appendix S2: Figure S1, solid curve; see references in Gillooly, 2002). This is largely because the metabolic theory of ecology (Brown, 2004; Savage et al., 2004), the prevailing framework for temperature dependence at the time, did not consider the high temperature decline in their formulations. The advent of climate warming has necessitated a broadening of the framework for characterizing trait response functions. Given the importance of climate warming in driving species distributions, future empirical studies should concentrate on quantifying the maturation rate at high temperature extremes so that the decline at these extremes can be quantified. Based on our experience, extending the temperature measurements to four or five temperature treatments above the optimal temperature for reproduction (T_{opt_b} in Equation 11) should suffice to obtain statistically significant fits to the two parameters that characterize the high temperature decline (Equation 12; Ardelan et al., 2023; Scranton & Amarasekare, 2017).

The framework we present applies broadly across multicellular ectotherm species despite life-history differences in the number of pre-reproductive stages. Such differences do not require modification to the model when density dependence acts only on adults or on all juvenile stages equally because pre-reproductive (juvenile) stages then simply act as a time lag (Murdoch et al., 2003). In systems for which density dependence acts at some but not all juvenile stages, the juvenile class in Equations (1) and (8) can be split into multiple juvenile classes, each with its own corresponding equation (e.g., Johnson et al., 2016).

Our framework is sufficiently general to apply to abiotic factors other than temperature (e.g., humidity, salinity) so long as the response of life-history traits and self-limitation can be measured at different magnitudes of the abiotic condition of interest. It is also feasible to make predictions based on the joint effects of multiple abiotic factors by modifying the existing framework, which is an important area for future research. Quantifying the temperature response (or other abiotic response) of life-history traits of long-lived or very large ectotherms may not be possible in lab-controlled settings. For these cases, the use of well-controlled field settings using large numbers per replicate could be a viable alternative. Research into this possibility is needed.

The key innovation of our framework is the development of metrics (intrinsic growth rate, abundance, and recovery time as a function of temperature) that can be used to generate thermal range plots for native and invasive species. These allow us to predict, a priori, the likelihood of competitive interactions and the proportion of each species' range within which such interactions are likely to occur. These thermal plots can be compared with temperature–abundance data from the field to determine where a species could be but is absent due to interactions with competitors and/or natural enemies or due to dispersal limitation and to where it could potentially expand under various scenarios of climate warming. By characterizing both necessary and sufficient conditions for population viability in terms of species abundances, we are able to obtain a complete description of the fundamental niche under both DI (e.g., invasive species in their initial establishment phase) and DD (e.g., native species' typical dynamics) population growth.

Our trait-based framework yields two important insights into the fundamental thermal niche of ectotherms. First, maximum abundance occurs at warmer temperatures in populations experiencing DI growth compared to populations experiencing DD growth. Second, the type of population growth determines the degree of congruence between the temperature at which abundance is maximized and the temperature at which the species can increase most quickly from low abundance. In populations exhibiting unbounded growth, the temperature at which abundance is maximized is the same as the temperature at which the species can increase most quickly from low abundances; in populations exhibiting bounded growth, the temperature at which abundance is maximized is lower than the temperature at which the species can increase most quickly from low abundances. Importantly, these are general outcomes that prevail regardless of which life-history trait density dependence operates on or the qualitative nature (monotonic vs. unimodal) of the temperature response of intraspecific competition. They suggest that climate warming will have differential effects on native or

naturalized versus invasive species. For instance, the fact that the temperature of maximum abundance and temperature of fastest recovery from low abundances coincide suggests an advantage of climate warming for species exhibiting unbounded growth (e.g., crop pests, newly introduced species). Similarly, the fact that the temperature of maximum abundance is lower than the temperature of fastest recovery suggests a disadvantage for species exhibiting bounded growth (e.g., native species well-established in their habitats). Putting this in the context of interactions between native and invasive species, their ability to increase when rare at warmer temperatures at which native species exhibit lower abundances and, hence, weaker competitive pressure give invasive species a greater advantage in establishing in newly colonized habitats. The important implication for native species, which is particularly relevant when generating climate envelopes for such species, is that the temperature at which one is likely to observe highest abundance in the field is not the temperature that is optimal for reproduction and population growth, but the one at which effects of self-limitation are minimal.

Our findings support the widespread expectation that climate warming will increase the spread of invasive pests and pathogens. An increase in the environmental temperature at a given location will draw native species away from the cooler temperatures at which their abundance and competitive pressure on invasive species are greatest. At the same time, it will subject the invasive species to the warmer temperatures at which their ability to increase when rare is greater. The faster an exotic species can increase when thermal conditions are favorable, the greater the likelihood of its successful establishment. The advantage of our framework is that we can predict, a priori, which native species will be at greater risk and which invasive species have the greater advantage, based on how their life-history traits respond to temperature. It is customary for entomologists and pest management specialists to quantify temperature effects on the life-history traits of pests and newly invaded species through laboratory experiments. In fact, the pest management and entomological literature is replete with such studies (e.g., Correa et al., 2021; Karpicka-Ignatowska et al., 2021; Sun et al., 2022), meaning that the information required for quantifying the thermal niche of invasive species is likely to be widely available.

Tests of our model predictions with data for the naturalized (harlequin bug) and invasive species (bagrada) confirm the key conceptual insights of our trait-based framework. First, when population growth is DI, the temperature at which abundance is maximized coincides with the temperature at which $r(T)$, and hence the ability to increase when rare, is maximized. Second, when population growth is DD, the temperature at which abundance is maximized is lower than that at which the intrinsic growth rate, $r(T)$, is maximized. Third, the range of thermal niche overlap between the two species includes the temperatures for which the harlequin bug's intrinsic growth rate and recovery time are maximized and the temperature at which the bagrada's abundance (under DD population growth) is maximized. Interestingly, we found that the bagrada achieved its maximum abundance at a temperature very close to that for which the harlequin's recovery time was the shortest, suggesting that competitive interactions with the invasive bagrada could impact the naturalized harlequin's ability to respond to external perturbation. We additionally found that the bagrada achieved its maximum abundance at a temperature close to that at which the harlequin bug's intrinsic growth rate was maximized. In contrast, bagrada's intrinsic growth rate was maximized at a temperature that was above the upper temperature limit for the harlequin bug's viability and was very close to the maximum temperature observed in the CSS habitat (~36°C in the University of California San Joaquin Marsh Reserve, Irvine, CA, USA; Simon, 2017). The upper temperature limit for bagrada's viability is slightly above the maximum observed CSS temperature.

The ability to increase when rare is a critical component of invasion success. However, if the temperature at which a species' ability to increase when rare is the greatest coincides with the temperature at which its competitor's abundance is maximized, invasibility will be hindered by strong competition from the resident species. Since the harlequin bug's (the resident species) abundance is maximized at a temperature much lower than that at which the bagrada's (the invasive species) ability to increase when rare is the greatest, one would expect the bagrada's invasion of the CSS community to be relatively unhindered by competitive pressure from the harlequin bug. Had their roles been reversed (i.e., bagrada had been the naturalized species), the harlequin bug would have had difficulty increasing from initially small numbers because the temperature at which it has the greatest ability to increase when rare is also the temperature at which competitive pressure from bagrada is the greatest (at least when density dependence acts on fecundity).

This finding illustrates an interesting asymmetry between species in their invasion success based on their latitudinal origin. Invasion by an exotic species is most likely to succeed when the temperature at which the exotic species' intrinsic growth is maximized (i.e., the temperature at which its ability to increase when rare is the greatest) is greater than the temperature at which the native (or naturalized) species' abundance is maximized. An ectotherm species of Mediterranean or temperate origin introduced to a tropical habitat may be at a

disadvantage because the temperature at which its ability to increase when rare is likely to coincide with the temperature at which the native species is the most abundant (and, hence, exerts the strongest competitive pressure on an incoming species). In contrast, an ectotherm species of tropical origin introduced to a Mediterranean or temperate habitat is likely to have greater invasion success because the temperature at which its invasibility is the greatest is likely to be higher than the temperature at which competitive pressure from the native species is the strongest. Such a directionality in invasion success, with tropical species having greater success in invading temperate habitats, has been reported based on data of both extant and extinct species (Jablonski et al., 2006, 2013), which recent theory (Amarasekare & Johnson, 2017; Amarasekare & Simon, 2020) attributes to tropical species having higher optimal temperatures for reproduction and lower mortality during temperate summers compared to temperate species. An interesting future direction would be to conduct a broader analysis, based on available data from the literature, to determine whether warm-adapted invasive species from lower latitudes have an intrinsic advantage when interacting with cold-adapted native species from higher latitudes.

ACKNOWLEDGMENTS

The research was supported in part by National Science Foundation (NSF) DDIG DEB-1502071 to MWS and NSF Grant DEB-1949796 to PA. The project described was also supported by Grant Number T32GM008185 from the National Institute of General Medical Sciences. The content is solely they responsibility of the authors and does not necessarily represent the official views of the National Institute of General Medical Sciences or the National Institute of Health. We thank two anonymous reviewers and Editor-in-Chief Kathryn Cottingham for constructive comments that improved the manuscript.

CONFLICT OF INTEREST STATEMENT

The authors declare no conflicts of interest.

DATA AVAILABILITY STATEMENT

Data (Simon & Amarasekare, 2024a) are available in Dryad at https://doi.org/10.5061/dryad.rxwdbrvfp. Code (Simon & Amarasekare, 2024b) is available in Zenodo at https://doi.org/10.5281/zenodo.8245092.

ORCID

Margaret W. Simon https://orcid.org/0000-0001-8269-2589
Priyanga Amarasekare https://orcid.org/0000-0001-8896-1532

REFERENCES

Amarasekare, P. 2015. "Effects of Temperature on Consumer–Resource Interactions." *Journal of Animal Ecology* 84(3): 665–679.

Amarasekare, P., and C. Johnson. 2017. "Evolution of Thermal Reaction Norms in Seasonally Varying Environments." *The American Naturalist* 189(3): E31–E45.

Amarasekare, P., and M. W. Simon. 2020. "Latitudinal Directionality in Ectotherm Invasion Success." *Proceedings of the Royal Society B* 287: 20191411.

Amarasekare, P., and R. Coutinho. 2013. "The Intrinsic Growth Rate as a Predictor of Intrinsic Growth Rate under Climate Warming." *Journal of Animal Ecology* 82: 1240–53.

Amarasekare, P., and R. Coutinho. 2014. "Effects of Temperature on Intra-Specific Competition in Ectotherms." *The American Naturalist* 184: E50–E65.

Amarasekare, P., and R. Sifuentes. 2012. "Elucidating the Temperature Response of Survivorship in Insects." *Functional Ecology* 26: 959–968.

Amarasekare, P., and V. M. Savage. 2012. "A Mechanistic Framework for Elucidating the Temperature Dependence of Fitness." *The American Naturalist* 179: 178–191.

Ardelan, A., A. Tsai, S. Will, R. McGuire, and P. Amarasekare. 2023. "Increase in Heat Tolerance Following a Period of Heat Stress in a Naturally Occurring Insect Species." *Journal of Animal Ecology* 92: 2039–51.

Bebber, D., M. Ramotowski, and S. Gurr. 2013. "Crop Pests and Pathogens Move Polewards in a Warming World." *Nature Climate Change* 3: 985–88.

Bernhardt, J. R., J. M. Sunday, and M. I. O'Connor. 2018. "Metabolic Theory and the Temperature-Size Rule Explain the Temperature Dependence of Population Carrying Capacity." *The American Naturalist* 192: 687–697.

Blatchley, W. S. 1934. "Notes on a Collection of Heteroptera Taken in Winter in the Vicinity of Lost Angeles, California." *Transactions of the American Entomological Society (1890-)* 60(1): 1–16.

Brown, J. H., J. F. Gillooly, A. P. Allen, V. M. Savage, and G. B. West. 2004. "Toward a Metabolic Theory of Ecology." *Ecology* 85: 1771–89.

Buckley, L. B., M. C. Urban, M. J. Angilletta, L. G. Crozier, L. J. Rissler, and M. W. Sears. 2010. "Can Mechanism Inform Species' Distribution Models?" *Ecology Letters* 13: 1041–54.

CaraDonna, P. J., A. M. Iler, and D. W. Inouye. 2014. "Shifts in Flowering Phenology Reshape a Subalpine Plant Community." *Proceedings of the National Academy of Sciences of the United States of America* 111: 4916–21.

Carrière, Y., and G. Boivin. 1997. "Evolution of Thermal Sensitivity of Parasitization Capacity in Egg Parasitoids." *Evolution* 51(6): 2028–32.

Chesson, P. 2000. "Mechanisms of Maintenance of Species Diversity." *Annual Review of Ecology and Systematics* 31: 343–366.

Corless, R., G. Gonnet, D. Hare, D. J. Jeffrey, and D. E. Knuth. 1996. "On the Lambert W Function." *Advances in Computational Mathematics* 5: 329–359.

Correa, C. P., S. S. Parreiras, L. A. Beijo, P. M. de Ávila, I. R. V. Teixeira, and A. R. Barchuk. 2021. "Life History Trait Response to Ambient Temperature and Food Availability

Variations in the Bean Weevil *Zabrotes subjasciatus*." *Physiological Entomology* 46: 189–199.

Couture-Beil, A., J. T. Schnute, R. Haigh, S. N. Wood, and B. J. Cairns. 2023. "PBSddesolve: Solver for Delay Differential Equations." R Package Version 1.13.3. https://CRAN.R-project.org/package=PBSddesolve.

Dannon, E. A., M. Tamò, A. van Huis, and M. Dicke. 2010. "Functional Response and Life History Parameters of *Apanteles taragamae*, a Larval Parasitoid of *Maruca vitrata*." *BioControl* 55(3): 363–378.

Dell, A., S. Pawar, and S. M. Savage. 2011. "Systematic Variation in the Temperature Dependence of Physiological and Ecological Traits." *Proceedings of the National Academy of Sciences of the United States of America* 108: 10591–96.

Dreyer, H., and J. Baumgärtner. 1996. "Temperature Influence on Cohort Parameters and Demographic Characteristics of the Two Cowpea Coreids *Clavigralla tomentosicollis* and *C. shadabi*." *Entomologia Experimentalis et Applicata* 78(2): 201–213.

Dukes, J., and H. Mooney. 1999. "Does Global Change Increase the Success of Biological Invaders?" *Trends in Ecology & Evolution* 14: 135–39.

Englund, G., G. Ohlund, C. Hein, and S. Diehl. 2011. "Temperature Dependence of the Functional Response." *Ecology Letters* 14: 914–921.

Forrest, J. 2016. "Complex Responses of Insect Phenology to Climate Change." *Current Opinion in Insect Science* 17: 49–54.

Gao, G., Z. Z. Lu, D. Xia, P. Sun, J. H. Ma, and Y. C. Xu. 2013. "Effects of Temperature and Density on the Mortality and Reproduction of Cotton Aphid *Aphis gossypii*." *Chinese Journal of Applied Ecology* 24: 1300–1304.

Gillooly, J. F., E. L. Charnov, G. B. West, V. M. Savage, and J. H. Brown. 2002. "Effects of Size and Temperature on Developmental Time." *Science* 293: 2248–51.

Gillooly, J. F., J. H. Brown, G. B. West, V. M. Savage, and E. L. Charnov. 2001. "Effects of Size and Temperature on Metabolic Rate." *Science* 293: 2248–51.

Harvey, J. A., R. Heinen, R. Gols, and M. P. Thakur. 2020. "Climate Change-Mediated Temperature Extremes and Insects: From Outbreaks to Breakdowns." *Global Change Biology* 26: 6685–6701.

Hellmann, J. J., J. E. Byers, B. G. Bierwagen, and J. S. Dukes. 2008. "Five Potential Consequences of Climate Change for Invasive Species." *Conservation Biology* 22(3): 534–543.

Hill, D. S. 2008. *Pests of Crops in Warmer Climates and their Control*. Berlin, Germany: Springer Science + Business Media.

Hochachka, P., and G. Somero. 2002. *Biochemical Adaptation: Mechanism and Process in Physiological Evolution*. Oxford: Oxford University Press.

Holt, R. D. 2009. "Bringing the Hutchinsonian Niche into the 21st Century: Ecological and Evolutionary Perspectives." *Proceedings of the National Academy of Sciences of the United States of America* 106(supplement_2): 19659–65.

Hou, Y., and Z. Weng. 2010. "Temperature-Dependent Development and Life Table Parameters of Octodonta nipae (Coleoptera: Chrysomelidae)." *Environmental Entomology* 39(5): 1676–84.

IPCC. 2018. "An IPCC Special Report on the Impacts of Global Warming of 1.5°C above Pre-Industrial Levels and Related Global Greenhouse Gas Emission Pathways in the Context of Strengthening the Global Response to the Threat of Climate Change, Sustainable Development, and Efforts to Eradicate Poverty." https://www.ipcc.ch/sr15/.

Jablonski, D., C. Belanger, S. Berke, S. Huang, A. Z. Krug, K. Roy, A. Tomasovych, and J. W. Valentine. 2013. "Out of the Tropics, but how? Fossils, Bridge Species, and Thermal Ranges in the Dynamics of the Marine Latitudinal Diversity Gradient." *Proceedings of the National Academy of Sciences of the United States of America* 110: 10487–94.

Jablonski, D., K. Roy, and J. Valentine. 2006. "Out of the Tropics: Evolutionary Dynamics of the Latitudinal Diversity Gradient." *Science* 312: 102–6.

Jandricic, S. E., S. P. Wraight, K. C. Bennett, and J. P. Sanderson. 2010. "Developmental Times and Life Table Statistics of *Aulacorthum solani* (Hemiptera: Aphididae) at Six Constant Temperatures, With Recommendations on the Application of Temperature-Dependent Development Models." *Environmental Entomology* 39(5): 1631–42.

Johnson, C., R. M. Coutinho, E. Berlin, K. E. Dolphin, J. Heyer, B. Kim, A. Leung, J. L. Sabellon, and P. Amarasekare. 2016. "Effects of Temperature and Resource Variation on Insect Population Dynamics: The Bordered Plant Bug as a Case Study." *Functional Ecology* 30: 1122–31.

Johnson, F. H., and I. Lewin. 1946. "The Growth Rate of E. Coli in Relation to Temperature, Quinine and Coenzyme." *Journal of Cellular and Comparative Physiology* 28: 47–75.

Karpicka-Ignatowska, K., A. Laska, B. G. Rector, A. Skoracka, and L. Kuczyński. 2021. "Temperature-Dependent Development and Survival of an Invasive Genotype of Wheat Curl Mite, *Aceria tosichella*." *Experimental & Applied Acarology* 83: 513–525.

Kingsolver, J. G. 2009. "The Well-Temperatured Biologist." *The American Naturalist* 174: 755–768.

Kingsolver, J. G., H. Arthur Woods, L. B. Buckley, K. A. Potter, H. J. MacLean, and J. K. Higgins. 2011. "Complex Life Cycles and the Responses of Insects to Climate Change." *Integrative and Comparative Biology* 51: 719–732.

Lehmann, P., T. Ammunét, M. Barton, A. Battisti, S. D. Eigenbrode, J. U. Jepsen, G. Kalinkat, et al. 2020. "Complex Responses of Global Insect Pests to Climate Warming." *Frontiers in Ecology and the Environment* 18(3): 141–150.

Lin, T., Y. Chen, Y. Chen, S. Lin, J. Hu, J. Zhao, G. Yang, F. Yang, and H. Wei. 2023. "Temperature-Dependent Functional Response of the Arboreal Rove Beetle, *Oligota flavicornis* (Coleoptera: Staphylinidae), a Voracious Predator of *Tetranychus urticae* (Acarina: Tetranychidae)." *Journal of Economic Entomology* 116(1): 90–97. https://doi.org/10.1093/jee/toac170.

Long, M. A., and M. S. Fee. 2008. "Using Temperature to Analyse Temporal Dynamics in the Songbird Motor Pathway." *Nature* 456(7219): 189–194.

Ludwig, S. W., and L. T. Kok. 1998. "Phenology and Parasitism of Harlequin Bugs, *Murgantia histrionica* (Hahn) (Hemiptera Pentatomidae), in Southwest Virginia." *Journal of Entomological Science* 33(1): 33–39.

Miller-Rushing, A. J., T. T. Hoye, D. W. Inouye, and E. Post. 2010. "The Effects of Phenological Mismatches on Demography." *Philosophical Transactions of the Royal Society B* 365: 3177–86.

Morgan, D., K. F. A. Walters, and J. N. Aegerter. 2001. "Effect of Temperature and Cultivar on Pea Aphid, *Acyrthosiphon pisum*

(Hemiptera: Aphididae) Life History." *Bulletin of Entomological Research* 91(1): 47–52.

Murdoch, W. W., C. J. Briggs, and R. M. Nisbet. 2003. *Consumer Resource Dynamics*. Princeton: Princeton University Press.

Nijhout, H. F. 1994. *Insect Hormones*. Princeton: Princeton University Press.

Nisbet, R. M., and W. S. C. Gurney. 1983. "The Systematic Formulation of Population-Models for Insects with Dynamically Varying Instar Duration." *Theoretical Population Biology* 23: 114–135.

Nisbet, R. M. 1997. "Delay-Differential Equations for Structured Populations." In *Structured-Population Models in Marine, Terrestrial, and Freshwater Systems*, edited by S. Tuljapurkar and H. Caswell, 89–116. New York: Chapman and Hall.

Palumbo, J. C., T. M. Perring, J. G. Millar, and D. A. Reed. 2016. "Biology, Ecology and Management of an Invasive Stink Bug, *Bagrada hilaris*, in North America." *Annual Review of Entomology* 61: 453–473.

Parmesan, C. 2006. "Ecological and Evolutionary Responses to Recent Climate Change." *Annual Review of Ecology and Systematics* 37: 637–669.

Pereira, H., P. Leadley, V. Proença, R. Alkemade, J. P. W. Scharlemann, J. F. Fernandez-Manjarrés, M. B. Araújo, et al. 2010. "Scenarios for Global Biodiversity in the 21st Century." *Science* 330: 1496–1501.

Post, E., B. Steinman, and M. Mann. 2018. "Acceleration of Phenological Advance and Warming with 148 Latitude over the Past Century." *Scientific Reports* 8: 3927.

R Core Team. 2017. *R: A Language and Environment for Statistical Computing*. Vienna: R Foundation for Statistical Computing.

Ratkowsky, D. A., J. Olley, and T. Ross. 2005. "Unifying Temperature Effects on the Growth Rate of Bacteria and the Stability of Globular Proteins." *Journal of Theoretical Biology* 233: 351–362.

Root, T. L., J. T. Price, K. R. Hall, S. H. Schneider, C. Rosenzweig, and J. A. Pounds. 2003. "Fingerprints of Global Warming on Wild Animals and Plants." *Nature* 421: 57–60.

Sala, O. E., F. S. Chapin, III, J. J. Armesto, E. Berlow, J. Bloomfield, R. Dirzo, E. Huber-Sanwald, et al. 2000. "Global Biodiversity Scenarios for the Year 2100." *Science* 287(5459): 1770–74.

Savage, V. M., J. F. Gillooly, J. H. Brown, G. B. West, and E. L. Charnov. 2004. "Effects of Body Size and Temperature on Population Growth." *The American Naturalist* 163: 429–441.

Schoolfield, R. M., J. H. Sharpe, and C. E. Magnuson. 1981. "Non-linear Regression of Biological Temperature-Dependent Rate Models Based on Absolute Reaction-Rate Theory." *Journal of Theoretical Biology* 88: 719–731.

Scranton, K., and P. Amarasekare. 2017. "Predicting Phenological Shifts in a Changing Climate." *Proceedings of the National Academy of Sciences of the United States of America* 114(50): 13212–17.

Sharpe, P. J. H., and D. W. DeMichele. 1977. "Reaction Kinetics of Poikilotherm Development." *Journal of Theoretical Biology* 64: 649–670.

Sherwood, S. C., M. J. Webb, J. D. Annan, K. C. Armour, P. M. Forster, J. C. Hargreaves, G. Hegerl, et al. 2020. "An Assessment of Earth's Climate Sensitivity Using Multiple Lines of Evidence." *Reviews of Geophysics* 58(4): e2019 RG000678.

Simon, M., and P. Amarasekare. 2024a. "Data and Code from: Predicting the Fundamental Thermal Niche of Ectotherms." Dryad, Dataset. https://doi.org/10.5061/dryad.rxwdbrvfp.

Simon, M., and P. Amarasekare. 2024b. Data and code from: "Predicting the Fundamental Thermal Niche of Ectotherms." Zenodo, Software. https://doi.org/10.5281/zenodo.8245092.

Simon, M. W. 2017. *Elucidating the Joint Effects of Biotic and Abiotic Factors on Species Invasion: A Trait-Based Approach*. Order No. 10638504 (Doctoral diss., University of California, Los Angeles). Philadelphia: ProQuest Dissertations Publishing.

Sorte, C., I. Ibanez, D. Blumenthal, N. A. Molinari, L. P. Miller, E. D. Grosholz, J. M. Diez, et al. 2013. "Poised to Prosper? A Cross-System Comparison of Climate Change Effects on Native and Non-native Species Performance." *Ecology Letters* 16: 261–270.

Stachowicz, J., J. Terwin, R. Whitlatch, and R. Osman. 2002. "Linking Climate Change and Biological Invasions: Ocean Warming Facilitates Nonindigenous Species Invasions." *Proceedings of the National Academy of Sciences of the United States of America* 99: 15497–500.

Sun, J., X. Tan, Q. Li, F. Francis, and J. Chen. 2022. "Effects of Different Temperatures on the Development and Reproduction of *Sitobion miscanthi* from Six Different Regions in China." *Frontiers in Ecology and Evolution* 10: 794495.

Sunday, J. M., A. E. Bates, and N. K. Dulvy. 2010. "Global Analysis of Thermal Tolerance in Ectotherms." *Proceedings of the Royal Society B* 278: 1823–30.

Uszko, W., S. Diehl, G. Englund, and P. Amarasekare. 2017. "Effects of Warming on Predator-Prey Interactions—A Resource-Based Approach and a Theoretical Synthesis." *Ecology Letters* 20: 513–523.

van der Have, T. M. 2002. "A Proximate Model for Thermal Tolerance in Ectotherms." *Oikos* 98: 141–155.

van der Have, T. M., and G. de Jong. 1996. "Adult Size in Ectotherms: Temperature Effects on Growth and Differentiation." *Journal of Theoretical Biology* 183: 329–340.

Vitasse, Y., F. Baumgarten, C. Zohner, T. Rutishauser, B. Pietragalla, R. Gehrig, J. Dai, H. Wang, Y. Aono, and T. H. Sparks. 2022. "The Great Acceleration of Plant Phenological Shifts." *Nature Climate Change* 12: 300–302.

Wallingford, A. K., T. P. Kuhar, P. B. Schultz, and J. H. Freeman. 2011. "Harlequin Bug Biology and Pest Management in Brassicaceous Crops." *Journal of Integrated Pest Management* 2(1): 1–4.

Walther, G. R., A. Roques, P. E. Hulme, M. T. Sykes, P. Pyšek, I. Kühn, M. Zobel, S. Bacher, Z. Botta-Dukát, and H. Bugmann. 2009. "Alien Species in a Warmer World: Risks and Opportunities." *Trends in Ecology & Evolution* 24(12): 686–693.

Walther, G. R., E. Post, P. Convey, A. Menzel, C. Parmesan, T. J. C. Beebee, J. M. Fromentin, O. Hoegh-Guldberg, and F. Bairlein. 2002. "Ecological Responses to Recent Climate Change." *Nature* 416: 389–395.

Wolfram Research, Inc. 2019. *Mathematica, Version 12.0*. Champaign, IL: Wolfram Research, Inc. https://www.wolfram.com/mathematica.

SUPPORTING INFORMATION

Additional supporting information can be found online in the Supporting Information section at the end of this article.

How to cite this article: Simon, Margaret W., and Priyanga Amarasekare. 2024. "Predicting the Fundamental Thermal Niche of Ectotherms." *Ecology* 105(5): e4289. https://doi.org/10.1002/ecy.4289

ARTICLES FOR FACULTY MEMBERS

GLOBAL WARMING EFFECTS ON ECTOTHERM SPECIES

Title/Author	**Temperature change effects on marine fish range shifts: A meta-analysis of ecological and methodological predictors / Dahms, C., & Killen, S. S.**
Source	***Global Change Biology*** **Volume 29 Issue 16 (2023) Pages 4459–4479** **https://doi.org/10.1111/gcb.16770** **(Database: Wiley Online Library)**

Received: 21 November 2022 | Revised: 12 April 2023 | Accepted: 30 April 2023

DOI: 10.1111/gcb.16770

Global Change Biology WILEY

REVIEW

Temperature change effects on marine fish range shifts: A meta-analysis of ecological and methodological predictors

Carolin Dahms[1,2] | Shaun S. Killen[1]

[1]School of Biodiversity, One Health and Veterinary Medicine, College of Medical, Veterinary & Life Sciences, University of Glasgow, Glasgow, UK

[2]Division for Ecology and Biodiversity, School of Biological Sciences, Faculty of Science, The University of Hong Kong, Hong Kong SAR, China

Correspondence
Carolin Dahms, Division for Ecology and Biodiversity, School of Biological Sciences, Faculty of Science, The University of Hong Kong, Hong Kong SAR, China.
Email: carolin.dahms.ac@gmail.com

Abstract

The current effects of global warming on marine ecosystems are predicted to increase, with species responding by changing their spatial distributions. Marine ectotherms such as fish experience elevated distribution shifts, as temperature plays a key role in physiological functions and delineating population ranges through thermal constraints. Distributional response predictions necessary for population management have been complicated by high heterogeneity in magnitude and direction of movements, which may be explained by both biological as well as methodological study differences. To date, however, there has been no comprehensive synthesis of the interacting ecological factors influencing fish distributions in response to climate change and the confounding methodological factors that can affect their estimation. In this study we analyzed published studies meeting criteria of reporting range shift responses to global warming in 115 taxa spanning all major oceanic regions, totaling 595 three-dimensional population responses (latitudinal, longitudinal, and depth), with temperature identified as a significant driver. We found that latitudinal shifts were the fastest in non-exploited, tropical populations, and inversely correlated with depth shifts which, in turn, dominated at the trailing edges of population ranges. While poleward responses increased with rate of temperature change and latitude, niche was a key factor in predicting both depth (18% of variation) and latitudinal responses (13%), with methodological predictors explaining between 10% and 28% of the observed variance in marine fish responses to temperature change. Finally, we found strong geographical publication bias and limited taxonomical scope, highlighting the need for more representative and standardized research in order to address heterogeneity in distribution responses and improve predictions in face of changing climate.

KEYWORDS
climate change, distribution changes, fish, marine, meta-analysis, methodological bias, range shift, temperature

1 | INTRODUCTION

Over the last century, global warming has had substantial impacts on marine ecosystems, with species locally extirpating (Pinsky et al., 2019), changing distributions in depth and latitude (Brown et al., 2016; Chen et al., 2011; Kortsch et al., 2012; Lenoir et al., 2020; Poloczanska et al., 2013), or in some cases shifting phenotypes in response to climatic pressures (Manhard et al., 2017; Perry et al., 2005; Ryu et al., 2020). In marine ectotherms such as fish, population distributional limits are influenced by physiological thermal constraints, as temperature affects critical functions such as metabolism, growth, and reproduction (Addo-Bediako et al., 2000; Angilletta et al., 2002; Roessig et al., 2004), and are restricted by narrower thermal safety margins (Pinsky et al., 2020). Accordingly, species' range changes in response to climate change have been up to sevenfold faster in the ocean as compared to on land (Poloczanska et al., 2013). As marine temperatures are forecasted to continue rising (Pörtner et al., 2019), the ability to predict fish redistributions will be vital to protect ecosystem functions, maintain food security, and other contributors to human well-being (Bonebrake et al., 2018; Pecl et al., 2017). A central challenge in predictive species range modeling has been the observation that, although many ranges have displayed anticipated poleward shifts in response to warming (Chen et al., 2011), a substantial number of range shifts have not followed projections and show significant variation in rate and direction of movements (Poloczanska et al., 2013; Urban, 2015), complicating population response predictions and conservation management. A key development in addressing this variation has been the acknowledgment that a suite of other non-temperature associated biotic factors, including species interactions (Ellingsen et al., 2020; Louthan et al., 2015), ecological and life history traits (MacLean & Beissinger, 2017), and eco-evolutionary dynamics (Cacciapaglia & van Woesik, 2018; Fredston et al., 2021; Nadeau & Urban, 2019), can also affect a population's ability to colonize and establish in novel environments, and should thus be incorporated into forecasts. However, an often overlooked factor in predicting and synthesizing climate change responses are differences in methodological approaches to measuring population distribution changes over time (Brown et al., 2016; Wolkovich et al., 2012), which might explain part of the observed variation in direction and velocity of responses to temperature, even within the same geographical and taxonomic context. For example, for some marine fish species within the same geographic regions seemingly contradictory responses are being reported. In the North Atlantic, for example, some studies suggest rapid environmental tracking at a rate corresponding to the local climate velocity (the pace and direction of climate shift across landscape; Frainer et al., 2017; Perry et al., 2005), while other multidecadal studies on range shifts suggest that only few are completely keeping pace with changing climate (Fredston-Hermann et al., 2020) and report significantly slower distribution responses (Campana et al., 2020). Addressing this variation will be key to improved response predictions informing conservation management, particularly as the magnitude of range shifts is likely to increase under climate change forecasts. Some syntheses have indeed highlighted the complexity of interacting functional and taxonomic predictors of climate responses in marine taxa (Lenoir et al., 2020), with Brown et al. (2016) demonstrating higher importance of methodological biases in marine range shift estimates than previously thought. To date, however, no recent synthesis with a focus on marine fish exists. As such, there is a need to build upon this initial work and to summarize the most recent literature to test an extended scope of interacting ecological factors influencing both the latitudinal and depth changes of marine fish species in response to climate change, and the confounding methodological factors that can affect their estimation.

The scarcity of analyses of methodological biases in marine range shift research is surprising considering the wide range of methods for data acquisition, processing, and modeling, resulting in high heterogeneity of research quality and results. While some methodological details need to be tailored to be suitable for specific taxa, ecosystems, and geographical conditions, large heterogeneity in other variables potentially affecting accuracy such as population sampling effort, temporal resolution, and statistical approaches remains. For example, redistribution inferences may be affected by sampling methods including choice of proxy for distribution measurement (Brown et al., 2011; Wernberg et al., 2012), including the "center of distribution" (COD) which constitutes the mean latitude of the spatial extent (e.g., Hsieh et al., 2009; Husson et al., 2022; Li et al., 2019), or a population's most extreme boundaries of longitude, latitude, or depth, inferred, for instance, by presence–absence data (e.g., Fredston-Hermann et al., 2020). How these distribution indices are obtained also affects the predictions that are produced (Brown et al., 2016): common data sources include abundance data from survey trawls by long-term fisheries or research programs (Perry et al., 2005; Yemane et al., 2014), tagging–recapture data (Hammerschlag et al., 2022; Neat & Righton, 2007), historical records (Kumagai et al., 2018), or genetic molecular methods (Knutsen et al., 2013; Spies et al., 2020). Each of these methods has various costs and benefits, such as tradeoffs associated with monetary expense, sampling effort, and feasibility in contrast to the likelihood of observing specific species or species types, achieving adequate sample sizes, and spatial–temporal resolution. Variation also exists in the data analysis stage, including the decision of whether to report movement estimates for a single species or cumulative inferences for whole assemblages reflecting changes in community traits and composition (e.g., Dulvy et al., 2008; Frainer et al., 2017). Response estimates in marine taxa were also shown to be affected when climatic predictors, other than temperature, such as salinity (Champion et al., 2021), oscillation indexes (Han et al., 2021; Nye et al., 2009), bathymetry (Hammerschlag et al., 2022; Li et al., 2019), or non-climatic drivers, such as food availability (Smith et al., 2021) or exploitation by fishing (Bell et al., 2015; Engelhard et al., 2014), were included (Brown et al., 2016). Nevertheless, robust data from wild marine fish populations incorporating both biotic and abiotic drivers of climate responses remain scarce (but see Adams et al., 2018), with potential differential effects on response estimates between single and multi-predictor models remaining unexplored. Overall, while this methodological variation is known to exist, it remains unclear whether

it has generated any systematic biases in the existing literature which may distort estimates of geographical shifts across fish species.

This review aims to summarize the current state and remaining gaps of knowledge on ecological and methodological factors influencing latitudinal and depth shifts in response to ocean warming in marine fish. First, we carried out a systematic literature review to gather data from existing original articles meeting criteria of measuring range shifts in response to temperature change. The aim was to investigate trends between rate of temperature change and range shifts across different niches, habitats, and other ecological factors such as life stage and marine exclusivity. Second, we summarized the current state of methodology prevalent across these studies, such as data acquisition and analysis methods, temporal and spatial resolution, and estimated the effects of study methods on population redistribution inferences.

2 | METHODS

2.1 | Literature search

The methodology of this review and meta-analysis was guided by the Preferred Reporting Items for Systematic reviews and Meta-analyses (PRISMA; Page et al., 2021).

Studies were identified by performing a literature search on the electronic database Web of Science in June 2022 with different combinations of the keywords '*fish geograph**', '*distribution*', '*range*', '*shift*', '*contract**', '*expan**' on studies dating until present, and were limited to articles in the research area of Zoology published in English language (Table 1). Additionally, suitable articles were identified further by scanning reference lists and review articles on related topics. Authors of four studies were contacted via email to obtain missing information on results and methodology. Of these, Dr. Maria Fossheim and Dr. Raul Primicerio provided species-wise raw data of latitudinal changes in distribution from the paper by Husson et al. (2022). The three remaining studies, for which no data were received, were dropped from analyses.

2.2 | Study selection

Records retrieved from the database were screened for duplicates, and for the first round of eligibility abstracts were manually checked to confirm the study focus included marine fish and distributional range changes in response to temperature (Figure 1). Four further rounds of filtering were performed according to inclusion and exclusion criteria (Table 2). This process was performed independently by one reviewer, while the second reviewer randomly selected a sample of five studies in every stage to assess, with disagreements between reviewers being resolved by consensus. Articles extracted from references were simultaneously screened for eligibility in the same manner.

Only original research papers documenting latitudinal or depth responses to temperature in marine fish were considered (Table 2). The terms range and distribution shifts are used in this study interchangeably and refer to, based on definitions used by Parmesan et al. (2005) and Sorte et al. (2010), a change in the distribution of native species' boundaries from their historical boundaries, including relocations, expansions, contractions along range edges. For a study to be included in the analysis, it had to discuss temperature as a likely driver of distributional range changes (preferably by statistical association) and have a span of at least 5 years, as fewer temporal sampling points may increase bias of short-term responses to climate fluctuations rather than long-term redistribution trends (Poloczanska et al., 2013). Studies looking at seasonal distribution responses or being only concerned with response predictions were excluded as this review is focused on historical long-term range changes. This review was limited to studies reporting quantified measurements of spatial change in mean latitude, either of centers of distribution (COD), or range edges (mean maximum and minimum latitudes, or lower and upper 5th latitudinal percentile), or estimates of depth changes (in meters) over a defined time span. The final step (Table 2) selected studies based on reliability of implemented methodologies. Studies were included if their methodology included presence–absence data, abundance data combined with another type of data, or molecular

TABLE 1 Search strategy and information sources. Six searches were performed in the online database Web of Science (WoS) including different combinations of the search terms 'fish geograph*', 'distribution', 'range', 'shift', 'contract*', 'expan*' with no date limitation for English original articles within the Zoology research area in June 2022; with results showing number of hits for each search term.

Search number	Search engine	Search term	Results	Type	Research area
1	WoS	fish geograph* distribution contract* temperature	45	Articles	Zoology
2	WoS	fish geograph* range shift temperature	210	Articles	Zoology
3	WoS	fish geograph* range expan* temperature	149	Articles	Zoology
4	WoS	fish geograph* range contract* temperature	44	Articles	Zoology
5	WoS	fish geograph* distribution shift temperature	280	Articles	Zoology
6	WoS	fish geograph* distribution expan* temperature	168	Articles	Zoology

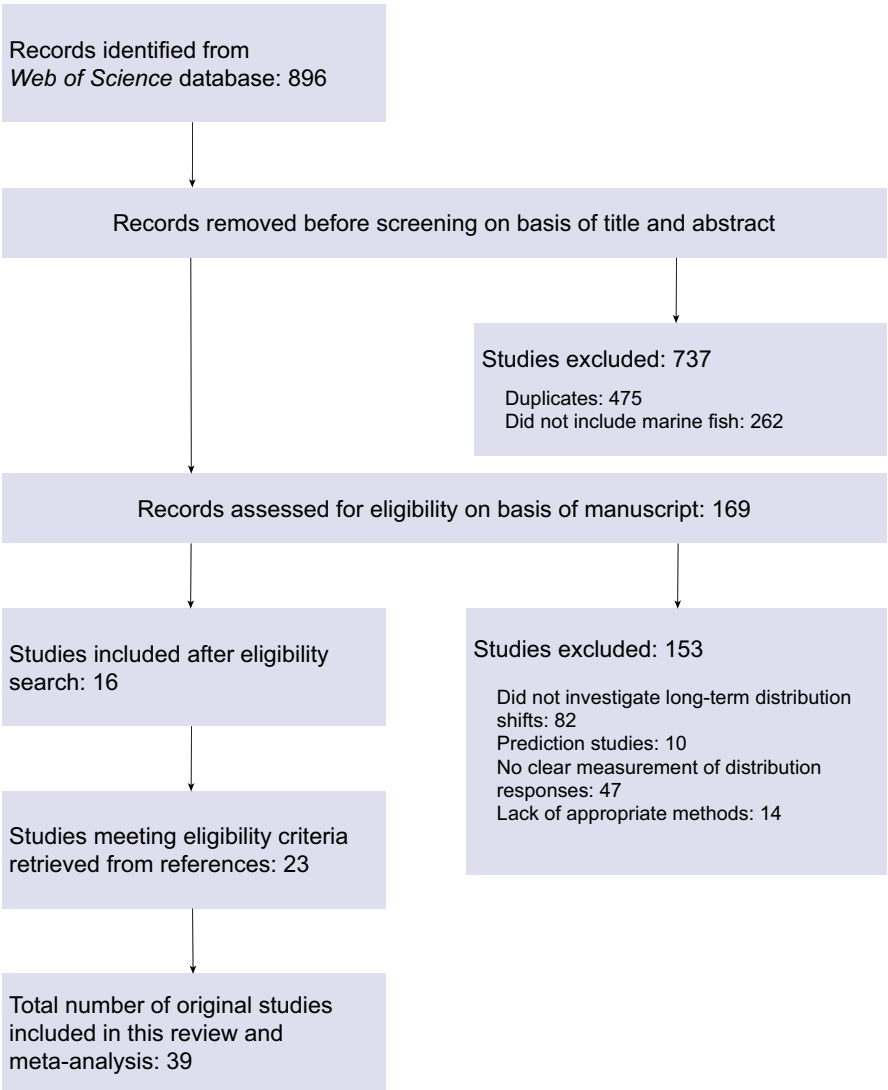

FIGURE 1 Flow Chart representing stages of the study selection process. From the original 896 records found in the bibliographic database Web of Science with search terms shown in Table 1, studies were scanned first by title and abstract for eligibility, and further filtered by criteria concerning methodology (see Table 2). 23 additional studies meeting criteria were retrieved from relevant references, totaling a final of 39 articles included in this analysis.

TABLE 2 Study selection criteria. After removal of duplicates from the database search, five rounds of screening were performed according to criteria concerning study focus and appropriate methodology, with the number of unique articles left after each selection round shown.

Filtering number	Study selection criterium	Criterium description	No. of unique studies
1	Fish and marine ecotype	Sampling marine fish	169
2	Range shift criteria	Change in range over latitudes, distribution changes, long-term (min. 5 years), not seasonal, no first sightings	87
3	No projections	Exclude prediction studies	77
4	Clear measurement	Calculated shift in latitude (by degrees or kilometers), e.g., of center of distribution or range edges	30
5	Appropriate data type	Abundance data combined with presence absence data (or clear measurement provided), or other methods such as long-term studies, tagging, or genetic molecular methods	16

methods or long-term tagging studies (at least 10 years with at least 10 individuals). Public science-based studies were only included if steps to reduce bias and false reporting were taken, such as verifying sightings by taxonomic experts. Reports based on new sightings only were excluded, as this type of data usually has low sample sizes and is prone to extreme outliers or misidentification. While sightings, including new sightings outside of previously known population limits, have been suggested to confirm range shifts or expansions (Fogarty et al., 2017), such measurements should be treated with particular caution due to increased chance

of detection bias and representing outliers (Brown et al., 2016). Accordingly, due to their reduced spatial and temporal resolution, many studies based on sightings failed to meet the minimum selection criteria. To avoid biases due to local population abundance changes, we excluded estimates based on changes in relative community composition and species richness or stemming solely from abundance data with sparse time points (less than 5 years).

2.3 | Data collection process

After the filtering process, an extraction sheet with variables of interest (described under *Data Items*) was created (Supporting Data S1). We pilot-tested five records and refined the sheet accordingly. In cases where variables were provided only in graphical rather than numerical representations (either not provided or authors were unresponsive to requests), numeric data were extracted manually from graphs using WebPlotDigitizer version 4.5 (Rohatgi, 2021). Numerical values of distribution responses over time, obtained by digitizing raster maps, were used to calculate latitudinal changes by fitting simple regression models between yearly mean latitude of species presence data and sampling years. For temperature, yearly temperature values were extracted from available graphs and fitted into linear regression models to obtain estimates of annual temperature change (°C year^{-1}) if not provided in the original articles; for studies comparing cold versus warm periods, yearly estimated mean values for each period were calculated, to then compare the difference in cold periods relative to the warm periods.

2.4 | Data items

Information from each study was extracted covering the following:

1. Species name (scientific and common), their habitat (demersal, pelagic, or reef associated) and niche affinity (deep-water, polar, temperate, or tropical), and commercial exploitation status, as provided by the study or otherwise sourced from the online fish catalog fishbase.org (version 02/2022); information on taxa and life stage, for example, whether sampled individuals were bony or non-bony fish and life stage (eggs, larvae, juveniles, or adults); and whether fish were marine exclusive or diadromous;
2. Whether a latitudinal redistribution was observed and the type (range shift, expansion, or contraction) and direction (north, east, south, west-wards, and whether this constituted a poleward direction);
3. Whether depth changes were recorded and if changes were significant and according to temperature predictions with deeper or shallower depth changes;
4. Temperature and its measurement type (sea surface or bottom water temperature), whether temperature was statistically tested for association with range shifts and whether it was a significant predictor of the changes; as well as yearly temperature change, as reported for sampling locations or approximate study area. If temporal temperature data were not provided, monthly sea surface temperature (SST) estimates in 1° resolution for each sampled raster grid within each study's duration were derived from the Hadley Centre Global Sea Ice and Sea Surface Temperature dataset (Rayner et al., 2003);
5. Whether other significant predictors of distribution changes, such as chlorophyll-*a* concentrations, ocean currents, pH, and oxygen concentrations in addition to water temperature, were identified by the study;
6. Methods of measurement which were classified into three categories: observations based on abundance data (A), presence–absence data (P), or a combination of both (AP), where we expect abundance-only data to bias toward lower range shift estimates as it is less influenced by potential outliers as in occurrence data. For the study by Husson et al. (2022), of which raw data were obtained for 29 species, two sets of LRS estimates were included in this study—one set of COD estimates weighted by abundance data and another weighted by presence–absence data, totaling 58 entries included in further analyses. We also considered which portion of a species' range was measured—the center (usually as the mean latitude or abundance weighed centroid), the leading or trailing edge (the upper and lower percentiles of a species distribution range), as we expect faster response rates at the leading front and center compared to the trailing edge;
7. If and how the overall size of shift (OSS) in depth and longitude/latitude was provided in a quantifiable form (e.g., °latitudes, km year^{-1}, or km °C^{-1}). Some studies provided only combined averages for grouped species (such as by habitat affinities) either for latitudinal and depth or latitudinal changes only and were marked appropriately (OSS_C, OSS_{C*}, respectively), which may reduce accuracy and statistical power in further meta-analyses. Distinguishing between different OSS reporting approaches (single or multi-population averages) allowed to test for their potential effect on reported distribution responses, as averages from multiple taxa are expected to be less accurate. Studies were further divided into three categories according to sampling frequency: those which measured distributional and temperature changes annually, irregularly (e.g., excluding some years during the study period), or between two points in time, such as studies which divided the study period into cold and warm years according to yearly temperature anomaly estimates and based further analyses on the comparison between cold and warm years;
8. Yearly rate of change in latitudinal, longitudinal range and depth, with estimates standardized into km year^{-1} and m year^{-1}, respectively, by extracting means from manuscripts or fitting linear regressions of yearly shift estimates if not provided. Where range shifts were reported in degrees, the result was converted into kilometers by the approximate conversion of 1 °latitude ≈ 110.574 km. While many studies reported shifts along the west–east axis, only six separate longitudinal response estimates

could be extracted, thus further analysis focused on latitudinal and depth shifts. Annual latitudinal range shift (LRS) rates were represented relative to poleward direction, where positive values represent poleward shifts and negative values represent shifts toward the equator. Positive depth shift estimates represent increasing depth and negative decreasing depth;

9. Data on the mean coordinates and sampling area size (in km^2): where not provided, approximate estimates were estimated based on extracted sampling map coordinates;
10. Location (continent, sea, or ocean) of the respective study and the number of sampled years. All data items were extracted separately where studies subdivided sampling location and time periods. For example, in the case when studies divided population distributions within an ecoregion into different areas, for example, round fish areas in the North Sea (Bluemel et al., 2022) or subregions in the Eastern Pacific based on fishing management areas or local oceanographic conditions (e.g., Li et al., 2019). Separate data entry points for analyses in this study also constituted instances of divided study periods, reflecting relevant temporal trends in biomass, or (seasonal) water temperature fluctuations (e.g., Bell et al., 2015; Bluemel et al., 2022);
11. Type of sampling method used to calculate distribution location, either from fisheries, such as through trawling, or from cameras and diving records, tagging studies, observations from long-term sightings, revision of historical records or information from genetic molecular analyses. Methods were grouped into trawl (486 observations), historical records (64), diving surveys (snorkel or camera, 9), tagging (3), or other fishing methods (33); and
12. The number of species per study investigated; and, depending on type of data collection method, the sample size in number of individuals collected, such as in tagging–recapture studies (e.g., Hammerschlag et al., 2022; Neat & Righton, 2007), reports based on long-term sighting records (e.g., Kumagai et al., 2018) or using population genetic techniques (e.g., Knutsen et al., 2013); and the yearly average of stations fished, such as in studies relying on abundance data from trawling surveys, were extracted. All data are provided in Supporting Dataset S1.

2.5 | Summary measures

The aim was to estimate standardized responses of latitudinal and depth shifts in marine fish distributions over time from studies that used a diversity of measurement methods. The meta-analyses were performed by selecting multivariate models with random effects, with the best models chosen according to likelihood ratio tests. We included 'Study' as a random effect to account for multiple estimates derived from the same paper. The primary analytical unit was the estimate for a given species or group of species of distance in latitude moved per year (LRS; km $year^{-1}$) in response to temperature. As the dataset to which the full model was fitted was reduced to 179 data points (which had estimates of both LRS and presence or absence of depth shifts), not all collected variables could be tested to avoid overfitting. We separately tested the effect of rate of depth change (m $year^{-1}$, 72 estimates), sampling method (trawl, historical records, diving surveys, and other fishing methods), and geographical location (the ocean basin of study site) on LRS estimates by fitting simple mixed-effect models with study as a random effect.

Factors which may affect LRS in response to *ΔTemperature* (°C $year^{-1}$) and were tested in linear mixed-effect models included:

a. Methodological factors: *OSS reporting*—whether shifts were reported per species (1) or groups of species for latitude and depth (C) or latitude only (C*); *Data type*—abundance (A), presence–absence (P), or their combination (AP); *Years sampled*—number of study years for which data were obtained; *First study year*; *Area size* (geographical area of sampling locations in km^2); *Marine exclusivity*—whether the taxa were diadromous or exclusively marine-dwelling; *Number of species*; *Study sampling frequency*—if data were collected every year (yearly), not for every year within the study period (irregular), or compared between two time periods; and *Non-temperature predictors*, a binomial factor indicating whether the study identified any other non-temperature predictors (which were not tested separately in this study due to low sample sizes);
b. Ecological predictors: *ΔTemperature*, the annual rate of temperature change (°C $year^{-1}$), to investigate whether degrees of distribution responses correlate with rates of temperature changes, as one might expect higher rates of temperature warming to provoke increased range shift responses; *Niche* (four categories: deep-water, polar, temperate, tropical); *Depth change* (binomial factor indicating whether depth change occurred or not); *Commercial exploitation status*, *Mean study latitude* and *Habitat*—seven categories (bathydemersal, bathypelagic, benthopelagic, demersal, pelagic–neritic, reef associated) grouped into pelagic, demersal, and reef associated. *Taxonomy* included five groups: bony fish, bony fish(eggs), bony fish (juvenile), bony fish (larval), and non-bony fish; *Range location* was either center, trailing, or leading edge of a distribution range. Testing of additional variables or interactions, such as between *Depth change* and *Niche* or *ΔTemperature* was limited by number of data points included ($n = 179$) after filtering for both estimated LRS and presence or absence of depth change. To investigate the effect of depth changes on latitudinal range changes, initially annual depth change rates (m $year^{-1}$) were included, however, the former yielded small model sample size ($n = 72$) and was thus replaced by the binomial *Depth change* predictor ($n = 179$), as many studies investigated the occurrence of depth changes without estimating rates.

The best model was selected by a back-ward selection process, starting with the "full" model (Equation 1) and reducing predictors until the best configuration was identified based on the lowest Bayes information criterion (BIC), calculated in the *lmerTest* package (v3.1-3, Kuznetsova et al., 2017) by maximum likelihood method.

From the full model, one outlier (i.e., one population's response estimate) identified with a Bonferroni outlier test was removed

(Bonferroni $p < .001$), which improved model likelihood (ΔlogLik = 5). Log-transformations to improve data normality were included for numerical predictors if model fit was improved. For each model (Table S2), log-likelihoods, p-values were calculated using Satterthwaite's approximations and three-way ANOVAs were performed for model comparison in the *lmerTest* package. The assumption of residual normality was determined to be satisfactory by visually inspecting residual and QQ plots.

For the best fitting model, marginal and conditional effect sizes (R^2) for mixed-effect models were calculated in the *MuMIn* package (v.1.46.0, Barton & Barton, 2015) according to Equations (1) and (2), respectively. The marginal R^2 represents variance explained by fixed predictors, while the conditional statistic shows the variance explained by both fixed and random effects, f representing the variance of fixed effects, α the variance of random effects, and ε the observation-level variance (Nakagawa & Schielzeth, 2013). Relative contributions of predictors to explained variation in range shift rates were compared by calculating partial marginal R^2 estimates (Nakagawa & Schielzeth, 2013).

$$R^2_{\text{marginal}} = \frac{\sigma^2{}_f}{\sigma^2{}_f + \sigma^2{}_\alpha + \sigma^2{}_E}, \tag{1}$$

$$R^2_{\text{conditional}} = \frac{\sigma^2{}_f + \sigma^2{}_\alpha}{\sigma^2{}_f + \sigma^2{}_\alpha + \sigma^2{}_E}. \tag{2}$$

The same model selection procedure was performed to identify the best model for depth change responses. After removing two outliers we fitted the full model to 104 observations, which included *ΔTemperature*, *Data type*, *Niche*, *Habitat*, *Commercial exploitation status*, *Sampled years*, *Mean study latitude*, and *Range location*. For the significant predictors according to BIC partial effects were estimated and plotted, estimates are reported in Table S4.

2.6 | Effect size estimation by correlation coefficients

The relationship between temperature change and LRS was quantified by extracting correlation coefficient (r) values from retrieved studies. Where coefficients were not reported, numerical values were obtained by digitizing figures when available and performing linear regressions. We used Fisher's z transformation to calculate a standardized effect size for each individual observation, where $z = 0.5 \times \log[(1+r)/(1-r)]$. The variance of z was calculated as $1/\sqrt{(n-3)}$ (Borenstein et al., 2009), where n corresponds to sample sizes which were normalized, as they originated from studies reporting either the number of individual fish caught or trawled stations and constituted different value ranges.

The overall significance of the temperature–LRS relationship was assessed by a random-effects model in R package *metafor* v.3.8-1 (Viechtbauer, 2010) using the transformed effect sizes. We assessed the heterogeneity within significant predictors with identified by the best multivariate model by an inverse-variance-weighted hierarchical mixed-effects meta-regression of z, including Study as a random effect to account non-independence of multiple observations within a single study. Among categorical predictors from the best fitting model, only Data type and Niche category had sufficient data (>1 r estimates per level). All parameters were calculated using maximum likelihood, which is preferred when fitting hierarchical mixed-effects models (Zuur et al., 2009).

We combined effect sizes across all studies for each Data type and Niche affinity to obtain the mean effect sizes which represent the weighted average of relationships between temperature and LRS. As the conditional variance is inversely related to n, studies with larger sample sizes had a greater weight. Effects were considered statistically significant if the 95% confidence interval (CI) did not include zero. Back-transformed z values to correlation coefficients were plotted for each data type and niche, where positive r values indicate increasing latitudinal change (km year^{-1}) per °C year^{-1}.

2.7 | Assessment of methodology

Summary statistics for the frequency of publication years, mean study period, and mean study area size with standard deviations were calculated. Methodological aspects of investigated studies, such as the type of data used to calculate range shifts, and how and if LRS was reported, were summarized.

To identify geographical publication biases, studies were grouped into locations (North Sea, Barents Sea, Northwest Atlantic, East Pacific, Bering Sea, Yellow Sea, Southwest Atlantic, central Indian Ocean, central Atlantic, and central Pacific) based on their central coordinates of sampling area and visualized on a map with frequencies representing number of studies per location. Study locations in central Indian, central Atlantic, and central Pacific originated from a single study (Worm & Tittensor, 2011) which had large sampling areas. Total numbers of each type of range change (shift, expansion, or contraction), and direction of shift (north, south, west, and east) of retained population responses ($n = 595$) were calculated. Trends of shift directions were reported as the proportion of populations per location moving in either of the four directions.

To assess potential publication bias, a funnel plot and regression of the effect sizes (reported LRS estimates) on sample sizes (n) was computed. Depending on the study method, n was either the total number of fish sampled per population or average number of stations per year trawled. Symmetry of the funnel shape was inspected visually and tested with a regression of effect sizes (y) on $1/\sqrt{n}$ (Tang & Liu, 2000), where p-values below significance threshold ($\alpha = 0.05$) suggest potential publication bias (Figure S2a,b). While for funnel plot regression analyses the weighted standard error of effect sizes is most commonly used (e.g., Egger's test; Egger et al., 1997), this measure was not available for most studies and was replaced by sample size in Tang and Liu's test (2000), which addresses the inflated false positive rates associated with the former regression test (Jin et al., 2015).

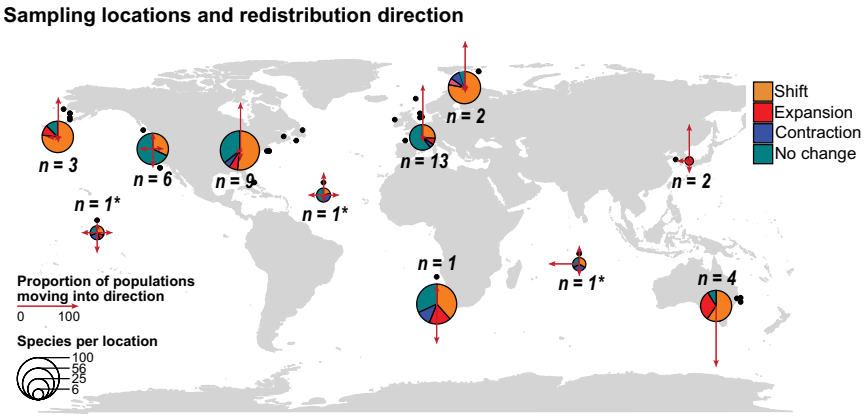

FIGURE 2 Map of sampling locations and sizes with type of range shift. From articles included in this review ($n = 39$), study locations were grouped into 11 locations which are represented by pie charts. Cumulative number of species sampled per location is shown as pie chart circle size, with number of studies per location denoted as n. Type of range change is color-coded: range shift (orange), range expansion (red), range contraction (blue), no change (green), and shown in proportions from total counts of sampled populations per location. Arrows indicate proportions of populations per location moving along four directions (north, east, south, and west). Black points represent the center of individual study sampling locations. Range shift estimates from multi-species estimates ($n = 92$) were excluded. Asterisks (*) indicate the same single study by Worm and Tittensor (2011) covering most of the Pacific, Atlantic and Indian oceans.

Average LRS estimates were expressed in medians and respective interquartile ranges (IQRs), that is, the difference between the upper lower quartile range of the data, due to the tendency for the data to have skewed distributions and outliers. For predictors from mixed-effect models, marginal effects (β) were reported with 95% confidence intervals (package *marginaleffects* v.0.9.0, Arel-Bundock, 2023). Data were analyzed and visualized in R (version 4.2.3; R Core Team, 2023).

3 | RESULTS

3.1 | Study selection

A total of 39 studies were identified for inclusion in the review (Table S1; Alheit et al., 2012; Bell et al., 2015; Bluemel et al., 2022; Champion et al., 2021; Chust et al., 2019; Dulvy et al., 2008; Engelhard et al., 2011, 2014; Fossheim et al., 2015; Fowler et al., 2017; Fredston-Herman et al., 2020; Hammerschlag et al., 2022; Han et al., 2021; Hsieh et al., 2008, 2009; Hughes et al., 2014; Hurst et al., 2012; Husson et al., 2022; Kotwicki & Lauth, 2013; Kumagai et al., 2018; Last et al., 2011; Li et al., 2019; Mueter & Litzow, 2008; Neat & Righton, 2007; Nicolas et al., 2011; Nye et al., 2009; Olafsdottir et al., 2018; Overholtz et al., 2011; Perry et al., 2005; Pinsky et al., 2013; Rose et al., 2000; Sabatés et al., 2006; Smith et al., 2018; Swain & Benoit, 2006; van Hal et al., 2010; Vestfals et al., 2016; Worm & Tittensor, 2011; Yasumiishi et al., 2020; Yemane et al., 2014). The search of Web of Science databases provided a total of 896 records. After adjusting for duplicates and studies which did not include marine fish, 169 studies remained. Of these, another 153 studies were discarded during the filtering process through reviewing the abstracts and examining article methods in detail. An additional 24 studies that met the criteria for inclusion were identified by checking the references of relevant papers and searching for studies that have cited these papers (Figure 1).

3.2 | Geography

The average sample size across the 11 major locations was 54.1 (±39.3) species per location, with more than half (77%) of all populations displaying a range shift, of which 16% expanded range, and 9% contracted their range, when excluding multi-species LRS estimates (Figure 2). Overall, more than half (54%) of the populations moved poleward, particularly in Asia (4 of 4), Australia (50 of 55), the North Sea (52 of 80), the Bering Sea (40 of 56), and the Barents Sea (49 of 59). Regarding longitudinal shifts, populations shifted overall eastwards (median = 1.7 km year^{-1}; IQR = 11.8, $n = 6$). While in some regions such as in the East Pacific, central Atlantic and Indian oceans responses were less significant or multidirectional (Figure 2), many studies investigated movements only across the north–south axis, which could have biased lower frequencies of shifts on the east–west axis.

When comparing individual LRS rates among major geographical locations, the southwest Pacific (Australian coast) had by far the fastest latitudinal range changes (median$_{LRS}$ = 20.7 km year^{-1}; IQR = 11.9), followed by the North Atlantic (median$_{LRS}$ = 8.5 km year^{-1}; IQR = 18.4) and South African populations (median$_{LRS}$ = 7.6 km year^{-1}; IQR = 17.0). In the Northeast Pacific, marine fish shifted around 0.8 km year^{-1} (IQR = 0.1; $n = 5$), while the Bering Sea saw shifts of 1.0 km year^{-1} (IQR = 2.5, $n = 57$), and the Northwest Atlantic 3.2 km year^{-1} (IQR = 3.9, $n = 61$).

3.3 | Methodology

The mean study duration was 41 (±49) years, at a sampling area size of 356,628 (±358,127) km^2 on average. Strong geographical bias of study location was observed—half of the studies originated from North America, with almost a third (31%) performed in Europe. Australia, Asia, and Africa had less representation with 11%, 6%, and 3% of the identified research articles, respectively. No eligible reports from South America and Antarctica were identified.

Most frequently investigated taxa were classified as tropical ($n=65$), followed by temperate ($n=52$), deep-water ($n=37$), and 19 polar populations (Figure S1). The most frequently studied fish families included *Pleuronectidae* ($n=80$, particularly *Microstomus*, *Atheresthes*, *Eopsetta*, and *Pleuronectes* spp.), *Gadidae* ($n=52$, *Gadus*, *Melanogrammus*, *Pollachius* spp.), *Scombridae* ($n=28$, *Scomber* and *Thunnus* spp.), *Rajidae* ($n=21$, including *Amblyraja radiata* and *Leucoraja* spp.), and *Sebastidae* ($n=18$ such as *Helicolenus dactylopterus*, *Sebastes* spp.).

Nearly 80% of studies implemented statistical tests to investigate range shift association with temperature changes, and assessed range changes annually (Figure 3), with only few studies measuring changes irregularly or comparing two time periods. From those studies confirming range shifts, most reported LRS sizes for individual species (77%), with four reporting combined shift sizes for groups of at least two species. The most common types of data used across studies included abundance (81%) and presence–absence data (67%), which in some studies were used in combination. Most samples originated from trawling (74%) or other fishing data, while 10% and 5% of studies revised historical occurrence records from literature and carried out tagging–recapture experiments, respectively.

From visual inspection of funnel plots of regressed LRS effect sizes on sample sizes, there was little evidence for risk of publication bias, particularly when the sample size proxy was individuals sampled per population (Figure S2a). Although a regression test suggested significantly asymmetrical funnel shape ($F_{1,152}=396$; $p=.048$) when expressing n as mean yearly rate of stations trawled, this proxy provided considerably less resolution of effect size distribution due to sampling of multiple populations with high heterogeneity in LRS across the same fishing stations (Figure S2b).

3.4 | Factors affecting range shift estimation

The best model (ΔBIC = 53.4 compared to full model) included ecological predictors *ΔTemperature*, *Niche*, *Depth change*, and *Mean study latitude* and methodological variables *OSS reporting*, *Data type*, *First study year*, and *Other predictors* (Table S2). The model had an intermediate effect size when considering only fixed effects ($R^2_{\text{marginal}}=0.30$), with methodological factors explaining 10% of the variance in range shifts, and combined ecological factors accounting for 7%, while niche affinity had the highest single proportion of 13% (Table S5; due to shared variances, individual predictors did not add up to total marginal variance).

From the filtered dataset for outliers, from which the highest likelihood model was fitted, 179 individual population-wise LRS estimates were retained, while 92 entries provided LRS estimates for grouped populations, such as species combined into assemblages according to niche or temperature affinity (e.g., Dulvy et al., 2008; Li et al., 2019; Pinsky et al., 2013). LRS was on average higher among studies which reported range shift sizes for individual populations as compared to those that grouped populations (Figure 4c); and lower when based on occurrence data compared to those derived from abundance data or a combination of the two (Figure 4d). Moreover, estimates tended to be lower if studies started in earlier years (Figure 4h). As sea temperature significantly increased over the years (ANOVA test: $F_{1,340}=9.81$, $p=.002$) and was positively correlated with LRS, this effect might be rather due to methodological biases, driven by significantly earlier study start among the fastest shifting temperate and tropical species, as study timing differed significantly among niche affinities (ANOVA: $F_{3,38}=34.8$, $p<.001$).

Range shift estimates were lower in studies which found significant effects of other non-temperature predictors (Figure 4e). Besides temperature, the most common explanatory variable for changes in marine fish ranges included oceanic oscillation indexes such as from the Atlantic and Pacific oceans, which was reported nine times across reviewed studies (Table 3). Other factors included abiotic marine factors such as ocean currents, salinity, depth and chlorophyll-a concentration ($n=9$), and exploitation by fishing ($n=7$). Density dependence was mentioned five times, which in some cases had larger effect sizes than temperature.

For individual estimates, the rate of latitudinal shifts was greater in populations which did not change mean depth ($\beta=9.68$ km year^{-1}; 95% CI (6.54–12.82); $p<.001$), compared to populations which were reported to shift their depth distribution ($\beta=6.58$ km year^{-1}; 95% CI (3.47–9.69); $p<.001$; Figure 4b). The deeper populations moved, the less latitudinal change was observed ($\beta=-3.95$ km year^{-1} for every meter in depth increase, $p<.001$, Figure 5e). LRS increased with annual temperature change, with tropical taxa moving the fastest at 18.46 km C^{-1} (95% CI (14.62–22.3); $p<.001$), while deep-water populations were the slowest at 8.23 km C^{-1} (95% CI (4.95–11.5); $p<.001$; Figure 4a), the latter having the highest proportion of non-poleward shifts (43% of responses). Responses also varied with a population's geographical location, as LRS estimates were highest among high-latitude taxa (Figure 4g).

The positive correlation between LRS and temperature change was supported by weighted means of correlation coefficients, with a grand mean effect size of 0.29 (95% CI (0.16–0.43)). The effect of temperature on climate responses varied as a function of niche and the type of data used by studies, with polar taxa showing nearly a twofold larger correlation coefficient ($r=.53$) compared to temperate counterparts (Figure S3).

Although not included in the final model, differences in responses between range locations were observed with leading edge populations moving poleward the fastest (median$_{\text{LRS}}=7.2$ km year^{-1}) compared to trailing and center populations (4.2 and 1.6 km year^{-1}, respectively; Figure 5a); and exploited

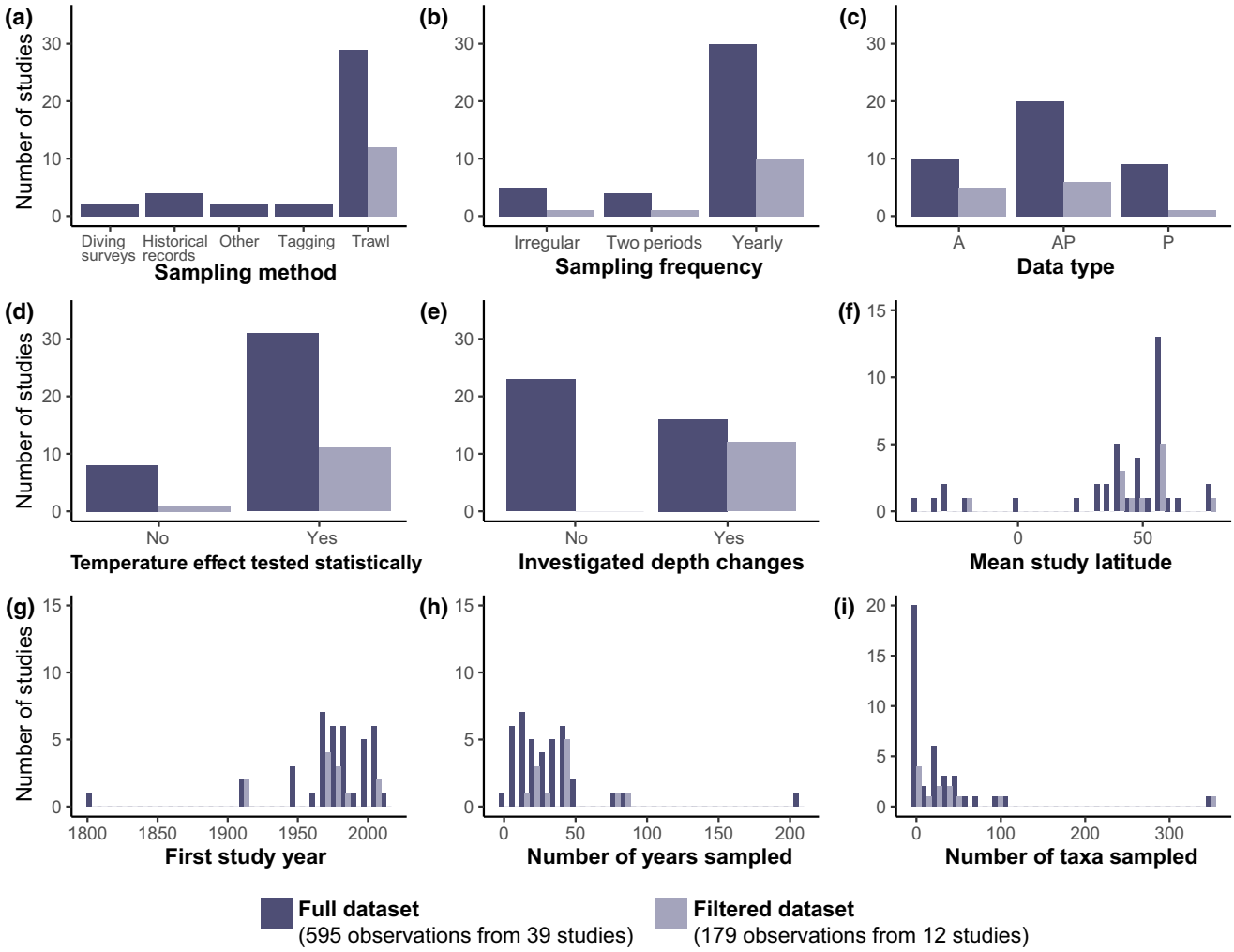

FIGURE 3 Frequency of methodological aspects across studies. Colors indicate counts for the complete dataset (dark) from 39 retained studies yielding 595 range shift responses to temperature change, or the data included in multivariate models (light) to test latitudinal range shift responses (12 studies with 179 observations). The reduction from 342 latitudinal shift estimates was due to only 179 observations investigating depth changes (e). Plots show (a) data acquisition method; (b) sampling frequency: whether sampling every year, sporadically or comparing two time points; (c) data type: based on abundance (a), presence–absence data (P) or a combination of the two (AP); (d) whether the study performed statistical analyses to confirm temperature effects on range shifts; (f) mean current latitude of sampling area; (g) first year of study period; number of sampled years (h) and taxa (i).

populations moving slightly less (2.1 km year^{-1}) than non-exploited counterparts (3.0 km year^{-1}; Figure 5c). Bony juvenile fish shifted poleward faster (15.2 km year^{-1}) than adults (2.8 km year^{-1}), while non-bony fish on average moved equatorward by 0.2 km year^{-1} (Figure 5j).

Variance in depth changes was best explained by niche affinity (18% of variation), commercial exploitation status (7%), position within the range distribution and rate of temperature change (3% each), as well as data type (28% of variance), according to the best model which explained overall 47% of the variance in depth responses (ΔBIC = 12.6 between full and final model). Depth shifting populations ($n = 104$) moved to overall shallower depths with higher rates of temperature change (Figure 6b), while non-exploited species deepened their distributions significantly faster ($\beta = 1.96$ m year^{-1}; 95% CI: 1.3–2.6) than exploited taxa (0.59 m year^{-1}; 95% CI: 0.9–3.4; Figure 5d).

Studies estimating depth changes based on abundance data found overall decreasing depth responses, while abundance–occurrence data tended to suggest increasing depths (Figure 6c). Individuals at the trailing edge of population distributions were showing the largest move toward deeper waters (Figure 6a), particularly among deep-water species. Tropical taxa showed the slowest depth responses, with shallowing trends at the center and leading edge (Figure 5a). Out of 104 estimated depth shift responses, the majority (73%) shifted in the direction as expected from temperature changes (i.e., to cooler waters).

4 | DISCUSSION

We found that the majority of fish populations have responded to thermal warming with a poleward change in their geographical

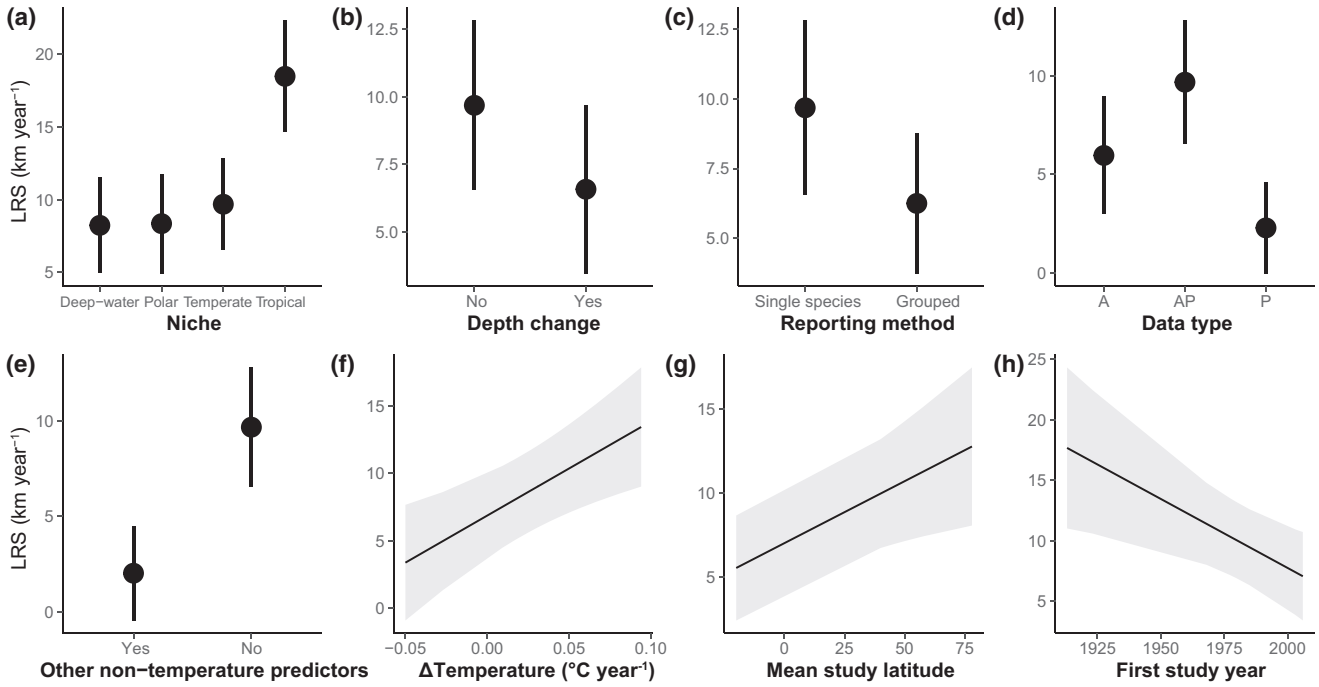

FIGURE 4 Latitudinal range shift predictors. Partial effects of fixed predictors included in the final mixed-effect model ($\Delta BIC_{full\text{-}final\ model} = 53.4$) explaining latitudinal range shift (LRS; km year^{-1}) in response to temperature in marine fish. Points indicate predicted means, and bars and grey shading the 95% confidence intervals. Positive LRS estimates indicate poleward shifts, while negative estimates represent equatorward movements. OSS reporting method had two categories for studies reporting LRS either for taxa individually (single) or the mean of multiple taxa (grouped). Data type was either abundance (A), presence–absence data (P) or a combination of the two (AP). According to temperature change estimates from included studies, tropical populations experienced the slowest yearly temperature increase (0.02 ± 0.02°C year^{-1}), followed by deep-water (0.03 ± 0.03°C year^{-1}), temperate (0.04 ± 0.03°C year^{-1}) and polar taxa (0.05 ± 0.1°C year^{-1}).

TABLE 3 Frequency of other significant predictors of range changes. Predictors other than temperature with significant effects on redistribution in the 39 reviewed studies were summarized into the shown categories, and counted as unique occurrences across studies (*n*).

Other identified predictors	*n*
Oceanic oscillation indexes	9
Other oceanic variables (currents, salinity, depth, chlorophyll-a concentration)	9
Fishing pressure	7
Population abundance/density dependence	5
Reproductive (recruitment, spawning stock biomass, buoyancy)	3
Food availability	1

distribution (Figure 2), which is consistent with forecasts for future responses to further climate change (García Molinos et al., 2015; Schickele et al., 2020). Importantly, however, we also found substantial heterogeneity in degree and direction of biogeographical shifts (Champion et al., 2021), which was influenced by both ecological factors such as niche and depth changes, and methodological factors associated with data collection and reporting (Figure S3).

4.1 | Ecological factors influencing distribution responses

We found a significant positive correlation between rate of LRS and latitude which bolsters previous findings by Lenoir et al., 2020, confirming the expectation of faster poleward movements in the Northern Hemisphere where oceans have been warming at faster rates than in the South (Friedman et al., 2013). However, mean current latitude explained only 2% of the variance in LRS, while niche affinity was a more important predictor of latitudinal and depth shifts globally. Results also show that tropical species shift latitudinally more rapidly (Chaudhary et al., 2021; McLean et al., 2021) in response to warming than other marine fishes (Figure 4a), with disproportionate poleward movements (Figure 2). This is consistent with high sensitivity to temperature change in stenothermic species with narrow thermal tolerance limits and restricted spatial ranges, such as tropical species inhabiting shallow waters close to their tolerance limits (Storch et al., 2014). Indeed, we found that reef-associated fish tended to display the most rapid latitudinal shifts compared to other habitat affinities, although this trend was not significant (Figure 5b). Other studies have shown that, in comparison to temperate fish, tropical species may have increased sensitivity and lower adaptability to thermal increase (Comte &

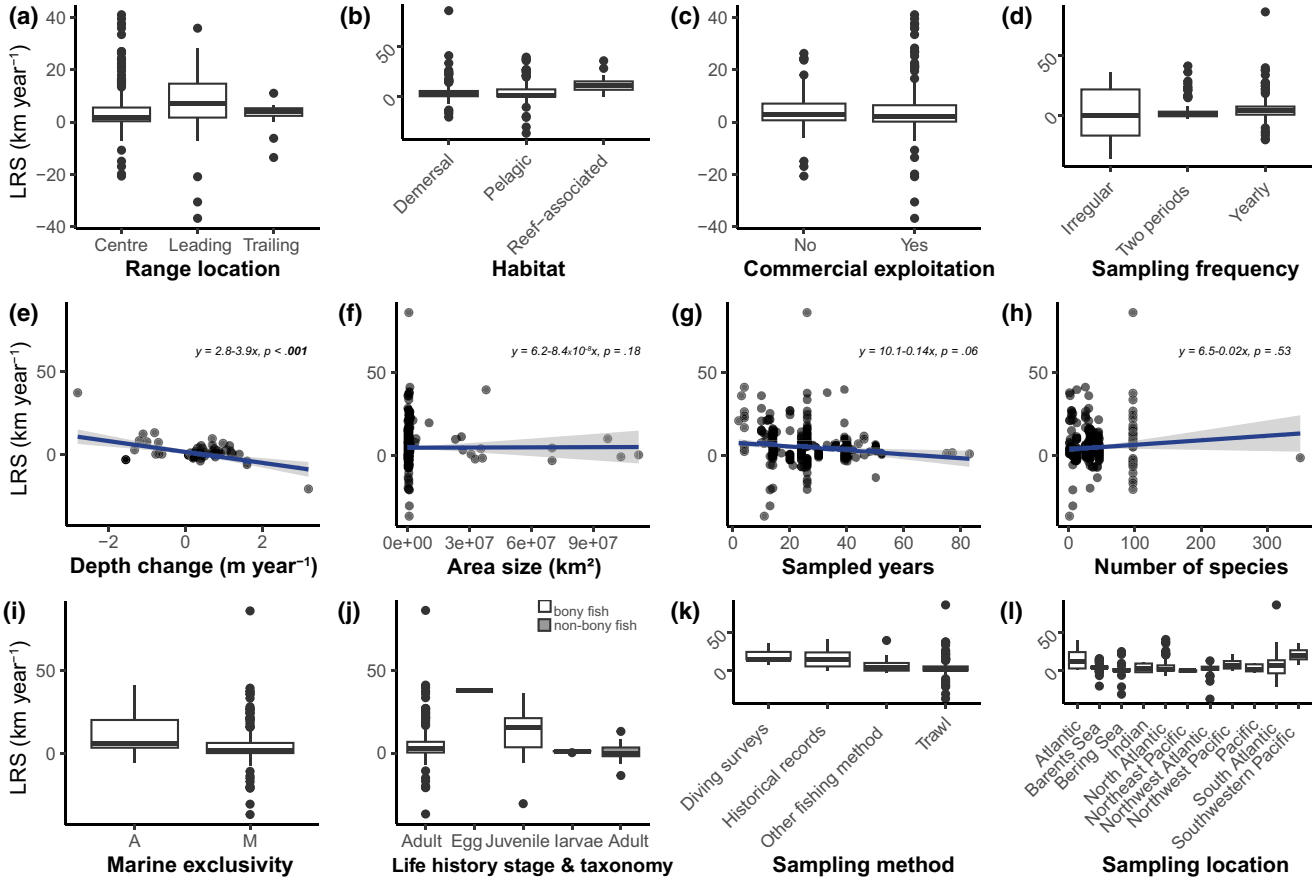

FIGURE 5 Non-significant latitudinal range shift predictors. Effects of excluded predictors from simple mixed-effect models with Study as a random effect. Rate of depth change (e, 72 estimates), sapling method (k) and location (l) were tested separately and were not included in the models to avoid overfitting due to limited data. Depth change showed a significantly negative correlation with LRS ($p < .001$). Positive LRS estimates indicate poleward shifts, while negative values indicate equatorward movements.

Olden, 2017; Nati et al., 2021) and may thus be more likely to shift distributions to track suitable thermal habitat.

Changes in depth in response to warming influenced rate of LRS, with depth shifting taxa on average moving latitudinally by 3.95 km year^{-1} less for every meter in depth increase per year. This suggests that fish populations might not need to shift horizontally if they can adjust their depth to track their favorable temperature niche (Hollowed et al., 2007), which was demonstrated in groundfish finding thermal refuge across rugged seabeds and canyons in the Western Gulf of Alaska (Li et al., 2019) and illustrated by tropical species having the slowest and shallowing depth changes (Figure 6a). In line with predicted narrow temperature tolerance limits of stenotherms (Storch et al., 2014), we found polar species to experience some of the fastest increases in depth of occurrence. It is well established that polar fish communities can experience rapid and disruptive community structure changes due to arrivals of poleward shifting boreal species (Fossheim et al., 2015; Frainer et al., 2017). Experiencing the fastest temperature increase (Stocker, 2014), but being limited in poleward expansion due to the edge of the sea shelf (Wassmann et al., 2006), arctic fish species might depend on moving to deeper waters as a last resort to avoid extirpation (Fossheim et al., 2015). Although leading edges showed faster poleward LRS rates compared to the trailing edge and center (Figure 5a), this difference was not significant, which is in line with previous findings suggesting similar warming sensitivities at opposite distribution fronts (Brown et al., 2016; Lenoir et al., 2020; Sunday et al., 2012), but in contrast to other reports (Poloczanska et al., 2013). Interestingly, faster depth increases were observed at the trailing edge across all niches (Figure 6a), despite similar rates of warming at the trailing and leading edges ($\text{mean}_{\Delta\text{temperature}} = 0.03°\text{C year}^{-1}$), suggesting that depth responses at contracting range fronts may be a response to other drivers. While additional drivers such as habitat and prey availability or resource competition for these responses were not investigated by studies, we found that commercially exploited species changed their mean depths at lower rates than non-target counterparts (Figure 6d). Restricted responsiveness to climate change in exploited populations might be due to reduced ability to establish in new areas due to localized effects of fishing pressure on abundance and age structure (Rindorf & Lewy, 2006), which has been observed in fish stocks globally (Engelhard et al., 2014; Hsieh et al., 2008; Last et al., 2011).

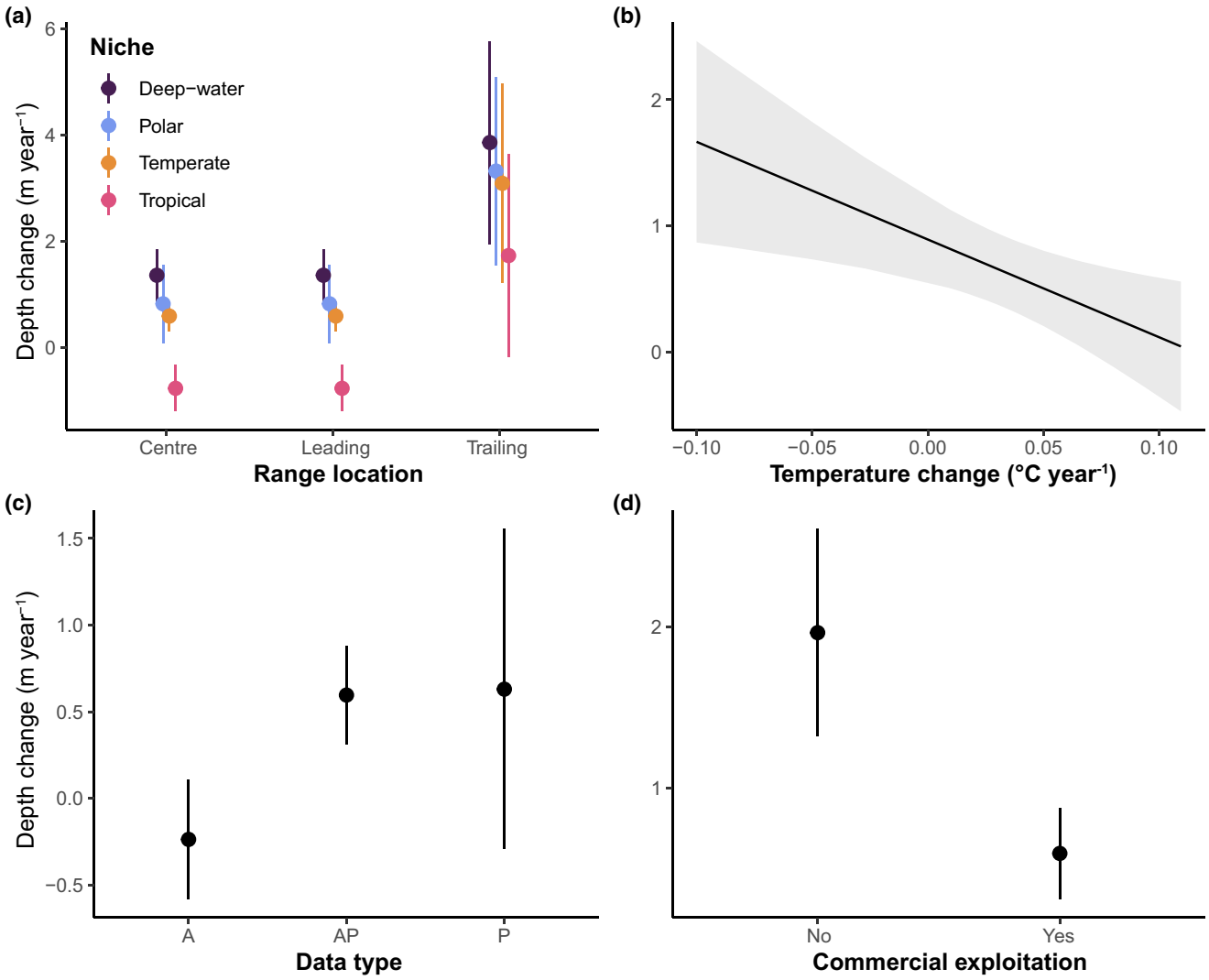

FIGURE 6 Depth shift predictors. Term plots of fixed predictors included in the final model (selected according to BIC) explaining changes in average depth (m year^{-1}) in response to temperature change. Points indicate predicted marginal means, and bars and grey shading the 95% confidence intervals. Data type was either abundance (A), presence–absence data (P) or a combination of the two (AP). Positive depth change values represent deepening, while negative values indicate distribution changes to shallower waters.

Other factors, such as life stage and taxonomy, were not found to significantly affect latitudinal range shift response, even though sensitivity to warming is thought to be partly dictated by thermal tolerances changing throughout the marine fish life cycle (Killen et al., 2007; Pörtner & Farrell, 2008; Whitney et al., 2013). Early life stages, embryos in particular, are most sensitive with their thermal limit being on average 8°C lower than in other stages (Dahlke et al., 2020), and are likely a major predictor of population responses to warming (Dahlke et al., 2020). Although we found faster range shifts for larvae and juveniles compared to adult fish, our inferences might have been affected by limited statistical power and unequal sample sizes (15 and 254 population responses, respectively). Similarly, the number of responses for anadromous marine species was limited ($n_{populations}=14$, mostly *Oncorhynchus* spp. ($n=8$); Fredston-Hermann et al., 2020; Mueter & Litzow, 2008; Nye et al., 2009; Yasumiishi et al., 2020). Thus, robust empirical data of more diverse marine life stages or life cycles could facilitate important hypotheses on non-adult temperature response outside laboratory settings (but see Barbeaux & Hollowed, 2018) or inferences of potential range shift limitations in diadromous fish species due to affinity to natal homing grounds (Hare et al., 2016).

4.2 | The effects of variable study methods

Both LRS and depth responses were greater when estimated from both abundance and presence–absence data together than from abundance data alone (Figures 4d and 6c). Abundance data, mostly obtained from fishery or research trawling data, such as from the Nansen Survey Program in Namibia and Angola (Yemane et al., 2014), has been widely used across population distribution literature as it is thought to represent the whole population

range, and to be less sensitive to search effort and misleading outliers (Brown et al., 2016). While fishery survey data can provide temporally and spatially high-resolution data, and decade-long records can be conveniently retrieved for new analyses, its frequent usage has created publication bias toward commercially important fish species in the northern hemisphere (Figure S1). Alternatively, recent studies measuring changes in range limits, such as by Fredston-Hermann et al. (2020), use only presence–absence data to infer changes in leading and trailing edges in the Northwest Atlantic, arguing that abundance data do not truly reflect potential changes of species ranges, but is rather confounded by density dependence effects through abundance changes caused by non-climatic factors such as fishing (Quinn & McCall, 1991). However, abundance and climate driven distribution shifts should be possible to distinguish by direction of shift: the former should be unselective in direction while the latter is expected to move along the temperature gradient. In line with findings by Brown et al. (2016), we observed that studies incorporating occurrence-based data had substantially higher range shift estimates than those using abundance data only, suggesting that presence–absence data may be more sensitive to outliers. Although response estimates from presence–absence data only were lower than estimates derived from a combination of occurrence and presence–absence data, all former observations originated from one single study and should thus be interpreted with caution.

Previous climate response syntheses have argued that single-species studies confirming range shifts consistent with warming may be more likely to be published and thus bias meta-analyses (Parmesan, 2007). While we did not identify publication bias due to low numbers of investigated species or sampled years, we found that range shift estimates reported as the average of multiple taxa were lower than those derived from individual species estimates. This could be due to random bias due to lower sample size in the four studies from which all group-wise estimates were obtained (Dulvy et al., 2008; Li et al., 2019; Perry et al., 2005; Pinsky et al., 2013) or indeed indicate that single-taxa studies are over-represented (Figure 3i). Unexpectedly, estimates of LRS decreased with date of the first study year (Figure 4h), which likely reflects methodological biases of earlier and longer reporting history of faster shifting temperate and tropical taxa. This also highlights that climate response studies for deep-water and polar species encompass shorter and more recent time periods, possibly biasing climate response estimations.

Contrary to expectations, we found only a weak negative effect of study area size on LRS values (Figure 5f). A plausible source of distributional response variation is the geographical scope of each study, with spatial sampling extents varying widely, and often spanning across whole oceans (e.g., Worm & Tittensor, 2011). The common assumption of marine ecosystems being almost barrier free with species generally occupying all thermally suitable areas (Sunday et al., 2011) has been challenged by accumulating evidence of local population subdivision due to a wide range of biotic and abiotic factors (Baker & Hollowed, 2014; Barbeaux & Hollowed, 2018; Sandoval-Huerta et al., 2019; Sherman et al., 2008) which likely causes variation in exposure and responses to water temperature changes (Poloczanska et al., 2013). Only a few studies have accounted for subregional differences in topography and oceanic factors such as currents or salinity gradients, which all might delineate divisions across marine species distributions (Kleisner et al., 2016; Marshall et al., 2016; Momigliano et al., 2019). For example, a study in the Northeast Pacific by Li et al. (2019) demonstrated significant heterogeneity in marine fish responses to marine warming due to subregional topography and geography characteristics. Other studies have measured shifts separately for identified central population areas based on ecologically relevant locations, such as known breeding grounds (Bluemel et al., 2022). A promising tool to investigate heterogeneity in range shift responses is genetic molecular techniques which help delineate cryptic diversity (Jokinen et al., 2019) and estimate dispersal velocity of locally adapted genotypes (Jonsson et al., 2018). These techniques may improve response predictions and infer historic range changes and migration routes for both ancient and contemporary distribution responses (Knutsen et al., 2013; Robalo et al., 2020; Spies et al., 2020), although such genetic applications to climate range shift research are still scarce.

The variation in species' responses to climate change has been addressed through various predictors such as local adaptation (Jonsson et al., 2018), phenotypic plasticity (Donelson et al., 2019; Reusch, 2014), species interactions (Figueira et al., 2019; Torres et al., 2008), food availability (Fossheim et al., 2015), and even social behavior (Smith et al., 2018). In some marine fishes, the likelihood of successful range expansions and colonization of new habitats was explained by species-level traits such as dispersal ability and being a generalist (Sunday et al., 2015), although trait-based range shift forecasts seem to have generally little explanatory power (Angert et al., 2011). While the majority of reviewed studies investigated (but not always statistically tested) temperature as the sole predictor, a significant proportion of climate response variation is likely explained by a multitude of climatic and biotic factors instead of temperature alone (McHenry et al., 2019). For example, some studies suggest that range shifts may be driven by abundance changes, as density dependence may lead to range expansions during high abundance and vice versa (Kotwicki & Lauth, 2013; Olafsdottir et al., 2018; Swain & Benoit, 2006; Worm & Tittensor, 2011; Yasumiishi et al., 2020). Our results suggest that marine range shift estimates from single-predictor studies focusing solely on temperature were higher than those originating from studies which identified at least one additional driver to temperature (Figure 4e), possibly due to the confounding effects of additional variables explaining part of the LRS variation. While some studies found effects of fishing pressure (Bell et al., 2015; Engelhard et al., 2014; Neat & Righton, 2007; Rose et al., 2000; Worm & Tittensor, 2011), recruitment level (Hurst et al., 2012) and spawning stock biomass (Hughes et al., 2014), marine studies including multiple climatic and non-climatic effects into climate response models are generally scarce. The multi-factor approach was shown to have elevated phenology response estimates in marine organisms when compared to inferences from studies

including temperature only (Brown et al., 2016). Thus, further research is needed to explore interactions between climatic and other ecological factors, and to test how these compare to single-predictor response estimates.

4.3 | Opportunities for future improvement

Our conclusions might have been affected by multiple statistical issues and biases associated with meta-analysis (Gurevitch & Hedges, 1999). First, the identified studies mostly originate in the northern hemisphere, particularly Northern Europe and North America with a limited number of fish species ($n_{species}=345$) of the estimated ~30,000 fish species present globally (Froese & Pauly, 2022). This suggests a significant research bias and limited taxonomic scope in marine fish climactic research. A common paradox in ecological research is observed whereas taxonomically rich ecoregions, such as the tropics, are strongly underrepresented (Hansen & Cramer, 2015). Very few or no studies could be identified from some of the most biodiverse regions such as Southeast Asia, South America, and Africa—highlighting the pressing need to expand research on climate responses in marine fish in face of increasing climate change pressures.

Sample sizes were low for some geographic regions, such as in the northwest Pacific where only two studies (Han et al., 2021; Kumagai et al., 2018) were retrieved, representing four species with an average sample size of 106 (±46) individuals per taxa. In other regions, disproportionate species sample sizes could have influenced interpretations, such as in the East Pacific, where contrasting, multi-directional range shift averages are mainly driven by one large study by Li et al. (2019), measuring depth and horizontal distribution shifts of 10 fish species in nine subregions. The latter example additionally illustrates the need for improved standardization in marine LRS measurement methods to improve comparability of results.

Large variation in publication of LRS and temperature estimates across studies also complicated our interpretations. For example, very few studies presented supporting numeric data of both yearly population center or range edge estimates and high-resolution water temperature data. While some estimates for either of these measures were not possible to extract, others were derived from figures within published papers, which could have affected the accuracy of estimates. Improved temporal and spatial resolution of water temperature estimates, including lagged effects, or implementing tags storing individually experienced water conditions (e.g., Hammerschlag et al., 2022) would likely improve response predictions to climate changes.

4.4 | Implications and recommendations

While no single formula for inferring marine fish distribution responses to warming exists, the local ecological factors as well as the extent of current methodological variation biases highlighted here will be key to improving the accuracy and usefulness of research comparing historical distribution data, creating new time series in the future, and synthesizing literature findings. To facilitate future climate impact research, increased standardization and robustness of range shift measurement methods could be achieved by identifying population structure shaped by relevant ecological variables, such as separate spawning grounds or timing (Oomen & Hutchings, 2015; Petrou et al., 2021) and larval retention (Sinclair & Power, 2015), as well as abiotic barriers due to bathymetry, geology, oceanography (Morgan et al., 2009), and genetic factors, such as cryptic diversity and shared local adaptations (DuBois et al., 2022). For underrepresented habitats such as deep-water or tropical niches, improved spatial and temporal resolution (i.e., robust sample sizes of sampled individuals and spatial and temporal sampling frequency in long-term studies), with measurement in all three dimensions (i.e., depth, latitude, and longitude) will be needed to identify vulnerable species and populations. Bias in LRS comparisons over time could be reduced by controlling for locally relevant confounding factors, including phenomena such as the Southern Oscillation affecting temperature trends in the tropics (Jakovlev et al., 2021), or density dependencies, such as in Bluemel et al. (2022) who accounted for biases by temporal biomass trends. There is an urgent need to expand geographical and taxonomic representation of marine fish range shift responses to climate change. In particular, expansion is needed in the highly biodiverse tropics and global south where marine taxa have been identified as the most vulnerable to warming (Comte & Olden, 2017). As in these regions marine research and long-term fisheries monitoring programs are less established than in the northern hemisphere, robust accounts of whether and how marine fish populations track their temperature niche are lacking.

Addressing the observed variation in marine range shifts will be fundamental for improving response predictions crucial to inform effective fisheries and conservation management strategies, particularly as the magnitude of distribution responses and extinction risk are likely to increase under climate change forecasts (Penn & Deutsch, 2022). In some of the most vulnerable marine ecosystems, such as the arctic, where species have limited thermal tolerance, food web structure and native biodiversity are already rapidly changing due to arrivals of invasive species from lower latitudes (Bartley et al., 2019; Fossheim et al., 2015; Kortsch et al., 2015). Globally, more frequent invasions and resulting novel community structures and interspecific interactions in temperate and arctic latitudes will have likely ecosystem-wide ramifications of yet unknown magnitude (Kortsch et al., 2015; Nadeau & Urban, 2019; Sorte et al., 2010). Therefore, addressing the natural complexity of distributional responses should rely on innovative and robust methods to allow assessment and comparison of findings.

AUTHOR CONTRIBUTIONS

Carolin Dahms and Shaun S. Killen conceived the project. Carolin Dahms collected the data and performed the analyses with the help of Shaun S. Killen. Carolin Dahms wrote the first version of the manuscript with input from Shaun S. Killen. All authors contributed to the final version.

ACKNOWLEDGMENTS

Thanks to Paolo Momigliano for comments and Maria Fossheim and Raul Primicerio for sharing their raw data supported by the Norwegian Institute of Marine Research. Shaun S. Killen was supported by a NERC Advanced Fellowship (NE/J019100/1) and a NERC Standard Grant (NE/T008334/1).

CONFLICT OF INTEREST STATEMENT

All authors declare that they have no conflict of interest.

DATA AVAILABILITY STATEMENT

The data that support the findings of this study are openly available in Zenodo at https://doi.org/10.5281/zenodo.7937671, reference number 7937671.

ORCID

Carolin Dahms https://orcid.org/0000-0002-3283-7820
Shaun S. Killen https://orcid.org/0000-0003-4949-3988

REFERENCES

Adams, C. F., Alade, L. A., Legault, C. M., O'Brien, L., Palmer, M. C., Sosebee, K. A., & Traver, M. L. (2018). Relative importance of population size, fishing pressure and temperature on the spatial distribution of nine Northwest Atlantic groundfish stocks. *PLoS ONE*, *13*, e0196583.

Addo-Bediako, A., Chown, S. L., & Gaston, K. J. (2000). Thermal tolerance, climatic variability and latitude. *Proceedings of the Biological Sciences*, *267*, 739–745. https://doi.org/10.1098/rspb.2000.1065

Alheit, J., Pohlmann, T., Casini, M., Greve, W., Hinrichs, R., Mathis, M., O'Driscoll, K., Vorberg, R., & Wagner, C. (2012). Climate variability drives anchovies and sardines into the North and Baltic Seas. *Progress in Oceanography*, *96*, 128–139. https://doi.org/10.1016/j.pocean.2011.11.015

Angert, A. L., Crozier, L. G., Rissler, L. J., Gilman, S. E., Tewksbury, J. J., & Chunco, A. J. (2011). Do species' traits predict recent shifts at expanding range edges? *Ecology Letters*, *14*, 677–689. https://doi.org/10.1111/j.1461-0248.2011.01620.x

Angilletta, M. J., Niewiarowski, P. H., & Navas, C. A. (2002). The evolution of thermal physiology in ectotherms. *Journal of Thermal Biology*, *27*, 249–268. https://doi.org/10.1016/S0306-4565(01)00094-8

Arel-Bundock, V. (2023). *marginaleffects: Predictions, comparisons, slopes, marginal means, and hypothesis tests*. R package version 0.9.0. https://vincentarelbundock.github.io/marginaleffects/

Baker, M. R., & Hollowed, A. B. (2014). Delineating ecological regions in marine systems: Integrating physical structure and community composition to inform spatial management in the eastern Bering Sea. *Deep Sea Research Part II: Topical Studies in Oceanography*, *109*, 215–240. https://doi.org/10.1016/j.dsr2.2014.03.001

Barbeaux, S. J., & Hollowed, A. B. (2018). Ontogeny matters: Climate variability and effects on fish distribution in the eastern Bering Sea. *Fisheries Oceanography*, *27*, 1–15. https://doi.org/10.1111/fog.12229

Bartley, T. J., McCann, K. S., Bieg, C., Cazelles, K., Granados, M., Guzzo, M. M., MacDougall, A. S., Tunney, T. D., & McMeans, B. C. (2019). Food web rewiring in a changing world. *Nature Ecology and Evolution*, *3*, 345–354. https://doi.org/10.1038/s41559-018-0772-3

Barton, K., & Barton, M. K. (2015). *Package "MuMIn"*. Version v.1.46.0. https://CRAN.R-project.org/package=MuMIn

Bell, R. J., Richardson, D. E., Hare, J. A., Lynch, P. D., & Fratantoni, P. S. (2015). Disentangling the effects of climate, abundance, and size on the distribution of marine fish: An example based on four stocks from the Northeast US shelf. *ICES Journal of Marine Science*, *72*, 1311–1322. https://doi.org/10.1093/icesjms/fsu217

Bluemel, J. K., Fischer, S. H., Kulka, D. W., Lynam, C. P., & Ellis, J. R. (2022). Decline in Atlantic wolffish *Anarhichas lupus* in the North Sea: Impacts of fishing pressure and climate change. *Journal of Fish Biology*, *100*, 253–267. https://doi.org/10.1111/jfb.14942

Bonebrake, T. C., Brown, C. J., Bell, J. D., Blanchard, J. L., Chauvenet, A., Champion, C., Chen, I.-C., Clark, T. D., Colwell, R. K., Danielsen, F., Dell, A. I., Donelson, J. M., Evengård, B., Ferrier, S., Frusher, S., Garcia, R. A., Griffis, R. B., Hobday, A. J., Jarzyna, M. A., … Pecl, G. T. (2018). Managing consequences of climate-driven species redistribution requires integration of ecology, conservation and social science. *Biological Reviews of the Cambridge Philosophical Society*, *93*, 284–305. https://doi.org/10.1111/brv.12344

Borenstein, M., Cooper, H., Hedges, L., & Valentine, J. (2009). Effect sizes for continuous data. *The Handbook of Research Synthesis and Meta-Analysis*, *2*, 221–235.

Brown, C. J., O'Connor, M. I., Poloczanska, E. S., Schoeman, D. S., Buckley, L. B., Burrows, M. T., Duarte, C. M., Halpern, B. S., Pandolfi, J. M., Parmesan, C., & Richardson, A. J. (2016). Ecological and methodological drivers of species' distribution and phenology responses to climate change. *Global Change Biology*, *22*, 1548–1560. https://doi.org/10.1111/gcb.13184

Brown, C. J., Schoeman, D. S., Sydeman, W. J., Brander, K., Buckley, L. B., Burrows, M., Duarte, C. M., Moore, P. J., Pandolfi, J. M., Poloczanska, E., Venables, W., & Richardson, A. J. (2011). Quantitative approaches in climate change ecology. *Global Change Biology*, *17*, 3697–3713. https://doi.org/10.1111/j.1365-2486.2011.02531.x

Cacciapaglia, C., & van Woesik, R. (2018). Marine species distribution modelling and the effects of genetic isolation under climate change. *Journal of Biogeography*, *45*, 154–163. https://doi.org/10.1111/jbi.13115

Campana, S. E., Stefánsdóttir, R. B., Jakobsdóttir, K., & Sólmundsson, J. (2020). Shifting fish distributions in warming sub-Arctic oceans. *Scientific Reports*, *10*, 16448. https://doi.org/10.1038/s41598-020-73444-y

Champion, C., Brodie, S., & Coleman, M. A. (2021). Climate-driven range shifts are rapid yet variable among recreationally important coastal-pelagic fishes. *Frontiers in Marine Science*, *8*. https://doi.org/10.3389/fmars.2021.622299

Chaudhary, C., Richardson, A. J., Schoeman, D. S., & Costello, M. J. (2021). Global warming is causing a more pronounced dip in marine species richness around the equator. *Proceedings of the National Academy of Sciences of the United States of America*, *118*, e2015094118. https://doi.org/10.1073/pnas.2015094118

Chen, I. C., Hill, J. K., Ohlemüller, R., Roy, D. B., & Thomas, C. D. (2011). Rapid range shifts of species associated with high levels of climate warming. *Science*, *333*, 1024–1026. https://doi.org/10.1126/science.1206432

Chust, G., Goikoetxea, N., Ibaibarriaga, L., Sagarminaga, Y., Arregui, I., Fontán, A., Irigoien, X., & Arrizabalaga, H. (2019). Earlier migration and distribution changes of albacore in the Northeast Atlantic. *Fisheries Oceanography*, *28*, 505–516. https://doi.org/10.1111/fog.12427

Comte, L., & Olden, J. D. (2017). Climatic vulnerability of the world's freshwater and marine fishes. *Nature Climate Change*, *7*, 718–722.

Dahlke, F. T., Wohlrab, S., Butzin, M., & Pörtner, H. O. (2020). Thermal bottlenecks in the life cycle define climate vulnerability of fish. *Science*, *369*, 65–70. https://doi.org/10.1126/science.aaz3658

Donelson, J. M., Sunday, J. M., Figueira, W. F., Gaitán-Espitia, J. D., Hobday, A. J., Johnson, C. R., Leis, J. M., Ling, S. D., Marshall, D., Pandolfi, J. M., Pecl, G., Rodgers, G. G., Booth, D. J., & Munday, P. L. (2019). Understanding interactions between plasticity, adaptation and range shifts in response to marine environmental change. *Philosophical Transactions of the Royal Society of London. Series B, Biological Sciences*, *374*, 20180186. https://doi.org/10.1098/rstb.2018.0186

DuBois, K., Pollard, K. N., Kauffman, B. J., Williams, S. L., & Stachowicz, J. J. (2022). Local adaptation in a marine foundation species:

Implications for resilience to future global change. *Global Change Biology*, *28*, 2596–2610. https://doi.org/10.1111/gcb.16080

Dulvy, N. K., Rogers, S. I., Jennings, S., Stelzenmller, V., Dye, S. R., & Skjoldal, H. R. (2008). Climate change and deepening of the North Sea fish assemblage: A biotic indicator of warming seas. *Journal of Applied Ecology*, *45*, 1029–1039. https://doi.org/10.1111/j.1365-2664.2008.01488.x

Egger, M., Smith, G. D., Schneider, M., & Minder, C. (1997). Bias in meta-analysis detected by a simple, graphical test. *BMJ*, *315*, 629–634.

Ellingsen, K. E., Yoccoz, N. G., Tveraa, T., Frank, K. T., Johannesen, E., Anderson, M. J., Dolgov, A. V., & Shackell, N. L. (2020). The rise of a marine generalist predator and the fall of beta diversity. *Global Change Biology*, *26*, 2897–2907. https://doi.org/10.1111/gcb.15027

Engelhard, G. H., Righton, D. A., Kerby, T. K., & Pinnegar, J. K. (2011). Cod behaves in mysterious ways: Shifting distribution in the North Sea during the last century. *ICES CM*, *500*, 6.

Engelhard, G. H., Righton, D. A., & Pinnegar, J. K. (2014). Climate change and fishing: A century of shifting distribution in North Sea cod. *Global Change Biology*, *20*, 2473–2483. https://doi.org/10.1111/gcb.12513

Figueira, W. F., Curley, B., & Booth, D. J. (2019). Can temperature-dependent predation rates regulate range expansion potential of tropical vagrant fishes? *Marine Biology*, *166*, 73. https://doi.org/10.1007/s00227-019-3521-5

Fogarty, H. E., Burrows, M. T., Pecl, G. T., Robinson, L. M., & Poloczanska, E. S. (2017). Are fish outside their usual ranges early indicators of climate-driven range shifts? *Global Change Biology*, *23*, 2047–2057. https://doi.org/10.1111/gcb.13635

Fossheim, M., Primicerio, R., Johannesen, E., Ingvaldsen, R. B., Aschan, M. M., & Dolgov, A. V. (2015). Recent warming leads to a rapid borealization of fish communities in the Arctic. *Nature Climate Change*, *5*, 673–677. https://doi.org/10.1038/nclimate2647

Fowler, A. M., Parkinson, K., & Booth, D. J. (2017). New poleward observations of 30 tropical reef fishes in temperate southeastern Australia. *Marine Biodiversity*, *48*, 1–6. https://doi.org/10.1007/s12526-017-0748-6

Frainer, A., Primicerio, R., Kortsch, S., Aune, M., Dolgov, A. V., Fossheim, M., & Aschan, M. M. (2017). Climate-driven changes in functional biogeography of Arctic marine fish communities. *Proceedings of the National Academy of Sciences of the United States of America*, *114*, 12202–12207. https://doi.org/10.1073/pnas.1706080114

Fredston, A., Pinsky, M., Selden, R. L., Szuwalski, C., Thorson, J. T., Gaines, S. D., & Halpern, B. S. (2021). Range edges of North American marine species are tracking temperature over decades. *Global Change Biology*, *27*, 3145–3156. https://doi.org/10.1111/gcb.15614

Fredston-Hermann, A., Selden, R., Pinsky, M., Gaines, S. D., & Halpern, B. S. (2020). Cold range edges of marine fishes track climate change better than warm edges. *Global Change Biology*, *26*, 2908–2922. https://doi.org/10.1111/gcb.15035

Friedman, A. R., Hwang, Y.-T., Chiang, J. C. H., & Frierson, D. M. W. (2013). Interhemispheric temperature asymmetry over the twentieth century and in future projections. *Journal of Climate*, *26*, 5419–5433.

Froese, R., & Pauly, D. (2022). *FishBase*. World Wide Web electronic publication. http://www.fishbase.org.

García Molinos, J., Halpern, B. S., Schoeman, D. S., Brown, C. J., Kiessling, W., Moore, P. J., Pandolfi, J. M., Poloczanska, E. S., Richardson, A. J., & Burrows, M. T. (2015). Climate velocity and the future global redistribution of marine biodiversity. *Nature Climate Change*, *6*, 83–88. https://doi.org/10.1038/nclimate2769

Gurevitch, J., & Hedges, L. V. (1999). Statistical issues in ecological meta-analyses. *Ecology*, *80*, 1142–1149. https://doi.org/10.1890/0012-9658(1999)080[1142:SIIEMA]2.0.CO;2

Hammerschlag, N., McDonnell, L. H., Rider, M. J., Street, G. M., Hazen, E. L., Natanson, L. J., McCandless, C. T., Boudreau, M. R., Gallagher, A. J., Pinsky, M. L., & Kirtman, B. (2022). Ocean warming alters the distributional range, migratory timing, and spatial protections of an apex predator, the tiger shark (*Galeocerdo cuvier*). *Global Change Biology*, *28*, 1990–2005. https://doi.org/10.1111/gcb.16045

Han, Q., Grüss, A., Shan, X., Jin, X., & Thorson, J. T. (2021). Understanding patterns of distribution shifts and range expansion/contraction for small yellow croaker (*Larimichthys polyactis*) in the Yellow Sea. *Fisheries Oceanography*, *30*, 69–84. https://doi.org/10.1111/fog.12503

Hansen, G., & Cramer, W. (2015). Global distribution of observed climate change impacts. *Nature Climate Change*, *5*, 182–185. https://doi.org/10.1038/nclimate2529

Hare, J. A., Morrison, W. E., Nelson, M. W., Stachura, M. M., Teeters, E. J., Griffis, R. B., Alexander, M. A., Scott, J. D., Alade, L., Bell, R. J., Chute, A. S., Curti, K. L., Curtis, T. H., Kircheis, D., Kocik, J. F., Lucey, S. M., McCandless, C. T., Milke, L. M., Richardson, D. E., … Griswold, C. A. (2016). A vulnerability assessment of fish and invertebrates to climate change on the northeast U.S. continental shelf. *PLoS ONE*, *11*, e0146756. https://doi.org/10.1371/journal.pone.0146756

Hollowed, A. B., Wilson, C. D., Stabeno, P. J., & Salo, S. A. (2007). Effect of ocean conditions on the cross-shelf distribution of walleye pollock (*Theragra chalcogramma*) and capelin (*Mallotus villosus*). *Fisheries Oceanography*, *16*, 142–154.

Hsieh, C., Reiss, C. S., Hewitt, R. P., & Sugihara, G. (2008). Spatial analysis shows that fishing enhances the climatic sensitivity of marine fishes. *Canadian Journal of Fisheries and Aquatic Sciences*, *65*, 947–961. https://doi.org/10.1139/f08-017

Hsieh, C.-H., Kim, H. J., Watson, W., Di Lorenzo, E., & Sugihara, G. (2009). Climate-driven changes in abundance and distribution of larvae of oceanic fishes in the southern California region. *Global Change Biology*, *15*, 2137–2152. https://doi.org/10.1111/j.1365-2486.2009.01875.x

Hughes, K. M., Dransfeld, L., & Johnson, M. P. (2014). Changes in the spatial distribution of spawning activity by north-east Atlantic mackerel in warming seas: 1977–2010. *Marine Biology*, *161*, 2563–2576. https://doi.org/10.1007/s00227-014-2528-1

Hurst, T. P., Moss, J. H., & Miller, J. A. (2012). Distributional patterns of 0-group Pacific cod (*Gadus macrocephalus*) in the eastern Bering Sea under variable recruitment and thermal conditions. *ICES Journal of Marine Science*, *69*, 163–174. https://doi.org/10.1093/icesjms/fss011

Husson, B., Lind, S., Fossheim, M., Kato-Solvang, H., Skern-Mauritzen, M., Pécuchet, L., Ingvaldsen, R. B., Dolgov, A. V., & Primicerio, R. (2022). Successive extreme climatic events lead to immediate, large-scale, and diverse responses from fish in the Arctic. *Global Change Biology*, *28*, 3728–3744. https://doi.org/10.1111/gcb.16153

Jakovlev, A. R., Smyshlyaev, S. P., & Galin, V. Y. (2021). Interannual variability and trends in sea surface temperature, lower and middle atmosphere temperature at different latitudes for 1980–2019. *Atmosphere*, *12*, 454. https://doi.org/10.3390/atmos12040454

Jin, Z. C., Zhou, X. H., & He, J. (2015). Statistical methods for dealing with publication bias in meta-analysis. *Statistics in Medicine*, *34*, 343–360. https://doi.org/10.1002/sim.6342

Jokinen, H., Momigliano, P., & Merilä, J. (2019). From ecology to genetics and back: The tale of two flounder species in the Baltic Sea. *ICES Journal of Marine Science*, *76*, 2267–2275. https://doi.org/10.1093/icesjms/fsz151

Jonsson, P. R., Kotta, J., Andersson, H. C., Herkül, K., Virtanen, E., Sandman, A. N., & Johannesson, K. (2018). High climate velocity and population fragmentation may constrain climate-driven range shift of the key habitat former *Fucus vesiculosus*. *Diversity and Distributions*, *24*, 892–905. https://doi.org/10.1111/ddi.12733

Killen, S. S., Costa, I., Brown, J. A., & Gamperl, A. K. (2007). Little left in the tank: Metabolic scaling in marine teleosts and its implications for aerobic scope. *Proceedings of the Biological Sciences*, *274*, 431–438. https://doi.org/10.1098/rspb.2006.3741

Kleisner, K. M., Fogarty, M. J., McGee, S., Barnett, A., Fratantoni, P., Greene, J., Hare, J. A., Lucey, S. M., McGuire, C., Odell, J., Saba, V. S., Smith, L., Weaver, K. J., & Pinsky, M. L. (2016). The effects of sub-regional climate velocity on the distribution and spatial extent of marine species assemblages. *PLoS ONE*, *11*, e0149220. https://doi.org/10.1371/journal.pone.0149220

Knutsen, H., Jorde, P. E., Gonzalez, E. B., Robalo, J., Albretsen, J., & Almada, V. (2013). Climate change and genetic structure of leading edge and rear end populations in a northwards shifting marine fish species, the corkwing wrasse (*Symphodus melops*). *PLoS ONE*, *8*, e67492. https://doi.org/10.1371/journal.pone.0067492

Kortsch, S., Primicerio, R., Beuchel, F., Renaud, P. E., Rodrigues, J., Lønne, O. J., & Gulliksen, B. (2012). Climate-driven regime shifts in Arctic marine benthos. *Proceedings of the National Academy of Sciences of the United States of America*, *109*, 14052–14057. https://doi.org/10.1073/pnas.1207509109

Kortsch, S., Primicerio, R., Fossheim, M., Dolgov, A. V., & Aschan, M. (2015). Climate change alters the structure of arctic marine food webs due to poleward shifts of boreal generalists. *Proceedings of the Royal Society B: Biological Sciences*, *282*, 20151546.

Kotwicki, S., & Lauth, R. R. (2013). Detecting temporal trends and environmentally-driven changes in the spatial distribution of bottom fishes and crabs on the eastern Bering Sea shelf. *Deep Sea Research Part II: Topical Studies in Oceanography*, *94*, 231–243. https://doi.org/10.1016/j.dsr2.2013.03.017

Kumagai, N. H., García Molinos, J., Yamano, H., Takao, S., Fujii, M., & Yamanaka, Y. (2018). Ocean currents and herbivory drive macroalgae-to-coral community shift under climate warming. *Proceedings of the National Academy of Sciences of the United States of America*, *115*, 8990–8995. https://doi.org/10.1073/pnas.1716826115

Kuznetsova, A., Brockhoff, P. B., & Christensen, R. H. (2017). lmerTest package: Tests in linear mixed effects models. *Journal of Statistical Software*, *82*, 1–26.

Last, P. R., White, W. T., Gledhill, D. C., Hobday, A. J., Brown, R., Edgar, G. J., & Pecl, G. (2011). Long-term shifts in abundance and distribution of a temperate fish fauna: A response to climate change and fishing practices. *Global Ecology and Biogeography*, *20*, 58–72. https://doi.org/10.1111/j.1466-8238.2010.00575

Lenoir, J., Bertrand, R., Comte, L., Bourgeaud, L., Hattab, T., Murienne, J., & Grenouillet, G. (2020). Species better track climate warming in the oceans than on land. *Nature Ecology and Evolution*, *4*, 1044–1059.

Li, L., Hollowed, A. B., Cokelet, E. D., Barbeaux, S. J., Bond, N. A., Keller, A. A., King, J. R., McClure, M. M., Palsson, W. A., Stabeno, P. J., & Yang, Q. (2019). Subregional differences in groundfish distributional responses to anomalous ocean bottom temperatures in the northeast Pacific. *Global Change Biology*, *25*, 2560–2575. https://doi.org/10.1111/gcb.14676

Louthan, A. M., Doak, D. F., & Angert, A. L. (2015). Where and when do species interactions set range limits? *Trends in Ecology & Evolution*, *30*, 780–792. https://doi.org/10.1016/j.tree.2015.09.011

MacLean, S. A., & Beissinger, S. R. (2017). Species' traits as predictors of range shifts under contemporary climate change: A review and meta-analysis. *Global Change Biology*, *23*, 4094–4105. https://doi.org/10.1111/gcb.13736

Manhard, C. V., Joyce, J. E., & Gharrett, A. J. (2017). Evolution of phenology in a salmonid population: A potential adaptive response to climate change. *Canadian Journal of Fisheries and Aquatic Sciences*, *74*, 1519–1527. https://doi.org/10.1139/cjfas-2017-0028

Marshall, A. M., Bigg, G. R., van Leeuwen, S. M., Pinnegar, J. K., Wei, H.-L., Webb, T. J., & Blanchard, J. L. (2016). Quantifying heterogeneous responses of fish community size structure using novel combined statistical techniques. *Global Change Biology*, *22*, 1755–1768. https://doi.org/10.1111/gcb.13190

McHenry, J., Welch, H., Lester, S. E., & Saba, V. (2019). Projecting marine species range shifts from only temperature can mask climate vulnerability. *Global Change Biology*, *25*, 4208–4221.

McLean, M., Mouillot, D., Maureaud, A. A., Hattab, T., MacNeil, M. A., Goberville, E., Lindegren, M., Engelhard, G., Pinsky, M., & Auber, A. (2021). Disentangling tropicalization and deborealization in marine ecosystems under climate change. *Current Biology*, *31*, 4817–4823.

Momigliano, P., Jokinen, H., Calboli, F., Aro, E., & Merilä, J. (2019). Cryptic temporal changes in stock composition explain the decline of a flounder (*Platichthys* spp.) assemblage. *Evolutionary Applications*, *12*, 549–559. https://doi.org/10.1111/eva.12738

Morgan, S. G., Fisher, J. L., Miller, S. H., McAfee, S. T., & Largier, J. L. (2009). Nearshore larval retention in a region of strong upwelling and recruitment limitation. *Ecology*, *90*, 3489–3502. https://doi.org/10.1890/08-1550.1

Mueter, F. J., & Litzow, M. A. (2008). Sea ice retreat alters the biogeography of the Bering Sea continental shelf. *Ecological Applications*, *18*, 309–320. https://doi.org/10.1890/07-0564.1

Nadeau, C. P., & Urban, M. C. (2019). Eco-evolution on the edge during climate change. *Ecography*, *42*, 1280–1297. https://doi.org/10.1111/ecog.04404

Nakagawa, S., & Schielzeth, H. (2013). A general and simple method for obtaining R^2 from generalized linear mixed-effects models. *Methods in Ecology and Evolution*, *4*, 133–142. https://doi.org/10.1111/j.2041-210x.2012.00261.x

Nati, J. J. H., Svendsen, M. B. S., Marras, S., Killen, S. S., Steffensen, J. F., McKenzie, D. J., & Domenici, P. (2021). Intraspecific variation in thermal tolerance differs between tropical and temperate fishes. *Scientific Reports*, *11*, 21272. https://doi.org/10.1038/s41598-021-00695-8

Neat, F., & Righton, D. (2007). Warm water occupancy by North Sea cod. *Proceedings of the Biological Sciences*, *274*, 789–798. https://doi.org/10.1098/rspb.2006.0212

Nicolas, D., Chaalali, A., Drouineau, H., Lobry, J., Uriarte, A., Borja, A., & Boët, P. (2011). Impact of global warming on European tidal estuaries: Some evidence of northward migration of estuarine fish species. *Regional Environmental Change*, *11*, 639–649.

Nye, J. A., Link, J. S., Hare, J. A., & Overholtz, W. J. (2009). Changing spatial distribution of fish stocks in relation to climate and population size on the Northeast United States continental shelf. *Marine Ecology Progress Series*, *393*, 111–129. https://doi.org/10.3354/meps08220

Olafsdottir, A. H., Utne, K. R., Jacobsen, J. A., Jansen, T., Óskarsson, G. J., Nøttestad, L., Elvarsson, B. Þ., Broms, C., & Slotte, A. (2018). Geographical expansion of Northeast Atlantic mackerel (*Scomber scombrus*) in the Nordic Seas from 2007 to 2016 was primarily driven by stock size and constrained by low temperatures. *Deep Sea Research Part II: Topical Studies in Oceanography*. https://doi.org/10.1016/j.dsr2.2018.05.023

Oomen, R. A., & Hutchings, J. A. (2015). Variation in spawning time promotes genetic variability in population responses to environmental change in a marine fish. *Conservation Physiology*, *3*. https://doi.org/10.1093/conphys/cov027

Overholtz, W. J., Hare, J. A., & Keith, C. M. (2011). Impacts of interannual environmental forcing and climate change on the distribution of Atlantic mackerel on the U.S. northeast continental shelf. *Marine and Coastal Fisheries*, *3*, 219–232. https://doi.org/10.1080/19425120.2011.578485

Page, M. J., McKenzie, J. E., Bossuyt, P. M., Boutron, I., Hoffmann, T. C., Mulrow, C. D., Shamseer, L., Tetzlaff, J. M., Akl, E. A., Brennan, S. E., Chou, R., Glanville, J., Grimshaw, J. M., Hróbjartsson, A., Lalu, M. M., Li, T., Loder, E. W., Mayo-Wilson, E., McDonald, S., … Moher, D. (2021). The PRISMA 2020 statement: An updated guideline for reporting systematic reviews. *Systematic Reviews*, *10*, 89. https://doi.org/10.1186/s13643-021-01626-4

Parmesan, C. (2007). Influences of species, latitudes and methodologies on estimates of phenological response to global warming. *Global Change Biology*, *13*, 1860–1872.

Parmesan, C., Gaines, S., Gonzalez, L., Kaufman, D. M., Kingsolver, J., Townsend Peterson, A., & Sagarin, R. (2005). Empirical perspectives on species borders: From traditional biogeography to global change. *Oikos*, *108*, 58–75. https://doi.org/10.1111/j.0030-1299.2005.13150.x

Pecl, G. T., Araújo, M. B., Bell, J. D., Blanchard, J., Bonebrake, T. C., Chen, I.-C., Clark, T. D., Colwell, R. K., Danielsen, F., Evengård, B., Falconi, L., Ferrier, S., Frusher, S., Garcia, R. A., Griffis, R. B., Hobday, A. J., Janion-Scheepers, C., Jarzyna, M. A., Jennings, S., … Williams, S. E. (2017). Biodiversity redistribution under climate change: Impacts on ecosystems and human well-being. *Science*, *355*, eaai9214. https://doi.org/10.1126/science.aai9214

Penn, J. L., & Deutsch, C. (2022). Avoiding ocean mass extinction from climate warming. *Science*, *376*, 524–526. https://doi.org/10.1126/science.abe9039

Perry, A. L., Low, P. J., Ellis, J. R., & Reynolds, J. D. (2005). Climate change and distribution shifts in marine fishes. *Science*, *308*, 1912–1915. https://doi.org/10.1126/science.1111322

Petrou, E. L., Fuentes-Pardo, A. P., Rogers, L. A., Orobko, M., Tarpey, C., Jiménez-Hidalgo, I., Moss, M. L., Yang, D., Pitcher, T. J., Sandell, T., & Lowry, D. (2021). Functional genetic diversity in an exploited marine species and its relevance to fisheries management. *Proceedings of the Royal Society B*, *288*, 20202398. https://doi.org/10.1098/rspb.2020.2398

Pinsky, M. L., Eikeset, A. M., McCauley, D. J., & Sunday, J. M. (2019). Greater vulnerability to warming of marine versus terrestrial ectotherms. *Nature*, *569*, 108–111. https://doi.org/10.1038/s41586-019-1132-4

Pinsky, M. L., Selden, R. L., & Kitchel, Z. J. (2020). Climate-driven shifts in marine species ranges: Scaling from organisms to communities. *Annual Review of Marine Science*, *12*, 153–179.

Pinsky, M. L., Worm, B., Fogarty, M. J., Sarmiento, J. L., & Levin, S. A. (2013). Marine taxa track local climate velocities. *Science*, *341*, 1239–1242. https://doi.org/10.1126/science.1239352

Poloczanska, E. S., Brown, C. J., Sydeman, W. J., Kiessling, W., Schoeman, D. S., Moore, P. J., Brander, K., Bruno, J. F., Buckley, L. B., Burrows, M. T., Duarte, C. M., Halpern, B. S., Holding, J., Kappel, C. V., O'Connor, M. I., Pandolfi, J. M., Parmesan, C., Schwing, F., Thompson, S. A., & Richardson, A. J. (2013). Global imprint of climate change on marine life. *Nature Climate Change*, *3*, 919–925. https://doi.org/10.1038/nclimate1958

Pörtner, H. O., & Farrell, A. P. (2008). Ecology. Physiology and climate change. *Science*, *322*, 690–692. https://doi.org/10.1126/science.1163156

Pörtner, H. O., Roberts, D. C., Masson-Delmotte, V., Zhai, P., Tignor, M., Poloczanska, E., & Weyer, N. M. (2019). The ocean and cryosphere in a changing climate. *IPCC Special Report on the Ocean and Cryosphere in a Changing Climate*, p. 1155.

Quinn, T. J., & McCall, A. D. (1991). Dynamic geography of marine fish populations. *Copeia*, *1991*, 861. https://doi.org/10.2307/1446418

R Core Team. (2023). *R: A language and environment for statistical computing*. R Foundation for Statistical Computing. https://www.R-project.org/

Rayner, N. A. A., Parker, D. E., Horton, E. B., Folland, C. K., Alexander, L. V., Rowell, D. P., Kent, E. C., & Kaplan, A. (2003). Global analyses of sea surface temperature, sea ice, and night marine air temperature since the late nineteenth century. *Journal of Geophysical Research: Atmospheres*, *108*(D14).

Reusch, T. B. (2014). Climate change in the oceans: Evolutionary versus phenotypically plastic responses of marine animals and plants. *Evolutionary Applications*, *7*, 104–122. https://doi.org/10.1111/eva.12109

Rindorf, A., & Lewy, P. (2006). Warm, windy winters drive cod north and homing of spawners keeps them there. *Journal of Applied Ecology*, *43*, 445–453.

Robalo, J. I., Francisco, S. M., Vendrell, C., Lima, C. S., Pereira, A., Brunner, B. P., Dia, M., Gordo, L., & Castilho, R. (2020). Against all odds: A tale of marine range expansion with maintenance of extremely high genetic diversity. *Scientific Reports*, *10*, 12707. https://doi.org/10.1038/s41598-020-69374-4

Roessig, J. M., Woodley, C. M., Cech, J. J., & Hansen, L. J. (2004). Effects of global climate change on marine and estuarine fishes and fisheries. *Reviews in Fish Biology and Fisheries*, *14*, 251–275. https://doi.org/10.1007/s11160-004-6749-0

Rohatgi, A. (2021). *Webplotdigitizer: Version 4.5*. https://automeris.io/WebPlotDigitizer

Rose, G. A., deYoung, B., Kulka, D. W., Goddard, S. V., & Fletcher, G. L. (2000). Distribution shifts and overfishing the northern cod (*Gadus morhua*): A view from the ocean. *Canadian Journal of Fisheries and Aquatic Sciences*, *57*, 644–663. https://doi.org/10.1139/f00-004

Ryu, T., Veilleux, H. D., Munday, P. L., Jung, I., Donelson, J. M., & Ravasi, T. (2020). An epigenetic signature for within-generational plasticity of a reef fish to ocean warming. *Frontiers in Marine Science*, *7*, 284. https://doi.org/10.3389/fmars.2020.00284

Sabatés, A. N. A., Martìn, P., Lloret, J., & Raya, V. (2006). Sea warming and fish distribution: The case of the small pelagic fish, *Sardinella aurita*, in the western Mediterranean. *Global Change Biology*, *12*, 2209–2219.

Sandoval-Huerta, E. R., Beltrán-López, R. G., Pedraza-Marrón, C. R., Paz-Velásquez, M. A., Angulo, A., Robertson, D. R., Espinoza, E., & Domínguez-Domínguez, O. (2019). The evolutionary history of the goby *Elacatinus puncticulatus* in the tropical eastern pacific: Effects of habitat discontinuities and local environmental variability. *Molecular Phylogenetics and Evolution*, *130*, 269–285. https://doi.org/10.1016/j.ympev.2018.10.020

Schickele, A., Goberville, E., Leroy, B., Beaugrand, G., Hattab, T., Francour, P., & Raybaud, V. (2020). European small pelagic fish distribution under global change scenarios. *Fish and Fisheries*, *22*, 212–225. https://doi.org/10.1111/faf.12515

Sherman, C. D., Hunt, A., & Ayre, D. J. (2008). Is life history a barrier to dispersal? Contrasting patterns of genetic differentiation along an oceanographically complex coast. *Biological Journal of the Linnean Society*, *95*, 106-116.

Sinclair, M., & Power, M. (2015). The role of "larval retention" in life-cycle closure of Atlantic herring (*Clupea harengus*) populations. *Fisheries Research*, *172*, 401–414. https://doi.org/10.1016/j.fishres.2015.07.026

Smith, S. M., Fox, R. J., Booth, D. J., & Donelson, J. M. (2018). "Stick with your own kind, or hang with the locals?" implications of shoaling strategy for tropical reef fish on a range-expansion frontline. *Global Change Biology*, *24*, 1663–1672. https://doi.org/10.1111/gcb.14016

Smith, S. M., Malcolm, H. A., Marzinelli, E. M., Schultz, A. L., Steinberg, P. D., & Vergés, A. (2021). Tropicalization and kelp loss shift trophic composition and lead to more winners than losers in fish communities. *Global Change Biology*, *27*, 2537–2548. https://doi.org/10.1111/gcb.15592

Sorte, C. J., Williams, S. L., & Carlton, J. T. (2010). Marine range shifts and species introductions: Comparative spread rates and community impacts. *Global Ecology and Biogeography*, *19*, 303–316. https://doi.org/10.1111/j.1466-8238.2009.00519.x

Spies, I., Gruenthal, K. M., Drinan, D. P., Hollowed, A. B., Stevenson, D. E., Tarpey, C. M., & Hauser, L. (2020). Genetic evidence of a northward range expansion in the eastern Bering Sea stock of Pacific cod. *Evolutionary Applications*, *13*, 362–375. https://doi.org/10.1111/eva.12874

Stocker, T. (2014). *Climate change 2013: The physical science basis: Working Group I contribution to the Fifth assessment report of the Intergovernmental Panel on Climate Change*. Cambridge University Press.

Storch, D., Menzel, L., Frickenhaus, S., & Pörtner, H.-O. (2014). Climate sensitivity across marine domains of life: Limits to evolutionary adaptation shape species interactions. *Global Change Biology*, *20*, 3059–3067. https://doi.org/10.1111/gcb.12645

Sunday, J. M., Bates, A. E., & Dulvy, N. K. (2011). Global analysis of thermal tolerance and latitude in ectotherms. *Proceedings of the Biological Sciences*, *278*, 1823–1830. https://doi.org/10.1098/rspb.2010.1295

Sunday, J. M., Bates, A. E., & Dulvy, N. K. (2012). Thermal tolerance and the global redistribution of animals. *Nature Climate Change*, *2*, 686–690.

Sunday, J. M., Pecl, G. T., Frusher, S., Hobday, A. J., Hill, N., Holbrook, N. J., Edgar, G. J., Stuart-Smith, R., Barrett, N., Wernberg, T., Watson, R. A., Smale, D. A., Fulton, E. A., Slawinski, D., Feng, M., Radford, B. T., Thompson, P. A., & Bates, A. E. (2015). Species traits and climate velocity explain geographic range shifts in an ocean-warming hotspot. *Ecology Letters*, *18*, 944–953. https://doi.org/10.1111/ele.12474

Swain, D. P., & Benoit, H. P. (2006). Change in habitat associations and geographic distribution of thorny skate (*Amblyraja radiata*) in the southern Gulf of St Lawrence: Density-dependent habitat selection or response to environmental change? *Fisheries Oceanography*, *15*, 166–182. https://doi.org/10.1111/j.1365-2419.2006.00357.x

Tang, J. L., & Liu, J. L. (2000). Misleading funnel plot for detection of bias in meta-analysis. *Journal of Clinical Epidemiology*, *53*, 477–484. https://doi.org/10.1016/s0895-4356(99)00204-8

Torres, L. G., Read, A. J., & Halpin, P. (2008). Fine-scale habitat modeling of a top marine predator: Do prey data improve predictive capacity. *Ecological Applications*, *18*, 1702–1717. https://doi.org/10.1890/07-1455.1

Urban, M. C. (2015). Climate change. Accelerating extinction risk from climate change. *Science*, *348*, 571–573. https://doi.org/10.1126/science.aaa4984

van Hal, R., Smits, K., & Rijnsdorp, A. D. (2010). How climate warming impacts the distribution and abundance of two small flatfish species in the North Sea. *Journal of Sea Research*, *64*, 76–84.

Vestfals, C. D., Ciannelli, L., & Hoff, G. R. (2016). Changes in habitat utilization of slope-spawning flatfish across a bathymetric gradient. *ICES Journal of Marine Science*, *73*, 1875–1889. https://doi.org/10.1093/icesjms/fsw112

Viechtbauer, W. (2010). Conducting meta-analyses in R with the metafor package. *Journal of Statistical Software*, *36*, 1–48.

Wassmann, P., Reigstad, M., Haug, T., Rudels, B., Carroll, M. L., Hop, H., Gabrielsen, G. W., Falk-Petersen, S., Denisenko, S. G., Arashkevich, E., Slagstad, D., & Pavlova, O. (2006). Food webs and carbon flux in the Barents Sea. *Progress in Oceanography*, *71*, 232–287. https://doi.org/10.1016/j.pocean.2006.10.003

Wernberg, T., Smale, D. A., & Thomsen, M. S. (2012). A decade of climate change experiments on marine organisms: Procedures, patterns and problems. *Global Change Biology*, *18*, 1491–1498. https://doi.org/10.1111/j.1365-2486.2012.02656.x

Whitney, C. K., Hinch, S. G., & Patterson, D. A. (2013). Provenance matters: Thermal reaction norms for embryo survival among sockeye salmon Oncorhynchus nerka populations. *Journal of Fish Biology*, *82*, 1159–1176. https://doi.org/10.1111/jfb.12055

Wolkovich, E. M., Cook, B. I., Allen, J. M., Crimmins, T. M., Betancourt, J. L., Travers, S. E., Pau, S., Regetz, J., Davies, T. J., Kraft, N. J. B., Ault, T. R., Bolmgren, K., Mazer, S. J., McCabe, G. J., McGill, B. J., Parmesan, C., Salamin, N., Schwartz, M. D., & Cleland, E. E. (2012). Warming experiments underpredict plant phenological responses to climate change. *Nature*, *485*, 494–497. https://doi.org/10.1038/nature11014

Worm, B., & Tittensor, D. P. (2011). Range contraction in large pelagic predators. *Proceedings of the National Academy of Sciences of the United States of America*, *108*, 11942–11947. https://doi.org/10.1073/pnas.1102353108

Yasumiishi, E. M., Cieciel, K., Andrews, A. G., Murphy, J., & Dimond, J. A. (2020). Climate-related changes in the biomass and distribution of small pelagic fishes in the eastern Bering Sea during late summer, 2002–2018. *Deep Sea Research Part II: Topical Studies in Oceanography.*, *181–182*, 104907. https://doi.org/10.1016/j.dsr2.2020.104907

Yemane, D., Kirkman, S. P., Kathena, J., N'siangango, S. E., Axelsen, B. E., & Samaai, T. (2014). Assessing changes in the distribution and range size of demersal fish populations in the Benguela Current Large Marine Ecosystem. *Reviews in Fish Biology and Fisheries*, *24*, 463–483. https://doi.org/10.1007/s11160-014-9357-7

Zuur, A. F., Ieno, E. N., Walker, N., Saveliev, A. A., & Smith, G. M. (2009). Mixed effects modelling for nested data. In *Mixed effects models and extensions in ecology with R* (pp. 101–142).

DATA SOURCES

Alheit, J., Pohlmann, T., Casini, M., Greve, W., Hinrichs, R., Mathis, M., O'Driscoll, K., Vorberg, R., & Wagner, C. (2012). Climate variability drives anchovies and sardines into the North and Baltic Seas. *Progress in Oceanography*, *96*, 128–139. https://doi.org/10.1016/j.pocean.2011.11.015

Bell, R. J., Richardson, D. E., Hare, J. A., Lynch, P. D., & Fratantoni, P. S. (2015). Disentangling the effects of climate, abundance, and size on the distribution of marine fish: An example based on four stocks from the Northeast US shelf. *ICES Journal of Marine Science*, *72*, 1311–1322. https://doi.org/10.1093/icesjms/fsu217

Bluemel, J. K., Fischer, S. H., Kulka, D. W., Lynam, C. P., & Ellis, J. R. (2022). Decline in Atlantic wolffish *Anarhichas lupus* in the North Sea: Impacts of fishing pressure and climate change. *Journal of Fish Biology*, *100*, 253–267. https://doi.org/10.1111/jfb.14942

Champion, C., Brodie, S., & Coleman, M. A. (2021). Climate-driven range shifts are rapid yet variable among recreationally important coastal-pelagic fishes. *Frontiers in Marine Science*, *8*. https://doi.org/10.3389/fmars.2021.622299

Chust, G., Goikoetxea, N., Ibaibarriaga, L., Sagarminaga, Y., Arregui, I., Fontán, A., Irigoien, X., & Arrizabalaga, H. (2019). Earlier migration and distribution changes of albacore in the Northeast Atlantic. *Fisheries Oceanography*, *28*, 505–516. https://doi.org/10.1111/fog.12427

Dulvy, N. K., Rogers, S. I., Jennings, S., Stelzenmller, V., Dye, S. R., & Skjoldal, H. R. (2008). Climate change and deepening of the North Sea fish assemblage: A biotic indicator of warming seas. *Journal of Applied Ecology*, *45*, 1029–1039. https://doi.org/10.1111/j.1365-2664.2008.01488.x

Engelhard, G. H., Righton, D. A., Kerby, T. K., & Pinnegar, J. K. (2011). Cod behaves in mysterious ways: Shifting distribution in the North Sea during the last century. *ICES CM*, *500*, 6.

Engelhard, G. H., Righton, D. A., & Pinnegar, J. K. (2014). Climate change and fishing: A century of shifting distribution in North Sea cod. *Global Change Biology*, *20*, 2473–2483. https://doi.org/10.1111/gcb.12513

Fossheim, M., Primicerio, R., Johannesen, E., Ingvaldsen, R. B., Aschan, M. M., & Dolgov, A. V. (2015). Recent warming leads to a rapid borealization of fish communities in the Arctic. *Nature Climate Change*, *5*, 673–677. https://doi.org/10.1038/nclimate2647

Fowler, A. M., Parkinson, K., & Booth, D. J. (2017). New poleward observations of 30 tropical reef fishes in temperate southeastern Australia. *Marine Biodiversity*, *48*, 1–6. https://doi.org/10.1007/s12526-017-0748-6

Fredston-Hermann, A., Selden, R., Pinsky, M., Gaines, S. D., & Halpern, B. S. (2020). Cold range edges of marine fishes track climate change better than warm edges. *Global Change Biology*, *26*, 2908–2922. https://doi.org/10.1111/gcb.15035

Hammerschlag, N., McDonnell, L. H., Rider, M. J., Street, G. M., Hazen, E. L., Natanson, L. J., McCandless, C. T., Boudreau, M. R., Gallagher, A. J., Pinsky, M. L., & Kirtman, B. (2022). Ocean warming alters the distributional range, migratory timing, and spatial protections of an apex predator, the tiger shark (*Galeocerdo cuvier*). *Global Change Biology*, *28*, 1990–2005. https://doi.org/10.1111/gcb.16045

Han, Q., Grüss, A., Shan, X., Jin, X., & Thorson, J. T. (2021). Understanding patterns of distribution shifts and range expansion/contraction for small yellow croaker (*Larimichthys polyactis*) in the Yellow Sea. *Fisheries Oceanography*, *30*, 69–84. https://doi.org/10.1111/fog.12503

Hsieh, C., Reiss, C. S., Hewitt, R. P., & Sugihara, G. (2008). Spatial analysis shows that fishing enhances the climatic sensitivity of marine fishes. *Canadian Journal of Fisheries and Aquatic Sciences*, *65*, 947–961. https://doi.org/10.1139/f08-017

Hsieh, C.-H., Kim, H. J., Watson, W., Di Lorenzo, E., & Sugihara, G. (2009). Climate-driven changes in abundance and distribution of larvae of oceanic fishes in the southern California region. *Global Change Biology*, *15*, 2137–2152. https://doi.org/10.1111/j.1365-2486.2009.01875.x

Hughes, K. M., Dransfeld, L., & Johnson, M. P. (2014). Changes in the spatial distribution of spawning activity by north-east Atlantic mackerel in warming seas: 1977–2010. *Marine Biology*, *161*, 2563–2576. https://doi.org/10.1007/s00227-014-2528-1

Hurst, T. P., Moss, J. H., & Miller, J. A. (2012). Distributional patterns of 0-group Pacific cod (*Gadus macrocephalus*) in the eastern Bering Sea under variable recruitment and thermal conditions. *ICES Journal of Marine Science*, *69*, 163–174. https://doi.org/10.1093/icesjms/fss011

Husson, B., Lind, S., Fossheim, M., Kato-Solvang, H., Skern-Mauritzen, M., Pécuchet, L., Ingvaldsen, R. B., Dolgov, A. V., & Primicerio, R. (2022). Successive extreme climatic events lead to immediate, large-scale, and diverse responses from fish in the Arctic. *Global Change Biology*, *28*, 3728–3744. https://doi.org/10.1111/gcb.16153

Kotwicki, S., & Lauth, R. R. (2013). Detecting temporal trends and environmentally-driven changes in the spatial distribution of bottom fishes and crabs on the eastern Bering Sea shelf. *Deep Sea Research Part II: Topical Studies in Oceanography*, *94*, 231–243. https://doi.org/10.1016/j.dsr2.2013.03.017

Kumagai, N. H., García Molinos, J., Yamano, H., Takao, S., Fujii, M., & Yamanaka, Y. (2018). Ocean currents and herbivory drive macroalgae-to-coral community shift under climate warming. *Proceedings of the National Academy of Sciences of the United States of America*, *115*, 8990–8995. https://doi.org/10.1073/pnas.1716826115

Last, P. R., White, W. T., Gledhill, D. C., Hobday, A. J., Brown, R., Edgar, G. J., & Pecl, G. (2011). Long-term shifts in abundance and distribution of a temperate fish fauna: A response to climate change and fishing practices. *Global Ecology and Biogeography*, *20*, 58–72. https://doi.org/10.1111/j.1466-8238.2010.00575.x

Li, L., Hollowed, A. B., Cokelet, E. D., Barbeaux, S. J., Bond, N. A., Keller, A. A., King, J. R., McClure, M. M., Palsson, W. A., Stabeno, P. J., & Yang, Q. (2019). Subregional differences in groundfish distributional responses to anomalous ocean bottom temperatures in the northeast Pacific. *Global Change Biology*, *25*, 2560–2575. https://doi.org/10.1111/gcb.14676

Mueter, F. J., & Litzow, M. A. (2008). Sea ice retreat alters the biogeography of the Bering Sea continental shelf. *Ecological Applications*, *18*, 309–320. https://doi.org/10.1890/07-0564.1

Neat, F., & Righton, D. (2007). Warm water occupancy by North Sea cod. *Proceedings of the Biological Sciences*, *274*, 789–798. https://doi.org/10.1098/rspb.2006.0212

Nicolas, D., Chaalali, A., Drouineau, H., Lobry, J., Uriarte, A., Borja, A., & Boët, P. (2011). Impact of global warming on European tidal estuaries: Some evidence of northward migration of estuarine fish species. *Regional Environmental Change*, *11*, 639–649.

Nye, J. A., Link, J. S., Hare, J. A., & Overholtz, W. J. (2009). Changing spatial distribution of fish stocks in relation to climate and population size on the Northeast United States continental shelf. *Marine Ecology Progress Series*, *393*, 111–129. https://doi.org/10.3354/meps08220

Olafsdottir, A. H., Utne, K. R., Jacobsen, J. A., Jansen, T., Óskarsson, G. J., Nøttestad, L., Elvarsson, B. Þ., Broms, C., & Slotte, A. (2018). Geographical expansion of Northeast Atlantic mackerel (*Scomber scombrus*) in the Nordic Seas from 2007 to 2016 was primarily driven by stock size and constrained by low temperatures. *Deep Sea Research Part II: Topical Studies in Oceanography*. https://doi.org/10.1016/j.dsr2.2018.05.023

Perry, A. L., Low, P. J., Ellis, J. R., & Reynolds, J. D. (2005). Climate change and distribution shifts in marine fishes. *Science*, *308*, 1912–1915. https://doi.org/10.1126/science.1111322

Pinsky, M. L., Worm, B., Fogarty, M. J., Sarmiento, J. L., & Levin, S. A. (2013). Marine taxa track local climate velocities. *Science*, *341*, 1239–1242. https://doi.org/10.1126/science.1239352

Rose, G. A., deYoung, B., Kulka, D. W., Goddard, S. V., & Fletcher, G. L. (2000). Distribution shifts and overfishing the northern cod (*Gadus morhua*): A view from the ocean. *Canadian Journal of Fisheries and Aquatic Sciences*, *57*, 644–663. https://doi.org/10.1139/f00-004

Sabatés, A. N. A., Martìn, P., Lloret, J., & Raya, V. (2006). Sea warming and fish distribution: The case of the small pelagic fish, *Sardinella aurita*, in the western Mediterranean. *Global Change Biology*, *12*, 2209–2219.

Smith, S. M., Malcolm, H. A., Marzinelli, E. M., Schultz, A. L., Steinberg, P. D., & Vergés, A. (2021). Tropicalization and kelp loss shift trophic composition and lead to more winners than losers in fish communities. *Global Change Biology*, *27*, 2537–2548. https://doi.org/10.1111/gcb.15592

Swain, D. P., & Benoit, H. P. (2006). Change in habitat associations and geographic distribution of thorny skate (*Amblyraja radiata*) in the southern Gulf of St Lawrence: Density-dependent habitat selection or response to environmental change? *Fisheries Oceanography*, *15*, 166–182. https://doi.org/10.1111/j.1365-2419.2006.00357.x

Tang, J. L., & Liu, J. L. (2000). Misleading funnel plot for detection of bias in meta-analysis. *Journal of Clinical Epidemiology*, *53*, 477–484. https://doi.org/10.1016/s0895-4356(99)00204-8

van Hal, R., Smits, K., & Rijnsdorp, A. D. (2010). How climate warming impacts the distribution and abundance of two small flatfish species in the North Sea. *Journal of Sea Research*, *64*, 76–84.

Vestfals, C. D., Ciannelli, L., & Hoff, G. R. (2016). Changes in habitat utilization of slope-spawning flatfish across a bathymetric gradient. *ICES Journal of Marine Science*, *73*, 1875–1889. https://doi.org/10.1093/icesjms/fsw112

Worm, B., & Tittensor, D. P. (2011). Range contraction in large pelagic predators. *Proceedings of the National Academy of Sciences of the United States of America*, *108*, 11942–11947. https://doi.org/10.1073/pnas.1102353108

Yasumiishi, E. M., Cieciel, K., Andrews, A. G., Murphy, J., & Dimond, J. A. (2020). Climate-related changes in the biomass and distribution of small pelagic fishes in the eastern Bering Sea during late summer, 2002–2018. *Deep Sea Research Part II: Topical Studies in Oceanography.*, *181–182*, 104907. https://doi.org/10.1016/j.dsr2.2020.104907

Yemane, D., Kirkman, S. P., Kathena, J., N'siangango, S. E., Axelsen, B. E., & Samaai, T. (2014). Assessing changes in the distribution and range size of demersal fish populations in the Benguela Current Large Marine Ecosystem. *Reviews in Fish Biology and Fisheries*, *24*, 463–483. https://doi.org/10.1007/s11160-014-9357-7

SUPPORTING INFORMATION

Additional supporting information can be found online in the Supporting Information section at the end of this article.

How to cite this article: Dahms, C., & Killen, S. S. (2023). Temperature change effects on marine fish range shifts: A meta-analysis of ecological and methodological predictors. *Global Change Biology*, *29*, 4459–4479. https://doi.org/10.1111/gcb.16770

ABOUT UMT FACULTY

SDI

Selective Dissemination of Information (SDI) service is a current-awareness service offered by the PSNZ for UMT Faculty Members. The contents selection criteria include current publications (last 5 years), highly cited and most viewed/downloaded documents. The contents with pdf full text from subscribed databases are organized and compiled according to a monthly theme which is determined based on the topics of specified interest.

For more information or further assistance, kindly contact us at 09-6684185/4298 or email to psnz@umt.edu.my/sh_akmal@umt.edu.my

Thank you.

Perpustakaan Sultanah Nur Zahirah
Universiti Malaysia Terengganu
21030 Kuala Nerus, Terengganu.

Tel. : 09-6684185 (Main Counter)
Fax : 09-6684179
Email : psnz@umt.edu.my